IMPLICATION OF DETERGENT-INSOLUBLE AGGREGATES OF SUPEROXIDE DISMUTASE 1 IN FAMILIAL AMYOTROPHIC LATERAL SCLEROSIS

By

MERCEDES PRUDENCIO ÁLVAREZ

A DISSERTATION PRESENTED TO THE GRADUATE SCHOOL
OF THE UNIVERSITY OF FLORIDA IN PARTIAL FULFILLMENT
OF THE REQUIREMENTS FOR THE DEGREE OF
DOCTOR OF PHILOSOPHY

UNIVERSITY OF FLORIDA

2009

To my family for their constant love and support

ACKNOWLEDGMENTS

I would like to thank my advisor Dr. David R. Borchelt for the great opportunity that joining his lab has been for my career. I also like to thank Dr. Borchelt for teaching me to work and think independently and to grow as a scientist. I would like to thank my committee members: Dr. Sue Semple-Rowland, Dr. Lucia Notterpek, Dr. Dennis Steindler, and Dr. William Dunn Jr. for their advice and interest on my research and career. In particular, I would like to thank Dr. Semple-Rowland for her constant help and support on writing skills, experimental techniques, and guidance on becoming a research scientist. I would like to thank Dr. Notterpek for her scientific and technical support. I also want to thank Dr. Dunn for his constant effort on trying to understand SOD1-associated ALS, and for his research advice. Finally, I want to thank Dr. Steindler for being up to date on my research progress and for finding time to look at my work. Additionally, I want to express my gratitude to all our collaborators: Dr. Julian Whitelegge, Dr. Armando Durazo, Dr. Joan Valentine, Dr. Madhuri Chattopadhyay, Dr. Herman Lelie, and Dr. John P. Hart for all their help and their example of wonderful collaborations. Furthermore, I cannot forget to thank past and current members of the Borchelt lab. In particular I want to thank Dr. Celeste M. Karch for all her support as a friend and as researcher, Ms. Hilda Slunt-Brown for her wonderful expertise and help with numerous research techniques, Dr. Guilian Xu and Mr. Andrew Tebbenkamp for their research advice and friendship. I also want to thank all the members of the Borchelt lab for all the good moments that made going to work a pleasure experience. Finally, I want to thank Mr. Ashton B. Manley for all his support and understanding, and to all my family (Máximo, Joaquina and Almudena) that despite the distance they are always there for me and I could not have done it without their love and support.

TABLE OF CONTENTS

page

LIST OF TABLES

LIST OF FIGURES

Abstract of Dissertation Presented to the Graduate School
of the University of Florida in Partial Fulfillment of the
Requirements for the Degree of Doctor of Philosophy

IMPLICATION OF DETERGENT-INSOLUBLE AGGREGATES OF SUPEROXIDE DISMUTASE 1 IN FAMILIAL AMYOTROPHIC LATERAL SCLEROSIS

By

Mercedes Prudencio Álvarez

December 2009

Chair: David R. Borchelt
Major: Medical Sciences - Neuroscience

Mutations in superoxide dismutase 1 (SOD1) are responsible for 10-20% of the familial cases of amyotrophic lateral sclerosis (ALS). Although it is unknown how these mutations lead to motor neuron degeneration, a yet unknown toxic property of mutant SOD1 is responsible for causing SOD1-associated ALS. One possible toxic property of mutant SOD1 proteins is their ability to misfold and aggregate. Specifically, my research project is focused on further evaluating the mechanism of mutant SOD1 protein aggregation. In particular, we determined the ability of experimental and ALS-associated SOD1 mutations to form detergent-insoluble aggregates, and the effect of these aggregates on disease by using both, cell culture and animal models (Chapters 2 and 3). Additionally, we have established the role of WT SOD1 in modulating aggregation of mutant SOD1 and its repercussions in animal models expressing WT and mutant SOD1 (Chapters 4 and 5). Finally, we have continued to use a cell culture model to further characterize detergent-insoluble aggregates of mutant SOD1 through immunofluorescence and biochemical techniques (Chapter 6).

Our studies demonstrate that all mutant SOD1 proteins that form detergent-insoluble aggregates cause ALS-symptoms in animal models. Additionally, higher rates of aggregate formation indicate a higher risk of developing a rapid disease in humans. A modulator of aggregation is WT SOD1; however, its effect on mutant SOD1 aggregation is complicated. While human WT SOD1 slows aggregation of mutant proteins in cell culture, both proteins eventually co-aggregate in cell culture and in endstage ALS mouse models. The effect of WT SOD1 on disease is detrimental in a dose dependent manner, suggesting an important role of WT on disease. Further characterization of detergent-insoluble aggregates of mutant SOD1 indicates that these species are of very small size, explaining the difficulty of identifying inclusions in cell culture and animal models. Fluorescent-tagged variants can form inclusions in cell culture. However, their large size makes this model not so adequate to establish possible sites of toxic action. In conclusion, we have demonstrated the importance of detergent-insoluble aggregates of mutant SOD1 in ALS. Thus, tools directed to slow down or block aggregate formation could alter the disease course in humans.

CHAPTER 1
INTRODUCTION

Amyotrophic Lateral Sclerosis: A General Overview

Amyotrophic lateral sclerosis (ALS) was first described as a late-onset degenerative motor neuron disease by Jean-Martin Charcot in 1869 (Charcot JM and AJ, 1869). Nowadays, ALS is one of the most common motor neuron diseases, with an incidence of 1 to 2 every 100,000 people (Cozzolino et al., 2008b), and about 15 new cases are diagnosed per day in North America (Wroe, 2009). ALS is usually diagnose as suspected, possible, probable or definite ALS, according to whether symptoms are identified in one or more areas of the body (bulbar, cervical, thoracic, and lumbar) and whether there is any other supporting information (genetic link, biopsy, pathology, etc). The criteria to diagnose ALS were not described till 1994 and they are commonly known as “El Escorial criteria”, which was defined at the World Federation of Neurology Research in Spain (Brooks, 1994). These criteria establish that a patient may be diagnosed as an ALS patient when:

1. There is clinical evidence of upper and lower motor neuron degeneration.
2. There are clinical symptoms that progress extending within a certain area or to other areas of the body; and,
3. There are not other symptoms or disease features that can explain the motor neuron degeneration.

Pathologically, ALS is characterized by the selective loss of upper and lower motor neurons in the spinal cord, brain stem and cortex. Interestingly the loss of motor neurons that control eye movements and the bladder are rarely affected (Kunst, 2004). Motor neuron degeneration in affected areas generally leads to muscular weakness, atrophy, twitching, and speech disabilities (Bendotti and Carri, 2004). As disease

progresses paralysis occurs, resulting in death by respiratory failure (Bruijn et al., 2004). A summary of affected areas in ALS patients is represented in Table 1-1 (table adapted from "The revised Escorial criteria" (Brooks, 1994).

Table 1-1. ALS affected areas.

Affected areas	Lower motor neuron signs	Upper motor neuron signs
Brain stem	Weakness, atrophy, fasciculations[a] of : -Jaw, face, palate, tongue, larynx.	Clonic jaw[b], gag reflex[c], exaggerated snout reflex[d], pseudobulbar features, forced yawning, pathologic deep tendon reflexes[e], spastic tone[f].
Spinal cord	Weakness, atrophy, fasciculations of: -Neck, arm, hand, diaphragm, back, abdomen, leg, foot.	Clonic deep tendon reflexes, Hoffman reflex[g], pathologic deep tendon reflexes, spastic tone, preserved reflex in weak wasted limb, loss of superficial abdominal reflexes

[a]Fasciculations = muscle twitching, involuntary muscle contractions
[b]Clonic jaw = rapid repetitive muscular contractions alternated by muscular relaxations of the muscles that control the jaw.
[c]Gag reflex = reflex that involves the contraction of the pharyngeal constrictor muscle
[d]Snout reflex = muscle contraction that makes the lips to purse
[e]Deep tendon reflex = contraction of the muscles in response to stretching forces
[f]Spastic tone = permanent muscle contraction that translates into stiffness of the muscles, interfering with movement, and sometimes speech.
[g]Hoffman reflex = test to determine corticospinal tract damage by tapping the terminal phalanx of the index, medium or ring fingers. A positive result is indicated by the flexion of the terminal phalanx of the thumb.

All ALS cases are clinically indistinguishable. However, in most cases, ALS arises from unknown causes (sporadic ALS), and only about 10% of the cases exhibit autosomal inheritance (familial ALS).

Genes Associated with ALS

In 1993, Rosen and colleagues found several cases of ALS that were associated with mutations in the gene that encodes the enzyme copper, zinc, superoxide dismutase 1 (SOD1) (Rosen et al., 1993). Since then, additional genes or loci have been associated with familial ALS cases. A list of the genes and loci that have been associated with familial ALS cases is represented on Table 1-2.

Table 1-2. Familial ALS-associated genes and loci.

Disease	Inheritance	Gene	Chromosomal location	References
ALS1[a]	Dominant (exceptions)	*SOD1, superoxide dismutase 1*	21q22.1	(Rosen et al., 1993;Al-Chalabi et al., 1998)
ALS2[b]	Recessive	*ALS2, alsin*	2q33	(Hadano et al., 2001;Yang et al., 2001)
ALS3[a]	Dominant	*Unknown*	18q21	(Hand et al., 2002)
ALS4[b]	Dominant	*SETX, senataxin*	9q34	(Chen et al., 2004)
ALS5[b]	Recessive	*Unknown*	15q15.1-q21.1	(Hentati et al., 1998)
ALS6[a]	Dominant	*FUS/TLS, fused in sarcoma/translated in liposarcoma*	16q12	(Vance et al., 2009;Kwiatkowski , Jr. et al., 2009)
ALS7[a]	Dominant	*Unknown*	20ptel-p13	(Sapp et al., 2003)
ALS8[a]	Dominant	*VAPB*, vesicle-associated membrane protein/ synaptobrevin-associated membrane protein B	20q13.33	(Nishimura et al., 2004)
ALS-FTD[a]	Dominant	*Unkown*	9q21-22	(Hosler et al., 2000)
ALS-D-PD[a]	Dominant	*MAPT, microtubule-associated protein tau*	17q21	(Lynch et al., 1994;Hutton et al., 1998)
Progressive lower motor neuron disease	Dominant	*DCTN1, dynactin*	2p13	(Puls et al., 2003)
Sporadic and familial ALS	Dominant	*TDP-43, TAR DNA binding Protein 43*	1p36.22	(Gitcho et al., 2008;Sreedharan et al., 2008;Kabashi et al., 2008)

[a]Adult onset, [b]Juvenile onset, FTD: Frontal-temporal dementia, D: Dementia, PD: Parkinson's disease.

***SOD1* Gene**

The *SOD1* gene composes a 11 kb fragment on chromosome 21, with 4 introns and 5 exons (Danciger et al., 1986). Two different transcripts are formed (0.7 and 0.9 kb) (Danciger et al., 1986), due to the existence of two different polyadenylation sites

(Figure 1-1). However, either transcript gives rise to the same SOD1 protein of 153 amino acids, with the same structural and functional features.

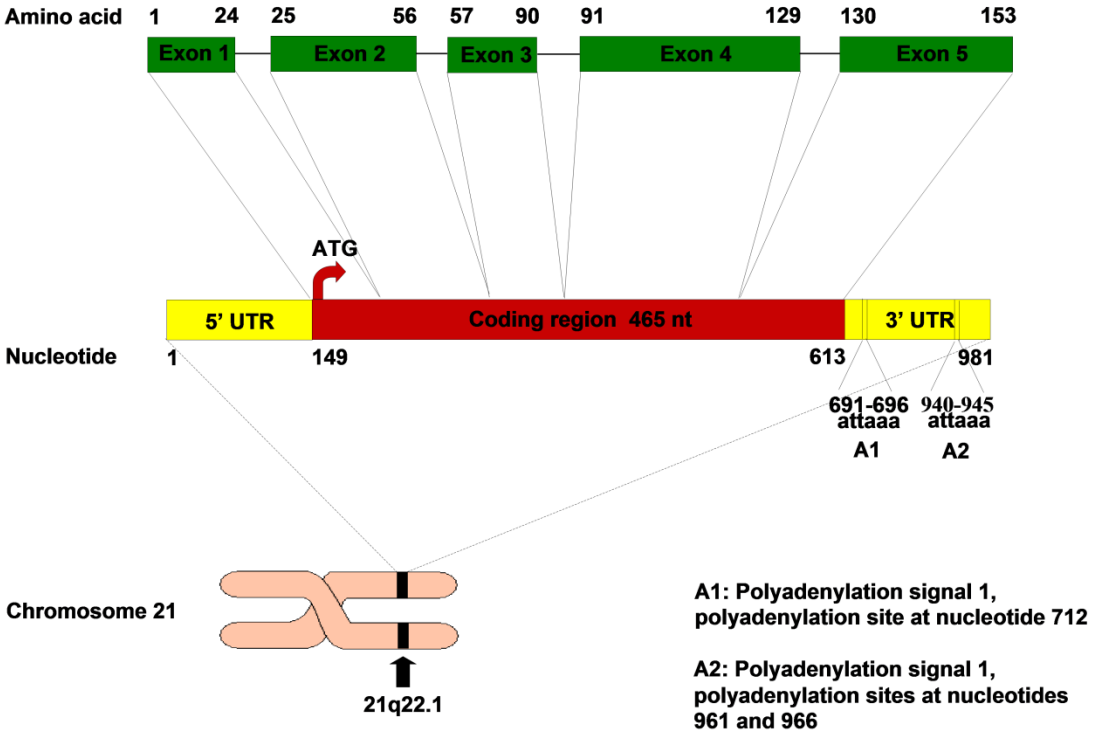

Figure 1-1. Schematic representation of the *SOD1* gene location in the human chromosome, the two polyadenylation signals in the SOD1 transcript and the SOD1 protein.

SOD1 Function

The human SOD1 protein was first isolated from blood erythrocytes in 1959 while studying the role of copper in erythropoiesis (MARKOWITZ et al., 1959), and it was then known as erythrocuprein. The enzymatic function of human SOD1 as a superoxide scavenger was first described by McCord and Fridovich, ten years after its isolation (McCord and Fridovich, 1969). In 1973, erythrocuprein was renamed superoxide dismutase 1 (SOD1) owing to its dismutase activity (Beckman and Pakarinen, 1973). The function of SOD1 protein is to catalyze the antioxidant reaction that converts superoxide radicals into oxygen and hydrogen peroxide. This reaction takes place

independently of pH (from 5 to 9.5) and occurs in two sequential steps, as indicated in Figure 1-2.

$$O_2^{\cdot -} + Cu^{2+}ZnSOD \longrightarrow O_2 + Cu^{+}ZnSOD$$

$$O_2^{\cdot -} + 2\,H^{+} + Cu^{+}ZnSOD \longrightarrow H_2O_2 + Cu^{2+}ZnSOD$$

Figure 1-2. Sequential steps in the dismutase activity of SOD1. $O_2^{\cdot -}$: superoxide radical, Cu^{2+}ZnSOD: oxidized, cupric SOD1, O_2: oxygen, Cu^{+}ZnSOD: reduced, cuprous SOD1, H^{+}: proton, H_2O_2: hydrogen peroxide.

Structural Properties of SOD1

The 32 kDa SOD1 homodimeric protein is very stable. SOD1 is resistant to heat (90ºC), detergent (4% sodium dodecyl sulfate, SDS) and chemical (10 M Urea) denaturation (Forman and Fridovich, 1973). The stability of this enzyme is due to its structural properties. Each of the two SOD1 monomers that compose the dimer forms a β-barrel of eight antiparallel β-strands and both SOD1 monomers are connected to each other by non-covalent forces (Figure 1-3).

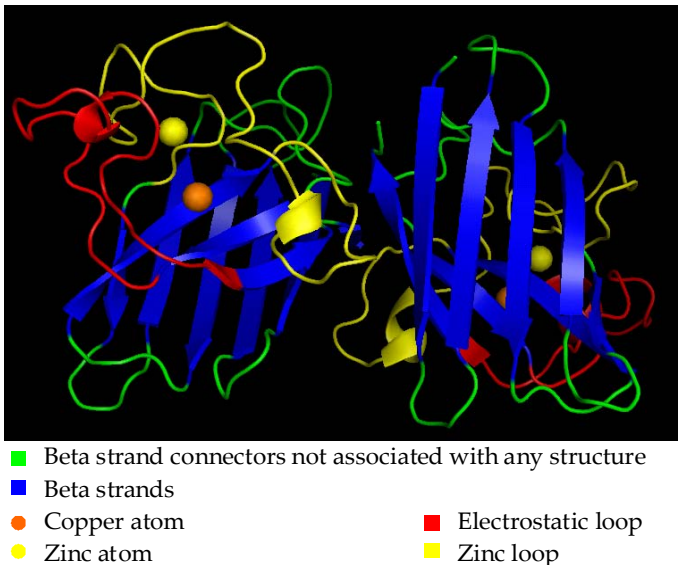

Figure 1-3. Dimeric structure of human G37R SOD1. The published structure (Resolution 1.90 Å, NCBI protein database, 1AZV) has been color coded using PyMOL Software (DeLano Scientific LLC, 2006).

There are two metal binding sites in each monomeric subunit, one for copper and another for zinc. Binding of copper is essential for activity and composes the catalytic site. The electrostatic loop (loop VII, residues 121–144) contains several positive amino acids that guide the superoxide substrate to the catalytic site. Binding of zinc and the zinc loop (loop IV, residues 49–84) confer structural stability to the folded SOD1 protein (Forman and Fridovich, 1973;Elam et al., 2003;Potter et al., 2007).

SOD1 Mutations

A total of 149 pathogenic mutations in the 153 amino acid SOD1 protein have been identified in ALS patients (Wroe, 2009), however only 113 have been documented in peer-reviewed journals (Figure 1-4) (See Appendix A for a list of published SOD1-associated ALS mutations). The majority of these mutations are single amino acid changes (point mutations); however a few deletion, insertion and frameshift mutations have also been associated to the disease. Point mutations predominate in the beta strand regions while frameshift mutations predominate in the C-terminus of SOD1 protein. To date there has not been a SOD1 mutation that produces a null protein. SOD1-associated ALS mutations are spread throughout the 153 amino acid protein sequence with the vast majority of point mutations occurring at highly conserved amino acids (Wang et al., 2006). Almost eighty codons in SOD1 are known to be targets of mutation that give rise to the ALS phenotype; in some cases multiple amino acid substitutions occur at one site (up to 6 for G93) (Figure 1-4).

Some mutations affect the residues that coordinate the binding of copper or zinc, thus affecting the overall SOD1 activity. These mutants are sometimes referred as metal binding mutants. Alternatively, several other mutants do not present reduced activity and have more shared characteristics with the WT SOD1 protein. These

mutants are commonly known as WT-like mutants. However, this terminology of metal binding and WT-like mutants is not appropriate as some mutants do not accurately fit in one of those two categories. Thus, a more recent classification that include β-barrel mutants, metal binding region mutants and disulfide loop mutants is more suitable (Seetharaman et al., 2009) (Also see Appendix A).

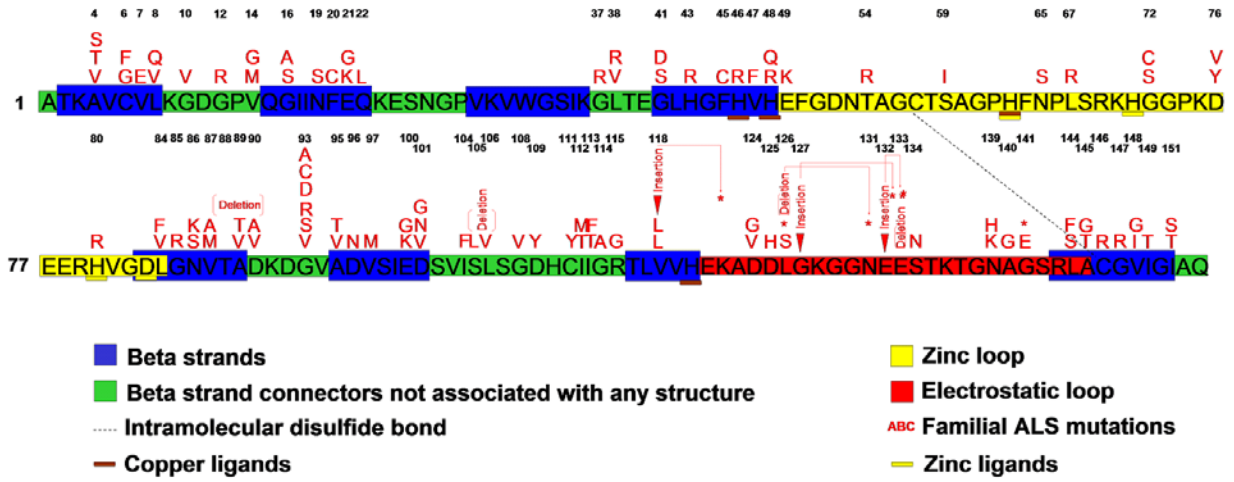

Figure 1-4. SOD1-associated ALS mutations represented in red in the SOD1 amino acid sequence. The different structural areas are color coded, as described in Figure 1-3.

Penetrance of SOD1 Mutations

Many SOD1-associated ALS mutations present complete penetrance, that is, all gene carriers of a SOD1 mutation develop ALS. However, a good number of mutations are known to skip generations and disease carriers do not always develop ALS. For a list of SOD1-associated mutations that present either complete or incomplete penetrance can be found in Table 3-3. A more complete table is represented in Table 1-3.

Certain SOD1 mutations are found in recessive cases, for example the D90A mutation causing ALS with recessive inheritance is found in Scandinavian countries,

while in other places one copy of D90A SOD1 mutation is enough to cause disease. Additionally, recessive cases seem to account for very aggressive phenotypes, these are the cases of G27ΔGP, L84F, N86S, and L126S (Boukaftane et al., 1998;Kato et al., 2001a;Hayward et al., 1998). This data suggest that the levels of SOD1 protein might be important to induce disease development.

Table 1-3. Penetrance of some SOD1-associated mutations.

Complete penetrance	Incomplete penetrance
A4V	A4T
G37R	L8Q
L38V	V14G
G41D	G16S
G41S	N19S
H43R	E21G
H46R	N65S
D76V	G72S
L84F	D76Y
L84V	N86S
G85R	A89V
N86K	D90Aheterozygous
G93A	G93S
G93C	A95T
E100G	E100K
D101H	D101N
I104F	S105L
G108V	I113T
C111Y	V118L
I112M	V118ins
G114A	L126S
L126X	N139H
G127X	
G141E	
L144F	
V148G	
V148I	

SOD1 Subcellular Location

The SOD1 protein is ubiquitously expressed and it is mainly located in the cytosol (Crapo et al., 1992). In lower quantities, SOD1 can also be found in the nucleus (Crapo

et al., 1992), intermembrane space of mitochondria (Sturtz et al., 2001;Jaarsma et al., 2001), and peroxisomes (Keller et al., 1991). Mutant SOD1 proteins are presumably located in the same compartments, although it is possible that misfolding and aggregation of mutant SOD1 proteins may alter the normal SOD1 location. Some studies suggest that misfolding and aggregation of mutant SOD1 proteins interfere with mitochondrial function/s which would lead then to motor neuron death. Although there are studies that showed mutant SOD1 protein association with the cytoplasmic face of the outer mitochondrial membrane (Liu et al., 2004), it does not appear that mutant SOD1 is internalized into mitochondria. However, it is yet to be elucidated the effect, if any, that protein aggregates may have on mitochondrial metabolism. Additionally, if toxicity derives from mutant SOD1 aggregates targeted to mitochondria, it is unclear how only certain cells are susceptible to this toxicity, or what type of cell death mechanism is triggered. Thus, further studies are required to elucidate the location of mutant SOD1 proteins, including mitochondria and other organelles, in order to further understand the disease mechanism of SOD1-associated ALS.

Potential Disease Mechanisms of SOD1-Associated ALS

Loss or Gain of SOD1 Function

Several mechanisms have been proposed to explain how mutations in SOD1 lead to the selective death of motor neurons in familial ALS. Initially, loss or increased protein activity were hypothesized as possible causes of ALS. However, it is now clear that SOD1 activity does not play a role in pathogenesis of familial ALS because:

1. Several SOD1-associated ALS mutations possess normal SOD1 activity (Ratovitski et al., 1999);
2. Some mice require to express the SOD1 mutant protein several folds higher than endogenous mouse WT SOD1 in order to develop familial ALS, thus increasing

overall SOD1 activity (Julien and Kriz, 2006;Jonsson et al., 2006b); while other models do not show increase in total SOD1 activity (Jonsson et al., 2004;Jonsson et al., 2006a);

3. Mice overexpressing WT SOD1 do not develop ALS (Gurney, 1994;Wong et al., 1995);
4. SOD1 knockout mice do not develop ALS (Reaume et al., 1996);
5. Reduction of SOD1 activity by depleting the copper chaperone for SOD1 (CCS) in transgenic mice does not change disease onset nor progression (Subramaniam et al., 2002).
6. Eliminating copper binding sites in human SOD1 of experimental transgenic mouse models does not abolish ALS development (Wang et al., 2002b;Wang et al., 2003).

Mutant SOD1 Damage through Oxidative Chemistry Mechanisms

The accumulation of reactive oxygen species is known to be able to cause cell death, and oxidative stress is known to increase with age and with neurodegenerative processes. In certain cases, free radical damage has been found in postmortem tissue of ALS patients (Beal et al., 1997;Ferrante et al., 1997;Tohgi et al., 1999). Thus, alteration in the oxidative chemistry has been suggested to be involved in SOD1-associated ALS, as mutations in SOD1 may alter its free radical scavenger activity or provide new functions to SOD1 that leads to increase oxidative damage.

The increase in oxidative chemistry may cause damage by peroxidation (Yim et al., 1990;Wiedau-Pazos et al., 1996;Yim et al., 1997), a mechanism by which WT SOD1 is known to react with hydrogen peroxide and produce highly toxic hydroxyl radicals at low levels (Figure 1-5).

Additionally, SOD1 could cause damage by covalent nitration of tyrosine residues (Beckman et al., 1993;Crow et al., 1997;Estevez et al., 1998). During this process, SOD1 reacts with peroxynitrite, which is produced from the reaction between superoxide and nitric oxide, and tyrosine residues of proteins acquire a nitro group. The

nitration of tyrosines residues may alter protein function or folding patterns. This chemical reaction may occur by one of two different proposed mechanisms that involve SOD1 (Figures 1-6 and 1-7).

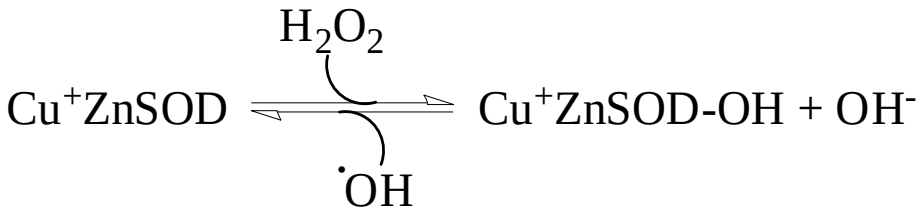

Figure 1-5. Peroxidation reaction. Cu^+ZnSOD: reduced, cuprous SOD1, H_2O_2: hydrogen peroxide, OH^- or $OH^{\cdot}$: hydroxyl radical.

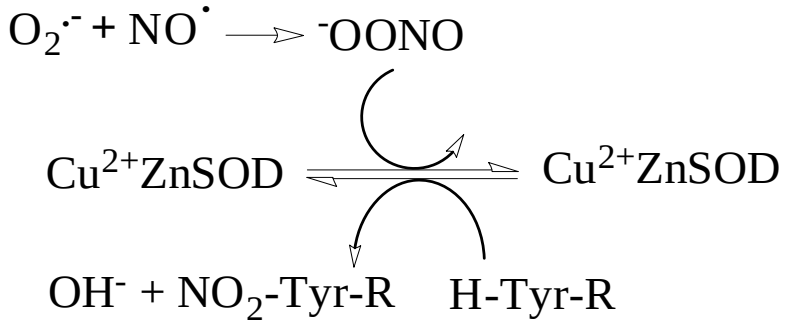

Figure 1-6. Mechanism of covalent nitration of tyrosine residues mediated by SOD1 (Beckman et al., 1993). $Cu^{2+}ZnSOD$: oxidized, cupric SOD1, $O_2^{\cdot -}$: superoxide radical, $NO^{\cdot}$: nitric oxide radical, ^-OONO: peroxynitrite anion, $OH^{\cdot}$: hydroxyl radical, NO_2: nitrogen dioxide, NO_2-Tyr-R: protein with 3-nitrotyroxine, H-Tyr-R: protein with tyrosine residue.

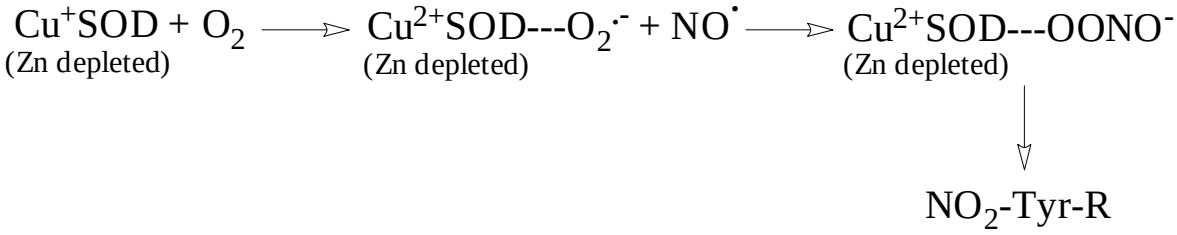

Figure 1-7. An alternative mechanism of covalent nitration of tyrosine residues mediated by SOD1 does not require zinc binding (Crow et al., 1997;Estevez et al., 1999). Cu^+SOD: reduced, cuprous, zinc depleted SOD1, O_2: oxygen, $Cu^{2+}SOD$: oxidized, cupric, zinc depleted SOD1, $O^{\cdot -}$: superoxide radical, $NO^{\cdot}$: nitric oxide radical, $OONO^-$: peroxynitrite anion, NO_2-Tyr-R: protein with 3-nitrotyroxine.

The caveat to these mechanisms of toxicity is that these reactions require mutant SOD1 to bind copper (Yim et al., 1997;Yim et al., 1996;Wiedau-Pazos et al., 1996), the essential cofactor for both dismutase activity and oxidative chemistry. However, a subset of SOD1 mutants (classified as metal binding mutants) have defects at or near metal binding sites or otherwise lower the enzyme affinity for copper (Valentine and Hart, 2003). Studies in transgenic mice have directly tested this mechanism by producing mutant forms of SOD1 with two (H46R/H48Q) or four (H46R/H48Q/H63G/H120G) of the copper binding residues mutated. Mice expressing either mutant develops ALS-like paralysis (Wang et al., 2003;Wang et al., 2002b). Thus, while these studies have demonstrated that the correct binding of copper is not required for ALS symptoms, the aberrant binding of copper to other residues in the protein to induce motor neuron-specific damage is still a possibility (Bush, 2002).

Mutant SOD1 and Protein Aggregation

SOD1 positive inclusions have been found in SOD1-associated ALS patients (Matsumoto et al., 1996;Shibata et al., 1996b;Sasaki et al., 1998;Kato et al., 1999b;Kato et al., 1999a;Kokubo et al., 1999;Watanabe et al., 2001) and SOD1 transgenic mice (Wong et al., 1995;Dal Canto and Gurney, 1997;Bruijn et al., 1997;Wang et al., 2002a;Wang et al., 2002b;Wang et al., 2003). However, the identification of inclusions has not always been possible and it does not tell us whether SOD1-positive inclusions correspond to WT and/or mutant SOD1, or whether it contains misfolded or aggregated protein. Thus, in our experience, the detection of mutant SOD1 aggregation is best accomplished biochemically, using a detergent extraction and sedimentation technique (Wang et al., 2003). Detergent-insoluble species of SOD1 are distinguished by the property of forming structures that are not dissociated by non-ionic detergents and are

of sufficient size to sediment upon centrifugation at high speed; properties associated with protein aggregation (Wang et al., 2003;Wang et al., 2006). For all familial mutant SOD1 proteins studied so far, detergent-insoluble and sedimentable forms of mutant SOD1 can also be generated in cell culture models (Wang et al., 2003;Wang et al., 2006). Thus, to date there has been a strong correlation between the aggregation of mutant SOD1 and toxicity. There are different hypothesis that explains aggregate toxicity in ALS through interference with cellular processes (Figure 1-8).

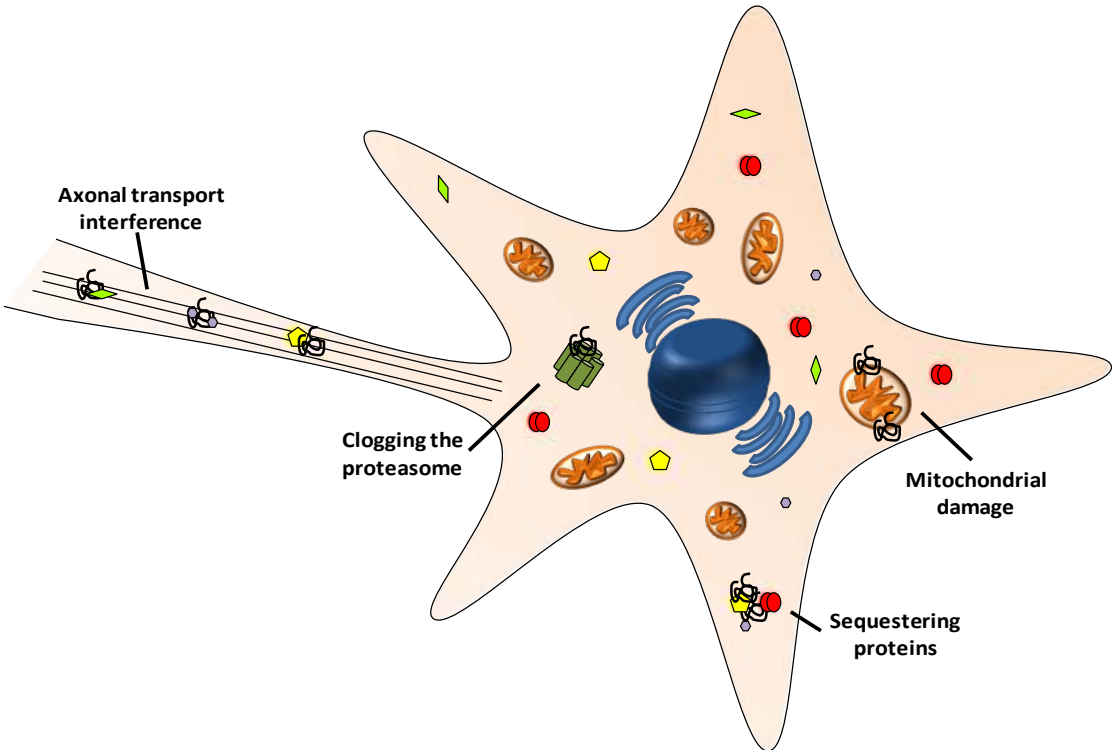

Figure 1-8. Schematic representation of the possible targets of mutant SOD1 aggregates in ALS, interfering with the normal cellular metabolism.

Some of these cellular processes include inhibition of the proteasome (Urushitani et al., 2002;Johnston et al., 2000;Kabashi et al., 2004), accumulation in mitochondria affecting their overall activity (Boillee et al., 2006a), interfering with axonal transport (Zhang et al., 1997;Borchelt et al., 1998;Williamson and Cleveland, 1999), or inhibition

of different cellular proteins by sequestering them into the SOD1 aggregates. Sequestered proteins may include those involved in the chaperone or proteasome system, and in apoptosis (Okado-Matsumoto and Fridovich, 2002;Kunst, 2004;Pasinelli et al., 2004).

Implication of WT SOD1 in ALS and in Aggregation

In SOD1-associated ALS, mutant SOD1 proteins are co-expressed with WT SOD1 at 1:1 ratios of synthesis (Borchelt et al., 1994). In some cases, WT SOD1 can heterodimerize with mutant SOD1protein (Borchelt et al., 1994;Borchelt et al., 1995). Whether toxicity of mutant SOD1 is modulated by interactions between WT and mutant protein, or by the activity of WT SOD1, has been addressed in several experimental models. Mice over-expressing just human WT SOD1 appear largely normal (Gurney et al., 1994;Wong et al., 1995), although there have been reports of mild abnormalities in mice that express very high levels of WT SOD1 (Dal Canto and Gurney, 1994;Tu et al., 1996). In a study of mice that express human G85R SOD1, eliminating the expression of normal endogenous mouse WT SOD1 or over-expressing human WT SOD1 [by crossing to a line of mice produced by Wong and colleagues (Wong et al., 1995)] had no obvious effects on disease onset, progression, or pathology (Bruijn et al., 1998). However, a later study found that mice co-expressing high levels of human WT [by crossing to a line of mice produced by Gurney and colleagues (Gurney et al., 1994)] and G93A SOD1 showed earlier disease onset than mice expressing the G93A mutant alone (Jaarsma et al., 2000). Recently, Deng and colleagues (Deng et al., 2006) reported that crossing the Gurney human WT SOD1 transgenic mice with mice harboring three different ALS mutants (A4V, G93A, and L126Z SOD1) caused accelerated disease onset, which was accompanied by the appearance of aggregated

SOD1. In the case of the A4V mutant mouse model, no evidence of mutant protein aggregation was detected in the absence of additional WT SOD1 or disease symptoms. A second interesting outcome was the observation that WT SOD1 protein co-purified with the mutant SOD1 aggregates in mice that co-expressed WT and L126Z SOD1 (Deng et al., 2006). Thus, one explanation for the decrease in age to onset could be that the addition of WT SOD1 promoted a more rapid aggregation of mutant protein.

Recent studies by Wang and colleagues have shown the results of crossing the same high expressor WT SOD1 mouse line from Gurney and colleagues to G85R SOD1 mice, obtaining similar results on accelerated disease onset and progression (Wang et al., 2009c). These results differ from the crosses made by Bruijn and colleagues with the lower expression WT SOD1 and G85R line (Bruijn et al., 1998). This suggests that the differences may lie in the different WT SOD1 lines of mice used. However, the G85R SOD1 mouse lines used in both studies are different, thus they may not express the same transgene levels, a feature important in mouse models for SOD1-ALS (see “Animal Models to Study SOD1-Associated ALS” in Chapter 1 and Chapter 2). Additionally, in neither study there is mention on whether aggregation is affected by the expression of WT SOD1 protein. Thus, the effect of WT SOD1 on disease and how they relate to aggregation of mutant SOD1 protein is still unclear, and further studies should be performed.

SOD1-Associated ALS: A Non Cell Autonomous Disease

SOD1-associated ALS is known to cause motor neuron degeneration. Several studies demonstrate that motor neurons are primarily targets of mutant SOD1 toxicity:

a) Reduction of mutant SOD1 from motor neurons slows disease onset (Raoul et al., 2002;Ralph et al., 2005;Miller et al., 2006;Boillee et al., 2006b).

b) Primary motor neuron cultures, but not of other cell types are susceptible to death pathways when the cells express a SOD1 mutation (Lino et al., 2002).

However, these studies do not explain whether the toxicity exerted from mutant SOD1 comes exclusively from motor neurons expressing mutant SOD1. It has been shown that mice with mutant SOD1 expression specifically targeted to motor neurons do not develop an ALS-like phenotype (Pramatarova et al., 2001;Lino et al., 2002). These studies suggest the involvement of other cell types in SOD1-associated ALS. Additionally, decreasing the amount of mutant SOD1 within motor neurons delays disease onset in transgenic mice, supporting the notion of motor neurons as the center of toxicity (Boillee et al., 2006b).

The Cleveland group has been pioneer in investigating the role of different cell types in SOD1-associated ALS pathology. The first indication that SOD1-associated ALS is a non-cell autonomous disease came by the creation of chimeric mice expressing human WT and mutant SOD1 proteins. These mice contained motor neurons with higher survival rates when they were surrounded by nonneuronal cells expressing WT SOD1. And degenerating motor neurons were in close proximity to non-neuronal cells expressing mutant SOD1. This study indicates that the motor neuron environment may be critical for their survival, as non-neuronal cells might help to trigger motor neuron death (Gong et al., 2000).

Astrocytes and Microglia

Gliosis is an early pathologic feature observed in SOD1-ALS mice at early stages of disease development (Feeney et al., 2001). Thus, an early thought was that actrocytes or microglia could be the inducers of motor neuron degeneration in ALS. Transgenic mice expressing mutant SOD1 exclusively in astrocytes do not develop

ALS, demonstrating that ALS might not initiate in this particular cell type. However, gliosis occurring within astroglia that express mutant SOD1 may be involved in aggravating disease once it has initiated (Yamanaka et al., 2008).

On the other hand, regarding microglia, depletion of mutant SOD1 from about 25% of microglial cells, but not from astrocytes, translates into longer survival in mutant SOD1 transgenic mice, with no differences in the number of activated astroglial or microglial cells (Boillee et al., 2006b). This data suggest the involvement of glial cells in ALS, although it is still unclear how they contribute to the disease.

Oligodendrocytes and Schwann Cells

Oligodendrocytes and Schwann cells form myelin sheets that envelop axons in the central and peripheral nervous system, respectively. Oligodendrocytes do not seem to be implicated in ALS as chimeric mice, which express mutant G37R SOD1 within all motor neurons and oligodendrocytes, do not develop ALS-like disease (Lobsiger et al., 2009). Surprisingly, Schwann cells seem to be protective as a 70% reduction of mutant G37R SOD1 transgene from Schwann cells shortens survival by over a month in mice (Miller et al., 2006).

Muscle Cells

Motor neurons synapse onto muscle cells through the formation of the neuromuscular junction. Retraction of nerve terminals is known to occur in ALS, likely to a consequence of motor neuron degeneration. However, it is still unclear whether the retraction mechanism starts in the neuron or the muscle cell. In a study of Miller and colleagues, by reducing mutant SOD1 expression from muscle cells alone there is no change in neither onset nor survival of mutant SOD1 transgenic mice (Deng et al.,

2006). These results suggest that mutant SOD1 acting from the muscle cells do not appear to play a role in toxicity.

Animal Models to Study SOD1-Associated ALS

Transgenic Rodents

From all identified genes or loci, mutations in SOD1 represent the largest group in familial ALS, constituting approximately 20% (1-2% of all ALS cases). Of the more than 100 mutations identified to cause disease in humans, only 11 have been expressed in transgenic animal models in order to unravel the molecular mechanisms of the disease. The most important models are represented in Table 1-4.

Additionally, several animal models harboring experimental mutations in the SOD1 transgene have also been created: H46R/H48Q (Wang et al., 2003), H46R/H48Q/H63G/H120G or QUAD (Wang et al., 2007), and SODMD: C6G, H43R, H46R, H48Q, H63G, H71R, H80R, C111S, H120G (for information on SODMD mice see Chapter 2).

Table 1-4. Transgenic rodent models for several SOD1 mutations.

SOD1 mutation	Animal model	References
A4V*	Mouse	(Deng et al., 2006)
G37R cDNA	Mouse	(Wang et al., 2005b)
G37R	Mouse	(Wong et al., 1995)
H46R	Mouse	(Chang-Hong et al., 2005;Sasaki et al., 2007)
H46R	Rat	(Nagai et al., 2001)
L84V	Mouse	(Tobisawa et al., 2003)
G85R	Mouse	(Bruijn et al., 1997;Wang et al., 2009c)
D90A	Mouse	(Jonsson et al., 2006b)
G93A	Mouse	(Gurney et al., 1994)
G93A	Rat	(Nagai et al., 2001;Howland et al., 2002)
G93R	Mouse	(Friedlander et al., 1997)
L126Z or L126stop	Mouse	(Wang et al., 2005a;Deng et al., 2006)
L126delTT(stop 131)	Mouse	(Watanabe et al., 2005)
Gins127TGGG	Mouse	(Jonsson et al., 2004)

*Asymptomatic mice

In all these models, there is evidence suggesting that the levels of expression are critical to induce disease. For example, there are mice that express the G37R or D90A SOD1 that do not develop disease unless bred to homozygosity (Wang et al., 2005b;Jonsson et al., 2006b). Similarly, disease is absent in mice expressing low levels of A4V SOD1 but evident when the levels of total SOD1 are raised by co-expression with WT SOD1 (Deng et al., 2006). Thus, the levels of expression of SOD1 mutant proteins seem to play an important role in ALS-rodent models.

Pathology in SOD1-Associated ALS and Rodent Models of the Disease

A few studies have tried to evaluate the cellular and subcellular changes in familial ALS. The availability of human tissue to evaluate such changes in familial ALS cases is scarce and only provides information of end stage disease since only post-mortem tissue is examined. Thus, most studies have been done using asymptomatic and symptomatic tissue of heterozygous transgenic animal models expressing SOD1 mutations associated with familial ALS. Only a few of the SOD1-associated ALS mutations have been studied for such intracellular and pathological changes in animal models, being the G93A SOD1 mice the most extensively studied and followed by G37R, G85R, H46R, H46R/H48Q, Quad and L126Z SOD1 mice. Some of these pathological changes include:

- Vacuolarization in anterior horns of spinal cords has been observed in the high expressor G93A and in G37R SOD1 mice (Dal Canto and Gurney, 1994;Wong et al., 1995). These vacuoles have been proposed to derive from mitochondria in the case of the G37R SOD1 mice (Wong et al., 1995), or from the Golgi apparatus and the endoplasmic reticulum in the G93A SOD1 mice (Stieber et al., 2000c;Stieber et al., 2000a). However, vacuolar pathology may be a consequence of high SOD1 activity and not a common pathological hallmark of ALS since the vacuolar pathology is also observed in transgenic mouse models expressing human WT SOD1 at high levels (Jaarsma et al., 2000;Sasaki et al., 1998), whereas it is absent in transgenic mice that express SOD1 mutants with none or reduced SOD1 activity such as G85R SOD1 mice (Bruijn et al., 1997;Watanabe et al., 2001), H46R/H48Q SOD1 mice

(Wang et al., 2002b), or even in the lower expressor G93A SOD1 mice (Dal Canto and Gurney, 1997).

- Golgi apparatus fragmentation have also been observed but only in the G93A SOD1 mice (Stieber et al., 1998;Stieber et al., 2000c;Stieber et al., 2000a). Although no other animal model for familial ALS has been used to study the changes in the Golgi apparatus, the same abnormalities have been previously described in some sporadic ALS cases (Wong et al., 1995;Matsumoto et al., 1996;Kato et al., 2000b;Kato et al., 2000a;Kato et al., 1999a;Sasaki et al., 2005;Sasaki et al., 1998;Shibata et al., 1996b). Thus, further studies in other transgenic models for mutant SOD1 should be used to explore the involvement of the Golgi apparatus in ALS.

- The presence of intracytoplasmic neural inclusions seems to be the common pattern observed in post-mortem human tissue and animal models that develop familial ALS-like disease (Kato et al., 1999b;Kato et al., 1999a;Watanabe et al., 2001;Wang et al., 2002b;Sasaki et al., 2007;Bruijn et al., 1997;Dal Canto and Gurney, 1997;Kokubo et al., 1999;Shibata et al., 1996b). These inclusions are usually observed with haematoxylin and eosin or other unspecific stains but some studies have gone further to characterize their composition. The most common inclusions are ubiquitin positive (Seilhean et al., 2004;Matsumoto et al., 1993;Schiffer et al., 1991) or immunoreactive for cystatin C, the latter component of the characteristics Bunina bodies (Shibata et al., 1996a;Okamoto et al., 1993). Familial ALS patients with the SOD1 mutations A4V or L126delTT also presented motoneurons filled with SOD1 inclusions (Bruijn et al., 1998;Wong et al., 1995). Likewise, H46R SOD1 ALS patients reveal inclusions that are reactive to SOD1 or ubiquitin (Ohi et al., 2002;Arisato et al., 2003). SOD1 positive inclusions are also observed in motoneurons of G37R (Wong et al., 1995), H46R (Sasaki et al., 2007), G85R (Bruijn et al., 1997;Watanabe et al., 2001), and G93A SOD1 transgenic mice (Watanabe et al., 2001;Stieber et al., 2000b;Sasaki et al., 2005). These SOD1 positive inclusions have been observed surrounding the pathologic vacuoles in G37R and G93A SOD1 mice (Wong et al., 1995;Higgins et al., 2003) and also in astrocytes before the appearance of disease symptoms in G85R SOD1 mice (Bruijn et al., 1997;Watanabe et al., 2001).The astrocyte SOD1-positive inclusions have also been reported in an earlier study of a familial ALS frameshift mutation, L126delTT SOD1 (Kato et al., 1996). However, the observation of SOD1 immunopositive inclusions has not always been possible. For example, poorly SOD1 stain has been reported for G37R, G85R, G93A, H46R/H48Q and Quad SOD1 transgenic mice (Wang et al., 2003). In addition, Watanabe and colleagues also did not detect any types of inclusions in symptomatic G37R SOD1 mice (Watanabe et al., 2001). Thioflavin S or T staining has been used to characterize the type of inclusions in familial ALS. Thioflavin is a dye that reacts with stacked beta sheet structures and is a typical stain to detect β-amyloid-like inclusions (Kelenyi, 1967;VASSAR and CULLING, 1959). The use of thioflavin stain in sporadic ALS human tissue has not been useful since control samples also show fluorescent material (Wang et al., 2002b;Wang et al., 2003;Wang et al., 2005b). However, thioflavin positive inclusions have been observed in some familial ALS transgenic mice (Wang et al., 2006) but not in the

L126Z SOD1 mouse model (Wang et al., 2005a). These data suggest that there may be different types of SOD1 aggregates in tissues expressing different SOD1 mutations and the difficulty in some cases to stain these aggregates indicates that further analyses are required.

- Detergent-insoluble aggregates of mutant SOD1: all transgenic animal models expressing SOD1-associated ALS mutation consistently form structures of mutant SOD1 proteins that can be isolated with a biochemical assay through detergent extraction and high speed centrifugation. The appearance of these detergent-insoluble species accumulate significantly at disease endstage of hindlimb paralysis, while they are undetectable when mice are asymptomatic (Wang et al., 2006;Karch et al., 2009). However, there is no evidence that the biochemically isolated aggregates of mutant SOD1 are the SOD1 immunoreactive species (inclusions) seen in mouse or human tissues expressing a SOD1-associated ALS mutation. Further studies regarding detergent-insoluble aggregates of mutant SOD1 can be found in the subsequent chapters.

Other Transgenic Animal Models for SOD1-Associated ALS

SOD1-expressing fruit flies.

The fruit fly, *Drosophila melanogaster*, has been used as a model to study SOD1. Flies null for WT SOD1, present a phenotype characterized by a shortened lifespan, decreased fertility and increased oxidative stress (Parkes et al., 1998). The shortened lifespan is recovered by the expression of WT SOD1, and overexpression of WT SOD1 in motorneurons induces a 40% increase in *D. melanogaster* lifespan (Mockett et al., 2003). Additonally, flies expressing SOD1-associated ALS mutations have also been made (A4V, G37R, G41D, G93C, I113T) (Elia et al., 1999;Mockett et al., 2003). These mutant SOD1 flies can partially restore the shortened lifespan observed in SOD1 null flies (Elia et al., 1999). However, the mutant SOD1 flies do not present symptoms of paralysis or premature death and do not manifest the toxic gain of function phenotype that is observed in human patients, as in flies the effect on lifespan is a recessive trait (Elia et al., 1999;Mockett et al., 2003). Thus, the use of this model system does not

seem suitable to study ALS, but might be important to better understand how mutations affect the SOD1 protein.

Worms models for SOD1-associated ALS

Recently, transgenic animal models of *Caenorhabditis elegans* have been created to express SOD1 proteins (WT, G85R, G93A, G127X) (Wang et al., 2009a;Gidalevitz et al., 2009). These transgenic worm models express SOD1 proteins with a C-terminal yellow fluorescent protein (YFP)-tag. Worms expressing mutant SOD1::YFP (SOD1 fused to YFP) proteins form visible inclusions, which translates into locomotor dysfunction (Wang et al., 2009a;Gidalevitz et al., 2009). Thus, this model represents a useful tool to assess toxicity of SOD1 mutant proteins. Although worms expressing WT SOD1::YFP do not present locomotor dysfunction or apparent inclusions, it is uncertain to whether the YFP could modify certain SOD1 properties that would not make this particular worm model useful to replicate all disease related features. Additionally, it would be more interesting to study SOD1 in non-tagged scheme in these *C. elegans* models.

Other models

Other transgenic animal models have been created as an attempt to obtain a better model to study SOD1-associated ALS. An example is the Danish pig, harboring the G93S mutation (Dr. Peter M. Andersen, personal communication). The use such pigs as a model to study ALS may not be, however, cost-effective or convenient. In any case, data on such models has not yet been published, thus we cannot determine the viability of this possible new ALS model.

Recent studies have published the existence of dogs with motor neuron disease that resembles ALS. These dogs express the E40K SOD1 mutation, which might be

equivalent to the E40G ALS mutation in humans. Dogs heterozygous for E40K mutation are asymptomatic but develop motor neuron disease when they are homozygous for the same mutation. If more cases of dogs harboring SOD1 mutations are found and disease features resemble those of ALS, then these animals would represent the first sporadic model to study ALS.

Therapies

Currently, there are no drugs that can cure ALS. Only Riluzole is commonly used to treat ALS. Many different drugs have gone into clinical trials, but no one represents a better alternative treatment.

Riluzole

Riluzole is the only drug approved by The Food and Drug Administration for treatment of ALS. In the best of cases, Riluzole extends lifespan by 2 to 3 months (Lacomblez et al., 1996;Lacomblez et al., 2002;Miller et al., 2007b). However, it is still unclear how this drug prolongs survival in ALS patients. Several Riluzole biological effects have been identified: modulation of glutamate release from the presynaptic terminal (Albo et al., 2004;Fumagalli et al., 2008), inhibition of G-protein dependent processes (Huang et al., 1997a), voltage-gated sodium channel blocker (Zona et al., 1998;Urbani and Belluzzi, 2000), voltage-gated potassium inhibitor (Zona et al., 1998), and voltage-activated calcium channel inhibitor (Huang et al., 1997a;Huang et al., 1997b). More recently, Riluzole has been shown to have a protective role against the slowing of neurofilament axonal transport that is induced by glutamate (Stevenson et al., 2009).

In ALS patients, Riluzole is thought to act mainly as an anti excitotoxicity agent, inhibiting excessive glutamate release from synaptic terminals. This property of Riluzole

is thought to compensate the abnormal glutamate metabolism, which has been reported in some ALS patients. Additionally, the following studies support this anti excitotoxic role of Riluzole in ALS:

- The glial glutamate transporter EAA2 is lost in rat models for SOD1-associated ALS (Howland et al., 2002).
- In ALS patients the activity of glutamate transporter GLT-1 is decreased in spinal cord and motor cortex (Rothstein et al., 1992).
- Protein expression of EAA2 is reduced in the motor cortex of ALS patients (Rothstein et al., 1995).

Glutamate transporters are in charge or recycling glutamate released from neurons into glia, where they are transformed into glutamine and transported back to neurons for glutamate neurotransmitter formation. The lost or deficiency of these transporters leads to an increase in extracellular glutamate, which translates into exitotoxicity. This exitotoxicity may include influx of calcium into cells, extensive depolarizations, or other events that may lead to cell death. However, the exact mechanism by which Riluzole may regulate glutamate release is still unknown. Additionally, this particular toxic event does not appear to represent an extremely important factor in ALS as the benefits of Riluzole are small or non-existent. Thus, further drugs are still to be discovered to obtain a better treatment to slow or stop ALS development.

Other Tested Drugs

A wide number of drugs have been tested in human clinical trials. However, none of these drugs has proven to be beneficial in slowing or curing the disease. A list with tested drugs that have gone into clinical trials is represented in Table 1-5.

Table 1-5. Past clinical trials conducted in ALS patients.

Drug	Mechanism of action	References
3,4-diaminopyridine	Slow potassium channel blocker	(Aisen et al., 1996;Aisen et al., 1995)
Omigapil (TCH346)	Anti-apoptotic, binds glyceraldehyde 3-phosphate deshydrogenase	(Miller et al., 2007a)
Brain-derived neurotrophic factor	Growth factor	(Beck et al., 2005;Kalra et al., 2003)
Branched chain amino acids	Increase muscle protein synthesis	(Tandan et al., 1996;Testa et al., 1989)
Celecoxib	Cyclooxigenase-2 inhibitor	(Cudkowicz et al., 2006)
Ciliary neurotrophic factor	Motor neuron survival	(Al-Chalabi et al., 2003)
Creatine monohydrate	Dietary supplement thought to increase muscle strength	(Groeneveld et al., 2003)
Cyclophosphamide	Immunosuppressor	(Gourie-Devi et al., 1997;Brown, Jr. et al., 1986;Smith et al., 1994)
Dextromethorphan	NMDA-glutamate receptor antagonist	(Gredal et al., 1997)
Gabapentin	Glutamate blocker	(Miller et al., 2001)
Ganglioside	Immunomodulator	(Harrington et al., 1984)
Glutathione	Antioxidant	(Chio et al., 1998)
Insulin-like growth factor 1	Growth factor	(Sorenson et al., 2008)
Interferon beta-1a	Immunomodulator	(Beghi et al., 2000)
Lamotrigine	Glutamate release inhibitor	(Ryberg et al., 2003)
Minocycline	Anti-apoptotic and anti-inflammatory	(Gordon et al., 2007)
N-acetylcysteine	Anti-oxidant	(Vyth et al., 1996)
Nimodipine	Calcium channel blocker	(Miller et al., 1996a)
Pentoxifylline	Anti-apoptotic	(Levin et al., 2006;Meininger et al., 2006)
Physostigmine	Interfere with acetylcholine metabolism	(Norris et al., 1993)
Selegiline	Anti-oxidant	(Lange et al., 1998;Mazzini et al., 1994)
Thyrotropin-releasing hormone	Trophic factor	(Munsat et al., 1992)
Topiramate	Inhibitor of excitatory neurotransmission	(Cudkowicz et al., 2003)
Total lymphoid irradiation	Immunosuppressor	(Drachman et al., 1994)
Verapamil	Calcium channel blocker	(Miller et al., 1996b)
Vitamin E	Anti-oxidant	(Graf et al., 2005)
Xaliproden	Serotonin receptor agonist	(Meininger et al., 2004)

Future Clinical Trials

Several other drugs are currently being tested in humans or will be in the near future. A list of some of them is indicated in Table 1-6. Note that some trials have been completed, but the studies have not been published yet.

Table 1-6. Ongoing clinical trials for the treatment of ALS.

Drug	Mechanism of action	Status[1]
Antisense oligonucleaotide SOD1	Reduce SOD1 protein expression levels	Unknown
Arimoclomol	Upregulate heat shock proteins	Phase II/III trial (NCT00706147) ongoing
Ceftriaxone	Anti-oxidant	Phase III trial (NCT00349622) ongoing
Coenzyme-Q-10	Cofactor in mitochondrial electron transfer	Phase II trial (NCT00243932) completed
Diaphragm conditioning	Diaphragm conditioning with electrodes	Trial (NCT00420719) ongoing
MCI-186	Anti-oxidant	Phase III trial (NTC00330681) completed
Memantine	NMDA-glutamate receptor antagonist	Phase II trial (NCT00353665) completed
ONO-2506	Cyclooxigenase-2 (COX2) inhibitor	Phase II trial (NCT00403204) completed,
R(+)pramipexol	Anti-oxidant	Phase II trial (NCT00600873) ongoing
Talampanel	Regulator of AMPA receptors	Phase II trial (NCT00696332) ongoing
TRO19622	Mitochondrial transition pore inhibitor	Phase II/III trial (NCT00868166) not yet started

[1]Information on the status of the trials were obtained from the U. S. National Institute of Health web page of clinical trials (Clinical Trials, 2009). The identifier number was also included.

CHAPTER 2
LACK OF TOXICITY IN A NOVEL VARIANT OF HUMAN SOD1 HARBORING ALS-ASSOCIATED AND EXPERIMENTAL MUTATIONS IN METAL-BINDING RESIDUES[1]

Introduction

Mutations in SOD1 are found in familial cases of ALS. The enzymatic function of SOD1 is to catalyze the antioxidant reaction that converts superoxide radicals ($O_2^{\cdot-}$) into hydrogen peroxide (H_2O_2) and oxygen (O_2) (McCord and Fridovich, 1969). The mature homodimeric SOD1 protein binds copper and zinc ions, which are either required for activity or provides structural stability, respectively (Forman and Fridovich, 1973;Elam et al., 2003;Potter et al., 2007). Histidines coordinate the copper (H46, H48, H63, and H120) and zinc (H63, H71, H80) binding sites. Additionally, an aspartate also forms part of the zinc site (D83). The two monomers in the SOD1 homodimer are maintained together by non-covalent forces, while an intramolecular disulfide bond between cysteines 57 and 146 confers structural stability within each monomer. Two cysteines, C6 and C111, are free in the normally folded protein, and it is known that C111 can bind metals aberrantly (Watanabe et al., 2007).

Of the 148 described SOD1 disease-causing mutations, a small portion presents defects in metal binding capability, thus affecting the overall enzymatic activity of SOD1. However, many other SOD1 mutant proteins do not present significant alterations in metal binding or activity. *In vitro* studies suggest that normally folded SOD1 can misfold and aggregate upon the loss of metals and/or reduction of its intramolecular disulfide bond (Chattopadhyay et al., 2008;Oztug Durer et al., 2009). Further studies demonstrate that metal binding prevents the dissociation of the intramolecular disulfide

[1] The work presented here is a manuscript in preparation that will be submitted shortly for publication.

bond, suggesting that metal binding is required to prevent aggregation (Tiwari and Hayward, 2005).

Transgenic mouse models expressing experimental SOD1 mutant proteins that abolish either two (H46R/H48Q) or four (H46R/H48Q/H63G/H120G or QUAD) of the normal copper binding sites develop ALS, which is accompanied by the characteristic formation of detergent-insoluble SOD1 aggregates (Wang et al., 2002b;Wang et al., 2003). These mice are unable to bind copper in their catalytic site; thus, copper binding does not appear to be required for aggregation. However, additional studies suggest that copper can interact with free cysteines, in particular cysteine 111 (Watanabe et al., 2007). Thus, the present models may not account for aberrant copper binding that might have a role in aggregation. On the other hand, nothing is known about the role that zinc binding might have in aggregation of mutant SOD1 and/or disease.

In order to study the implication of SOD1 metal binding and aggregation and its role in disease, we created mice expressing a SOD1 protein (termed SODMD) in which we abolished all possible sites of metal binding (H43, H46, H48, H63, H71, H80, H120), including the two free cysteine amino acids, C6 and C111. SOD1 in these mice is incapable of binding either copper or zinc in its normal binding site, or aberrantly in any of the reported possible sites. We analyzed the effect of the SODMD protein in mice, and we extensively characterized the ability of SODMD and SODMD protein variants to sediment in non-ionic detergent.

Materials and Methods

A list of materials used can be found in Appendix B. Methodology used for the work presented in this chapter is described in “Chapter 2 Methods” of Appendix C.

Results

To study the role of metal binding in aggregation and disease, we created transgenic mice expressing the metal deficient genomic SOD1 variant, or SODMD. Mutations within this protein comprise all histidine residues known to be involved in metal binding (H43, H46, H48, H63, H71, H80, H120) and the two free cysteines that do not form part of the intramolecular disulfide bond (C6 and C111). A diagram with the SODMD mutations is represented in Figure. 2-1.

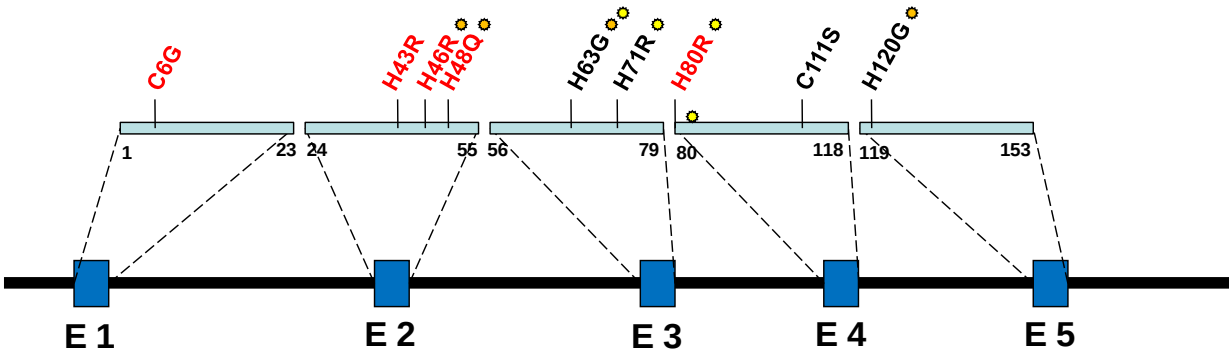

Figure 2-1. Schematic representation of genomic SODMD. The SODMD DNA is mutated within each of the 5 exons (E) that compose SOD1. Red denotes single amino acid substitutions in the SOD1 protein that have been previously found in different human ALS patients. The rest of the single point mutations in black are experimental mutations. Orange circles indicate copper binding sites, while yellow circles indicate zinc binding sites. The first and last amino acid locations of each exon are also indicated in the figure.

A total of seven founder lines were initially produced, from which we selected the two highest expressing lines (I-32 and U-69 lines) to be maintained (Figure 2-2). The rest of the lines produced very low or non-detectable levels of transgene. To determine whether the expression of mutant SOD1 in either line of these MD mice was sufficiently high to induce disease, we compared the levels of transgene mRNA in our highest expressor SODMD mice (line U-69) to several of our lines of mutant SOD1 mice (Figure 2-3). For each line of mice we used 3 mice of similar ages, however even for the same

SOD1 mutation, mRNA levels were different among each animal (especially note the error bars for G93A and L126Z line 44 in Figure 2-3B). Mice expressing the mutations G93A or double histidine (H46R/H48Q) mutants present the highest mRNA levels, followed by WT L76, G37R and two different lines of L126Z SOD1 mice (L44 and L45). A line of L126Z mice (L171) expresses the lowest levels of transgene of all lines analyzed here. Compared to L126Z L171, the SODMD line U-69 mice present equivalent levels of mRNA (Figures 2-3A and 2-3B). These data suggest that mice harboring the SODMD mutations present expression levels that are in the lower range of transgene expression but that are high enough to manifest an ALS phenotype if the mutation is pathogenic.

The L126Z line 171 mice represent the level of expression that is approximately at the threshold required to induce disease. The SODMD I-32 line expresses mRNA SOD1 at lower levels than L126Z line 171, whereas the SODMD U-69 line expresses at levels equivalent to L126Z line 171 mice (see Figure 2-2). Thus, for the purpose of these studies we used exclusively animals from the SODMD U-69 line of mice.

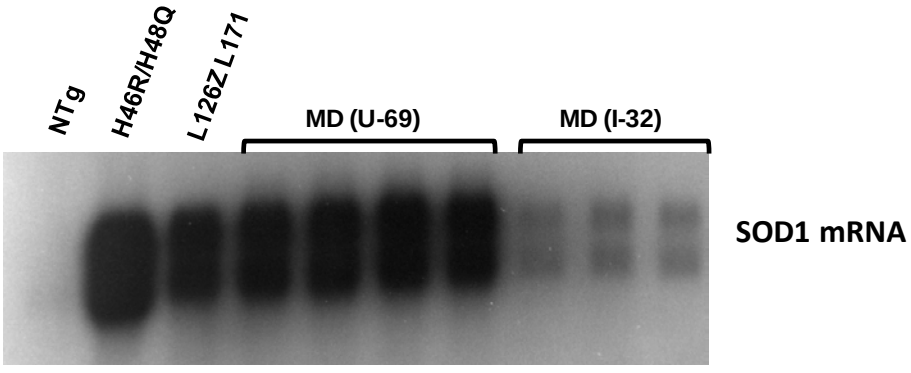

Figure 2-2. Northern blot showing the two lines of SODMD mice with the best expression levels. The SODMD mRNA levels are compared to those of L126Z L171 which expresses SOD1 at very low levels. This blot was exposed for a long time in order to allow visualization of mRNA levels of the SODMD line I-32. This figure was kindly provided by Ms. Hilda Slunt-Brown.

We have previously observed that the levels of transgene expression relate to disease development in our SOD1 mice. For example, there are cases in which transgenic mice homozygous for a certain mutant SOD1 protein present a shorter lifespan than heterozygous mice for the same SOD1 mutation. However, it is uncertain to whether we can predict when animals develop ALS based on data from different transgenic lines, expressing different mutant SOD1 proteins at different levels. Thus, to determine whether we can use mouse lifespan data available from other SOD1 lines to estimate when SODMD mice should get sick, we collected data on age of disease endstage –defined by weakness followed by paralysis of the hindlimbs- in different transgenic lines. When we compared such data with transgene expression levels, we observed that mice presenting a shorter lifespan, present higher levels of transgene expression (Figure 2-3B). For example, G93A mice express the highest levels and develop paralysis at the earliest times, around 5 months old (159.1 ± 4.03 days), while the lowest expression mice (L126Z L171) do not develop symptoms till they are 13 months old (400.3 ± 22.56 days; Figure 2-3B).

Additionally, correlation analysis demonstrates that the age of onset of symptoms in transgenic mice is dependent on the level of mutant SOD1 mRNA (Figure 2-4). Thus, we can expect to observe onset of symptoms in our SODMD mice (line U-69) at similar ages than L126Z L171 mice (around 1 year old), since both lines of mice present similar levels of SOD1 mRNA.

In our experience the mRNA levels of SOD1 in mouse spinal cords predict the levels of SOD1 protein present in spinal cords. Furthermore, we have shown that mRNA levels are similar for SODMD and L126Z L171 mice. Thus, to corroborate that protein

levels are also similar between these two lines of mice, we evaluated total protein levels for mice belonging to each line. Our data demonstrate that protein levels in the low expressor L126Z L171 mice do not differ from that of SODMD mice (Figure 2-5). These results, together with our analysis in mRNA SOD1 levels, assure us that disease development in SODMD would be predicted to occur around the age of onset of L126Z L171 mice if the SODMD protein is a disease causing variant.

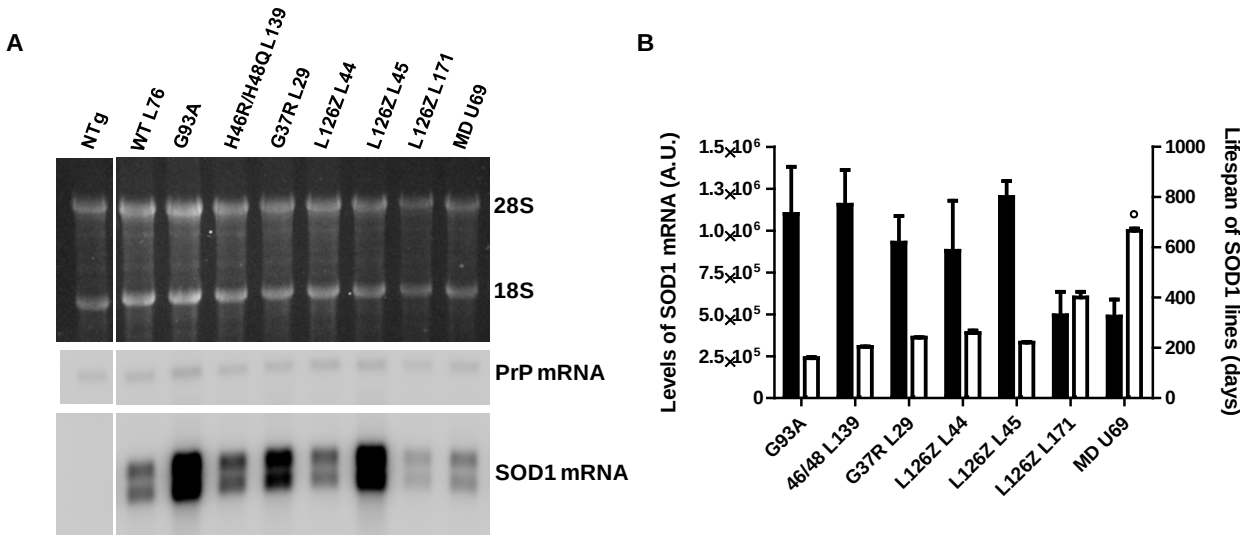

Figure 2-3. Lower mRNA SOD1 expression levels predict a longer lifespan in mice. A) Northern blot showing the mRNA levels of different lines of mice expressing WT or mutant SOD1 proteins. The 28S and 18S RNAs and PrP mRNA are also shown, the latter serving as a loading control. For these experiments Ms. Hilda Slunt-Brown contributed with invaluable help. B) Quantifications of mRNA levels of three different Northern blots are represented by the black bars. White bars indicate the survival times of SOD1 lines calculated from data collected in our lab from animals harvested during more than 4 years. The “o” symbol over the survival time of SODMD line indicates that the data bar represents mean of lifespan to sacrifice, however no disease symptoms were noted in these mice.

In terms of disease development, we did not observe apparent weakness, or paralysis in SODMD mice. At ages closer to 2 years of age (normal lifespan of laboratory mice), animals were monitored daily. In some cases some SODMD mice were found dead, but no symptoms of weakness or paralysis were noted.

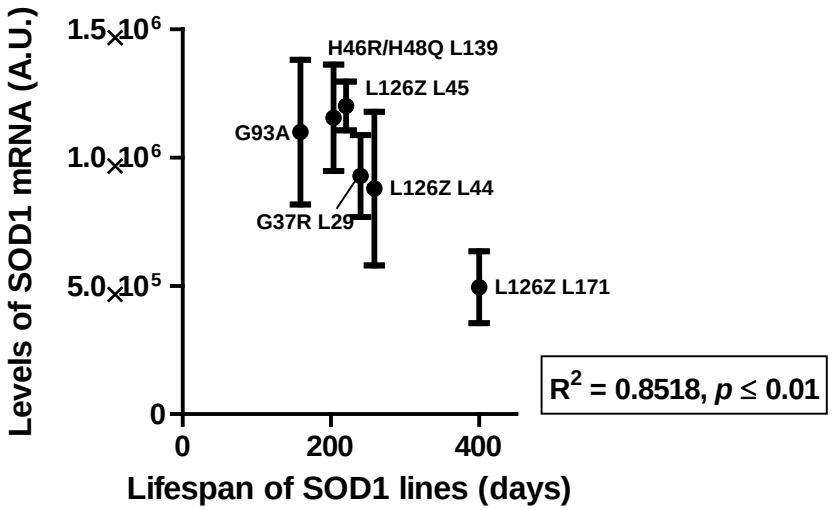

Figure 2-4. The levels of SOD1 mRNA and lifespan of SOD1 mice statistically correlate. The levels of SOD1 mRNA were obtained from experiments performed in Figure 2-3. Data on the lifespan of SOD1 mice were collected from a minimum of 10 mice per paralyzed line of mice that were harvested along the course of 4 years.

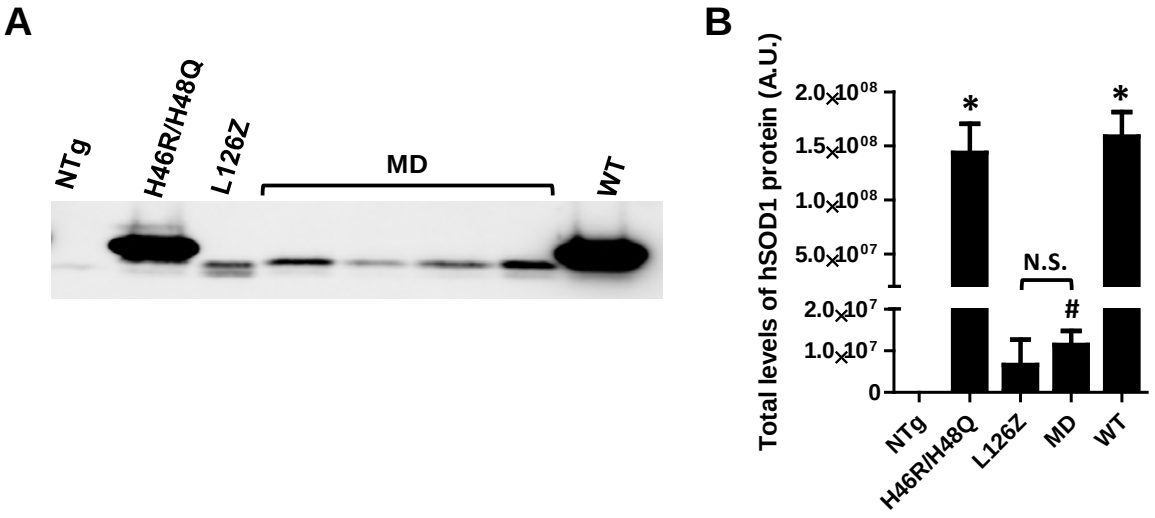

Figure 2-5. Protein levels in the spinal cord of SODMD mice resemble those of L126Z SOD1 mice. A) Western blot of total protein levels of indicated mouse lines, which has been incubated with an antibody that recognizes human SOD1. Note that L126Z truncation mutant and SODMD (MD in figures) run faster than other SOD1 proteins in SDS-PAGE gels. B) Quantification of the total human SOD1 protein levels. Non-significant differences are found between MD and symptomatic L126Z. NTg denotes Non-transgenic animals, N.S. non-significant differences, $^{*}p \leq 0.05$, $^{\#}p. \leq 0.005$.

The levels of transgene expression are an important feature to cause ALS symptoms in transgenic animal models. For example, mice expressing the G37R mutation under the mouse prion promoter do not develop motor neuron disease unless levels of expression are raised through homozygosity (Wang et al., 2005b). Similar examples occur for a line of mice that express the D90A mutant of SOD1 (Jonsson et al., 2006b). Thus, we self-crossed SODMD mice with the intention to increase SOD1 protein levels through homozygosity, which should translate into a more rapid disease development. A total of 20 mice were positive for the SODMD transgene, from which approximately 33% should be homozygous. However, we did not observe disease symptoms in any of these mice suggesting that the SODMD variant is not pathogenic.

Analysis of the SODMD mice for their ability to form detergent-insoluble aggregates demonstrates that the lack of disease development correlates with the inability of the mutant protein to aggregate (Figure 2-6). SODMD proteins appear to turnover rapidly as the SOD1 protein levels in the detergent-soluble fraction (S1) are low. The L126Z truncation SOD1 mutant protein is also rapidly degraded, but when mice become symptomatic the aggregated protein is not so easily degraded and accumulates in the cell as detergent-insoluble aggregates (P2), which can be detected by our biochemical assay (Figure 2-6). However, we did not observe detectable levels of SODMD protein in the insoluble or P2 fraction. Thus, SODMD mice lack of pathology that includes mutant SOD1 aggregates that are detergent-insoluble and centrifuge at high speed.

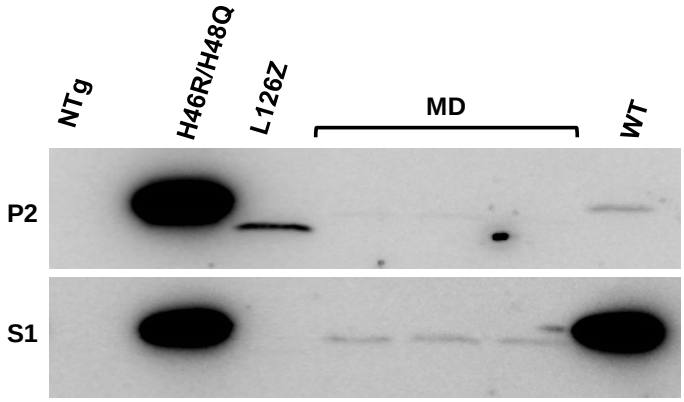

Figure 2-6. Spinal cord of old SODMD mice do not contain aggregated SOD1 proteins. Immunoblot of detergent-insoluble (P2) and detergent-soluble (S1) protein fractions of mouse spinal cords, blotted with a human SOD1 antibody. NTg: non-transgenic mice. Note that the L126Z protein although is quite unstable in spinal cords (undetectable in S1), it is aggregated at detectable levels while SODMD protein does not aggregate.

We further analyzed old SODMD mice histologically, in order to look for pathological features that may occur at time points previous to significant accumulations of detergent-insoluble aggregates. Axon denervation is an earlier disease feature observed in G93A SOD1 transgenic mice (Fischer et al., 2004). A consequence of this phenomenon is axon demyelination. Thus, we performed myelin staining in sciatic nerve sections from non-transgenic, symptomatic H46R/H48Q, and old SODMD mice (Figure 2-7). In transverse sciatic nerve sections, only symptomatic H46R/H48Q mice appear to present a lower number of myelinated axons as well as smaller diameter of myelin sheaths, while SODMD sections did not differ from those of non-transgenic mice (Figures 2-7A to 2-7I). Similarly, longitudinal sciatic nerve sections showed reduced number of myelinated fibers in sick H46R/H48Q SOD1 mice, while old SODMD mice appear largely normal (Figures 2-7J to 2-7R). Thus, SODMD mice do not present any obvious abnormality in myelinated fibers at old ages.

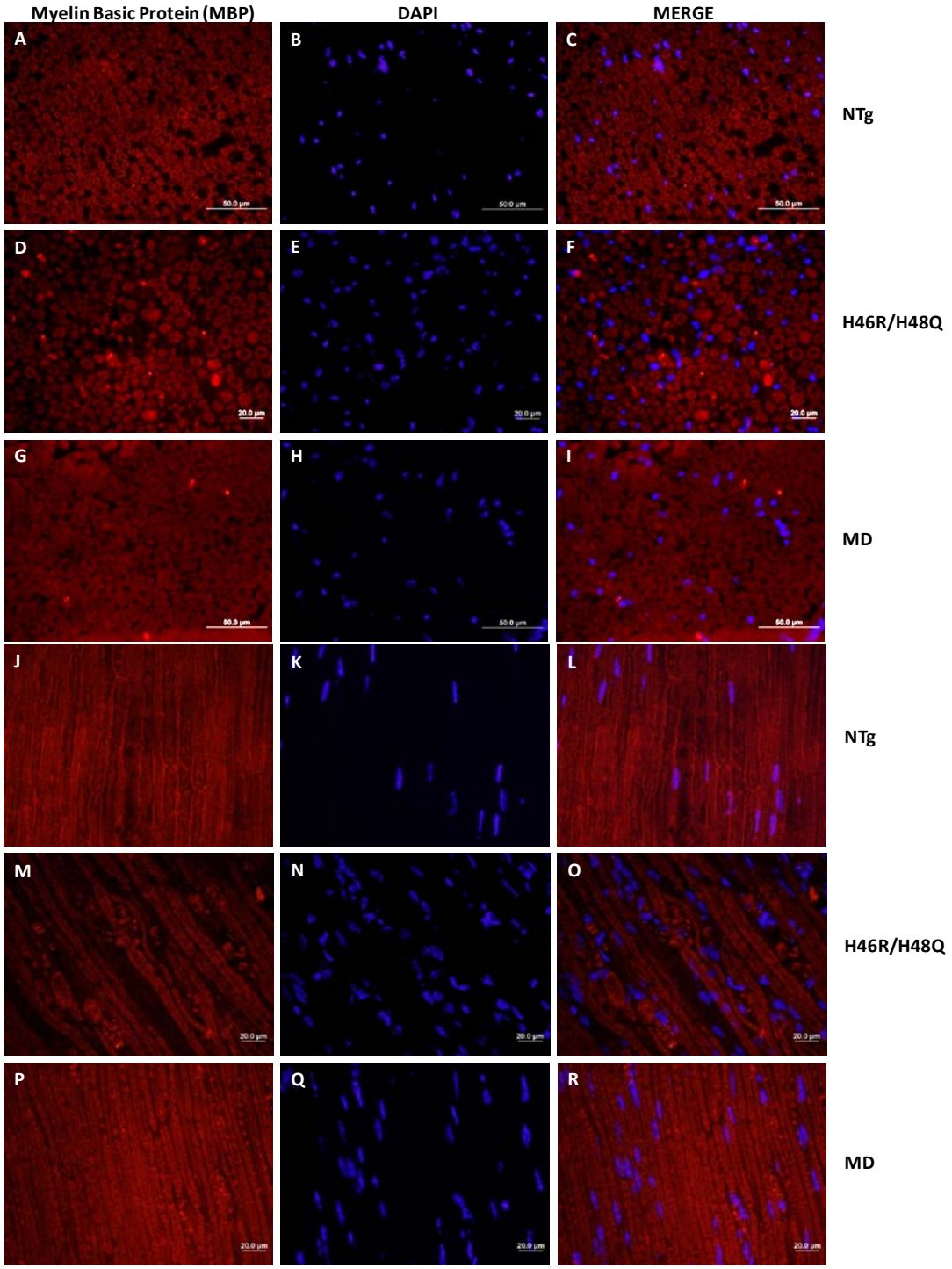

Figure 2-7. Myelin abnormalities are observed in symptomatic H46R/H48Q SOD1 mice, while SODMD do not differ from non-transgenic (NTg) mice. A-R) Transverse (A-L) or longitudinal (M-R) sciatic nerve sections stained with myelin basic protein. Nuclear stain was applied with secondary antibody incubations. All micrographs were taken with a 40x objective, bars 50 (A-C, G-I) or 20 (D-F, M-R) µm.

Gliosis is another of the earliest characterized abnormalities in SOD1 transgenic mice (Feeney et al., 2001). To determine whether SODMD mice present some early abnormalities at times prior the accumulation of detergent-insoluble SOD1 species or the appearance of hindlimb weakness/paralysis, we performed studies on histological sections to look for reduced number of motor neurons, reduced axonal fibers and GFAP immunoreactivity. Haemmatoxylin and eosin staining indicates reduced presence of motor neurons in the ventral horn of symptomatic H46R/H48Q SOD1 mice (Figures 2-8A and 2-8B). However, the number of motor neurons in WT and SODMD mice do not qualitative differ (Figures 2-8A and 2-8C). Silver impregnation stains axonal fibers. Here, silver staining demonstrates that symptomatic mice expressing mutant SOD1 proteins present reduced number of fibers compared to WT or SODMD mice (Figures 2-8D to 2-8F). Additionally, GFAP immunoreactivity is only markedly increased in our ssymptomatic H46R/H48Q SOD1 control (Figures 2-8G to 2-8I). Thus, our histological analysis demonstrate that mice expressing the SODMD variant are healthy and do not present any of the characteristic mutant SOD1 pathology.

One question that might rise from these studies is to whether the 10 single-point mutations in the SODMD protein alter too many of the SOD1 protein features. In order to address this issue we created a SODMD cDNA version for its analysis in cell culture. In cell culture, SODMD is more highly expressed such that it is clearly detected in the detergent-soluble S1 fractions (Figure 2-9A, lower panel); however, as in our mouse model, we do not observe significant accumulation of protein that sediment in the detergent-insoluble fraction (P2), not different from WT at 48 hours following transfection (Figures 2-9A and 2-9B). This data confirms the inability of this mutant to

aggregate. One feature of the WT SOD1 protein in cell culture is its ability to slow the aggregation rates of normally aggregating SOD1 mutants and to ultimately co-aggregate with mutant proteins at longer, 48 hour transfection intervals (Prudencio et al., 2009a). Taking advantage of the more rapid migrating ability of SODMD protein in SDS-PAGE gels, compared to most SOD1 mutant proteins, we co-transfected SODMD with the highly aggregating mutant G93A for 24 hours. At 24 hour transfection intervals, SODMD protein slows aggregation of G93A SOD1 proteins maintaining both proteins in the detergent-soluble S1 fraction (Figure 2-9C). This significant reduction in aggregation of G93A is not different from the effect of WT on G93A aggregation (Figure 2-9D). Thus, SODMD mutant proteins conserve features of the WT SOD1 protein, suggesting that the amino acid substitutions in SODMD may only alter the metal binding capability and activity of SOD1.

Transgenic mice co-expressing mutant SOD1 and WT protein at very high level present an accelerated disease phenotype. In particular, WT SOD1 is able to trigger disease and aggregation in asymptomatic mice that expresses the A4V SOD1 mutation at very low levels (Deng et al., 2006). In an attempt to induce disease development in SODMD mice, we mated these mice to those expressing WT SOD1 at very high levels. Out of 59 animals that resulted from such mating, 11 presented both, WT and SODMD transgenes. The youngest doubly transgenic WT/SODMD mice were born in April 2008, and at the time of writing (October 2009) such animals do not present visible disease symptoms. Additionally, co-expression of WT and SODMD does not induce aggregation in cell culture (Figure 2-10). These data support the notion of SODMD as being the first

experimental SOD1 mutant protein that is unable to cause an ALS phenotype in transgenic mice.

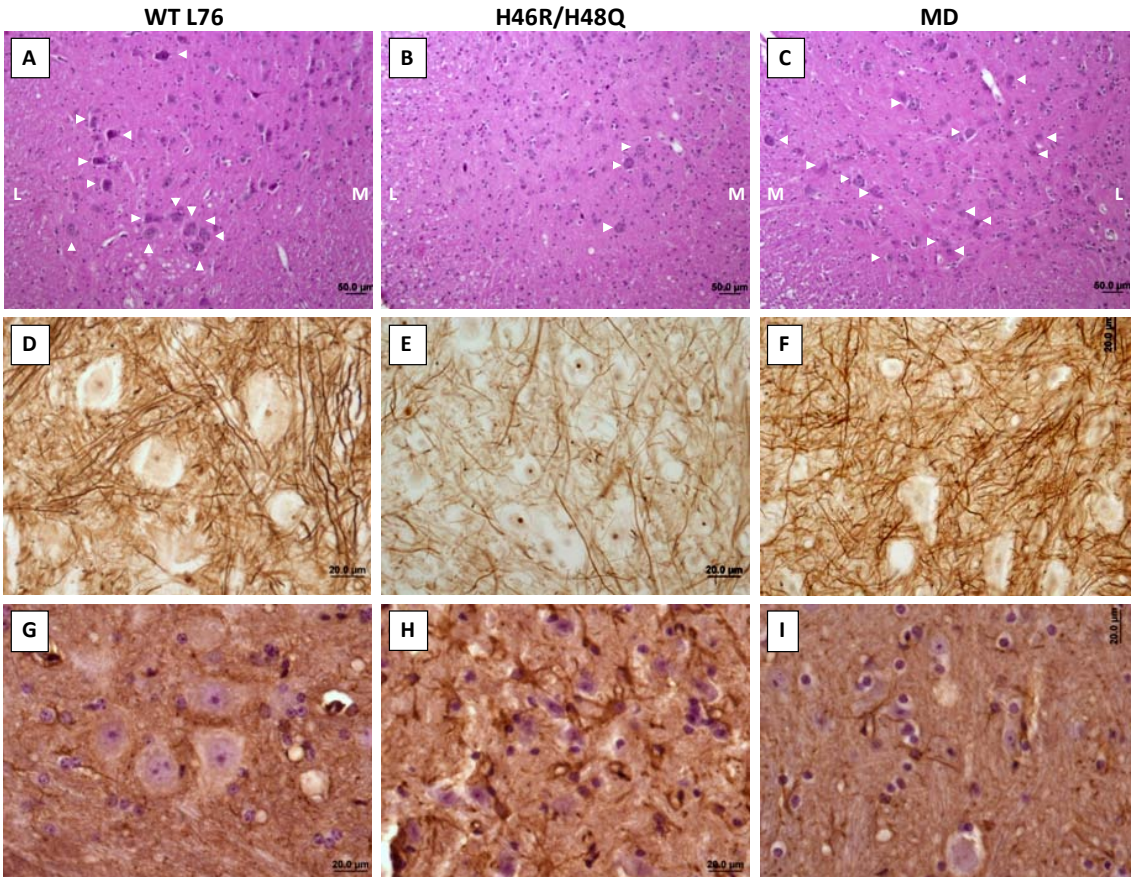

Figure 2-8. SODMD mice, like WT SOD1 mice, lack of any ALS-like pathology.A-I) Mice expressing WT (A, D, G), H46R/H48Q (B, E, H) and MD (C, F, I) SOD1 proteins were characterized histologically to determine the appearance of any kind of pathology. A-C) Heammatoxylin and eosin stain on paraffin embedded sections at low power (10x) demonstrates significant lower number of motor neurons (indicated by white arrowheads) in the ventral horn of symptomatic H46R/H48Q (B) mice than in WT (A) SOD1 mice. No differences are noted between WT (A) and SODMD (C) mice. M: medial portion of the spinal cord, L: lateral portion of the spinal cord. D-F) Silver staining of paraffin embedded sections indicates the existence of a very low number of axons in symptomatic H46R/H48Q (E), while WT (D) and MD (F) spinal cords appear largely normal. Note that all staining was done simultaneously for all sections, thus the low fiber staining in H46R/H48Q mice is due to a lower number of axons present. G-I) GFAP-DAB staining on paraffin embedded sections demonstrate none or low GFAP immunoreactivity in WT (G) and MD (I) mice, while strong gliosis is apparent in symptomatic H46R/H48Q (H) SOD1 mice. Bar represents 50 µm in A-C and 20 µm in D-I, and are located in the ventral portion of the spinal cord.

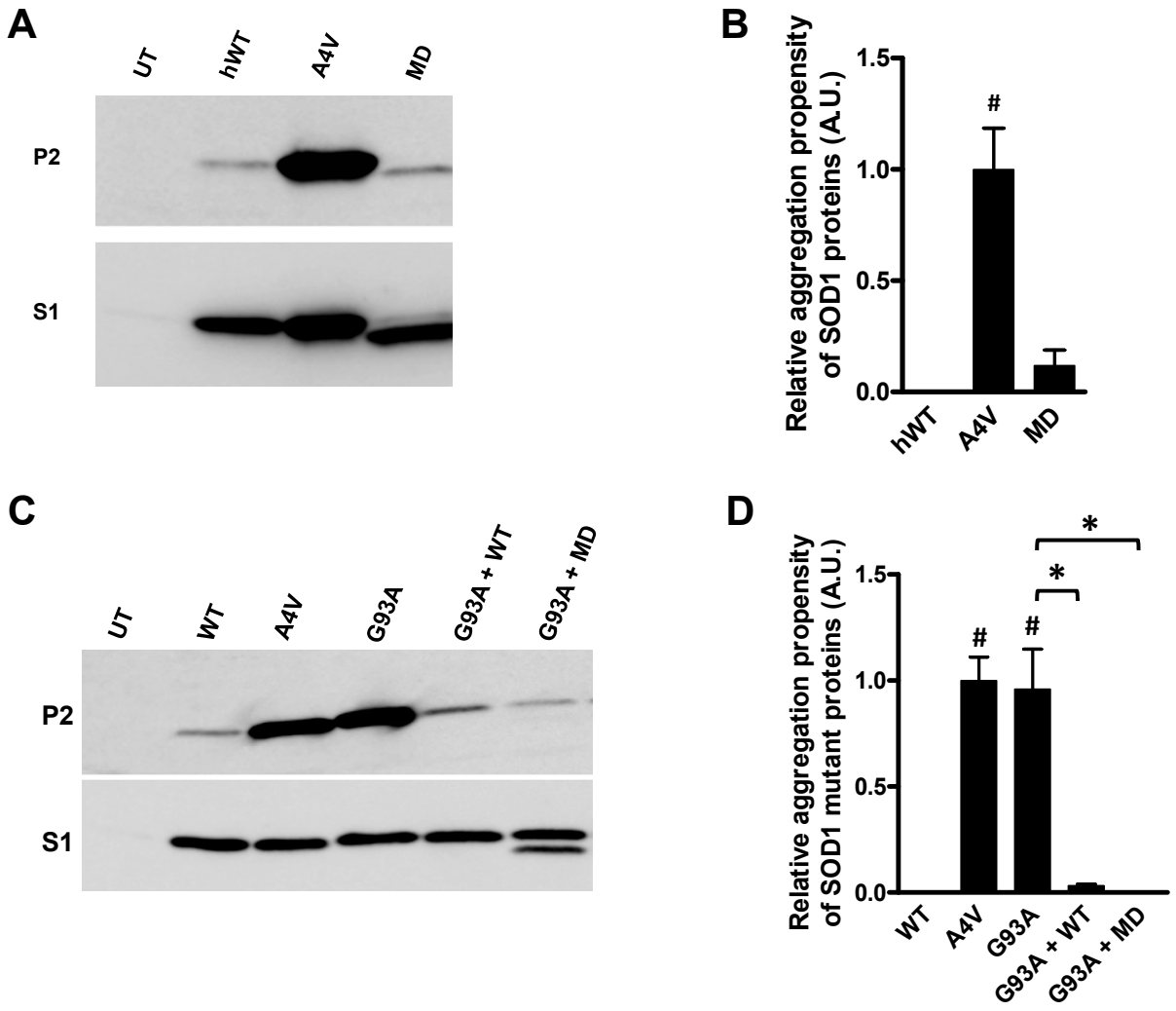

Figure 2-9. The non-aggregating SODMD cDNA variant present WT-like features in cell culture. A, C) Immunoblots of detergent-insoluble (P2) and detergent-soluble (S1) protein fractions of HEK293FT cells expressing the indicated SOD1 constructs for 48 (A) or 24 (C) hours. UT denotes untransfected cells. B, D) Quantification of the relative aggregation propensity of the indicated SOD1 mutant proteins expressed in cells for 48 hours (B) or of G93A in the 24 hour co-transfection experiment (D). Paired student *t*-tests were performed to compare the aggregation propensities of the mutant proteins with the aggregation propensity of the human WT SOD1 protein (hWT or WT), or of indicated pairs. Non-significant differences were found between human WT and SODMD; and SODMD protein significantly slows aggregate accumulation of G93A SOD1. $^{*}p \leq 0.05$, $^{\#}p \leq 0.005$.

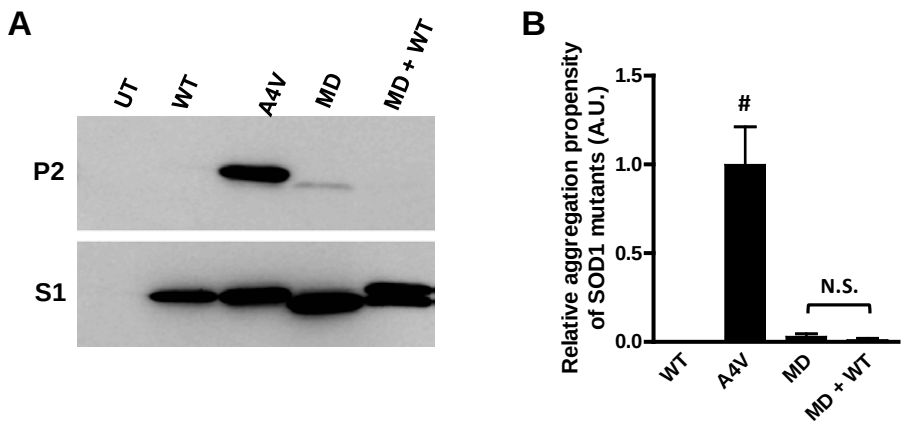

Figure 2-10. SODMD co-expression with WT SOD1 does not induce a rapid increase in aggregation of either protein after 48 hour transfection interval in cell culture. A) Immunoblot of detergent-insoluble (P2) and soluble (S1) fractions of indicated SOD1 proteins expressed in HEK293FT cells for 48 hours. B) Quantification of the aggregation propensity indicates than in this set of transfections, only A4V SOD1 is able to significantly aggregate. Paired student *t*-tests were performed to evaluate significant differences in terms of aggregation propensity. $^{\#}p \leq 0.005$, N.S.: non-significant differences.

Discussion

We present here an experimental SOD1 mutation that eliminates metal binding sites in SOD1 and is unable to cause ALS in animal models. In addition to the lack of disease development, mice overexpressing the SODMD mutant protein are healthy, without any obvious pathology or protein aggregation during their lifespan. Attempts to increase the pathogenicity of this protein by raising the levels of mutant protein or the overall protein levels by overexpressing human WT SOD1, have not been translated into development of an ALS-like disease. Thus, SODMD mice present a human SOD1 protein that is non-toxic. Further understanding of this protein may help us to determine requirements for the SOD1 protein to induce disease.

SODMD Mice and Expression Levels

Mice overexpressing experimental SOD1 mutations that abolish copper binding (H46R/H48Q, Quad) have been shown to present the ability to aggregate and produce

the toxicity observed with disease associated variants (Wang et al., 2002b;Wang et al., 2003). The metal deficient SODMD mice however, do not develop ALS-like symptoms of hindlimb paralysis. We carefully analyzed expression levels on different lines of mice expressing mutant SOD1 and found correlations between mRNA levels and onset of symptoms. The expression levels of the SODMD variant were in the lower end of expression but they were not different from those of L126Z L171 mice, which develop disease at 1 year of age. Additionally the levels of mutant protein in SODMD and L126Z L171 were quite similar. Thus, we are confident that SODMD mice express protein above the normal threshold to induce disease. In addition we crossed transgenic SODMD mice to obtain homozygous SODMD mice. From a total of 20 animals, 6 should be homozygous mice with higher levels of expression. None of these 20 mice developed disease symptoms or pathology, which should have been obvious at earlier time points than heterozygous mice since they have a higher dose of mutant protein. Therefore, the SODMD protein lacks of the toxicity inherent of other SOD1 mutant proteins.

SODMD Protein Does Not Produce ALS-Like Pathology

The lack of toxicity in SODMD mice is reflected by the absence of detergent-insoluble SOD1 aggregates. In recent studies we have demonstrated that the formation of aggregates of mutant SOD1 in mice are a late event (Karch et al., 2009), and earlier abnormalities are known to occur previous to aggregate formation (Wong et al., 1995;Kennel et al., 1996;Borchelt et al., 1998;Watanabe et al., 2001;Fischer et al., 2004;Hegedus et al., 2007). However, we did not observe any other pathology that might occur at earlier stages in mice generated from SODMD x SODMD cross. In particular, we found no significant changes in myelination, fiber or motor neuron

numbers, or gliosis. Additionally, SODMD does not possess even a mild toxic property that could be enhanced by co-overexpressing it with WT SOD1. Thus, we are convinced that SODMD is a non-toxic variant of mutant SOD1.

Metal Binding, Aggregation and Disease

Relating metal binding to disease is a difficult endeavor, since our animals also lack of the aggregate pathology. Eliminating the copper ligands does not abolish aggregation in cell culture or animal models. The binding of zinc is known to confer structural stability, thus abolishing zinc binding could in theory increase the potential of the protein to misfold and aggregate. Rather it seems that the inability of SODMD to aggregate may be related to its lack of pathogenicity. A different explanation would be that metal binding plays a role in disease. From our studies we cannot discard that, however, that metals or aberrant SOD1 activity plays a role in the disease.

The inability of SODMD to aggregate could be linked to the presence of an amino acid substitution in cysteine 111 to a serine (C111S). This particular cysteine in position 111 has recently shown to play an important role in aggregation, and substitution to a serine does not make WT SOD1 to aggregate (Karch and Borchelt, 2008;Prudencio et al., 2009a). More importantly, C111S reduces aggregation rates in combination with other aggregation prone proteins. Thus, it is likely that the lack of aggregating ability of SODMD might come from this particular mutation. Further studies should then be focused on obtaining an SODMD variant that lack of same metal binding sites but is able to aggregate. In this way we would be able to assess whether the lack of toxicity of SODMD comes from the lack of metal binding or the inability of the protein to aggregate.

SODMD and WT SOD1

The 10 point mutations in SODMD make it different from WT in terms of SOD1 activity, since this cannot take place without metal binding. As an experimental mutation, there exists the possibility that this mutant SOD1 protein may be very different from other disease causing mutations. However, when possible, we mutated the metal binding sites to known ALS causing mutations and other models that abolish 2 or 4 of the copper binding sites develop a typical ALS phenotype in mice. Additionally, we were able to determine some similarities of SODMD with the normal WT SOD1 protein. SODMD retains the WT SOD1 feature of modulating aggregation, and as WT it lacks of the inherent propensity to aggregate. Additionally, the double or quadruple histidine experimental mutants develop and ALS-like disease in transgenic mice (Wang et al., 2002b;Wang et al., 2003). Thus, we believe that SODMD retains SOD1 properties suitable to study the role of aggregation and metal binding in ALS.

Previous studies have shown the ability of WT to slow aggregation in cell culture when expressed for short periods of time (Prudencio et al., 2009a). At longer intervals co-aggregation of mutant and WT proteins is a clear event (Deng et al., 2006;Prudencio et al., 2009a). In our hands, SODMD exhibits the aggregation blocking property of WT SOD1 and thus appears to be able to interact with mutant SOD1 in some manner that is similar to WT SOD1. However SODMD lacks the property of WT that allows it to ultimately co-aggregate with mutant SOD1 proteins when incubation periods are extended to 48 hours. The mutated amino acids within SODMD may inhibit intramolecular contacts that would make the protein self-aggregating. Thus, the SODMD protein could be seen as a way to further study likely hotspots within the amino acid sequence that makes SOD1 prone to misfold and aggregate.

Toxicity in ALS

As mentioned earlier, aggregation is a late event and does not appear to determine onset in transgenic mice. However, it is possible that more soluble aggregated species, termed oligomers, may be the initiators of disease. Detergent-insoluble SOD1 aggregates become detectable as symptoms develop rapidly (Karch et al., 2009). Thus, lack of toxicity from SODMD protein could be due to the inability of this mutant to aggregate. However, we are unable to isolate more soluble protein species of SODMD since this protein is quite unstable. Thus far, this work demonstrates the SODMD protein as another example that supports aggregation as a present feature in symptomatic ALS mice.

Future Directions

Future studies should be in part focus on obtaining an SODMD variant that can aggregate and still be able to not bind metals. Previous studies have shown the importance of cysteines 6 and 111 in modulating aggregation of mutant SOD1 (Karch and Borchelt, 2008). While SOD1 with C6G and C111S mutations (also present in SODMD variant) do not produce an aggregating mutant SOD1 protein, modifications in these 2 cysteines can make SOD1 more prone to aggregate. Thus, as part of future work, we performed modifications in the cDNA sequence of SODMD to produce a protein that is able to aggregate. Restoring either cysteine 6 or 111 allows for this mutant SOD1 protein to aggregate, and when both are restored the overall aggregation levels are much higher (Figure 2-11). Mutations in SODMD changing amino acid 111 (in MD a serine) to tyrosine (C111Y is a disease causing mutation) produces a protein which aggregation propensity is similar to that of restoring cysteine 111 in SODMD, and when restoring cysteine 6 in S111Y SODMD variant, the aggregation propensity is even

higher than when restoring both cysteines in SODMD (Figure 2-11). The C6F SOD1 variant is a highly aggregating mutant, and a phenylalanine in amino acid 6 (another disease mutation) of SODMD produces a highly aggregating protein. Thus, we created a SODMD variant with amino acid 6 mutated to a phenylalanine, and cysteine 111 changed to a tyrosine (C6F, H43R, H46R, H48Q, H63G, H71R, H80R, C111Y, H120G) that produces a protein that highly aggregates (see MD-G6F-S111Y in Figure 2-11). In conclusion, it is possible to have a SOD1 protein with all mutations that abolish metal binding but can aggregate.

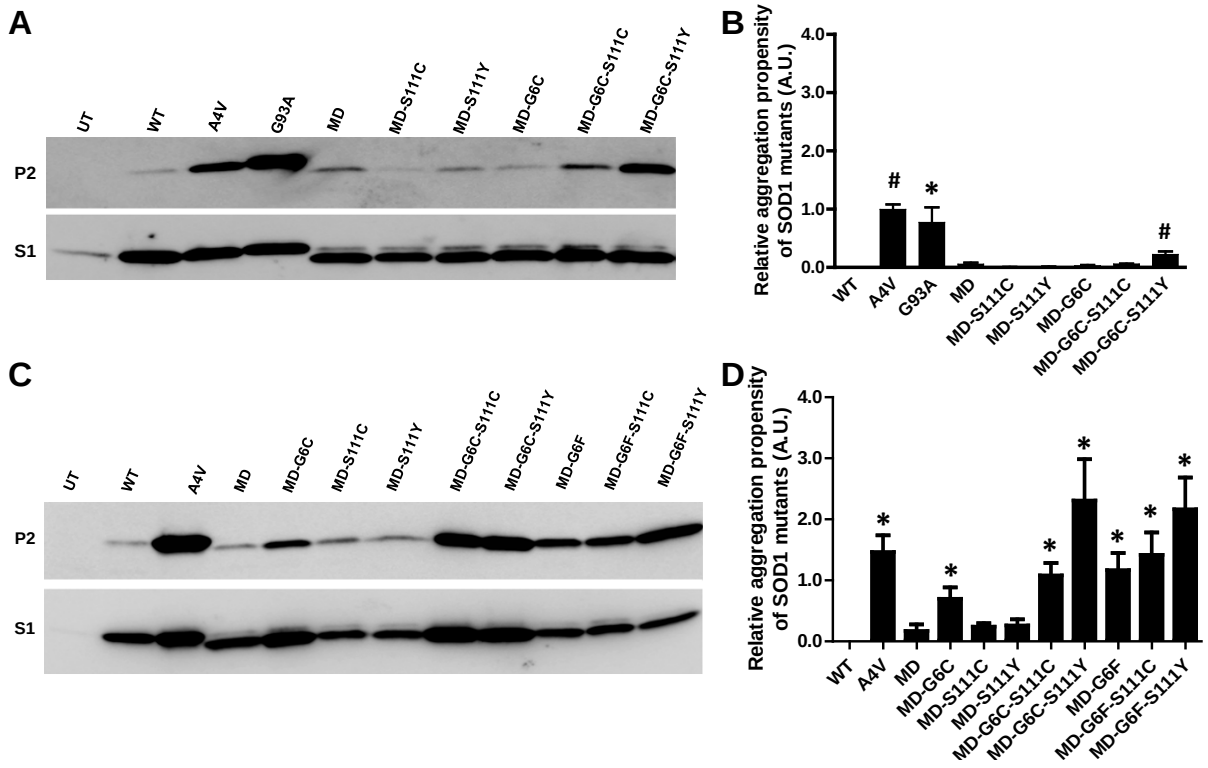

Figure 2-11. Mutations in amino acids 6 and 111 in the context of SODMD mutations can reestablish the aggregation propensity of SODMD. HEK293FT were transfected for 24 (A, B) or 48 (C, D) hours. A, C) Immunoblots of detergent-extracted HEK293FT expressing the indicated SOD1 proteins. B, D) Quantification of the aggregation propensity at 24 (B) or 48 (D) hours following transfection. All values are normalized to the aggregation propensity of A4V at 24 hours (set to 1). Paired student *t*-tests were performed to compare aggregation propensities of SOD1 proteins to SODMD. $^{*}p \leq 0.05$, $^{\#}p \leq 0.005$.

A better understanding of metals on disease would be better addressed through the creation of mice with these two different cysteine modifications. Based on our preliminary cell culture studies, metal binding does not seem to be required for aggregation. We suggest that it might be possible to create mice that express a version of SOD1 that lacks all of the known metal binding sites and which develop typical ALS.

CHAPTER 3
VARIATION IN AGGREGATION PROPENSITIES AMONG ALS-ASSOCIATED VARIANTS OF SOD1: CORRELATION TO HUMAN DISEASE[1]

Introduction

In all mouse models, the manifestation of disease symptoms is accompanied by the accumulation of detergent-insoluble aggregated forms of mutant SOD1 (Watanabe et al., 2001;Jonsson et al., 2004;Wang et al., 2005a;Wang et al., 2005b;Deng et al., 2006;Jonsson et al., 2006a). Additionally in Chapter 2 we have seen that an experimental SOD1 mutation unable to form such aggregates cannot cause disease in animal models. In human SOD1-associated ALS there is similar evidence that mutant SOD1 aggregation is a pathologic feature (Watanabe et al., 2001). Thus, there seems to be a clear correlation between the presence of detergent-insoluble aggregated forms of mutant SOD1 in spinal cords and disease (Wang et al., 2003). Importantly, aggregated forms of mutant SOD1 that display similar properties of detergent-insolubility can be produced in cultured cells (Wang et al., 2003;Wang et al., 2006;Karch and Borchelt, 2008;Prudencio et al., 2009a), representing an efficient system to screen and study aggregation of ALS mutants.

It is well established that specific mutations are associated with disease of short or long clinical course (Cudkowicz et al., 1997). Examples of short disease course include the A4V mutation (< 2 years) (Rosen et al., 1994) whereas mutations such as H46R are associated with a long disease course (> 10 years) (Arisato et al., 2003). A recent study used a variety of biophysical data to calculate aggregation rates for

[1]The work presented in this chapter has been published in *Human Molecular Genetics* 18(17):3217-26 (2009). Mercedes Prudencio and David R. Borchelt designed the experiments, Mercedes Prudencio, Peter M. Andersen and David R. Borchelt interpreted the data and wrote the manuscript. Mercedes Prudencio carried out all the experiments, Peter M. Andersen provided all the clinical data, and P. John Hart provided cDNA SOD1 constructs in a yeast expression vector.

different ALS mutants, suggesting that aggregation of mutant protein could be a key factor in disease progression (Wang et al., 2008). Here, we have used our cell culture model to analyze a total of 33 SOD1-associated ALS mutations in regards to their ability to form detergent-insoluble aggregates, including different mutation substitutions at the same codon. By this approach, we assess how measured aggregation potentials relate to known biophysical/biochemical characteristics, and examine whether aggregation propensities correlate to disease features in human ALS patients.

Materials and Methods

A list of materials used can be found in Appendix B. Methodology used for the work presented in this chapter is described in “Chapter 3 Methods” of Appendix C.

Results

Our first analysis of 21 mutant SOD1 proteins demonstrated that all are capable of forming detergent-insoluble SOD1 aggregates in cells within 24 hours (Figure 3-1A). Quantification of the aggregation propensity, which is calculated from the ratio of insoluble to soluble forms of mutant SOD1 in cell lysates, of different mutations showed significant differences from WT SOD1. To normalize data from different experiments, we chose to use the aggregation propensity of A4V SOD1 as the reference mutant (assigning 1 to the mean aggregation propensity of A4V, as previously described (Wang et al., 2003;Prudencio et al., 2009a)). Most mutations analyzed in Figure 3-1A are of similar, or higher, aggregation propensity to A4V. Several mutants possessed aggregation propensities lower than that of A4V (G93D, E21G, E21K and G41D). In cases in which more than one mutation occurred at a particular codon, we often observed significantly different levels of aggregated protein for each individual mutation at one position (Figure 3-1B); examples include A4V *vs*. T ($p = 0.0168$); G93A *vs*. D ($p =$

0.0078), R (p = 0.0056), or S (p = 0.0222); G41D *vs*. S (p = 0.0128); and E100G *vs*. K (p = 0.0160). We also observed examples in which different amino acid changes at the same position did not differentially affect the aggregation propensity: G93A *vs*. C (p = 0.4934), V (p = 0.111); V14G *vs*. M (p = 0.8766); and E21G *vs*. K (p = 0.6213). Further studies on additional SOD1 mutants involving different amino acid substitutions at the same site demonstrated very high variability in aggregation propensities. Mutation of D101 or V148 to G induced the formation of very high levels of detergent-insoluble proteins in 24 hours (Figure 3-1C). D101G together with E100K SOD1 represent the most aggregation prone proteins analyzed so far. However, D101N and V148I showed dramatically lower aggregation levels at 24 hours, not different from that of WT SOD1 (Figure 3-1D).

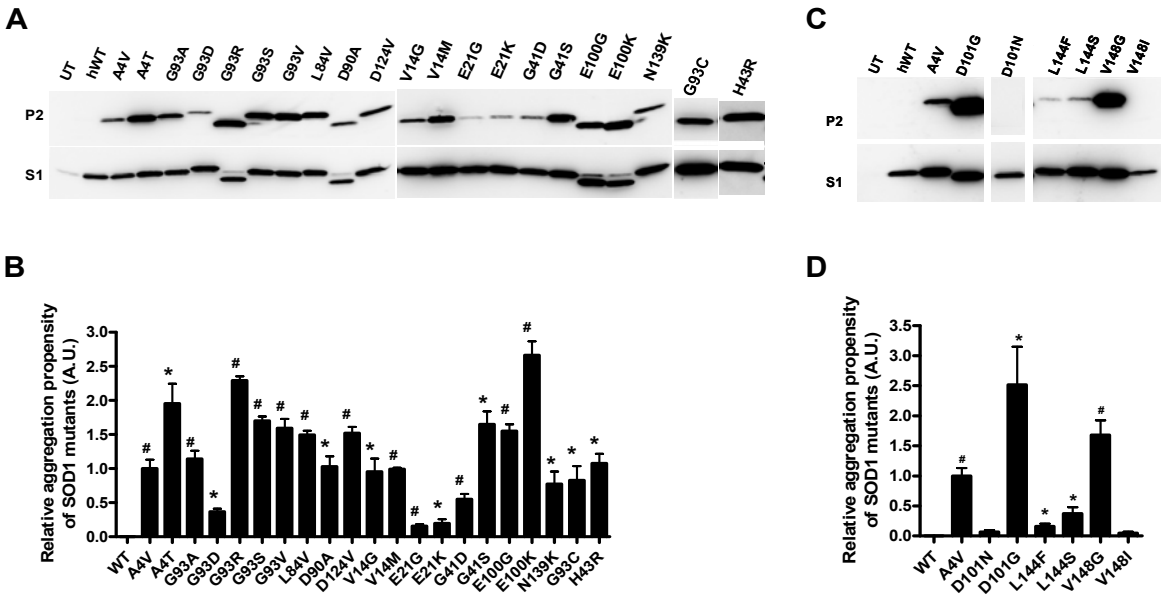

Figure 3-1. Large variability in aggregation among SOD1-associated ALS mutants. A, C) Immunoblots of detergent insoluble (P2) and soluble fractions (S1) of HEK293FT cells transfected with WT or mutant SOD1 for 24 hours. UT: untransfected cells. B, D) Quantification of the relative aggregation propensity of WT and mutant SOD1 proteins as described in Methods. Bars represent mean ± SEM of 3 or more independent transfection experiments. $^{*}p \leq 0.05$, $^{\#}p \leq 0.001$.

In addition to the slow aggregating D101N and V148I mutants, we found other mutations in which aggregation levels resemble those of WT SOD1 protein at 24 hours (Figure 3-2A). Compared to G37R, which to date had been representative of mutants with low potentials to aggregate (Wang et al., 2006), the H80R, D101N, D125H, E133ΔE, S134N and V148I SOD1 mutants showed even lower potentials to aggregate (Figure 3-2A, upper panels). In all cases, high levels of soluble SOD1 protein were detected for each of the mutants indicating robust protein expression (Figure 3-2A, lower panels). Quantification and statistical analysis indicated that the aggregation propensity of these mutants in 24 hours was not different from WT SOD1 (Figure 3-2B). Thus, we identified, for the first time, SOD1 mutants that do not readily form detergent-insoluble aggregates in 24 hours, showing a similar behavior to WT SOD1. These findings were initially viewed as an indication that aggregation, a priori, may not be necessarily linked to disease development. In order to more rigorously determine whether these mutants remain completely soluble, we extended the interval between transfection and harvest of the cells from 24 to 48 hours. With longer incubation times all mutants formed detectable levels of detergent-insoluble protein, while WT SOD1 still remained completely soluble (Figure 3-2C). At 48 hours, the aggregation propensities of these mutants were significantly different from WT SOD1 (Figure 3-2D).

Although we have shown that all SOD1 mutants ultimately form detergent-insoluble aggregates, we were somewhat surprised to find several mutants that were not statistically different from WT SOD1 in regards to aggregate formation in 24 hours. To further explore how closely these mutants resemble WT SOD1, we employed a technique of co-transfection in which the mutants with low aggregation potential were

co-transfected with mutants of high aggregation potential. We have previously shown that WT SOD1 is able to slow aggregation of SOD1 mutant proteins in cell culture, while co-expression of two highly aggregation prone mutants does not interfere with aggregate formation (Prudencio et al., 2009a). Similar to WT SOD1, co-transfection of H80R, D101N, D125H, E133ΔE, or S134N with G85R SOD1 reduced considerably the amount of detergent-insoluble G85R protein present in cells 24 hours after transfection (Figure 3-3A). Similar results were obtained with V148I SOD1 (data not shown). The aggregation propensity of G85R was quantified revealing that these WT-like mutants reduced significantly the aggregation of G85R; no longer different from WT SOD1 (Figure 3-3B). Notably, when we extended the post-transfection incubation period to 48 hours, then clear evidence of aggregation of both mutants (for all tested here) was observed (Figure 3-3C). At these longer incubation intervals, WT SOD1 can also be captured into mutant SOD1 aggregates (Prudencio et al., 2009a). These results suggest that the H80R, D101N, D125H, E133ΔE, S134N and V148I SOD1 mutants share two features with WT SOD1: low inherent propensity to aggregate over 24 hours, and the ability to slow the aggregation of mutant SOD1 proteins that exhibit high aggregation rates.

It has been suggested that mutations in SOD1 that decrease the net negative charge of the protein (eliminating negatively charged or introducing positively charged amino acids) causes misfolding and aggregation of mutant SOD1 (Shaw and Valentine, 2007;Sandelin et al., 2007). Many of the ALS associated point mutations in SOD1 reduce the net negative charge of SOD1; however, three ALS mutants would be expected to possess a protein charge more negative than WT SOD1 (Figure 3-4, Table

3-1). Thus, we asked whether differences in protein charge among the ALS mutants may explain the variability in the relative rates of mutant SOD1 aggregation. Some of these changes in protein charge can be observed in mutations occurring at amino acid G93. Although some mutations in G93 do not alter the overall protein charge (Table 3-1), there is a reduction in the negative charge of SOD1 when mutating G93 to R, increasing the aggregation propensity significantly compared to those mutants that do not produce a change in protein charge (G93R *vs.* A, $p = 0.0056$; G93R *vs.* C, $p = 0.0262$; G93R *vs.* S, $p = 0.0012$; G93R *vs.* V, $p = 0.0325$). Additionally, when G93 is mutated to D, which increases the negative charge of SOD1, then the levels of aggregated protein are significantly reduced compared to neutral change mutants (e.g., G93D *vs.* A, $p = 0.0078$). Another example of similar findings is that of mutations at G41, where G41S presented an aggregation propensity higher than that of the more negatively charged G41D ($p = 0.0128$). Additionally, when mutations occur in E100 (E100G, E100K) the resulting mutant proteins present less negative charge than WT SOD1; the E100K mutant shows a more substantial decrease in negative charge and significantly higher aggregation potential as compared to E100G ($p = 0.016$). Overall, these findings support the hypothesis that changes in negative charge may play an important role in modulating aggregation of SOD1. However, this apparent correlation does not apply to all mutants that alter the negative charge of SOD1. A good example is the case of mutations in E21, which can be mutated to either G or K, similar to mutations in E100. Although E21K SOD1 has a higher decrease in negative charge, the aggregation propensity levels of E21G and E21K are not statistically different from each other ($p = 0.6213$), with both being very low (see Figure 3-1). Another example is that of

changes in D101. Decreasing the negative charge of SOD1 by substituting amino acid D101 by either G or N produces mutant proteins in which aggregation levels are either very high (D101G) or very low (D101N). In this case the same magnitude of decrease in negative charge produces a very large variability in aggregation rates (D101G *vs*. D101N, $p = 0.0296$). Additional examples, in which a reduction in the negative charge of SOD1 does not produce dramatic increases in aggregation, are the cases of H80R, D125H, and E133ΔE (Table 3-1).

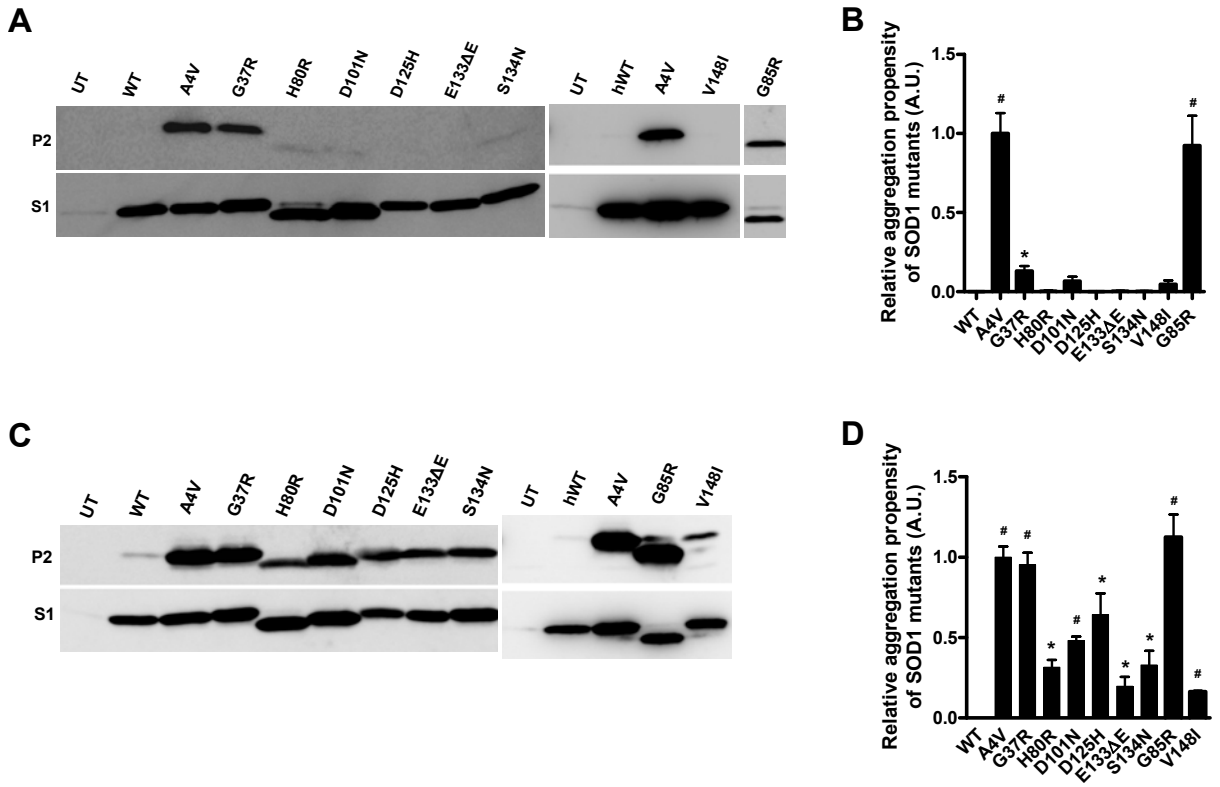

Figure 3-2. Some SOD1-associated ALS mutant proteins aggregate slowly. A, C) Immunoblots of P2 and S1 fractions of HEK293FT cells transfected with human WT (hWT) or mutant SOD1 for 24 (A) or 48 (C) hours. UT: untransfected cells. B, D) Quantification of the relative aggregation propensity of SOD1 proteins at 24 (B) and 48 (D) hours. Bars represent mean ± SEM of 3 or more independent transfection experiments. $^{*}p \leq 0.05$, $^{\#}p \leq 0.001$.

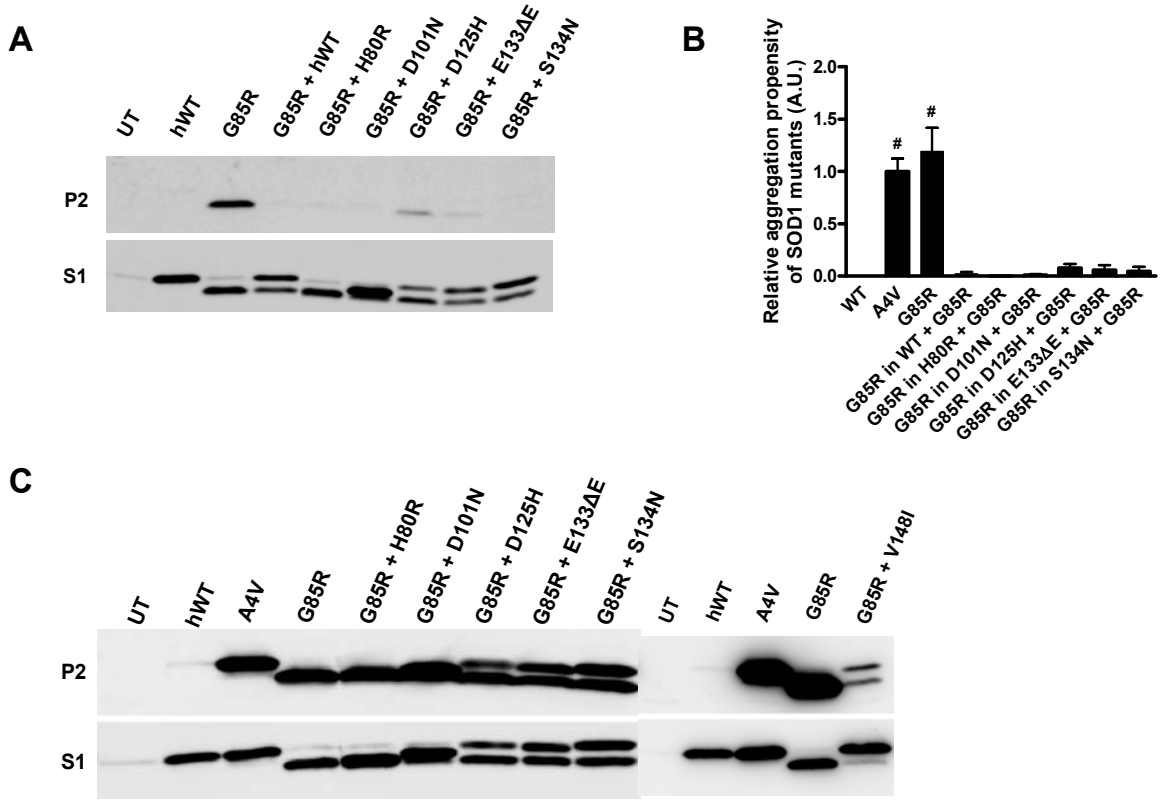

Figure 3-3. Mutants with low aggregation propensity behave like human WT (hWT) SOD1 in terms of modulating aggregation. A, C) Immunoblots of P2 and S1 fractions of cells singly transfected with SOD1 constructs or doubly transfected with G85R and a low aggregating SOD1 variant, for 24 (A) or 48 (C) hours. B) Quantification of the aggregation propensity of G85R when co-transfected for 24 hours. Bars represent mean ± SEM of 3 or more independent transfection experiments. $^{\#}p \leq 0.001$.

Table 3-1. Changes in protein charge do not explain aggregation propensity.

Aggregation propensity (24 h)	No change in net negative charge	Reduce net negative charge	Increase net negative charge
Low	S134N, V148I	H80R, D101N, D125H, E133ΔE	
Moderate	I113T, L144F, L144S, C111Y	E21G, E21K, G37R	G41D, G93D, N139K
High	C6G, G93C, V14G, C6F, V14M, A4V, G93A, L84V, G93V, G41S, V148G, G93S	H43R, G85R, D90A, E100G, D124V	
Extreme	A4T	G93R, E100K, D101G	

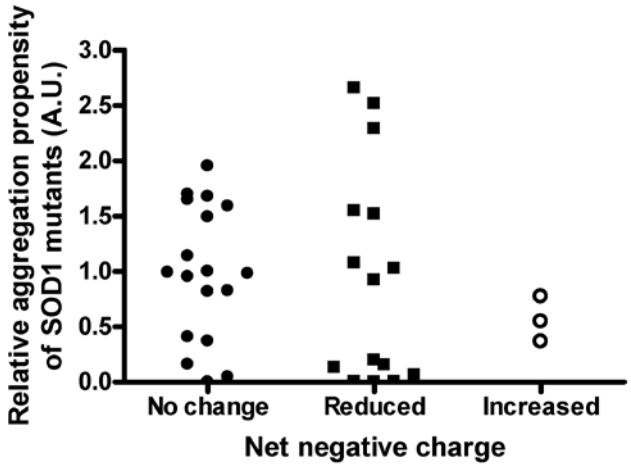

Figure 3-4. Changes in the net negative charge of SOD1 do not predict aggregation propensity. Mutations in SOD1 that reduce, increase, or do not modify the negative charge of SOD1 present aggregation propensity values that range from very low to very high; with no particular group representing mutants of high or low aggregation propensities. Unpaired Student t-tests: no change in charge mutants *vs*. mutants with reduced charge ($p = 0.8711$), no change in charge mutants *vs*. mutants with increased charge ($p = 0.2556$), mutants with reduced charge *vs*. mutants with increased protein charge ($p = 0.5213$).

To further probe as to whether the location of the mutation within the protein may interact with the change in net charge, we graphed measured aggregation propensity as a function of mutation location and charge (Figure 3-5). No obvious pattern emerges to link change in net charge to inherent aggregation propensities.

Further, there were no obvious correlations between changes in net charge and disease onset or duration (Figure 3-6). Thus, our data suggest that the relative aggregation propensity of mutant SOD1 is not inextricably linked to changes in net protein charge.

Additionally we did not find correlations between aggregation propensity and other protein features such as metal binding or protein thermostability (Table 3-2). However, we do not discard the possibility that a combination of two or more protein

characteristics (changes in protein charge, protein stability, metal binding, etc), could explain the different aggregation propensities of ALS mutants.

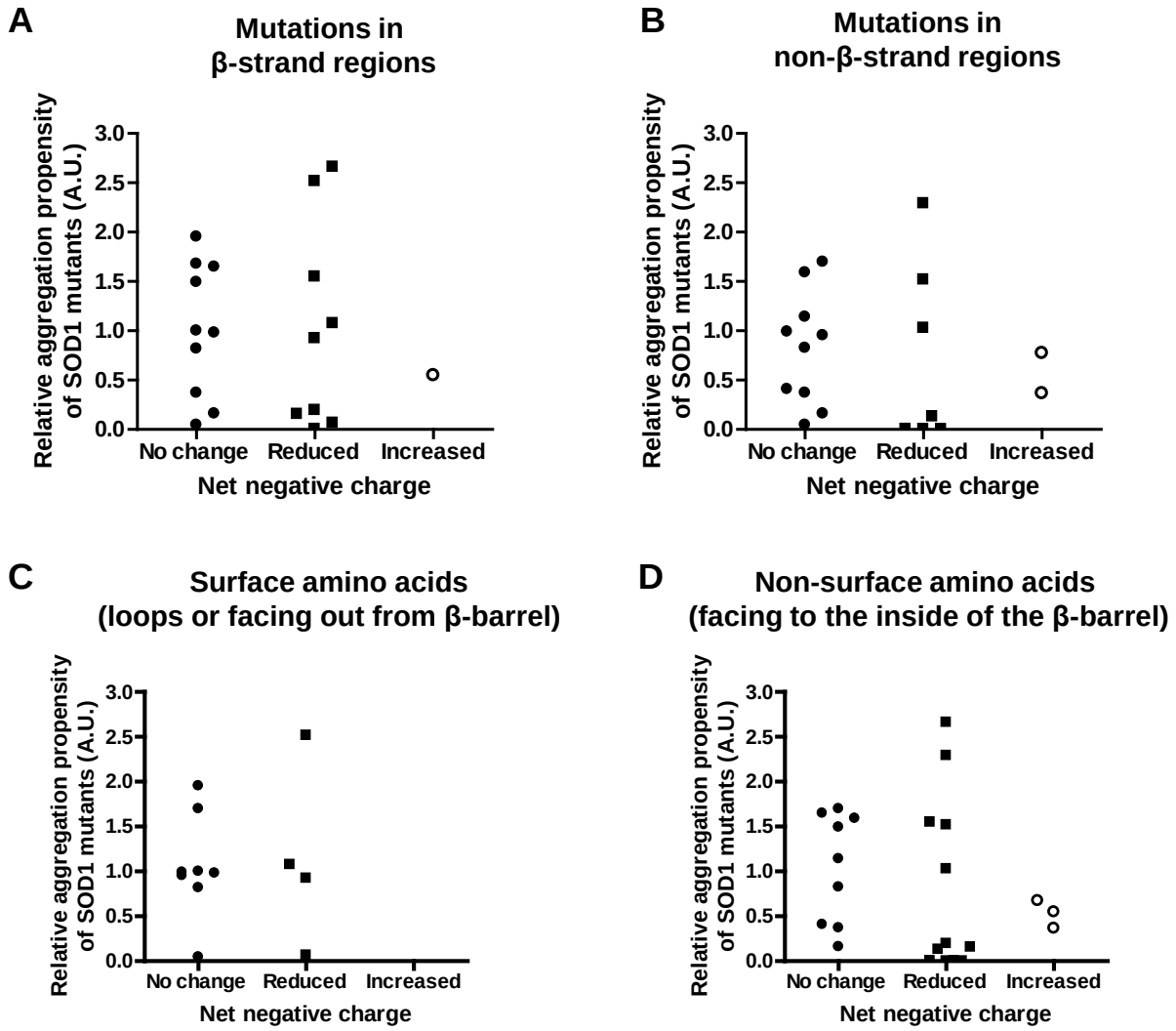

Figure 3-5. Changes in protein charge do not explain differences in aggregation propensity. Representation of changes in net negative charge of SOD1 *vs*. aggregation propensity based on the structural location of the different SOD1-associated ALS mutations: in beta strand (A) *vs*. non-beta strand (B) regions, and by mutations affecting amino acids located on surface of the protein (C) *vs*. amino acids facing the interior of the beta barrel (D). Determination of the structural location of the mutated amino acids was performed using the pdb online structure of G37R SOD1 mutant protein and visualized with PyMOL software (DeLano Scientific, LLC).

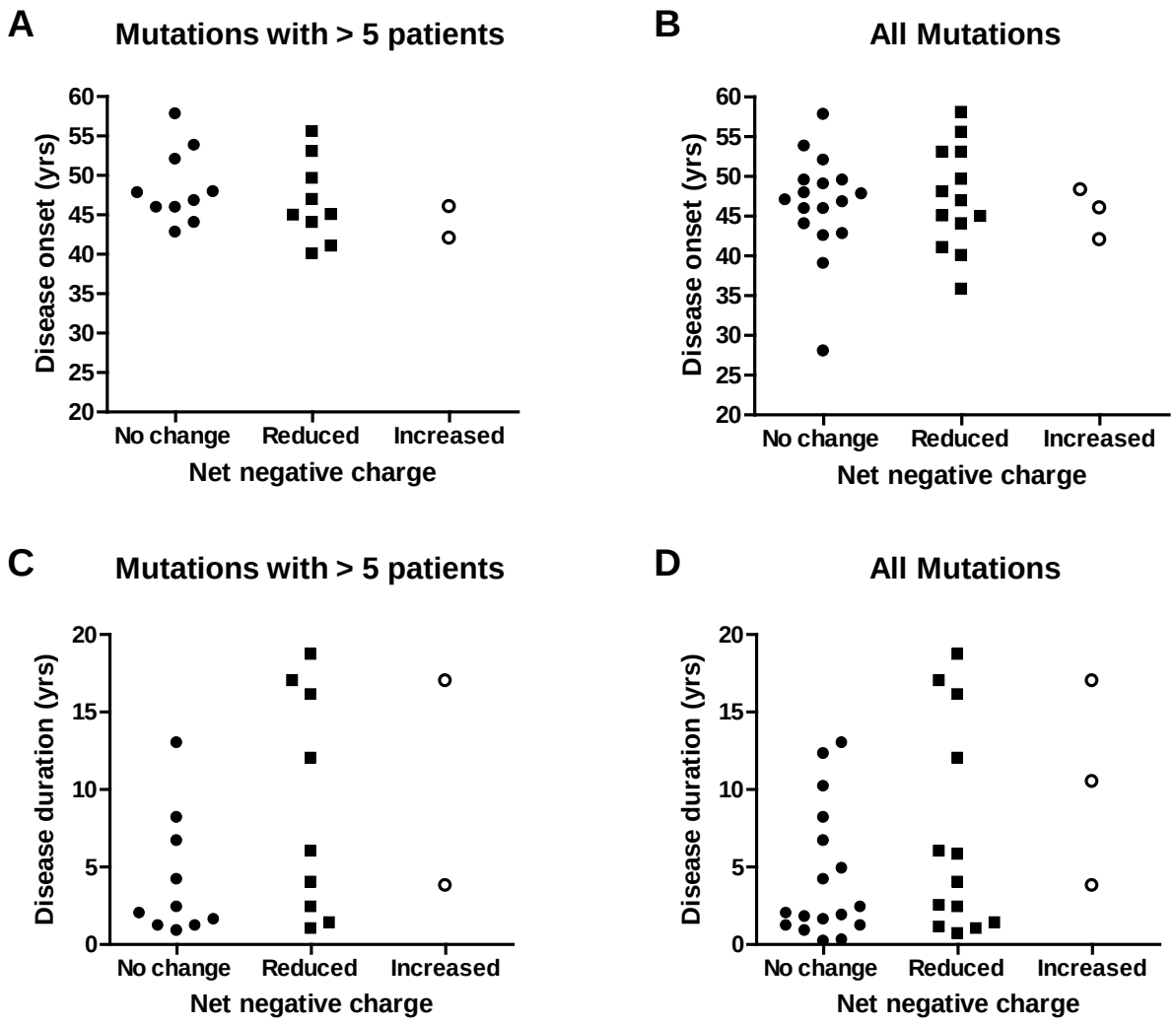

Figure 3-6. Changes in protein charge do not predict onset or survival. Mean aggregation *vs*. mean disease onset (A, B); or *vs*. mean disease duration (C, D) for SOD1 mutations with a significant number of patients (> 5) (A, C), or for all SOD1 mutations with some patient data available (B, D).

Table 3-2. Biophysical and biochemical characteristics of SOD1 variants.

SOD1 variant	Change in negative charge	Aggregation levels at 24 h	Copper binding	Stability	References
WT	No	No	High	High	(Rodriguez et al., 2002;Hayward et al., 2002)
V148I	No	Low	ND	ND	NA
C6F	No	Moderate	ND	Low[a]	(Lindberg et al., 2002)
C6G	No	Moderate	ND	ND	NA
V14G	No	Moderate	ND	ND	NA
V14M	No	Moderate	ND	ND	NA

Table 3-2. Continued.

SOD1 variant	Change in negative charge	Aggregation levels at 24 h	Copper binding	Stability	References
G93C	No	Moderate	High[c]	Low[a]	(Lindberg et al., 2002;Borchelt et al., 1994)
C111Y	No	Moderate	ND	ND	NA
I113T	No	Moderate	High[c]	Low[a]	(Borchelt et al., 1994;Rodriguez et al., 2005;Valentine et al., 2005)
L144F	No	Moderate	High	Low	(Shaw and Valentine, 2007)
L144S	No	Moderate	High	ND	(Valentine et al., 2005)
A4T	No	High	ND	Low[b]	(Nakano et al., 1996)
A4V	No	High	Low	Low[a]	(Borchelt et al., 1994;Rodriguez et al., 2002;Hayward et al., 2002;Lindberg et al., 2002;Rodriguez et al., 2005)
G41S	No	High	High	Low[a]	(Rodriguez et al., 2002;Hayward et al., 2002;Shaw and Valentine, 2007)
L84V	No	High	Low	Low[a]	(Rodriguez et al., 2005;Shaw and Valentine, 2007)
G93A	No	High	High	Low[a]	(Rodriguez et al., 2002;Hayward et al., 2002;Lindberg et al., 2002;Shaw and Valentine, 2007)
G93S	No	High	ND	ND	NA
G93V	No	High	High	ND	(Valentine et al., 2005)
V148G	No	High	High	High	(Valentine et al., 2005)
H80R	Reduced	Low	Low	ND	(Rodriguez et al., 2002;Valentine et al., 2005)
D101N	Reduced	Low	High	High[a]	(Rodriguez et al., 2005;Shaw and Valentine, 2007)
D125H	Reduced	Low	Low	High[a]	(Rodriguez et al., 2002;Hayward et al., 2002;Rodriguez et al., 2005;Shaw and Valentine, 2007;Valentine et al., 2005)
E133ΔE	Reduced	Low	High	Low[a]	(Rodriguez et al., 2002;Hayward et al., 2002)
S134N	Reduced	Low	Low	High[a]	(Rodriguez et al., 2002;Hayward et al., 2002;Rodriguez et al., 2005;Shaw and Valentine, 2007;Valentine et al., 2005),

Table 3-2. Continued.

SOD1 variant	Change in negative charge	Aggregation levels at 24 h	Copper binding	Stability	References
E21G	Reduced	Moderate	ND	ND	NA
E21K	Reduced	Moderate	ND	ND	NA
G37R	Reduced	Moderate	High[c]	Low[a]	(Borchelt et al., 1994;Rodriguez et al., 2005;Shaw and Valentine, 2007)
H46R	Reduced	Moderate	Low	High[a]	(Rodriguez et al., 2002;Rodriguez et al., 2005;Antonyuk et al., 2005;Shaw and Valentine, 2007)
H48Q	Reduced	Moderate	Low	High[a]	(Hayward et al., 2002;Rodriguez et al., 2002;Rodriguez et al., 2005)
H43R	Reduced	High	High	ND	(Valentine et al., 2005)
G85R	Reduced	High	Low	Low[a, b]	(Borchelt et al., 1994;Borchelt et al., 1995;Rodriguez et al., 2002;Valentine et al., 2005)
D90A	Reduced	High	High	Low[a]	(Rodriguez et al., 2002;Lindberg et al., 2002)
E100G	Reduced	High	High	Low[a]	(Rodriguez et al., 2005;Shaw and Valentine, 2007)
D124V	Reduced	High	Low	High[a]	(Rodriguez et al., 2005;Shaw and Valentine, 2007)
G93R	Reduced	Extreme	High	Low[a]	(Rodriguez et al., 2005;Valentine et al., 2005;Shaw and Valentine, 2007)
E100K	Reduced	Extreme	High	High[a]	(Rodriguez et al., 2005;Shaw and Valentine, 2007)
D101G	Reduced	Extreme	High	ND	(Valentine et al., 2005)
G41D	Increased	Moderate	High[c]	Low[b]	(Borchelt et al., 1995;Valentine et al., 2005)
G93D	Increased	Moderate	ND	ND	NA
N139K	Increased	Moderate	High	High[a]	(Rodriguez et al., 2005;Shaw and Valentine, 2007)
L126stop	Increased	Very unstable	Low	Low	NA
L126deltt	Increased	Extreme	Low	Low[b]	(Ratovitski et al., 1999)

[a]Stability calculated of purified apo-protein, or [b]by its half-life when expressed in mammalian cell systems.
[c]Copper binding content high or low based on levels of activity
ND: Not determined
NA: Not available

A recent study, using mathematical models, suggested that the predicted aggregation propensity of SOD1 mutants correlates with disease duration in humans (Wang et al., 2008). Here we used data from our cell culture model to analyze whether our measured aggregation propensity correlates with patient data on disease onset and/or duration. We imposed a filter on the patient data, focusing on cases in which the number of affected individuals with a particular mutation met or exceeded 5 individuals. We chose 5 individuals as the lower limit because it emerged as a natural breakpoint in our data and because this number of patients allows for a more rigorous estimation of reproducibility of observed phenotypes. After filtering our patient data set, we were able to identify 21 different mutations for which we possessed data on an adequate number of patients. The data on aggregation propensities of the different mutants were stratified into 4 categories as explained in Figure 3-7. For the 21 mutations in the patient data sets we analyzed, 2 mutations were categorized as exhibiting extreme aggregation propensity, 12 of the mutations fit criteria for high aggregation propensity, 6 fit criteria as moderate, and one fits criteria for low aggregation propensity (Table 3-3). No obvious correlation between aggregation propensity and age of onset was noted (Figure 3-7). This outcome was expected because the mean age of onset is 45-47 years of age for all SOD1 mutants (Table 3-3).

When we stratified the mutants by the 4 criteria described above and graphed these groups as a function of disease duration, we noted that mutants exhibiting aggregation propensities equivalent to or greater than the A4V mutation largely predicted shorter disease duration in patients (Figure 3-8A). Statistical analysis demonstrated significant differences between the groups of high and moderate

aggregation propensities (unpaired *t* test, $p = 0.0008$). However, inverse correlations do not exist between aggregation propensity and disease duration ($p = 0.1440$, Figure 3-8B), possibly because disease duration in patients with mutations of moderate or low aggregation propensity is less predictable. Still, when we focus on the mutants that show high aggregation propensities, we find that the majority of patients with these mutations exhibit a rapid disease course.

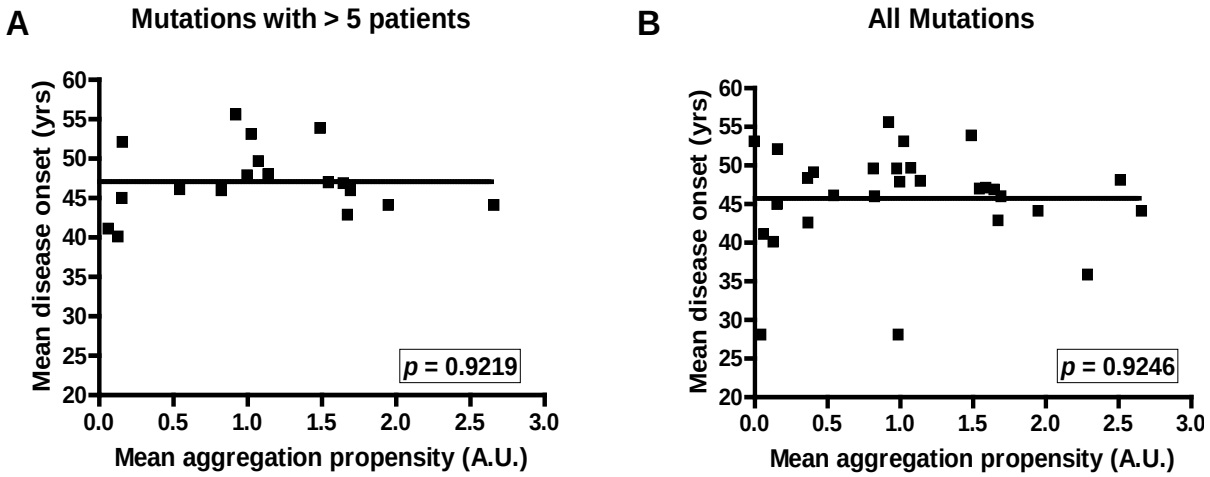

Figure 3-7. Disease onset is not driven by changes in aggregation propensity. SOD1 mutations with a significant number of patients (> 5) (A), or all available compiled data (B) grouped in terms of aggregation propensity: Extreme (produces a level of insoluble mutant protein in 24 hours that is equal to or greater than twice that of A4V SOD1- always set at 1), High (aggregate load is similar to A4V in 24 hours; aggregation propensities range between 0.7 and 1.7), Moderate (aggregate load is detectable but < 0.5 in 24 hours), Slow (no aggregates detected in 24 hours –only visible at 48 hours). No correlation was found between aggregation and age of onset ($p \geq 0.05$). Note that the mean onset for ALS patients with a SOD1 mutation occurs between 45-47 years of age.

Table 3-3. Clinical data ordered by relative aggregation potential values.

Mutation	Aggregates 24 h	Age of onset	Survival time	Penetrance	*N*
L126deltt	Extreme	NA	NA	NA	NA
E100K	**Extreme**	**44.0 ± 6.1**	**12.0 ± 4.1**	**Incomplete**	**16**
D101G^{+}	Extreme	48.0 ± 9.1	2.5 ± 0.4	NA	3
G93R	Extreme	35.8 ± 4.3	5.8 ± 4.5	NA	4
A4T^{+}	**Extreme**	**44.0 ± 11**	**1.2 ± 0.4**	**Incomplete**	**14**
G93S	**High**	**45.9 ± 4.4**	**8.2 ± 4.0**	**Incomplete**	**9**

Table 3-3. Continued.

Mutation	Aggregates 24 h	Age of onset	Survival time	Penetrance	*N*
V148G⁺	**High**	**42.8 ± 10.5**	**2.0 ± 0.9**	**Complete**	**7**
G41S⁺	**High**	**46.8 ± 13.5**	**0.9 ± 0.2**	**Complete**	**8**
L126X‡	**Very unstable**	**42.0**	**3.8**	**Complete**	**14**
G93V	High	47.0	4.9 (variable: 4 to >9)	NA	3/2
E100G	**High**	**46.9 ± 12.0**	**4.0 ± 2.3**	**Complete**	**22**
D124V	High	NA	NA	NA	NA
L84V	**High**	**53.8 ± 15.3**	**1.6 ± 0.5**	**Complete**	**6**
G93A⁺	**High**	**47.9 ± 17.7**	**2.4 ± 1.4**	**Complete**	**11**
H43R⁺	**High**	**49.6 ± 15.1**	**1.4 ± 0.8**	**Complete**	**7**
D90A mc	**High**	**53.0 ± 17.3**	**< 1 (variable)**	**Incomplete**	**5/2**
A4V⁺	**High**	**47.8 ± 13.3**	**1.2 ± 0.9**	**Complete**	**84**
V14M	High	NA	NA	NA	NA
C6F⁺	High	49.5 ± 4.95	0.29 ± 0.06	NA	2
V14G	High	39.0	1.9	Apparently sporadic	1
G85R	**High**	**55.5 ± 12.6**	**6.0 ± 4.5**	**Complete**	**11**
G93C	**High**	**45.9 ± 10.6**	**13.0 ± 4.0**	**Complete**	**20**
C6G⁺	High	49.5	0.2	NA	2
N139K	High	NA	NA	NA	1
G41D	**Moderate**	**46.0 ± 7.3**	**17.0 ± 6.3**	**Complete**	**7**
C111Y	Moderate	49.0 ± 4.4	10.2 ± 3.1	Complete	3
L144S	Moderate	42.5 ± 10.6	12.3 ± 3.7	NA	2
G93D	Moderate	48.3 ± 16.2	10.5 ± 5.5	NA	3
E21K	Moderate	NA	NA	Apparently sporadic	1
L144F	**Moderate**	**52.0**	**6.7 (variable: 3 to 20)**	**Complete**	**13/11**
E21G	**Moderate**	**44.9**	**16.11**	**Incomplete**	**18**
G37R	**Moderate**	**40.0 ± 9.9**	**18.7 ± 11.4**	**Complete**	**8**
I113T	**Moderate**	**57.8 ± 15.1**	**4.2 ± 3.2**	**Incomplete**	**10**
H46R	**Moderate**	**45.0 ± 10.2**	**17.0 ± 7.0**	**Complete**	**56**
H48Q⁺	Moderate	58.0	1.1	NA	2
D101N	**Low†**	**41.0 ± 10**	**2.4 ± 0.9**	**Incomplete**	**14**
V148I⁺	Low†	28.0 ± 3.8	1.8 ± 0.5	Complete	4/3
H80R	Low†	NA	NA	Apparently sporadic¥	1
E133ΔE	Low†	NA	NA	Apparently sporadic	2
S134N⁺	Low†	NA	NA	NA	2
D125H⁺	Low†	53.0	0.7	NA	2

†Moderate aggregate levels when expressed for 48 hours; ‡High aggregate levels when expressed for 48 hours; ⁺Very aggressive mutations; ¥De novo mutation; mc: indicates D90A heterozygous cases; NA: not available; *N:* number of patients analyzed, when more than one number is given in this column, the first number indicates the total number of patients (used to calculate onset) and the second number represents the total number of deceased patients (used for calculation of survival times); Mutations in bold font are those in which the number of patients is higher than 5.

Statistical tests indicate that when all available data are included, then the there is no significant correlation between disease duration and aggregation propensity (p = 0.2257, Figure 3-9). Whether data on patients with very few cases is reliable is uncertain, but these data are included to allow the reader to predict what might happen as more data becomes available. The pattern that becomes apparent when all data is analyzed is that mutants with low to moderate inherent aggregation propensities are associated with a wide variation in disease duration. The association between high aggregation propensity and short duration seems to hold; data we interpret as an indication that high aggregation propensity is a risk factor for disease of short duration.

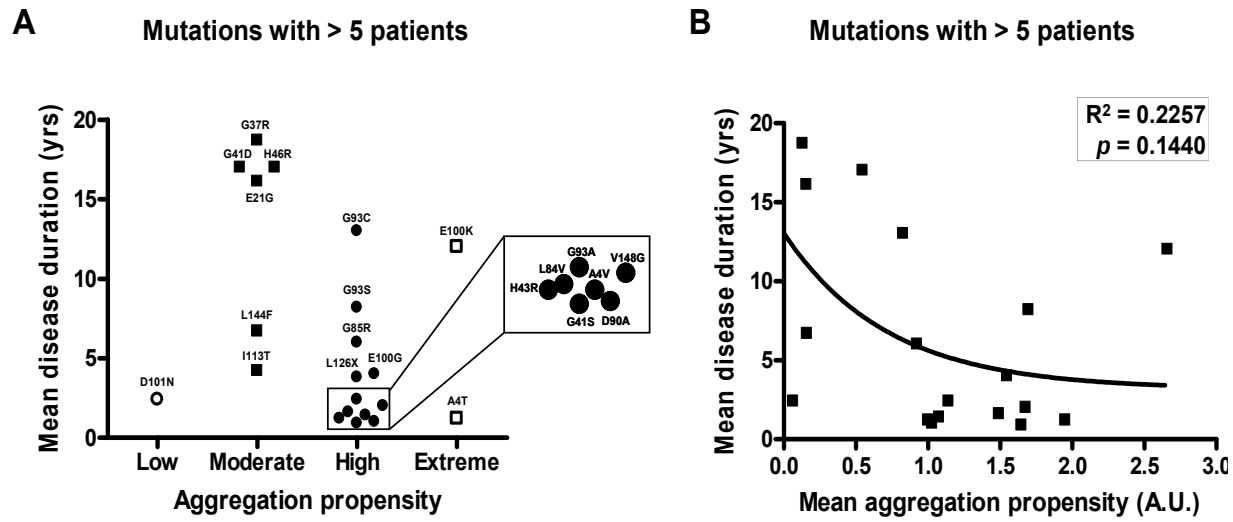

Figure 3-8. Mutants possessing a higher aggregation propensity correlate with shorter disease duration. A) Mutations with a significant number of patients (> 5) grouped in terms or aggregation propensity categories, as explained in Figure 3-7. Mutations associated with shorter disease durations belong to a group that present high or extreme aggregation propensities. B) Non-linear regression of aggregation propensity and disease duration. A statistically significant correlation between aggregation and disease duration was not found ($p \geq 0.05$).

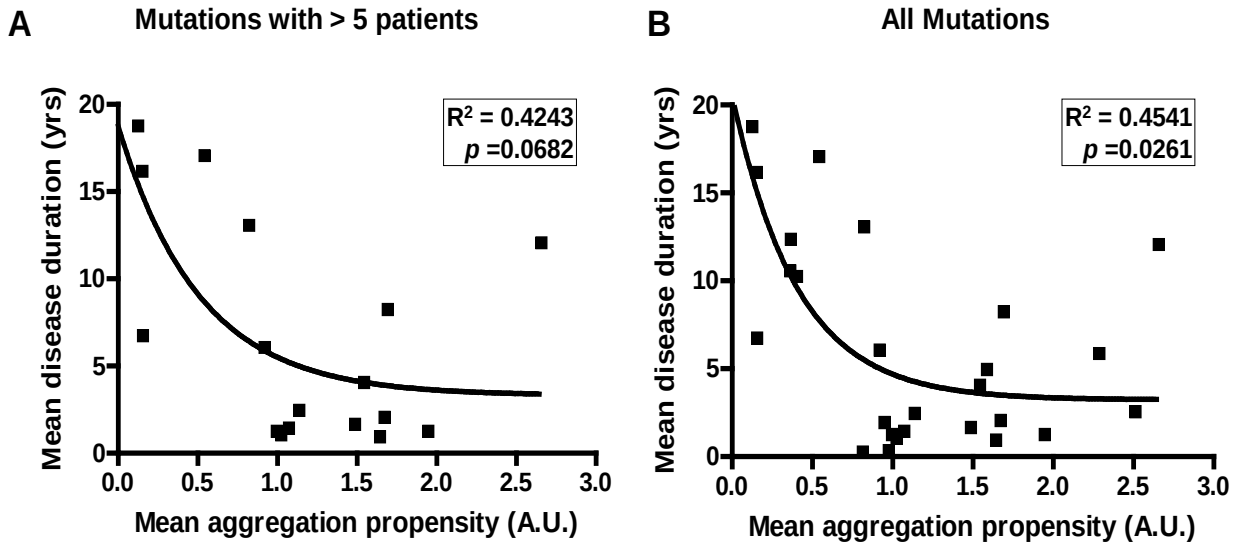

Figure 3-9. Mutants possessing low or moderate aggregation propensities are associated with a large variation in disease duration. A) All SOD1 mutations with some patient data available grouped in terms of aggregation propensity values (see legend in Figure 3-7) and plotted against mean disease duration in years. Significant differences are found between the groups of moderate and high aggregation propensity (unpaired *t*-test, $p = 0.0003$). B) Non-linear regression of aggregation propensity and disease duration.

To determine whether the results obtained in human HEK293FT cells are specific to these cells, or are more broadly applicable to other cell types, we have attempted to replicate our findings in a different cell line to determine whether different results are achieved. We chose to use mouse neuroblastoma N2a cells which transfect reasonably well and which have also been used to study mutant SOD1 (Borchelt et al., 1995;Pasinelli et al., 1998;Krishnan et al., 2006). We chose a set of mutants with a range of aggregation propensities (A4V, G37R, G93D, G93R, D101G, D101N, V148G, V148I) to express in N2a cells for 24 hours (time point in which we can see mutants with low to extreme aggregation propensity ratios in HEK293FT, Figure 3-10). Unfortunately, for most of the vectors tested, the levels of human SOD1 expression were much lower than what is obtained in HEK293FT cells and we were unable to ascertain aggregation

propensities. However, we were able to observe good expression of the D101G and D101N mutants, which show extremely high versus extremely low aggregation propensities in HEK293FT cells. In the N2a cells, we find a similar outcome in that D101G produces a very high level of detergent insoluble SOD1 whereas the D101N mutant remains largely soluble at 24 hours (Figure 3-10).

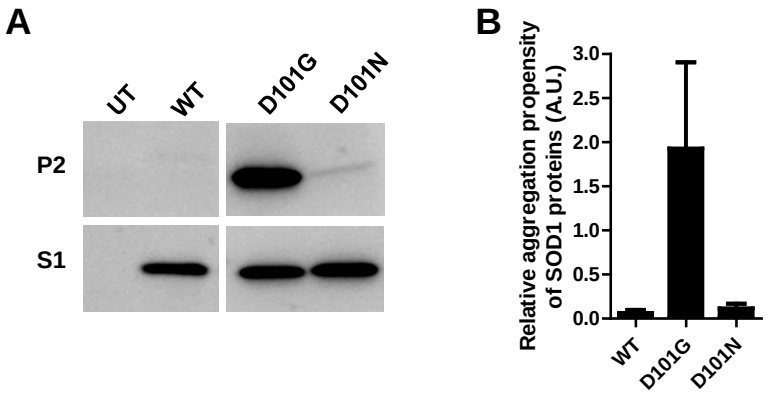

Figure 3-10. Aggregation of mutant SOD1 in mouse N2a cells. Mouse neuroblastoma N2a cells were transiently transfected following protocols described in Methods. A minimum of 3 repetitions were attempted to assess aggregation propensity in mouse N2a cells at 24 hours. Using the same protocol as HEK293FT cells, only 2 of the mutants tested reliably produced sufficient levels of expression to allow for assessments of aggregation propensity. A) Immunoblots of P2 and S1 fractions. B) Quantification of aggregation propensity (P2/S1).

Discussion

Studies to date, which have examined a relatively small percentage of all ALS mutants, have demonstrated that ALS mutations in SOD1 increase the propensity of the protein to form detergent-insoluble aggregates. Data from our present study raises the total number of SOD1-associated mutants for which we have measured aggregation propensities to 30% of all known mutants, providing definitive evidence that increased aggregation propensity is highly likely to be a universal feature of mutant SOD1. However, the inherent propensity of different mutants to produce aggregated protein

varies, even in cases in which multiple mutations target a single amino acid position. We could not identify a specific biochemical or biophysical property of the SOD1-associated ALS mutants that adequately explains the variability in the propensity of these mutant proteins to aggregate. Although causality for variability is unknown, we find that the inherent aggregation propensity of ALS mutants is related to the duration of disease in ALS patients such that mutants that show high aggregation propensities are associated with a greater risk for short disease duration.

Variability in Aggregation Propensity of SOD1 Mutants and Protein Charge

One aspect of our study sought to determine whether variability in mutant SOD1 aggregation propensity could be explained by the nature of the amino acid mutation. Mutations in SOD1 that bring the protein charge to neutrality, or decrease the negative charge, have been suggested to make it more prone to aggregate (Chiti et al., 2002;Calamai et al., 2003). More than half of the SOD1 proteins studied here represent mutations affecting a charged residue or introduce a charged amino acid in place of a non-charged (see Figure 3-4). Within this group of mutations that modify the negative charge of SOD1, we can find SOD1 mutants with all defined levels of aggregation propensity (low, moderate, high or extreme), not following a clear correlation between a decrease or increase in protein charge and aggregation rates. For example, eliminating aspartate in amino acid 101 produces a low (D101N) or very high (D101G) aggregating protein, with both proteins producing a decrease in negative charge. However, when mutations occur at E100, the mutant with a larger increase in net negative charge has the highest aggregation propensity (E100K *vs*. G). The E100 and D101 amino acids are in such close proximity that it seems unlikely that the different changes in charged amino acids at these two residues could have very different structural effects on the

protein. Additionally, we have found no obvious correlation between aggregation propensity and change in charge in amino acids that concentrate to a particular structure (beta strand *vs*. non beta strand regions, surface *vs*. interior; see Figure 3-5). Finally, we found no obvious correlation between the magnitude of change in charge by mutation and disease onset or duration (see Figure 3-6). Collectively, these data indicate that changes in protein charge cannot be the only determining factor that drives aggregation of mutant SOD1 and that there is no obvious correlation between charge changes and a disease feature.

Variability in Aggregation Propensity of SOD1 Mutants and Protein Stability

Thermostability is viewed as a measure of the inherent stability of protein conformation. The mutants we identify here as slow to aggregate (H80R, D101N, D125H, E133ΔE, S134N and V148I) exhibit some of the characteristics of WT SOD1 (see Figure 3-3). Biophysically, these mutants show similar H/D exchange kinetics (which assess the exposure of residues in the folded protein to solvent) to WT SOD1 as apo-proteins (Rodriguez et al., 2005), as well as high levels of activity (only when metallated) and high thermostability (in both fully metallated or demetallated states) (Rodriguez et al., 2005) (see Table 3-2). By contrast, the mutants that show higher aggregation propensities generally show reduced thermostability (see Table 3-2). However, in our tabulation of data on aggregation levels at 24 hours in comparison to thermostability, we noted no obvious association between low thermostability of the apo-protein (lacking Cu) and aggregation propensity (see Table 3-2).

Variability in Aggregation Propensity of SOD1 Mutants and Metal Binding

Sorting out the role of metal-binding in aggregation propensity is somewhat complicated in that different approaches of assessing metal-binding have yielded

different outcomes depending upon whether the protein was produced and isolated from yeast or Sf21 insect cell expression systems. From the available data, we find little evidence to relate poor metal binding capacity to the formation of detergent-insoluble SOD1 aggregates. Three of the low aggregating SOD1 mutants identified here appear to bind metals weakly (see Table 3-2). Moreover, experimental SOD1 mutants in which copper binding ligands have been abolished do not present a higher propensity to form detergent-insoluble aggregates than other SOD1-associated ALS mutations (Wang et al., 2003). Thus, it does not appear that low metal binding capacity correlates to high aggregation propensity.

Aggregation *vs*. Disease

To date, the specific role or impact that aggregates of mutant SOD1 have on disease pathogenesis remains unclear. In some settings, aggregation of mutant protein has been suggested to reduce toxicity by concentrating an otherwise toxic protein to a specific subcellular compartment (Arrasate et al., 2004;Gong et al., 2008); however, evidence linking aggregates to toxicity is still largely correlative. All of the SOD1 ALS murine models that have been analyzed accumulate significant amounts of detergent-insoluble aggregates in tissues most affected by the disease process (Johnston et al., 2000;Wang et al., 2002b;Wang et al., 2002a;Wang et al., 2003;Jonsson et al., 2004;Wang et al., 2005b;Wang et al., 2006;Karch et al., 2009). In certain cases in which the expression of mutant protein was low, disease development and/or aggregation was not observed (Wang et al., 2005b;Deng et al., 2006). The two interpretations of these findings are that: 1) aggregation of mutant SOD1 is critical to the development of disease, or 2) that some other process initiates disease onset and that cells damaged by the disease process are prone to aggregate mutant SOD1. Our cell model, however,

suggests that a high propensity to aggregate is an inherent characteristic of ALS mutant SOD1. Our studies have shown that SOD1-associated ALS mutants display a wide variety of aggregation propensities that are dependent upon the type and location of the mutation. Thus, if aggregates have an important role in disease pathogenesis, then some characteristic of human disease should correlate to the aggregation propensity of the individual mutant.

As noted in Results, the mean age of disease onset in SOD1-associated ALS is between 45-47 years of age, and we find no obvious correlation between aggregation propensity and age of onset (see Figure 3-7). However, in our analysis of clinical data regarding mutations with reliable patient information (see Table 3-3), we have observed that in general there is an inverse relationship between high aggregation propensity and disease duration (see Figure 3-8). Mutants with higher aggregation propensities compose a group of mutations in which the clinical data available is more abundant. In this set of mutants, survival intervals tend to be shorter; all exhibit a survival of less than 12 years, although most of them are characterized by survival times of 4 years or less. By contrast, SOD1 mutants with moderate aggregation propensities present survival times ranging 10-18 years. However, these relationships were not absolute as we found examples of mutants with moderate aggregation propensity in which disease duration is shorter than 10 years: I113T and L144F SOD1 (see Table 3-3, see Figure 3-8). The mutant I113T is known to have incomplete penetrance, thus it might be possible that additional factors regulate disease appearance in certain generations, which would be responsible for the large variability in disease duration among patients. Patients harboring the L144F mutation present complete penetrance, but exhibit a wide range of

survival times (see Table 3-3). It is possible that as more data becomes available, the number of exceptions (low aggregation potential linked to rapid progression) may rise. However, when we include in our analysis of patient data, all available data including cases with only 1 or 2 patients (see Figure 3-9), we continue to observe that high aggregation propensity shows a strong association with disease of short duration (< 5 years). Mutants that show low or moderate aggregation potentials are essentially unpredictable. Overall, we regard the high propensity of a particular mutant to aggregate as a risk factor for a more rapidly progressing disease.

HEK293FT Cells as a Model to Study SOD1-Associated ALS Aggregation

All of our data in the present study, as well as data derived from prior studies (Wang et al., 2003;Karch and Borchelt, 2008) have used the HEK293FT cell as the model system. We note that we were able to find one report in the literature in which inducible vectors were used in mouse NSC-34 cells to express a limited number of human mutant proteins (including A4V, C6F, H46R, G93A, and C146R SOD1) (Cozzolino et al., 2008a). These investigators used a very similar approach of determining the levels of mutant SOD1 in detergent soluble and insoluble fractions. After 48h of induced expression, they reported that A4V and G93A mutants showed ratios of soluble to insoluble SOD1 that were similar to what we report in our current study. We have previously examined the aggregation the C6F and C146R mutants in HEK293FT cells, and found high inherent rates of aggregation (Karch and Borchelt, 2008). Cozzolino reported a similar high rate of aggregation of these mutants in mouse NSC-34 cells (Cozzolino et al., 2008a). By contrast, the H46R mutant showed much lower levels of aggregated mutant SOD1 in NSC-34 cells; which again is similar to what we have previously reported for this mutant in our HEK293FT cell system (Wang et al.,

2003). We also examined aggregation propensities of human SOD1 by transient transfection of mouse neuroblastoma N2a cells (see Figure 3-10). One of the more interesting pairs of mutants, D101G and D101N, showed similar aggregation propensities in the N2a cells as was observed in the HEK293FT cells. Thus, we think that our findings in HEK293FT cells reflect inherent aggregation propensities of these mutants that are manifest in other cell types. It is possible that there are factors unique to motor neurons that modulate aggregation; and that such factors could significantly impact mutant SOD1 folding when present at physiologic levels. However, we argue that the HEK293FT cell model, which is dependent upon high levels of expression, overwhelms most of the cellular systems that might otherwise modulate mutant SOD1 aggregation (proteasome degradation, chaperone levels, etc) providing insight in the inherent propensity of these proteins to self associate. Even in the face of other modulating factors, the inherent propensity to aggregate would be the basic force behind aggregation. At this basic level, we find that mutants that exhibit a high aggregation propensity are often associated with disease of short duration.

One other factor to consider is that most of the human cases for which we have significant data are examples of disease of relatively short duration. Because the longer duration cases are not equally represented, the apparent association between high aggregation rates and short disease duration could be due to bias in data set. However, statistical analyses of the data indicate a non-random distribution of disease duration among the classes of mutants, with high aggregation propensity more often being found in patients with short duration. Moreover, within the group of patients that show short duration, 9 of the 12 mutants that exhibited high aggregation potential are associated

with disease durations of less than 5 years. However, we clearly identify mutants that in cell culture show aggregation propensities that do not fit with expectations for disease duration. Whether these exceptions are truly examples of mutants that aggregate slowly and yet are associated with rapidly progressing disease (e.g. D101N mutant) or mutants that aggregate rapidly and yet are associated with slowly progressing disease (e.g. E100K), is uncertain. These may be examples in which the cell culture system is not accurately predicting the *in vivo* situation, or these may be examples in which other modifying factors overshadow the role of aggregation in disease duration.

The association between aggregation of mutant SOD1 and symptomatic disease duration, rather than onset, is a particularly intriguing finding. In comparison to other neurodegenerative diseases that have been associated with protein misfolding, SOD1-associated ALS appears unique. For example, in neurodegenerative disorders with expansions of glutamine repeats regions there is an association between aggregation and age of disease onset rather than progression. Individuals with polyglutamine expansions in the huntingtin gene develop Huntington's disease (HD). In HD, the length of the polyglutamine tract strongly correlates with disease onset, the larger the expansion the earlier onset (Persichetti et al., 1994;Gusella and MacDonald, 2006); and longer repeat lengths correlate with higher aggregation propensities of mutant huntingtin (Scherzinger et al., 1999). In HD, disease duration is not noted to be variable and the length of the polyglutamine repeat does not correlate with disease duration (Gusella and MacDonald, 2006). Another example is Alzheimer's disease (AD), which is defined by pathologic accumulation of aggregated of β-amyloid peptides in the brain. Familial forms of AD linked to mutations in amyloid precursor protein or presenilin 1, lead to a net

increase in the amount of the highly aggregating β-amyloid peptide 1-42 (Duff et al., 1996;Borchelt, 1998). These inherited forms of AD generally show much earlier disease onsets, but disease durations are similar to the sporadic disease (Bertram and Tanzi, 2008;Bird, 2008). Thus, in other examples of neurodegenerative disease associated with protein misfolding and aggregation, the aggregation rates of the causative protein appears to best correlate with disease onset.

Conclusions

We provide evidence that mutations in SOD1 that are associated with a high aggregation propensity generally predict a more rapidly progressing disease. However, several exceptions are noted, and it becomes less predictable for mutants with lower aggregation propensities. Thus, it appears that at least two factors regulate disease progression; one of which is high inherent aggregation propensity of SOD1 mutant protein. In this view, we would categorize high aggregation propensity as a risk factor for rapidly progressing disease. Studies from our laboratory, and others, have demonstrated that, in mouse models of SOD1-associated ALS, the most significant accumulations of large mutant SOD1 aggregates occurs late in disease (Johnston et al., 2000;Wang et al., 2002b;Wang et al., 2002a;Wang et al., 2003;Jonsson et al., 2004;Wang et al., 2005b;Wang et al., 2005a;Wang et al., 2006;Karch et al., 2009). Importantly, significant accumulation of mutant SOD1 aggregates occurs well after the appearance of multiple pathologic abnormalities in these mouse models (Karch et al., 2009). Thus, we concur with others that have suggested that there must be a toxic form of mutant SOD1 that is distinct from larger protein aggregates with these entities initiating disease. However, aggregation of the mutant protein may be one of the forces capable of modulating the rate of disease progression. The mechanisms by which

aggregation of mutant SOD1 promotes disease progression are unclear at present. One hypothesis that could apply is the idea that the accumulation of SOD1 aggregates impairs the ability of the cell to maintain protein homeostasis (Gidalevitz et al., 2009). The idea is that as chaperones become occupied in unproductive attempts to dissolve protein aggregates, these activities are not available for productive functions in protein folding. There is also evidence that cells accumulating protein aggregates show reduced proteasome function (Bence et al., 2001). Together, the disruption of these critical protein homeostatic processes could cause a feed-forward cascade of impairment in the protein folding and metabolism that could underlie the rapid progression of disease that is seen in many of the mouse models. If these mechanisms apply, then compounds that modulate mutant SOD1 aggregation could be useful therapeutics in slowing the progression of this disease in humans.

CHAPTER 4
MODULATION OF MUTANT SUPEROXIDE DISMUTASE 1 AGGREGATION BY CO-EXPRESSION OF WILD-TYPE ENZYME1

Introduction

In SOD1-associated ALS, WT and mutant SOD1 proteins are co-expressed at 1:1 ratios of synthesis. Whether toxicity of mutant SOD1 is modulated by interactions between WT and mutant protein, or by the activity of WT SOD1, has been addressed in several experimental models (for more information about these studies see "Implication of WT SOD1 in ALS and Aggregation" in Chapter 1). Transgenic mouse studies conducted to determine the effect of human WT SOD1 on the toxicity of mutant human SOD1 have produced conflicted results. In one study mice overexpressing WT and G85R human SOD1 proteins revealed that WT human SOD1 had no effect on disease onset or survival (Bruijn et al., 1998), while in other studies the presence of WT human SOD1 in mice expressing a mutant human SOD1 protein (A4V, G85R, G93A, T116X, or L126Z) was found to accelerate disease onset (Jaarsma et al., 2000;Deng et al., 2006;Deng et al., 2008;Wang et al., 2009c). Additionally, in one of the latter studies, earlier disease onset was accompanied by the formation of SOD1 protein aggregates that contained both WT human SOD1 proteins (Deng et al., 2006). Thus, one explanation for the decrease in mouse lifespan could be that the addition of human WT SOD1 promoted a more rapid aggregation of mutant protein. Additionally, the lack of correlation between aggregation propensities of slow aggregating SOD1 mutants and

[1]The work presented in this chapter has been published in *The Journal of Neurochemistry* 108(4):1009-18 (2009). Mercedes Prudencio and David R. Borchelt designed the experiments, interpret the data and wrote the manuscript. Mercedes Prudencio carried out all the experiments with the exception of the FMTS analyses which were performed and interpreted by Armando Durazo and Julian Whitelegge at UCLA.

disease duration, studied in Chapter 3, may be due to the fact that WT could play an important role in modulating aggregation.

In this study we have used our cell culture model of mutant SOD1 aggregation to ask whether WT SOD1 directly promotes the aggregation of mutant SOD1. In order to address this issue, we co-expressed cells with WT SOD1 (human or mouse) and mutant human SOD1 (A4V, G85R, G93A SOD1) for different periods of time, and asses for aggregation of mutant SOD1 proteins. We observed an outcome not predicted in the mouse studies. Additionally, human and mouse WT SOD1 demonstrated similar, but not identical, ability on modulating mutant SOD1 aggregation. Further analyses are performed to explore such differences between human and mouse WT SOD1.

Materials and Methods

A list of materials used can be found in Appendix B. Methodology used for the work presented in this chapter is described in “Chapter 4 Methods” of Appendix C.

Results

Differential detergent extraction and centrifugation techniques have been demonstrated as an approach to separate mutant SOD1 complexes of high molecular weight (presumed aggregates and defined as such here); which occur in both transgenic mouse tissue and cell culture models (Wang et al., 2003;Wang et al., 2006;Karch and Borchelt, 2008;Karch et al., 2009)}. The formation of SOD1 aggregates can be modelled by high level expression of mutant SOD1 in human HEK293FT cells (Wang et al., 2003). Using this model system we sought to examine whether WT SOD1 modulates the aggregation of mutant SOD1.

Co-expression of WT and mutant human SOD1 proteins in cultured HEK293FT cells reduced the level of detergent-insoluble mutant SOD1 proteins that accumulates in

24 hours (Figure 4-1). Cells transfected with A4V, G85R or G93A SOD1 alone formed detergent-insoluble aggregates that sedimented upon ultracentrifugation, whereas cells expressing both WT and mutant human SOD1 produced little or no detergent-insoluble SOD1 protein (Figures 4-1A and 4-1B, upper panel). Instead, both WT and mutant human SOD1 proteins were found only in soluble fractions (Figures 4-1A and 4-1B, lower panel). To control for non-specific effects of co-transfection, such as reduced mutant protein expression that may have caused a reduction in aggregation, we co-expressed the mutant SOD1 constructs (A4V, G85R and G93A SOD1) with a GFP construct and performed the detergent extraction and centrifugation assay. In each case, the expression of GFP did not affect the aggregation of mutant SOD1 (Figures 4-1A and 4-1B, upper panel); and a large fraction of the mutant SOD1 remains fully soluble in detergent (Figures 4-1A and 4-1B, lower panels). The levels of soluble SOD1 protein provide a good indication of protein expression, indicating that all mutant proteins were expressed at high levels relative to non-transfected control cells. Immunoblot data from at least four experiments for each set of WT and mutant human SOD1 co-transfections was quantified and analyzed statistically (Figure 4-1C), providing clear evidence that in our cell culture model the co-expression of WT SOD1 modulates mutant human SOD1 aggregation.

To examine the effects of WT human SOD1 on mutant SOD1 aggregation over time, we extended the interval between transfection and harvest to 48 hours. Interestingly we found that WT human SOD1 differentially affected the aggregation of the different SOD1 mutants (A4V, G85R and G93A SOD1; Figures 4-1D and 4-1E). As compared to cells expressing A4V human SOD1 alone, cells co-transfected with vectors

for WT and A4V human SOD1 continued to accumulate less detergent-insoluble mutant protein (Figure 4-1D, upper panel). However, aggregation was not blocked as these cells contained significantly more detergent-insoluble SOD1 than cell cells transfected with WT human SOD1 (Figure 4-1E). The levels of detergent-soluble SOD1 protein in extracts from cells co-transfected with WT and A4V human SOD1 indicated relatively high levels of expressed protein (Figure 4-1D, lower panel). However, because the WT and A4V human SOD1 proteins could not be distinguished by SDS-PAGE and the low amount of detergent-insoluble SOD1 in the co-transfected cells, we could not determine whether the insoluble human SOD1 is limited to mutant protein. When WT human SOD1 was co-expressed with G85R human SOD1, it was possible to differentiate the WT and mutant human SOD1 proteins by SDS-PAGE; the G85R variant migrates anomalously in SDS-PAGE, running slightly faster than the expected size (Hayward et al. 2002; Wang et al. 2003; Wang et al. 2006). In cells co-expressing WT with G85R human SOD1, we observed significant accumulation of detergent-insoluble mutant protein at 48 hours. More interestingly, WT human SOD1 was clearly detected in the detergent-insoluble fraction (Figures 4-1D upper panel, and 4-1F). This result is consistent with the discoveries of detergent-insoluble WT human SOD1 in spinal cords of transgenic mice co-expressing WT and mutant human SOD1 (Deng et al., 2006). Similar to the result with the G85R variant, co-expression of WT and G93A human SOD1 for 48 hours showed similar levels of SOD1 protein in the detergent-insoluble fraction as compared to cells transfected with G93A human SOD1 expression plasmid alone (Figures 4-1D and 4-1E). However, whether WT human SOD1 co-aggregated with G93A SOD1 could not be determined by SDS-PAGE alone.

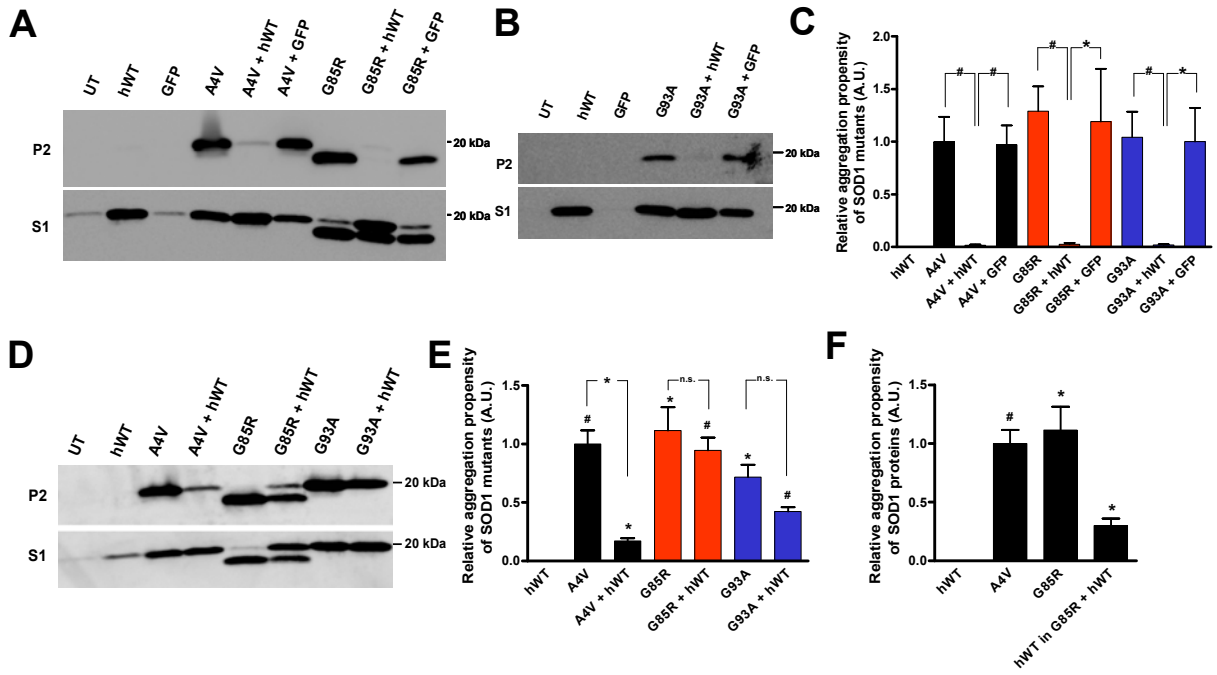

Figure 4-1. Human WT SOD1 modulates the aggregation of mutant SOD1 in cultured cells. A, B, D). Immunoblots of P2 and S1 fractions from HEK293FT cells co-transfected with WT human SOD1 (or GFP) and mutant SOD1 for 24 (A, B) or 48 (D) hours. UT: untransfected cells. hWT: cells transfected with WT human SOD1 construct. C, E, F). Quantification of the relative aggregation potentials of the SOD1 mutants, when expressed alone or with hWT (C, E); or of hWT when co-expressed with G85R for 48 hours (F). Bars represent mean ± SEM. N=3-9. Paired student *t*-tests *vs*. hWT, or as indicated. $^{*}p \leq 0.05$, $^{\#}p \leq 0.005$, n.s.: non-significant differences.

To determine whether the detergent-insoluble human SOD1 protein fraction of cells co-transfected with WT and G93A human SOD1 contain any trace of WT human SOD1 protein, we analyzed such fractions by hybrid linear ion-trap Fourier-transform ion cyclotron resonance mass spectrometry (FTMS). FTMS analysis revealed the presence of both WT and G93A human SOD1 in both the detergent-insoluble (P2) and the detergent-soluble (S1) fractions (Figure 4-2). In the detergent-insoluble fractions, there was about 10 fold more G93A than WT human SOD1 detected (Figure 4-2A, P2); while in the soluble fractions, the levels of WT and G93A human SOD1 were similar (Figure 4-2B, S1). These findings indicate that WT human SOD1 co-sediments with the G93A

SOD1 mutant protein, but WT protein is not a major component of the detergent-insoluble aggregated protein.

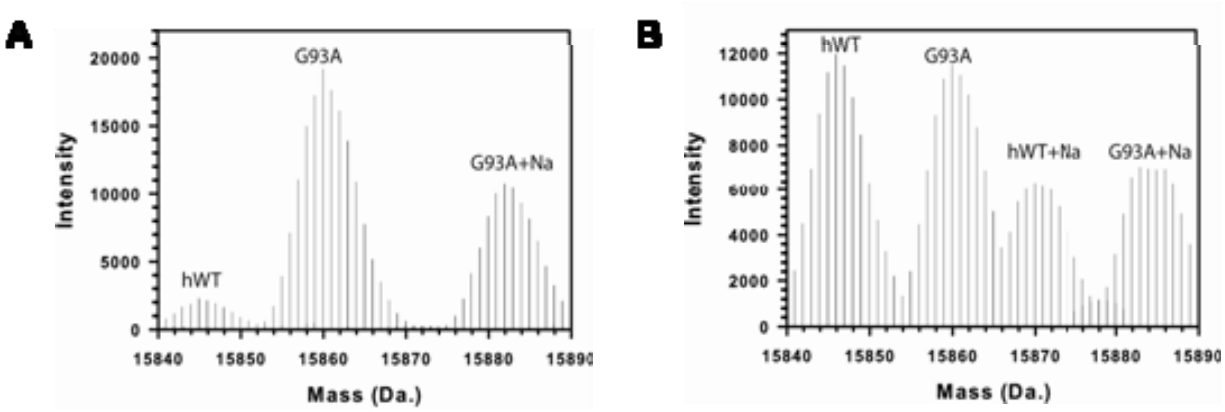

Figure 4-2. Comparison of SOD1 molecular mass profiles from S1 and P2 fractions of HEK293FT cells co-expressing human WT (hWT) and G93A human SOD1. A, B) SOD1 was recovered from spinal cord extracts, solubilized and purified (See Methods). An appropriate chromatographic fraction was analyzed by nano-electrospray using FTMS, with resolution 100,000 at m/z=400. Zero charge molecular mass profiles were deconvoluted from raw FTMS spectra of SOD1 recovered from P2 (A) and S1 (B) fractions using Xtract software (Thermo Fisher). Bars represent the individual ^{13}C isotopomers with the most intense approximating the average mass of the protein. Minor sodium (Na) adducts are typical in these experiments.

To control for the effects of co-transfection and for the possibility that SOD1 proteins of differing sequences might interfere with aggregation, we also co-transfected G85R human SOD1 with WT, A4V, and G93A human SOD1 constructs. In these experiments we took advantage of the anomalous migration of G85R human SOD1 to examine how the co-expression of two different SOD1 mutants might affect their aggregation. Cells co-expressing G85R SOD1 with either A4V or G93A SOD1 produced detergent-insoluble forms of each human SOD1 mutant (Figure 4-3A, upper panel). As described above, the presence of mutant human SOD1 protein in the S1 fraction for each transfection indicated that only a portion of the total protein adopted the detergent-insoluble conformation (Figure 4-3A, lower panel). Quantification of multiple

independent experiments demonstrated that whether expressed alone or in combination with the A4V or G93A SOD1 variants, the propensity of G85R SOD1 to aggregate was not significantly altered (Figure 4-3B). These data suggest that the apparent reduction in aggregation caused by the co-expression of WT with mutant human SOD1 is not due to some non-specific effect of co-transfection or some non-specific effect of interactions between two different SOD1 subunits, but rather appears to be due to a specific property of the WT human SOD1 protein.

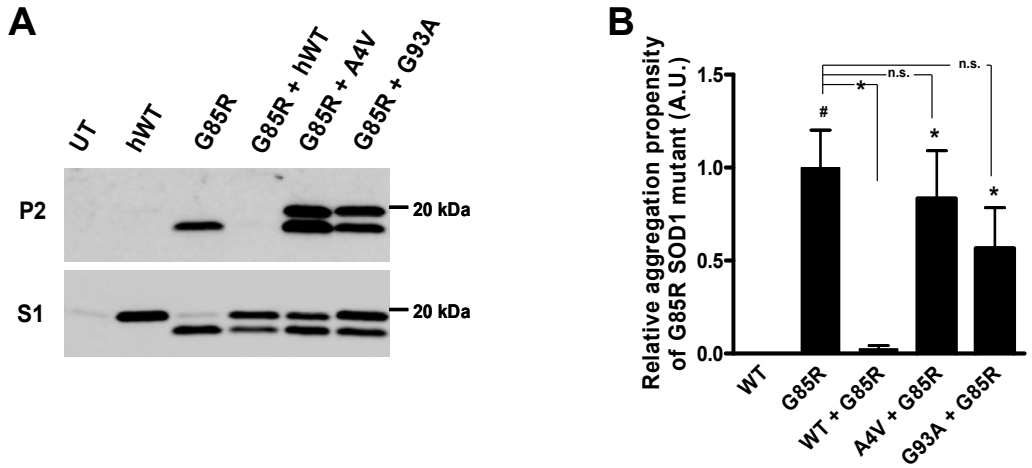

Figure 4-3. SOD1 mutants with high propensity to aggregate (A4V and G93A SOD1) do not interfere with aggregation of G85R SOD1. A) Immunoblot of P2 (upper panel) and S1 (lower panel) fractions of singly and doubly transfected HEK293FT cells. UT: untransfected cells. Notations are the same as in Figure 4-1. B) Quantification of the relative aggregation potentials of the G85R SOD1 when expressed alone and with other SOD1 constructs. Bars represent mean ± SEM (N = 4-8). Statistical analysis compares the aggregation of WT human SOD1 to G85R or G85R co-transfected with another construct $^{*}p \leq 0.05$, $^{\#}p \leq 0.005$. Only G85R + WT was significantly different from G85R alone $^{*}p \leq 0.05$; n.s. indicates non-significant differences.

The human and mouse WT SOD1 proteins share approximately 83.6% identity at the level of amino acid sequence (Figure 4-4), with 25 amino acid differences in the 153 residue protein. Thus, we next sought to investigate whether these differences in protein

sequence would affect the ability of WT SOD1 to modulate the aggregation rate of mutant human SOD1.

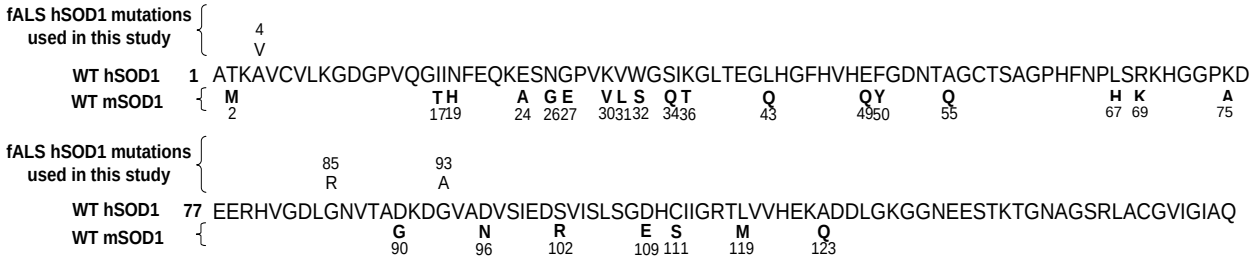

Figure 4-4. Alignment of human (h) and mouse (m) SOD1 protein sequences. Below the human SOD1 sequence, in bold font, we indicate the 25 differences between human and mouse SOD1. The ALS mutations used in this study are also indicated above the human SOD1 sequence.

HEK293FT cells co-transfected with WT mouse SOD1 and mutant human SOD1 proteins (A4V, G85R and G93A SOD1) showed a significant reduction in the amount of detergent-insoluble SOD1 aggregates produced in 24 hours (Figures 4-5A and 4-5B). Interpretation of the immunoblots of cells co-transfected with WT mouse SOD1 and G85R human SOD1 was complicated by the fact that these proteins migrated to very near the same position in SDS-PAGE. However, these proteins could be resolved in gels exposed for short intervals, allowing for the detection of both WT mouse SOD1 and G85R human SOD1 in the detergent-soluble protein fraction (Figure 4-5A, right lower panel). Despite a significant reduction in the amount of insoluble G85R human SOD1 in these co-transfected cells, aggregation was not blocked and it was possible to demonstrate that the detergent-insoluble fraction contained only G85R human SOD1 (Figure 4-5A, right upper panel). Quantification of the relative aggregation propensity of the human SOD1 mutants in cells co-transfected with WT mouse SOD1 revealed a significant reduction in the amount of detergent-insoluble mutant human SOD1 protein

that accumulated in 24 hours (Figure 4-5B). Thus, WT mouse SOD1 has the same capacity as WT human SOD1 to slow the rate of mutant human SOD1 to aggregate.

When we extended the interval between transfection and harvest to 48 hours, we observed that A4V, G85R and G93A human SOD1, when expressed with WT mouse SOD1, were able to form detectable amounts of detergent-insoluble SOD1 aggregates (Figure 4-5C). We observed that in measures of aggregation propensity, which compensates for any changes in the expression of mutant hSOD1 that may occur when co-transfected with WT mouse SOD1, the presence of WT mouse SOD1 had no significant effect on aggregation of mutant human SOD1 (Figure 4-5D). Interestingly, WT mouse SOD1, unlike WT human SOD1, did not seem to co-aggregate with any of the mutants even after the longer 48 hour interval (Figure 4-5C, upper panel). In co-transfections of A4V or G93A human SOD1 mutants with WT mouse SOD1, the amount of mouse SOD1 detected in the insoluble fraction was not different from that of cells transfected with mouse SOD1 alone (Figure 4-5C; $p \geq 0.05$, N = 4). Moreover, we did not detect mouse SOD1 in detergent-insoluble fractions of cells co-expressing WT mouse SOD1 and G85R human SOD1 ($p = 0.2028$, N = 3), which could be observed in gels exposed for short intervals (Figure 4-5C, right panel). Thus, although WT mouse SOD1 possesses an ability that is similar to WT human SOD1 in modulating the aggregation of mutant proteins, it lacks a feature that allows for co-sedimentation with mutant human SOD1.

The differing ability of WT mouse SOD1 and human SOD1 to co-aggregate with mutant human SOD1 is a finding that appears to be consistent with a recent report suggesting that a specific cysteine residue in human SOD1 may mediate the co-

aggregation of WT and mutant human SOD1 (Cozzolino et al., 2008a). The cysteine residue at position 111 of human SOD1 has been identified as a potential mediator of disulfide cross-linking between mutant and WT human SOD1 (Cozzolino et al., 2008a). Mouse SOD1 encodes serine at position 111, and thus could not generate such disulfide linkages. To directly test this hypothesis, we used a previously described human cDNA that encodes serine as position 111 (C111S) (Karch and Borchelt, 2008) in co-transfection with G85R human SOD1. The mutant C111S human SOD1 is not an ALS mutation; in most species the position equivalent to 111 encodes serine. Previous studies have established that this mutant does not spontaneously aggregate (Cozzolino et al., 2008a;Karch and Borchelt, 2008). In C111S and G85R human SOD1 co-transfections, cells were harvested after 48 hours, which was the interval needed to observe WT and G85R human SOD1 co-aggregation. Consistent with previous studies, all C111S human SOD1 fractionated to the detergent-soluble fraction (Figure 4-6A). However, in cells co-transfected with C111S and G85R human SOD1 and harvested 48 hours later, we found both proteins in the detergent-insoluble fraction. Quantification of the aggregation propensity of each SOD1 protein shows significant accumulation of aggregated C111S human SOD1 in the co-transfected cells (Figure 4-6B). This finding suggests that the co-aggregation of WT human SOD1 with mutant protein is not dependent upon a disulfide linkage between cysteine 111 of WT protein and cysteine residues of mutant human SOD1.

The implication of disulfide bonding can be further studied by including high concentrations of β-ME (30%) in the detergent extraction buffers. In this setting, in cells co-transfected with WT and G85R human SOD1, both proteins are detected in the P2

fractions (Figure 4-7, lanes 5 and 7). Notably, cells expressing WT human SOD1 alone in the presence of β-ME present somewhat higher levels of WT human SOD1 in P2 fraction (Figure 4-7, lane 2). This higher background of WT in P2 makes it difficult to interpret the meaning behind the presence of WT human SOD1 in insoluble fractions of cells co-expressing WT and G85R human SOD1. Whether some WT human SOD1 is disulfide cross-linked to mutant human SOD1 cannot be excluded by this experiment. However, overall, these data show that disulfide linkages are unlikely to be important in maintaining aggregate structure.

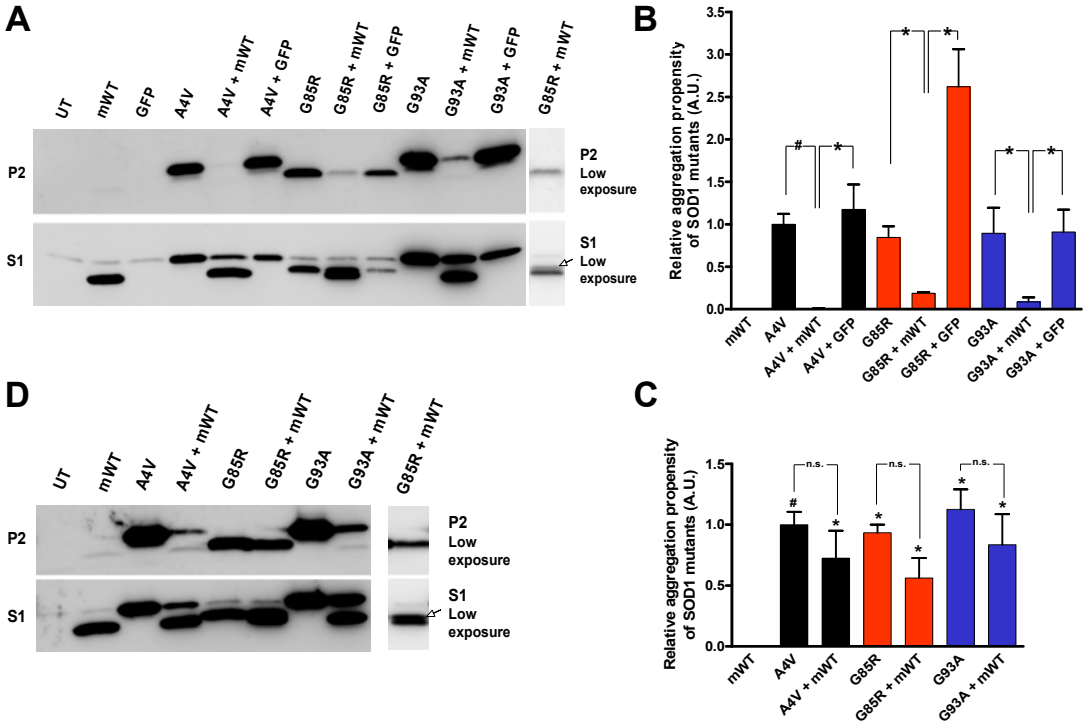

Figure 4-5. Mouse WT SOD1 also modulates the aggregation of mutant SOD1 in cultured cells, but without evidence of co-aggregation. A, D) Immunoblots of P2 and S1 fractions from 24 (A) and 48 (B) hour transfections and co-transfections in of HEK293FT cells. UT: untransfected cells. mWT: cells transfected with WT mouse SOD1 construct. B, C) Quantification of the relative aggregation potentials of the studied SOD1 mutants when expressed alone and with WT mouse SOD1. Bars represent mean ± SEM. N=3-6. Statistical analysis compares differences in aggregation propensity with mWT, or as indicated $^{*}p \leq 0.05$, $^{\#}p \leq 0.005$, n.s.: non-significant.

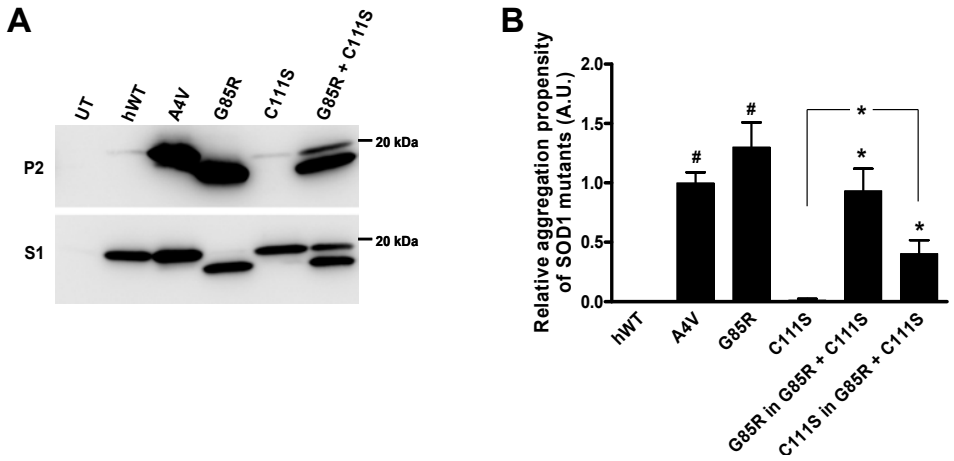

Figure 4-6. Cysteine 111 is not required for the co-aggregation of WT with G85R human SOD1. A) Immunoblots of detergent extracted cells that co-expressed C111S and G85R human SOD1 proteins for 48 hours. Notations are the same as in Figure 4-1. B) Quantification of the relative aggregation propensity of mutant human SOD1 proteins. Bars represent mean ± SEM. N=4. Student *t*-tests compare the aggregation of WT human SOD1 to each mutant, or as indicated on the figure. $^{*}p \leq 0.05$, $^{\#}p \leq 0.005$.

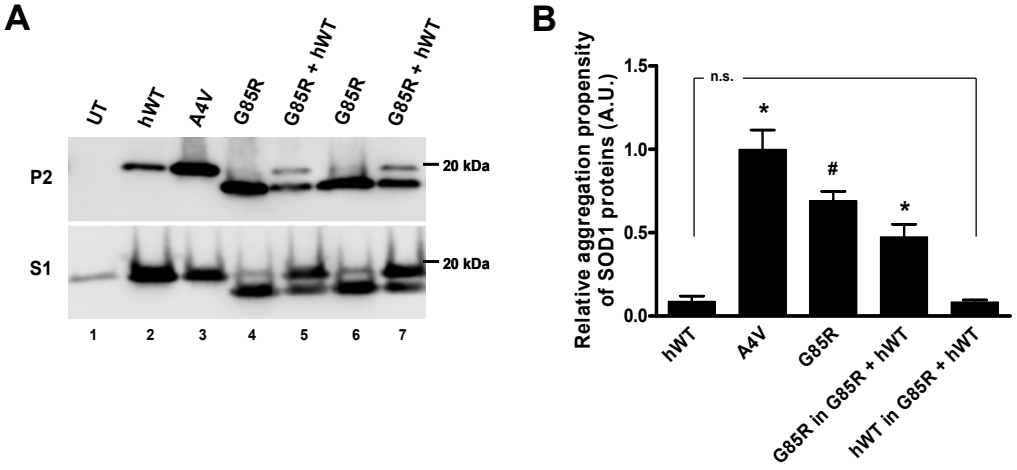

Figure 4-7. High concentration of β-ME does not reduce the amount of mutant SOD1 that fractionates to the P2 fraction at 48 hours. Detergent extractions followed the same protocols used for previous figures except all buffers were adjusted to contain 30% β-ME to break all disulfide bonds. A) Immunoblots of P2 and S1 fractions. B) Quantification of the relative aggregation propensity of WT or mutant human SOD1. Bars represent mean ± SEM (N = 3). Paired student t-tests compare the aggregation of WT human SOD1 to each mutant or as noted on the figure, *p ≤ 0.05, #p ≤ 0.005; n.s.: non-significant differences.

Discussion

In the present study, we examined the potential for WT SOD1 to influence the aggregation of mutant SOD1 as defined by the formation of structures that are insoluble in non-ionic detergent and sediment upon ultracentrifugation. In a cell culture model of mutant SOD1 aggregation, we found that the presence of WT human SOD1 or mSOD1 significantly lowered the amount of mutant human SOD1 (A4V, G85R and G93A) in aggregates after 24 hours. Upon longer incubation (48 hours), we observed significant aggregation of G85R and G93A human SOD1, but continued attenuation of A4V aggregate levels. We also observed that WT human SOD1 can co-sediment with mutant G85R and G93A SOD1 aggregates; however, the predominant species of SOD1 in these aggregates was mutant protein. Importantly, these effects of WT human or mouse SOD1 on the aggregation of mutant protein were specific to WT protein. Co-expression of G85R human SOD1 with either A4V or G93A human SOD1 showed no evidence of slowed aggregation rates; detergent-insoluble forms of both mutant proteins were readily detectable in 24 hours. From these findings, we conclude that WT SOD1 possess a capacity to modulate the aggregation of the mutant protein, with the primary effect being to slow aggregation rates.

Human But Not Mouse WT SOD1 Can Co-Aggregate with Mutant SOD1.

One mechanism by which WT protein could slow aggregation of mutant protein, but then ultimately become a component of such aggregates, is via direct protein-protein interactions between the WT and mutant proteins at the level of nucleation, or growth, of the aggregate. In many aggregate structures, the stacking of peptide chains of identical sequence is crucial to the formation of stable oligomeric structures (Petty and Decatur, 2005;Shorter and Lindquist, 2005). Such stacking forces have been

proposed in prion protein conformational changes and it is well established that the presence of two prion proteins with single amino acid substitutions can slow aggregation (Hsiao et al., 1994;Petty et al., 2005). With this notion in mind, we tested whether WT mouse SOD1 could produce the same effects as WT human SOD1 on the aggregation of mutant human SOD1. The WT mouse SOD1 protein contains 25 amino acid differences from the human protein (see Figure 4-4). Despite these numerous sequence differences, WT mouse SOD1 retains the ability to slow aggregation of mutant human SOD1, presumably through direct protein-protein interactions. However, WT mouse SOD1 does not co-sediment with the mutant human SOD1 aggregates. This latter outcome could indicate that the numerous sequence differences between human and mouse SOD1 disrupt the types of close protein-protein interactions that would be required in the assembly of SOD1 aggregates.

WT and Mutant Human SOD1 Protein-Protein Interaction: Role of Disulfide Bonding and Cysteine 111.

Our observation that WT mouse SOD1 does not co-aggregate with mutant human SOD1 is consistent with a recently a proposed mechanism of WT and mutant SOD1 co-aggregation that suggested a role for inter-subunit disulfide crosslinking between cysteine residues at position 111 (Cozzolino et al., 2008a). In a heterodimer of WT and mutant SOD1 subunits, these cysteines would be in close proximity near the dimer interface and thus could mediate an inter-subunit bridge. Mouse SOD1 encodes serine at position 111 and would be incapable of forming such a disulfide bridge. To test the role of disulfide linkages between cysteine 111 residues in the co-aggregation of WT and mutant human SOD1, we mutated cysteine 111 of WT human SOD1 to serine and then co-transfected this construct with G85R human SOD1; finding that we could still

detect co-aggregation of this modified WT human SOD1 with mutant protein. We cannot rule out the possibility that cysteine 111 of the mutant human SOD1 mediates a disulfide linkage with another cysteine in C111S human SOD1 (cysteines at positions 6, 57, or 146); however, it is clear that the linkage cannot be between cysteine 111 of the two proteins. Additionally, we have noted that we can supplement the buffers used in our detergent extraction protocols with as much as 30% β-mercaptoethanol (β-ME, a strong reducing agent) without noting significant reductions in the amount of mutant SOD1 that fractionates to detergent-insoluble fractions (see Figure 4-7). These data provide compelling evidence that disulfide cross-linking is not a primary mechanism by which the structure of aggregates are maintained [also see (Karch and Borchelt, 2008)]; and we think it unlikely that disulfide-linkages are responsible for the co-sedimentation of WT human SOD1 with mutant human SOD1. Rather, we suggest that the co-sedimentation of WT human SOD1 with mutant human SOD1 is likely to involve more intimate protein-protein interactions.

Role of WT and Mutant SOD1 Interactions in Disease

In a study by Deng and colleagues (Deng et al., 2006), the co-expression of WT and mutant human SOD1 in transgenic animals, produced by mating two distinct lines of mice, showed earlier onset of disease and earlier age to paralysis; with the symptomatic mice showing high levels of detergent-insoluble forms of both WT and mutant protein. If aggregation of mutant SOD1 were one of the driving forces in age to disease onset, then increasing the concentration of total SOD1, through the addition of WT human SOD1 protein, could potentially decrease the “nucleation” phase of protein aggregation; which is well established to be highly concentration-dependent (Jarrett and Lansbury, Jr., 1992). However, in our cell culture model, we find that the presence of

WT human SOD1 slows the aggregation of mutant protein. The most informative data in our experiment is a comparison of mutant SOD1 aggregate loads in cells co-transfected with mutant SOD1 constructs and constructs for GFP to cells co-transfected with mutant and WT SOD1 constructs. As compared to GFP, WT SOD1 co-expression reduced overall amounts of aggregated mutant SOD1 that accumulated in 24 hours. We interpret this finding as evidence that WT human SOD1 does not provide a concentration-dependent enhancement of mutant SOD1 aggregation. Whether the effect of WT SOD1 on mutant SOD1 aggregation occurs at the level of aggregate nucleation is difficult to address in our cell culture system. It is possible that WT SOD1 interferes with the growth phase of aggregation in which small oligomers of protein assemble into larger sedimentable aggregates.

If our cell culture studies accurately model events that occur *in vivo*, then our data would argue that the basis for accelerated disease onset in the mouse studies of Deng and colleagues (Deng et al., 2006) is not attributable to accelerated rates of mutant SOD1 aggregation. However, the foregoing study demonstrated that mice expressing low levels of A4V human SOD1 never develop disease and do not develop SOD1 aggregates, whereas mice that co-express high levels of WT human SOD1 with low levels of A4V human SOD1 develop disease with spinal cords that contain aggregated SOD1 protein (undetermined whether WT, A4V, or both) (Deng et al., 2006). This latter outcome suggests a direct involvement of SOD1 aggregation in disease pathogenesis.

However, other recent studies have demonstrated that aggregation of mutant SOD1 may be dissociable from the toxic events that drive disease onset. Co-expression

of high levels of the copper chaperone for SOD1 (CCS) with G93A SOD1 greatly accelerates the onset of disease while reducing the level of G93A SOD1 aggregation (Son et al., 2007). Moreover, we have recently determined that the accumulation of the larger sedimentable aggregates of mutant SOD1 in ALS mouse models occurs largely after disease onset (Karch et al., 2009). These recent findings indicate that disease onset may not be governed by the rate of mutant protein aggregation. Whether other aspects of disease, such as progression, are related to the rates of mutant protein aggregation is a subject of study.

Although the cell model we use here has high utility in assessing the aggregation propensity of mutant SOD1, it is not well suited for studies of toxicity. The advantage of the model is that aggregation occurs without an exogenous stimulus, such as inhibition of proteasomes or other toxic insult. However, the levels of expression achieved are admittedly well above physiologic levels and thus we are hesitant to conclude that any toxicity observed in this cell model over a 24 or 48 hour period would equate to events occurring over a much longer time frame in either mouse models or humans. Deciphering the mechanism by which WT human SOD1 overexpression heightens the toxicity of mutant SOD1 will require development of more physiologically relevant cell models, or innovative approaches to studying molecular events in animal models.

Conclusions

In a cell culture model of mutant SOD1 aggregation, we find evidence that WT SOD1 is a direct modulator of mutant human SOD1 aggregation, with the predominant effect being to slow aggregation rates. More than 100 mutations in SOD1 have been associated with ALS and, given the variability in the biophysical properties of these mutants, we think it is highly likely that the magnitude of the effect of WT protein on the

aggregation rate of mutant human SOD1 will vary. Indeed in our small sample of mutants in the present study, we find that that the effect of WT SOD1 on the aggregation of A4V human SOD1 appears to be distinct from that of the G85R or G93A variants. In human SOD1-associated ALS, disease occurs in a setting of equivalent expression of WT and mutant SOD1 subunits. We propose that the modulation of mutant human SOD1 aggregation by WT enzyme may introduce another factor that influences the age to onset, or rate of progression, of disease in humans.

CHAPTER 5
A COMPLEX ROLE FOR WILD-TYPE SOD1 IN THE TOXICITY AND AGGREGATION OF ALS-ASSOCIATED MUTANT SOD1[1]

Introduction

Work presented in the previous chapter (Chapter 4) describes the ability of WT SOD1 to modulate aggregation of mutant proteins in a cell culture model. Results from such studies demonstrate that the co-aggregation of WT and mutant human SOD1 proteins is not a consequence of increased amounts of expressed SOD1 protein, as WT SOD1 slows mutant SOD1 aggregation. However, the role of WT SOD1 on disease remains controversial (see "Implications of WT SOD1 in ALS and Aggregation" in Chapter 1, and introduction of Chapter 4).

The variability in the results of the different studies may be explained by the type of mutant SOD1 protein expressed in conjunction with WT human SOD1, the background of the strain of mice used, and/or the relative expression levels of WT and mutant human SOD1 proteins in the mice. In the present study we have directly compared the WT human SOD1 mouse line used in the Bruijn's study to the mouse line used in the other studies (Jaarsma, Deng and Wang's studies) to determine to what degree these mice contributed to the differences observed between these studies. With each of these WT human SOD1 lines of mice, we created double transgenic mice expressing WT human SOD1 and either L126Z or G37R human SOD1 mutant proteins. The results of our studies demonstrate that the variability in the rate of disease onset observed in previously published studies can be explained by differences between the WT human SOD1 lines of mice used, and by the specific mutant human SOD1 protein

[1]The work presented here is a manuscript in preparation that will be submitted shortly for publication.

expressed in these mouse lines. Further, all double WT and mutant human SOD1 transgenic mice created shared the ability to form detergent-insoluble SOD1 aggregates of WT and mutant human SOD1 proteins that accumulate at disease endstage. Thus, our data provide: 1) clarification of the effect of WT human SOD1 on disease progression in mutant SOD1 transgenic mice, and 2) insight into the role that WT human SOD1 has modulating aggregation of mutant human SOD1 proteins.

Materials and Methods

A list of materials used can be found in Appendix B. Methodology used for the work presented in this chapter is described in “Chapter 5 Methods” of Appendix C.

Results

A study by Bruijn and colleagues, reported that mice transgenic for both WT and G85R human SOD1 developed disease at the same age as mice transgenic only for the mutant gene (Bruijn et al., 1998). However, several recent studies have shown that the presence of WT human SOD1 in mice expressing mutant human SOD1 (A4V, G85R, G93A, T116X, or L126Z) accelerates disease onset (Jaarsma et al., 2000;Deng et al., 2006;Deng et al., 2008;Wang et al., 2009c). The study by Bruijn used a different line of WT SOD1 mice than used by the 4 studies that reported WT SOD1 co-expression accelerates disease. To determine if the different lines of WT human SOD1 mice used in these studies produce different outcomes, we crossed three different strains of WT human SOD1 mice to mice expressing either PrPG37R or L126Z human SOD1 proteins. The three WT human SOD1 strains of mice used were:1) B6SJL-Tg(SOD1)2Gur/J hybrid line (SJL WT for abbreviation) (Gurney et al., 1994) [previously shown to accelerate disease when co-expressed with A4V, L126Z, G93A (Deng et al., 2006), T116X (Deng et al., 2008), or G85R (Wang et al., 2009c)], 2) B6/L76 WT SOD1

Wong congenic line (L76 WT for abbreviation) (Wong et al., 1995) [shown not to have an effect on disease onset or duration when co-expressed with G85R) (Bruijn et al., 1998)], and 3) a variant of the B6SJL-Tg(SOD1)2Gur/J Gurney hybrid line, here termed congenic (Cg) WT, that was backcrossed to C57BL/6J (Gurney et al., 1994) to create a strain possessing a equivalent background to that of the B6/L76 WT SOD1 Wong congenic line. We compared side by side the levels of human SOD1 mRNA and protein in the different WT human SOD1 mouse strains used in this study, using northern and western blot analyses, respectively. The mRNA and protein levels of SOD1 in spinal cords isolated from each WT SOD1 strain of mice was normalized using PrP mRNA or β-tubulin III protein as loading controls, respectively. The results from these analyses showed that both mRNA and protein levels were approximately 30% higher in SJL and Cg WT strains of the Gurney mouse line compared to the L76 WT Wong line (Figure 5-1).

We further characterized the three WT mouse strains used in our study by analyzing the coding sequence of SOD1 in these mice. Thus, we performed real time polymerase chain reaction (RT-PCR) analysis from mRNA isolated from spinal cords of each strain. Each of the resulting RT-PCR products (Figure 5-2A) were then cloned into a vector and sequenced. The sequencing results revealed identical SOD1 cDNA sequences (Figure 5-2B), demonstrating that the three strains of the two transgenic WT human SOD1 lines used in this study contain identical WT SOD1 proteins, with the only difference of expressing such transgene at different levels.

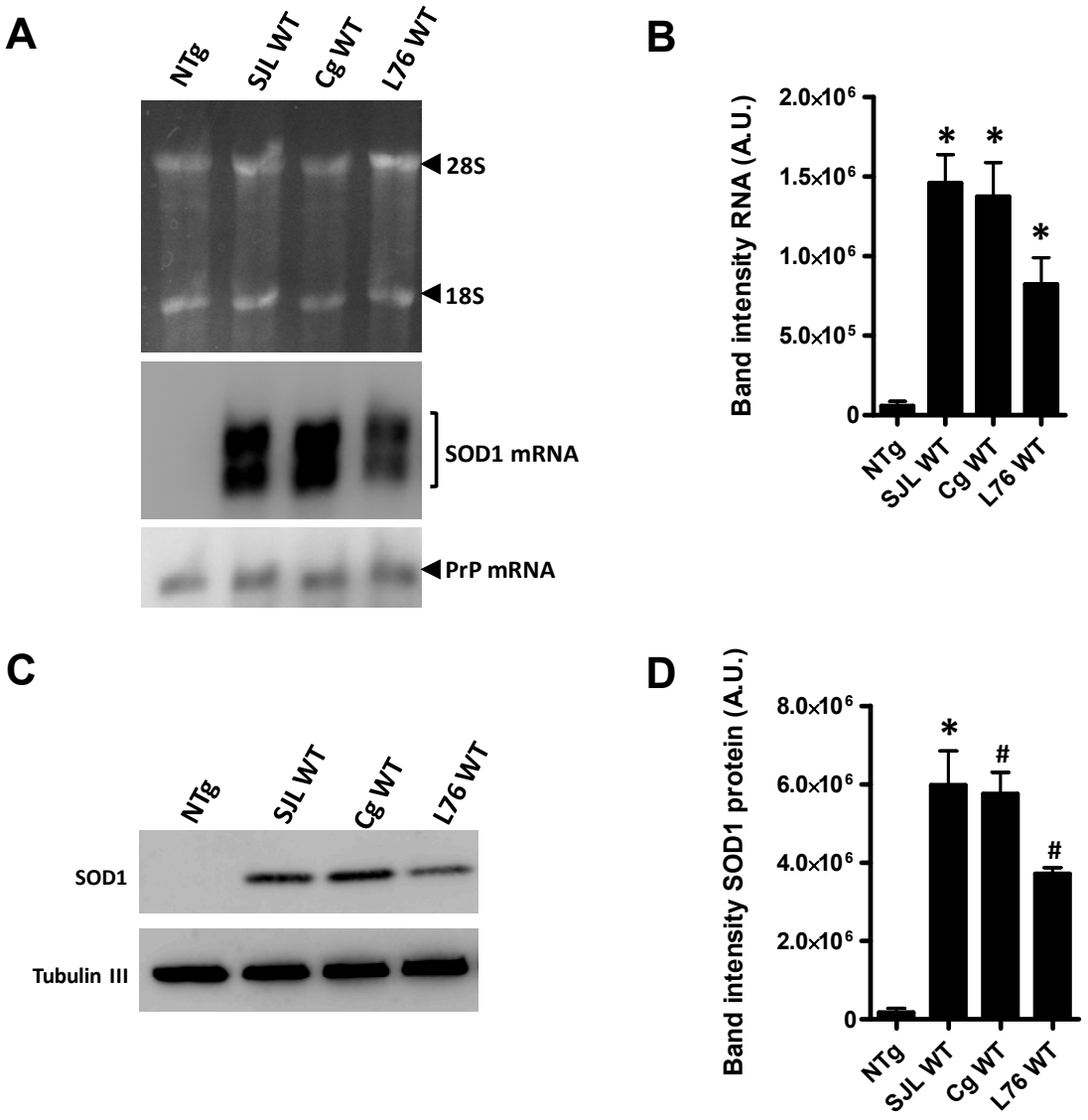

Figure 5-2. WT Gurney lines express higher mRNA and protein levels than WT Wong line. A) Northern blot showing the mRNA levels in the spinal cords of the WT lines used in this study for which mRNA of the mouse prion protein (PrP) was used as a loading control. B) Quantification of the mRNA levels normalized to the PrP control. C) Western blot analysis of same animal cords and detected with a human SOD1 antibody. Antibody recognizing β-tubulin III was used as a loading protein control. D) Quantification of the human WT protein levels normalized to loading control. Statistical differences in B) and D) were assessed thought unpaired student *t*-tests: $^{*}p \leq 0.05$, $^{\#}p \leq 0.005$. Bars represent mean ± SEM of three different spinal cords for each mouse line.

A

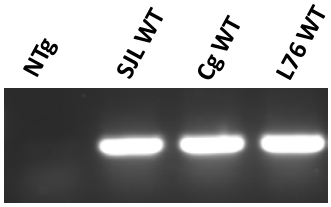

B

```
SOD1 cDNA      1 MATKAVCVLKGDGPVQGIINFEQKESNGPVKVWGSIKGLTEGLHGFHVHEFGDNTAGCTSAGPHFNPLSRKHGGPKDE
SOD1 SJL WT    1 MATKAVCVLKGDGPVQGIINFEQKESNGPVKVWGSIKGLTEGLHGFHVHEFGDNTAGCTSAGPHFNPLSRKHGGPKDE
SOD1 Cg WT     1 MATKAVCVLKGDGPVQGIINFEQKESNGPVKVWGSIKGLTEGLHGFHVHEFGDNTAGCTSAGPHFNPLSRKHGGPKDE
SOD1 L76 WT    1 MATKAVCVLKGDGPVQGIINFEQKESNGPVKVWGSIKGLTEGLHGFHVHEFGDNTAGCTSAGPHFNPLSRKHGGPKDE

SOD1 cDNA     79 ERHVGDLGNVTADKDGVADVSIEDSVISLSGDHCIIGRTLVVHEKADDLGKGGNEESTKTGNAGSRLACGVIGIAQ
SOD1 SJL WT   79 ERHVGDLGNVTADKDGVADVSIEDSVISLSGDHCIIGRTLVVHEKADDLGKGGNEESTKTGNAGSRLACGVIGIAQ
SOD1 Cg WT    79 ERHVGDLGNVTADKDGVADVSIEDSVISLSGDHCIIGRTLVVHEKADDLGKGGNEESTKTGNAGSRLACGVIGIAQ
SOD1 L76 WT   79 ERHVGDLGNVTADKDGVADVSIEDSVISLSGDHCIIGRTLVVHEKADDLGKGGNEESTKTGNAGSRLACGVIGIAQ
```

Figure 5-2. All WT SOD1 lines express the same cDNA WT SOD1 sequence. A) Agarose gel showing results from RT-PCR from non-transgenic (NTg) or WT mouse cords. B) Automated sequence analyses of the RT-PCR products indicate identical WT SOD1cDNA sequences (top lines).

One line of mutant SOD1 mice used in this study is heterozygous for the G37R SOD1 mutation, which is driven by the mouse prion promoter (PrPG37R SOD1). This promoter drives transgene expression primarily in muscle and neural tissue (Wang et al., 2005b). The expression levels of the PrPG37R *SOD1* transgene in heterozygous mice are known to be too low to produce an ALS phenotype in mice. However, when G37R expression levels are increased by breeding the mice to homozygosity, the resulting mice manifest typical ALS symptoms and pathology (Wang et al., 2005b). Thus, while heterozygous PrPG37R mice do not develop ALS over the course of their 2 year lifespan, homozygous PrPG37R mice develop paralysis at about 8 months of age (Wang et al., 2005b). The other mutant SOD1 mouse line that we also used expresses the L126Z SOD1 transgene, which is controlled by the normal SOD1 human promoter and consists of modified genomic SOD1 (Wang et al., 2005a). The survival time for this line of mice is also 8 months (Wang et al., 2005a).

To study *in vivo* the effect of WT SOD1 from different mouse lines on disease and aggregation of SOD1 proteins, we performed matings of WT human SOD1 mice to either PrPG37R or L126Z human SOD1 mice. We obtained five different types of double transgenic mice expressing WT and mutant human SOD1 proteins: PrPG37R/SJL WT, PrPG37R/Cg WT, PrPG37R/L76 WT, L126Z/SJL WT, and L126Z/L76 WT. In PrPG37R/SJL WT mice, we observed survival times of 5 months of age (160.1 ± 2.40 days, N = 18), which was even shorter than that of homozygous PrPG37R SOD1 mice (paralyzed at 8 months, 252.6 ± 4.75 days, N = 20). Mice co-expressing G37R protein, and the WT SOD1 from the congenic Gurney strain variant (Cg WT), also became paralyzed very early (190.1 ± 1.01 days, N = 7), but at about a month later than PrPG37R/SJL WT mice (Figure 5-3A). Mice expressing G37R/L76 WT became paralyzed at about 7 months (213.8 ± 4.35 days, N = 13), which represents an earlier age than for paralyzed homozygous PrPG37R mice (Figure 5-3A). Thus, although heterozygous PrPG37R SOD1 mice are asymptomatic, mice expressing G37R/WT human SOD1 proteins developed ALS-like disease and reached endstage at earlier time points than PrPG37R SOD1 homozygous mice.

Similar to the outcome described above, in double transgenic mice harboring human WT and the L126Z mutant human SOD1 proteins, were observed earlier onsets of paralysis in mice transgenic for both L126Z and WT human SOD1 that comes from the Gurney WT line of mice. L126Z/SJL WT mice developed disease between 5-6 months of age (170.1 ± 4.74 days, N = 10; Figure 5-3B), which represents about 2 to 3 months earlier than mice expressing just L126Z SOD1 (214.1 ± 3.74 days, N = 53). However, L126Z/L76 WT double transgenic mice did not develop paralysis until 8

months of age (224.8 ± 6.41 days, N = 16; Figure 5-3B), which is the same age of paralysis as for L126Z singly transgenic SOD1 mice. Thus, only the co-expression of WT SOD1 from the SJLWT strain, but not the L76 WT strain, of mice translated into a more rapid development of paralysis in mice harboring the L126Z SOD1 mutation.

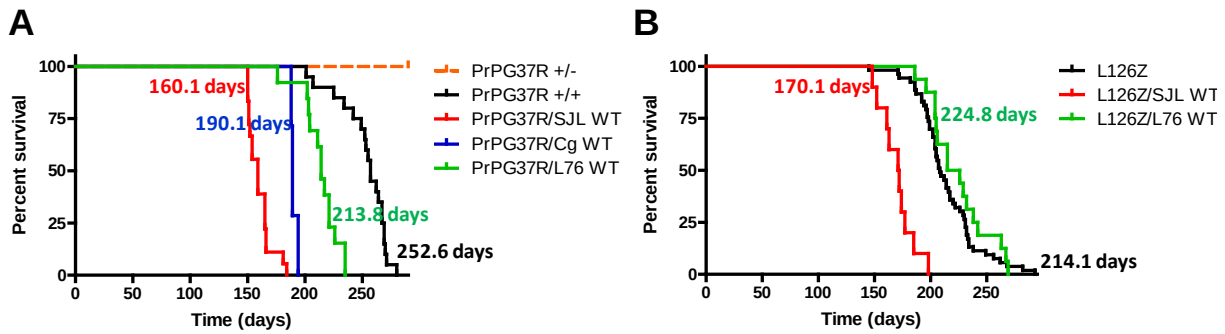

Figure 5-3**.** WT SOD1 protein from Gurney's mice significantly accelerates disease in mice harboring either PrPG37R or L126Z mutations, while the effect of WT SOD1 derived from Wong's mice (L76 WT) is not as strong. A) Survival curves of mice from PrPG37R crosses. B) Survival curves of mice from L126Z crosses. Survival times were estimated as the time comprised between birth and when animals are required to be sacrificed as hindlimb paralysis impeded them reach food and water. Unpaired *t*-test demonstrated statistical differences in lifespan between homozygous PrPG37R mice and PrPG37R/SJL WT ($p \leq 0.0001$), PrPG37R/Cg WT ($p \leq 0.0001$), and PrPG37R/L76 WT ($p \leq 0.0001$); and between L126Z mice and L126Z/SJL WT ($p \leq 0.0001$), but not with L126Z/L76 WT ($p = 0.5177$).

Previous studies have established that spinal cords of paralyzed mice expressing mutant SOD1 contain detergent-insoluble aggregates of mutant protein (Deng et al., 2006). Additionally, Deng and colleagues observed that the earlier disease phenotype in mice expressing both WT (SJL WT strain) and mutant SOD1 (L126Z) accumulated insoluble forms of WT and mutant SOD1 proteins (Deng et al., 2006). Thus, we sought to determine whether any of our double transgenic mice contain aggregated WT and/or mutant human SOD1 proteins. In order to do that, we use a biochemical assay and western blotting techniques to detect the proportion of SOD1 protein that becomes

insoluble in non-ionic detergent. With this assay, we detected the presence of detergent-insoluble aggregates in the spinal cords of endstage PrPG37R/WT mice (Figure 5-4A, P2). The levels of SOD1 in the detergent-insoluble (P2) and soluble (S1) fractions were quantified and graphed as the ratio of P2 to S1; we refer to this value as aggregation propensity. In all PrPG37R/WT mice the accumulation of detergent-insoluble SOD1 species is significantly higher than heterozygous PrPG37R mice, and similar to homozygous symptomatic PrPG37R SOD1 mice (Figure 5-4B). In L126Z/WT mice, we were able to distinguish WT from L126Z protein on immunoblots due to the smaller size of the truncated mutant protein. Thus, in all L126Z/WT mice we detected detergent-insoluble forms of WT and mutant SOD1 proteins (Figure 5-4C). Note that we were unable to detect detergent-soluble forms of the L126Z protein due to its very rapid turnover (Figure 5-4C). Because we can specifically detect WT SOD1 in detergent-soluble and insoluble fraction of these mice, we were able to estimate aggregation propensity (P2/S1). We found that the aggregation propensity of WT in L126Z/WT mice is much lower than the aggregation propensity of G37R SOD1 in homozygous PrPG37R mice (compare Figures 5-4B and 5-4D). Thus, much lower proportions of WT SOD1, compared to mutant SOD1 proteins, are able to become part of detergent-insoluble aggregates. In the case of L126Z/WT mice, approximately equivalent levels of WT and mutant SOD1 proteins were present in the detergent-insoluble fraction (Figure 5-4E). The observation of WT and L126Z human SOD1 proteins co-aggregating in double transgenic mice, is consistent with what has previously been described by Deng and colleagues (Deng et al., 2006).

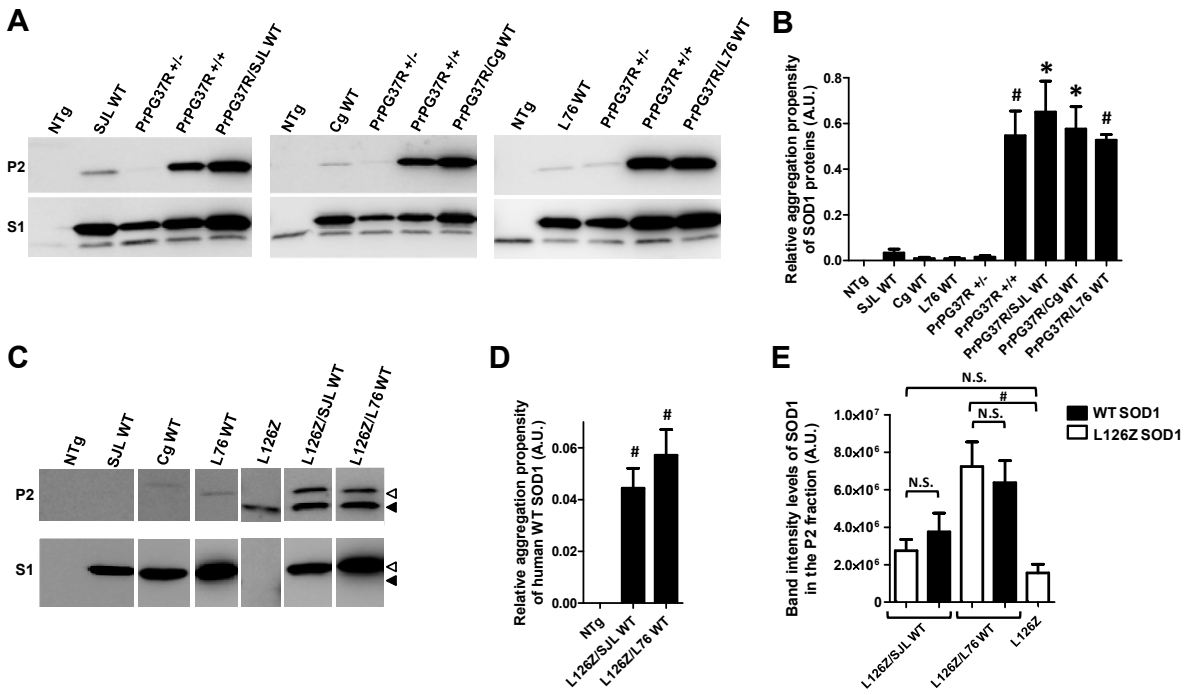

Figure 5-4. Symptomatic mice present significant accumulation of detergent-insoluble SOD1 aggregates at endstage. A, C) Western immunoblots of detergent-insoluble (P2) and detergent-soluble (S1) fractions of spinal cord transgenic mice. SOD1 protein was detected with an antibody that recognizes mouse and human SOD1 (A), or an antibody specific for human SOD1 (C). Note that the truncation mutant, due to its size, migrates faster (black arrowheads) than human WT SOD1 (open arrowheads). B, D) Quantification of aggregation propensity of PrPG37R/WT crosses (B) and human WT in L126Z/WT crosses (D). E) Quantification of the relative protein levels of WT (black bars) and L126Z (white bars) SOD1 present in double transgenic L126Z/WT mice. Statistical differences of aggregation propensity were compared to non-transgenic (NTg) animals by unpaired student *t*-test: $^{*}p \leq 0.05$, $^{\#}p \leq 0.005$, of at least three different spinal cords per line. N.S.: non-significant differences.

As described above, western blot analysis allowed us to determine the presence of WT and mutant human SOD1 in the detergent-insoluble fractions of L126Z/WT SOD1 mice. However, WT and G37R human SOD1 proteins cannot be distinguished by standard western blot techniques. Thus, to further explore whether WT human SOD1 is also present in the P2 fraction of PrPG37R/WT mice, we analyzed spinal cords of symptomatic PrPG37R/SJL WT mice through hybrid linear ion-trap Fourier-transform

ion cyclotron resonance mass spectrometry (FTMS) analyses. Data from such analyses indicated the presence of WT and G37R human SOD1 proteins in the detergent-insoluble P2 fraction of two different samples from spinal cords expressing PrPG37R and SJL WT transgenes (Figures 5-5A and 5-5B). Additionally, a portion of WT and G37R SOD1 proteins were also detected in the S1 fractions (Figures 5-5C and 5-5D). Notably, in both the P2 and S1 fractions, the intensity of the signal for WT SOD1 was much greater than that of the G37R protein. In the S1 fraction, the mass spectrometry data suggested that WT SOD1 was present in much greater quantities than the mutant in the double transgenic animals. However, these data did not appear to be congruent with the data we obtained from immunoblots of PrPG37R/WT mice, in which the levels of WT protein should be only about twice more abundant than for the G37R protein (Figure 5-6).

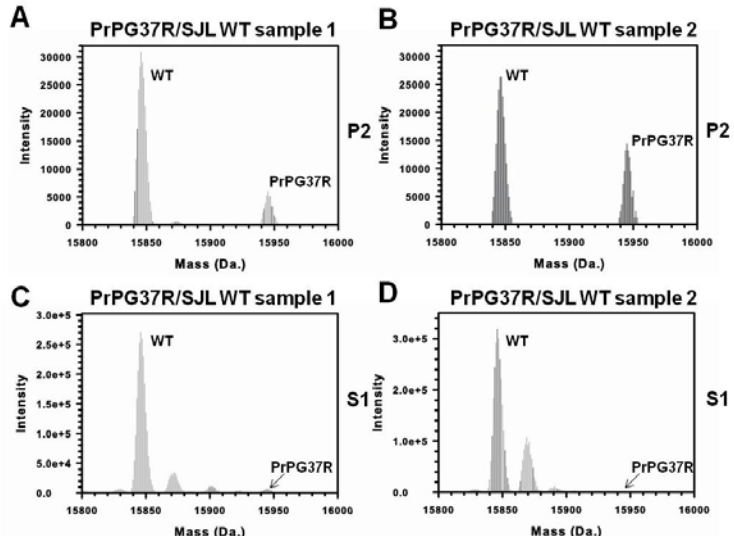

Figure 5-5. WT SOD1 is present in detergent-insoluble fractions of spinal cords of PrPG37R/SJL WT mice. A-D) FTMS analyses of P2 (A, B) and S1 (C, D) fractions from two different sets of spinal cord samples. For each sample, a total of three spinal cords were combined (from different symptomatic PrPG37R/SJL WT mice) and extracted in detergent as explained in methods. Volumes of 1.2 ml for S1 and 100 µl for P2 were obtained and sent for FTMS analysis.

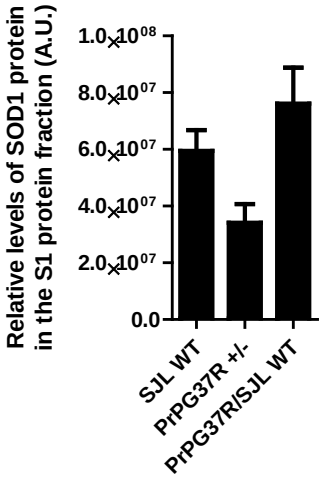

Figure 5-6. Protein levels in the detergent-soluble fraction of heterozygous SJL WT and PrPG37R are not more than two fold different. The amount of S1 protein was calculated from western blot data of samples presented in Figure 5-4. Although SJL WT protein levels are higher than the levels of G37R protein in heterozygous mice, this difference was not statistically significant.

Previous analyses in cell culture have demonstrated that the co-expresssion of WT and mutant SOD1 at 1:1 ratios does not lead to a rapid increase in aggregation of SOD1 proteins. Instead, we have previously demonstrated that WT SOD1 protein slows, but does not block, the aggregation of several human SOD1 variants (A4V, G85R, and G93A) (Prudencio et al., 2009a). However, as early as 48 hours of co-expression, both proteins (WT and mutant) co-sediment in the detergent-insoluble, aggregated fraction (Prudencio et al., 2009a). Here we evaluated the ability of WT human SOD1 to modulate aggregation of G37R and L126Z human SOD1 mutant proteins in cell culture. Co-transfections of WT and G37R human SOD1 proteins, at 24 hours did not produce detectable levels of aggregated human SOD1 proteins (Figures 5-7A and 5-7B, 24 hours), demonstrating the ability of WT human SOD1 in slowing aggregation of G37R SOD1 proteins. However, at 48 hours after transfection we observed significant accumulation of aggregated SOD1 proteins in the WT + G37R

human SOD1 co-transfection. Additionally, the total amount of aggregated SOD1 in the P2 fraction was lower when WT and G37R were co-expressed as compared to when G37R SOD1 was co-expressed with GFP (a control for nonspecific effects of co-transfection) (Figures 5-7A and 5-7, 48 hours). Thus, it appears that in the cell model, WT human SOD1 slows the aggregation of G37R SOD1.

In co-transfections of WT SOD1 with the L126Z SOD1 truncation mutant, we evaluated aggregation propensity only at the 48 hour transfection interval. Cells expressing only L126Z SOD1 presented high levels of aggregated protein and small quantities of soluble SOD1 protein (Figures 5-7C and 5-7D). However, in L126Z + WT SOD1 co-transfected cells there were virtually undetectable levels of aggregated WT or L126Z human SOD1 proteins (Figures 5-7C and 5-7D). In the co-transfection control (L126Z SOD1 + GFP), we observed levels of aggregated L126Z protein that were significantly higher than the aggregation propensity of L126Z in the WT + L126Z SOD1 co-transfection (Figures 5-7C and 5-7D). These findings indicate that, at least in our cell model, the presence of WT SOD1 produces a pronounced slowing of L126Z mutant SOD1 aggregation.

In previous work, we have demonstrated that a major portion of the mutant SOD1 that accumulates in aggregates lacks the normal intramolecular disulfide bond (Karch et al., 2009). Additionally, high levels of disulfide reduced mutant SOD1 protein have been associated, in specific settings, with a much shorter lifespan of mutant SOD1 mice (Proescher et al., 2008;Son et al., 2009). Thus, we sought to evaluate whether the high level expression of WT SOD1, in the double transgenic mice, might elevate the overall levels of reduced SOD1 in spinal cord. Using previously described western blotting

techniques (Jonsson et al., 2006a;Zetterstrom et al., 2007;Karch et al., 2009), we found that, in the three WT strains of mice, at steady-state levels about 10% of WT SOD1 protein lacked the normal disulfide bond at old ages (Figures 5-8A and 5-8B).

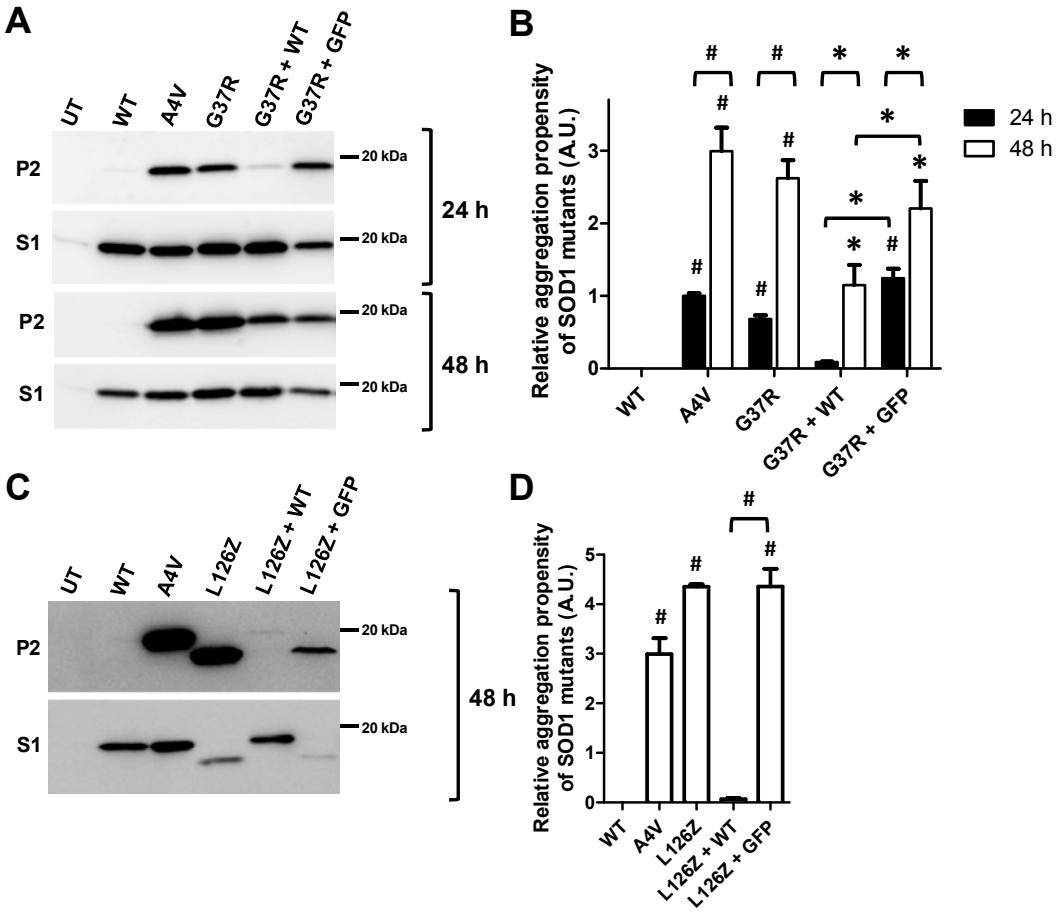

Figure 5-7**.** Human WT SOD1 slows aggregate formation in cell culture and such effect is stronger for the L126Z SOD1 truncation mutant. A, C) Aggregate formation determined by western blot of transiently transfected cells for 24 (A, upper panels) or 48 (A, lower panels; and C) hours. In co-transfections of WT and mutant SOD1 or mutant SOD1 and GFP (the latter as a control for co-transfection), we used equimolar amounts of each plasmids; with the total amount of transfected protein remaining the same for all reactions (4 µg). B, D) Relative aggregation propensity of SOD1 proteins were calculated as P2/S1 ratios, and paired student *t*-test were performed as statistical analyses. Note that relative values of aggregation propensity are normalized to P2/S1 value of A4V at 24 hour transfection (set to 1). Symbols over the bars indicate differences with human WT SOD1 transfected cells, or as indicated in the figure: $^{*}p \leq 0.05$, $^{\#}p \leq 0.005$. Bars represent mean ± SEM of a minimum of 3 independent transfection experiments.

Additionally, in younger SJL WT mice, about 10% of the WT protein also migrated on SDS-PAGE as expected for reduced SOD1 (Figures 5-8C and 5-8D). In double transgenic PrPG37R/SJL WT symptomatic mice, the levels of reduced SOD1 protein does not differ from aged matched SJL WT SOD1 singly transgenic mice (Figures 5-8C and 5-8D). Thus, it appears that the co-expression of WT and mutant SOD1 in double transgenic mice does not lead to an increase in the overall levels of reduced mutant SOD1 protein, and the total levels of reduced SOD1 appear to be the sum of the individual amounts of reduced WT and mutant SOD1.

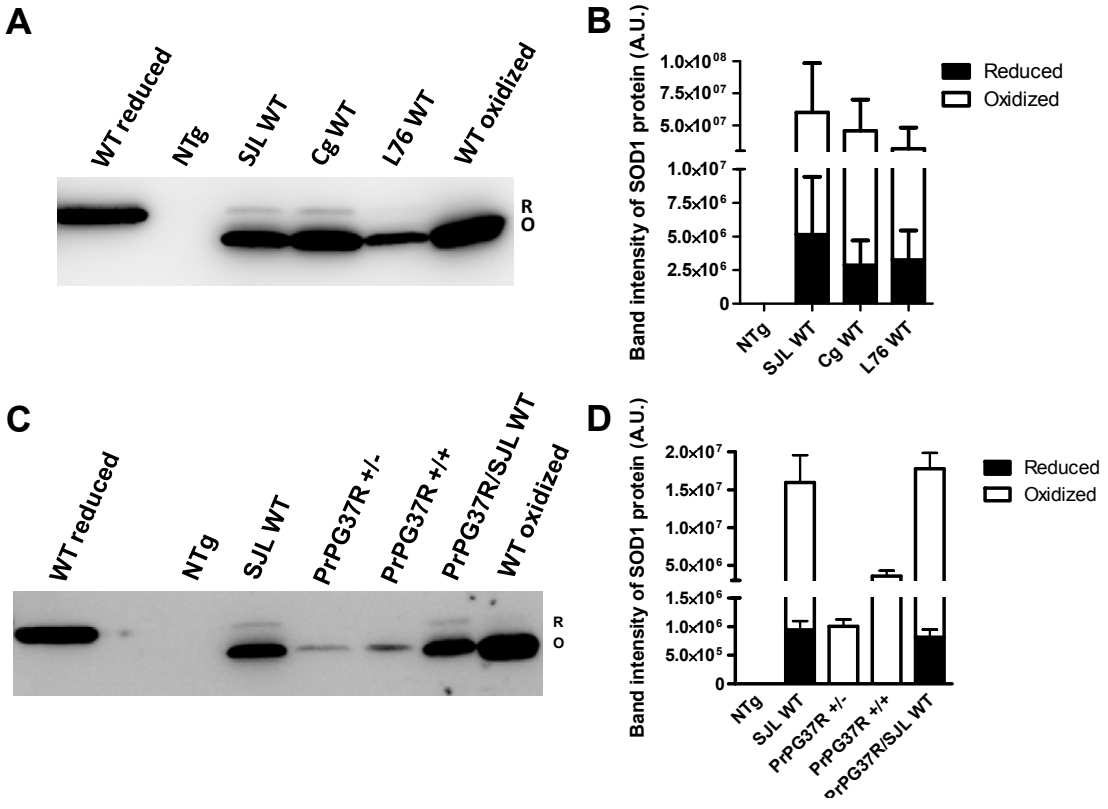

Figure 5-8. Low amounts of reduced WT SOD1 protein are present in all WT lines of mice. A, C) Immunoblots of reduced an oxidized proteins in spinal cord extracts of different lines of old (> 11 months) WT SOD1 mice (A), or in young (8 months) single and double transgenic mice (C). R: reduced, O: oxidized. B, D) Quantification of the band intensities of at least three independent experiments from reduced and oxidized WT or mutant proteins in old (B) or young (D) animals.

Recent *in vitro* studies have demonstrated that small quantities of immature disulfide reduced WT SOD1 protein can be induced to aggregate (Chattopadhyay et al., 2008). Thus, to investigate whether any of the strains of WT SOD1 mice may accumulate aggregates of SOD1 protein, we performed detergent extraction analyses and determination of aggregate levels at young (< 8 months) and old (> 11 months) ages. For the Gurney line, in both SJL and Cg WT strains, significant accumulations of aggregated WT SOD1 protein were found as early as 8 months (SJL WT), and increased to higher levels at 11 (SJL WT) and 17 (Cg WT) months of age (Figures 5-9A and 5-9C). However, WT SOD1 in the L76 WT SOD1 line did not show significant accumulation of detergent-insoluble protein by 17 months of age (Figures 5-9A and 5-9C). Importantly, the levels of aggregation propensity for WT human SOD1 protein in any of the lines were not as high as in symptomatic L29 G37R mice (Figures 5-9A and 5-9C), which accumulates relatively low levels of aggregated SOD1 at disease endstage (Karch et al., 2009).

Analyses of total protein levels at young and old ages showed that the amount of WT SOD1 protein in the different strains of mice increases with age, and the overall WT SOD1 levels at old ages between Gurney and Wong lines remain constant, that is the Gurney line (SJL and Cg WT) expressing about 30% higher protein levels than the Wong L76 WT line (Figures 5-9B and 5-9D). These data suggest that the higher expression levels of WT human SOD1 in the Gurney mice (SJL and Cg WT) translates into increased amount of misfolded WT SOD1.

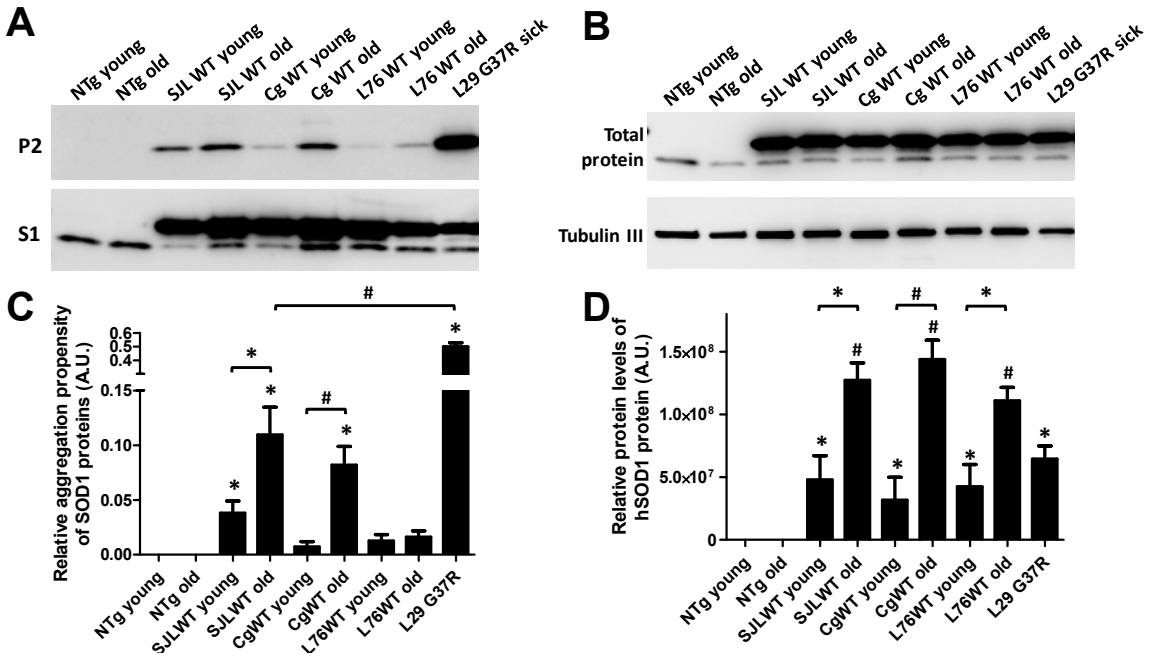

Figure 5-9. WT SOD1 from Gurney lines (SJL and Cg), but not from Wong line (L76), forms detergent-insoluble SOD1 aggregates at old ages. A, B) Immunoblots of S1 and P2 fractions (A), or of total SOD1 levels (B) of mice expressing WT SOD1 at young (4 months, or 8 months for SJL WT) or old (17 months, or 11 months for SJL WT) ages. An antibody that recognizes mouse and human SOD1 was used. NTg: non-transgenic mice. β-tubulin III was used as a loading control for total protein. C, D) Quantification of the aggregation propensity (C) or of total SOD1 protein levels (D). Paired student *t*-tests were performed to establish significant differences with NTg mice, or as indicated: $^{*}p \leq 0.05$, $^{\#}p \leq 0.005$. Bars represent mean ± SEM.

Discussion

In the present study, we investigated the apparent discrepancy in studies regarding the potential for WT human SOD1 to accelerate the course of disease caused by the expression of mutant SOD1 in transgenic mice. A study by Bruijn and colleagues reported that the course of disease caused by expression of the G85R variant of human SOD1 is not changed by either co-expression with human WT SOD1 or elimination of endogenous mouse SOD1 expression (Bruijn et al., 1998). However, more recently, using a different line of WT human SOD1 mice (B6SJL-Tg(SOD1)2Gur/J, here termed SJL WT), Wang and colleagues reported that co-expression of WT and mutant SOD1

accelerated disease caused by transgenic expression of human G85R SOD1 (a different line of G85R mice was used) (Wang et al., 2009c). Additionally, multiple studies using the SJL WT mice have demonstrated that mice transgenic for the transgene array in this line of WT SOD1 and transgenic for mutant SOD1 constructs, develop disease much earlier than mice transgenic for only the mutant SOD1 genes (Jaarsma et al., 2000;Deng et al., 2006;Deng et al., 2008). Our study clarifies this discrepancy by demonstrating that the effects of the two different mouse lines of WT SOD1 on disease in mice expressing mutant SOD1 is influenced by the nature of the mutation and the level of WT SOD1 expression.

We show that in WT and mutant (G37R or L126Z) human SOD1 double transgenic mice, there is acceleration in the development of hindlimb paralysis that is independent of the strain background in which the WT SOD1 transgenic lines were originally raised. The more rapid disease is associated with the appearance of detergent-insoluble SOD1 aggregates that contain both, WT and mutant human SOD1 proteins at disease endstage. Further, an earlier age of hindlimb paralysis correlates with a higher dose of WT human SOD1 protein expressed. These data demonstrate a potential role for WT human SOD1 in SOD1-associated ALS.

Acceleration of Disease by WT and Mutant SOD1 Overexpression is Independent of Strain Background.

Previous studies of WT and mutant human SOD1 transgenic mice have shown that WT human SOD1 either accelerates or has no effect on disease onset, compared to mice that only overexpress a given human SOD1 mutation (Bruijn et al., 1998;Deng et al., 2006;Deng et al., 2008;Wang et al., 2009c). In our hands, double transgenic mice expressing mutant human SOD1 and either high (from Gurney WT mice) or low (from

Wong L76 WT mice) levels of WT human SOD1 can induce an earlier disease onset of symptoms. However, while all mutant/WT mice with WT human SOD1 protein that derives from the Gurney mouse line (SJL hybrid and Cg congenic strains) present significant acceleration in the development of hindlimb paralysis, mutant/WT mice expressing a WT SOD1 protein that derives from L76 WT human SOD1 mice (from the line of Wong and colleagues) suffer a less severe effect (in PrPG37R/L76 WT mice) or no effect at all (in L126Z/L76 WT mice) in accelerating onset of paralysis. Thus, we observed clear differences on the effect of WT SOD1 derived from two different lines, even when the WT protein comes from mice of equivalent strains (L76 and Cg WT). This finding demonstrates that the strain background in which the Gurney and Wong's mouse lines were initially raised in does not account for the different outcomes. Rather, the different expression levels of WT human SOD1 from the different mouse lines may explain the stronger effect of the Gurney line *vs*. the Wong L76 line.

Earlier Disease in Mutant/WT Mice is Associated With Aggregated SOD1.

Mice expressing different human mutant SOD1 proteins are characterized by a significant accumulation of detergent-insoluble aggregates of mutant SOD1 at disease endstage (Karch et al., 2009). In all our doubly transgenic mutant/WT human SOD1 mice, hindlimb weakness and paralysis is accompanied by the accumulation of detergent-insoluble species of SOD1 proteins. The overall aggregated protein levels in the different PrPG37R/WT double transgenic mice are more or less equivalent, and similar to the levels of PrPG37R protein in symptomatic mice. For L126Z/WT mice the overall amount of detergent-insoluble species were higher than in L126Z singly transgenic mice (see Figure 5-4), and WT and L126Z human SOD1 are present at similar levels in the P2 fraction. Thus, it appears that in L126Z/WT mice the presence of

WT protein increases the amount of protein that is detergent-insoluble, with WT SOD1 protein becoming part of this aggregated fraction. However, in terms of aggregation propensity of L126Z/WT mice, only a small portion of total WT SOD1 protein becomes detergent-insoluble, while the totality of L126Z SOD1 protein that we able to detect by western blotting techniques remains detergent-insoluble. These data indicate that in L126Z/WT mice the ability of the mutant protein to aggregate is much higher than for WT SOD1 protein, with possibly mutant SOD1 increasing the ability of WT SOD1 to misfold and aggregate. Since double transgenic mice reach endstage at earlier time points than singly transgenic mice, detergent-insoluble aggregated SOD1 species are also detected earlier in double mutant/WT SOD1 mice. A possible explanation for the shorter lifespan of doubly transgenic mice is by acceleration on the formation of toxic species, which would translate into the appearance of aggregates at earlier times, as they reach the same aggregation propensity levels at endstage. In this case, WT human SOD1 contributes to this more rapid aggregation rates by being included into the aggregated fraction (see Figures 5-4 and 5-5). Alternatively, rates of aggregation may not change in double transgenic mice and WT SOD1 would only exert a role in disease initiation, thus moving disease development, and aggregate formation events, to earlier times. Still, whether the toxic effect of WT SOD1 in mutant SOD1 transgenic mice has something to do with the co-aggregation phenomenon remains uncertain.

Co-aggregation of WT and Mutant SOD1 is Dependent on SOD1 Protein Levels

For PrPG37R/WT and L126Z/WT mice, SOD1 aggregates at disease endstage contain WT and mutant human SOD1 proteins. Based on the western blot data from L126Z/WT mice, it appears that only a small proportion of total levels of WT human SOD1 protein accumulates in the detergent-insoluble SOD1 fraction, but constitutes

protein of equal levels of WT and L126Z human SOD1 in the P2 fraction (see Figure 5-4). However, we cannot distinguish WT and mutant human SOD1 in PrPG37R/WT mice through western blot analysis. To determine whether insoluble aggregates of WT SOD1 are generated in the PrPG37R/WT SOD1 mice, we used FTMS analysis to demonstrate the presence of WT SOD1 in the P2 fractions. Due to uncertainties regarding the relative ability of FTMS analysis to detect the WT and G37R proteins, we are not able to use the FTMS data to establish the relative abundance of WT and G37R SOD1 in the insoluble aggregates of these mice. However, it is possible that aggregates in the PrPG37R/WT SOD1 mice contain more WT than mutant protein. Thus, the larger effect of WT SOD1 on PrPG37R mice might rely on a higher proportion of WT human SOD1 that can be incorporated into detergent-insoluble aggregated protein fraction.

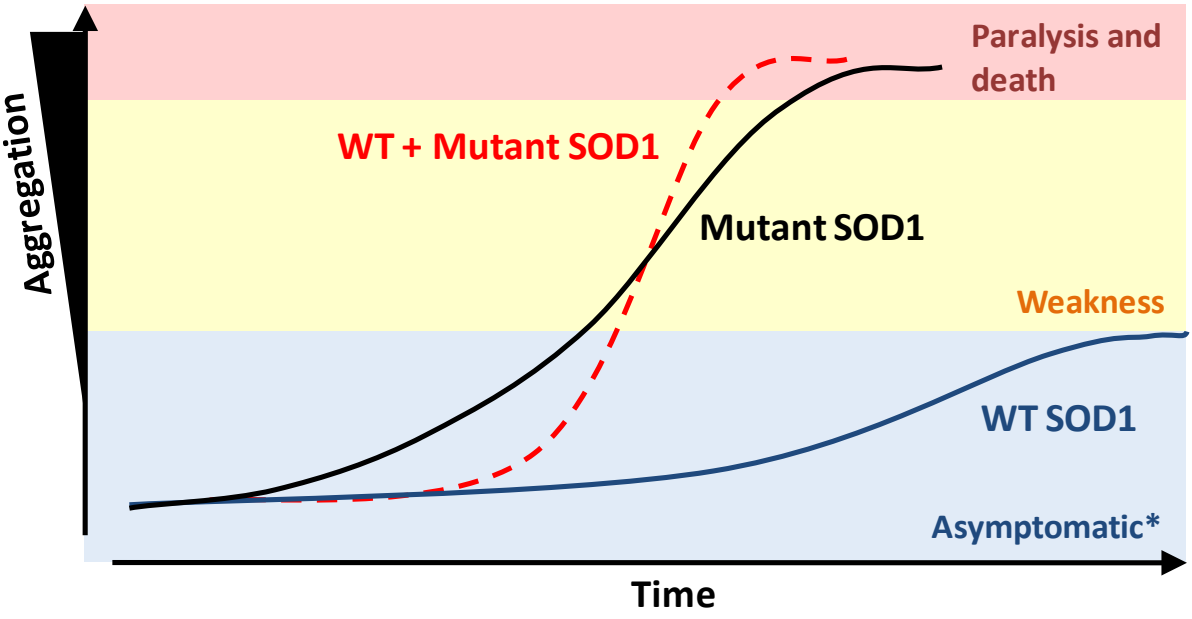

Figure 5-10. Hypothetical model on the effect of WT SOD1 on disease and aggregation in mice expressing a mutant SOD1 mutation. The asterisk (*) indicates asymptomatic mice with no obvious symptoms of weakness or other abnormalities.

The Complexity of WT-Mutant Co-aggregation

In cell culture mutant/WT SOD1 co-expression at 1:1 ratios translates into aggregation levels much lower than mutant alone (compare mutant aggregation propensity in co-transfection with that of mutant + GFP at 24 or 48 hours, see Figure 5-7). This data demonstrates that when WT human SOD1 is co-expressed with mutant SOD1, the rates of mutant SOD1 aggregation are different from those of cells expressing only mutant human SOD1 proteins, indicating that WT human SOD1 is an important modulator of mutant SOD1 aggregation. At longer transfection intervals (48 hours) WT and mutant (G85R or G93A) human SOD1 proteins can be seen to co-aggregate in cell culture (Prudencio et al., 2009a), while the aggregation propensity for other mutants is still reduced (see Figure 5-7). Thus, cell culture studies indicate that WT SOD1 protein does not readily co-aggregate with mutant SOD1 proteins.

A likely explanation on the delay of WT and mutant human SOD1 co-aggregation in cell culture may reside on the ability of WT and mutant human SOD1 to interact with each other. G37R and WT SOD1 protein are likely to easy interact which other, since previous reports demonstrate their ability to form active heretodimers of WT and G37R proteins (Borchelt et al., 1994). Thus, we explain the higher impact of WT human SOD1 protein in asymptomatic PrPG37R mice as a result of a better interaction between WT and G37R proteins. In the case of SOD1 truncation mutants, like L126Z, WT and mutant human SOD1 would be less likely to interact. Additionally, the very rapid turnover of this truncated mutant (hardly detected when soluble in detergent) would make harder for any interactions to occur. However, studies in cell culture and animal models expressing L126Z and WT human SOD1 proteins indicate that some kind of interactions take place between both proteins (Deng et al., 2006;Furukawa et al., 2006).

Thus, higher levels of WT human SOD1 protein (that come from Gurney WT line) are necessary to observe an effect of WT SOD1 on disease in L126Z/WT transgenic mice. A hypothetical model on the effect of WT human SOD1 in disease and aggregation is represented in Figure 5-10. In such model we propose that aggregation occurs in 3 steps: 1) A nucleation phase, in which initial subunits of disulfide immature or misfolded SOD1 come together to form a “core” from which aggregation can initiate; 2) A growth phase, where detergent-insoluble species start accumulating in the cells; and 3) A final phase, which coincides with onset of paralysis in mice and where cells are saturated with detergent-insoluble aggregates and may present other high molecular weight disulfide linked species. According to our model, aggregation of mutant SOD1 proteins (black line) occurs at a rate that varies depending on the SOD1 mutation expressed and that would reach final aggregation stages that coincided with paralysis. However, aggregation of WT SOD1 (blue line) occurs at much lower rates, with significant accumulation of detergent-insoluble species when expressed in cells for long periods of time and at very high levels. This late accumulation of WT SOD1 aggregates would then coincide with the appearance of subtle motor abnormalities. Finally, we propose that when co-expression of WT and mutant SOD1 takes place (dotted red line), the nucleation phase of aggregation is increased, compared to mutant protein alone, due to a) longer time required for WT-mutant interactions to occur, b) a more rapid degradation of soluble WT-mutant proteins, c) a less likely chance of mutant aggregating units to come together due to the existence of WT units, and/or d) nucleation event of WT-mutant complexes occurs at slower rates due to the more difficult ability of WT to nucleate and aggregate. Then, once nucleation of WT and mutant SOD1 proteins

occurs, the growth phase would be much faster than for mutant alone. This more rapid growth phase can be explained by either the fact that the presence of WT human SOD1 proteins exerts some kind of toxicity in mutant/WT SOD1 mice that translates into a more rapid accumulation of detergent-insoluble aggregates. Or alternatively, the addition of high amounts of SOD1 protein, in this case WT SOD1, allows a more rapid growth phase of aggregation.

Critical Levels of Reduced WT SOD1 Protein Can Initiate WT Aggregation.

Previously, Jonsson and colleagues showed the ability of WT human SOD1 protein to aggregate in SJL WT mice (Jonsson et al., 2006a). Here, we used higher detergent concentration to determine the portion of SOD1 that is detergent-insoluble. Also, with our assay, we observed that WT SOD1 protein expressed from Gurney line is able to form aggregates at old ages; but not from WT protein expressed from the Wong line (see Figure 5-9). Previous studies have shown that WT SOD1 in the apo, disulfide reduced form can aggregate *in vitro* (Chattopadhyay et al., 2008). Here, we determined that as much as 10% of the steady state levels of WT human SOD1 protein correspond to WT protein that is in a disulfide reduced state (see Figure 5-7). We have also shown that Gurney WT mouse line expresses about 30% more WT human SOD1 protein that the Wong line (see Figure 5-1). Thus, the overall levels of disulfide reduced WT SOD1 in the Gurney line are then higher than in the Wong mouse line. Since, the Wong L76 WT line does not appear to present the same ability to form significant levels of aggregated SOD1 protein at old ages, we may suggest that the overall protein levels of WT SOD1 protein required for aggregation are just below a required threshold. Additionally, it is possible that the required protein threshold could have something to do with the proportion of disulfide reduced SOD1 protein expressed. Overall, it appears

that in order for WT SOD1 to significantly aggregate, compared to mutant protein, WT SOD1 requires both higher protein expression levels and longer intervals.

We also noted that Gurney WT mice (SJL and Cg WT), but not L76 WT Wong mice, presented some motor abnormalities as early as a year of age (data not shown). And in many instances animals died unexpectedly or the veterinary recommended euthanasia before we could age them past 15 months of age. However, none of the WT lines showed ALS-like symptoms in their lifespan, supporting previously published data (Gurney et al., 1994;Wong et al., 1995). Abnormalities in these mice at about 15-20 months of age have been described previously.(Tu et al., 1996;Jaarsma et al., 2000;Jaarsma et al., 2008). These include neurofilament inclusions at about 135 days of age (Tu et al., 1996); and swollen mitochondria, vacuoles, as well as ubiquitinated inclusions that appear as early as 280 or 490 days of age respectively (Jaarsma et al., 2000;Jaarsma et al., 2008). However, such abnormalities have not been described for the L76 WT line of SOD1 mice (Wong et al., 1995). Thus, the ability of the Gurney WT, but not L76 WT Wong line, to form detergent-insoluble aggregates of SOD1 protein may account for the motor abnormalities observed in this WT SOD1 line.

Mechanisms of Toxicity

Previous studies by Witan and colleagues have shown that WT/mutant SOD1 heterodimers induce higher toxicity that mutant homodimers in *C. elegans* while the aggregation levels were reduced (Witan et al., 2008). Additionally, they suggest that the role of WT human SOD1 on disease is through stabilization of mutant SOD1 as a soluble protein (Witan et al., 2008;Witan et al., 2009). However, our results on the L126Z truncation mutant indicate that in the presence of WT SOD1, at different levels, soluble L126Z protein remains still undetectable. Thus, the instability of this protein in its

soluble state does not support higher toxicity of mutant through stability of soluble state by WT SOD1.

The overexpression of CCS in mutant SOD1 transgenic mice accelerates disease without the formation of SOD1 aggregates (Son et al., 2007;Proescher et al., 2008;Son et al., 2009). In this case it has been suggested that the ability of CCS to transport immature SOD1 into mitochondria translates into a more severe phenotype (Son et al., 2007;Proescher et al., 2008;Son et al., 2009). Additionally, increased mitochondrial toxicity and earlier disease onset due to CCS overexpression has only been observed in G37R and G93A SOD1 transgenic mice (Son et al., 2007;Son et al., 2009). The incorporation of CCS and SOD1 into mitochondria is thought to occur through a disulfide relay system (Kawamata and Manfredi, 2008), which may explain why in the presence of CCS there is only enhanced toxicity of mutant SOD1 proteins that can form disulfide bonds (Son et al., 2009). An additional study demonstrates that CCS-mutant SOD1 interactions can facilitate import of mutant SOD1 proteins into peroxisomes (Islinger et al., 2009). Thus, it is possible that the altered mutant SOD1 localization, due to CCS overexpression explains the enhanced toxicity in CCS/mutant SOD1 mice (Leitch et al., 2009). An interesting point of the CCS/mutant SOD1 studies is that co-expression of CCS with either L126Z or G86R mutant human SOD1 proteins in mice, does not change disease course (Son et al., 2009). However, the presence of WT human SOD1 that comes from Gurney WT line of mice induces an earlier onset of hindlimb paralysis in mice expressing either L126Z (Deng et al., 2006). or G85R (Wang et al., 2009c) SOD1 proteins. Additionally, the fact that WT SOD1 plays a role in modulating SOD1 aggregation, while this process is absent in CCS/SOD1 mice,

indicates that the toxic effect exerted by WT human SOD1 protein occurs through different mechanisms than those that might take place in the presence of CCS.

Still, it remains unclear whether mutant/WT SOD1 enhanced toxicity is related to any kind of mitochondrial abnormalities. It is known that a very small proportion of WT SOD1 is localized normally in the intermembrane space of mitochondria (Sturtz et al., 2001). Previous studies have found WT and mutant SOD1 accumulates in brain mitochondria, and mutant aggregates are found within this organelle (Vijayvergiya et al., 2005). Additionally, the presence of vacuoles, that in some cases have been shown to derive from mitochondria, have been found in transgenic animal models harboring G37R and G93A mutations (Dal Canto and Gurney, 1994;Wong et al., 1995), as well as in a high expressor WT Gurney line at very old ages (Jaarsma et al., 2000). However, mitochondrial abnormalities are not a common feature of ALS mouse models. Additionally, G93A/WT and L126Z/WT transgenic mice created by Deng and colleagues appeared to present some dysfunctional mitochondrial, but no obvious vacuolar pathology was reported in those mice (Deng et al., 2006). Furthermore, previous studies imply that mutant SOD1 does not translocate into mitochondria but it associates with its cytoplasmic membrane (Liu et al., 2004). These data suggest that although some association of mutant SOD1 with mitochondria might normally take place, the toxic effect of WT SOD1 in mice expressing mutant SOD1 proteins does not involve an internalization of mutant SOD1 proteins into these organelles. Rather, alternative toxic mechanisms are more likely to explain mutant/WT SOD1 toxicity.

In our studies, PrPG37R/WT mice develop disease at earlier times than PrPG37R homozygous mice (PrPG37R/PrPG37R). Thus, G37R/WT SOD1 complexes appear to

induce a higher toxicity than those composed of G37R/G37R, with G37R/WT aggregates appearing at earlier ages but always concomitant with paralysis. In the case of L126Z/WT mice, we observed that aggregates of L126Z are more abundant in the presence of WT SOD1 protein. Additionally, in mutant/WT SOD1 mice, WT becomes part of detergent-insoluble aggregates at endstage, suggesting that mutant/WT co-expression in SOD1 mice increases the levels of misfolded WT SOD1 protein. Thus, we propose that the presence of WT SOD1 protein may stabilize aggregates of SOD1 proteins by some kind of protein-protein interactions. Additionally, co-aggregation of WT and mutant proteins is not likely to require normal dimeric interactions, since the L126Z truncation mutant lack amino acids involved in the dimer interface. The presence of detergent-insoluble aggregated species of SOD1 at disease endstage is not likely to explain events that occur earlier that lead to a more rapid onset of paralysis induced by the presence of WT SOD1 protein. However, still remains a possibility that some other type of aggregated species (oligomers, undetectable multimers, etc.) is responsible for disease initiation. Here, we demonstrate that different levels of WT SOD1 protein have different effects on accelerating onset of symptoms in transgenic mice that express a specific SOD1 mutation. Additionally, stronger effects of WT SOD1 in mutant SOD1 toxicity appear to take place with mutants that present more similarities with WT protein. Co-aggregation of WT and mutant SOD1 indicates possible protein-protein interactions. Thus, further studies directed to elucidate what kind of mutant-WT interactions occur may give insight in the enhanced toxicity provided by the WT SOD1 protein.

CHAPTER 6
CHARACTERIZATION OF DETERGENT-INSOLUBLE AGGREGATES OF MUTANT SOD1 IN CELL CULTURE

Introduction

Animals models and human ALS patients expressing mutant SOD1 proteins are characterized by the presence of protein inclusions, that in some cases have been identified to contain SOD1 (Shibata et al., 1996b;Kato et al., 2000a;Kato et al., 2001b). However the ability to detect SOD1-positive inclusions in transgenic mice has not always been easy (see “Pathology in SOD1-associated ALS and Rodent Models of the Disease” in Chapter 1). In cell culture, examples in which protein aggregates can be visualized utilize techniques that modify the normal cell homeostasis through the use of proteasome inhibitors (Johnston et al., 2000), or by inducing ER stress (Yamagishi et al., 2007). An alternative technique that is increasingly being used to study SOD1 inclusions is by tagging SOD1 with fluorescent proteins (Matsumoto et al., 2005;Witan et al., 2008). The drawback of this technique is that either C- or N-terminal tags localize in the dimer interface of SOD1, thus any kind of tag can possibly affect the normal folding or interactions patterns of SOD1.

The presence of detergent-insoluble SOD1 aggregates is part of the pathology of SOD1-associated ALS. The best way we have to visualize such aggregated species is through a biochemical assay and western blotting (see Chapters 2 to 5). However, it is unclear whether these species are the same as the inclusions observed in cell culture or animal models. Thus, to further study this particular type of mutant SOD1 aggregates we have used fluorescence imaging techniques in cultured cells to a) localize them subcellularly and determine their morphology, and b) determine the implications of the tag in SOD1 aggregate and inclusion formation. These studies provide insight on the

location and morphology of mutant SOD1 aggregates, which could give us clues about their pathogenic role.

Materials and Methods

A list of materials used can be found in Appendix B. Methodology used for the work presented in this chapter is described in “Chapter 6 Methods” of Appendix C.

Results

In order to analyze the morphology and location of mutant SOD1 aggregates, we used our previously described HEK293FT cell culture model to express different SOD1 proteins. We chose A4V and D101N SOD1 mutant proteins for our studies because their different aggregation propensities, A4V high and D101N low (see Chapter 3 for values in aggregation propensity of different mutant SOD1 proteins). The use of these two mutants may help us to understand different stages of inclusion formation. We transiently transfected HEK293FT cells with untagged WT, A4V, or D101N human SOD1 constructs for 24 hours, and performed immunofluorescence SOD1 staining as described in Methods. Cells expressing WT, A4V or D101N SOD1 proteins present uniform SOD1 staining and no particular SOD1 protein inclusion appears to form spontaneously (Figure 6-1). Thus, in natural conditions (without any additional treatment that would modify protein homeostasis) we do not observe any obvious protein inclusion of SOD1.

A possible explanation for our inability to detect mutant SOD1 inclusions resides in the possibility that the amount of endogenous WT SOD1, produced by the human cell line used, may increase the overall SOD1 staining and interfere with the visualization of protein inclusions. Thus, to eliminate the background generated by the amount of endogenous WT SOD1 protein expressed by the use of a human cell line (HEK293FT

cells), we performed transient transfections in a mouse fibroblast cell line (TK negative cells, also commonly known as L cells) and used antibodies specific to human SOD1 to detect transfected protein. The transfection efficiency of our expression plasmids in this cell type is already quite low and in order to observe detergent-insoluble SOD1 aggregates biochemically we need to express such plasmid for at least 48 hours (data not shown). At 48 hours, mouse TK negative cells expressing WT and A4V SOD1 proteins showed a similar pattern of fluorescence than in HEK293FT cells, indicating that human SOD1 proteins in TK negative cells remain in a protein conformation that does not lead to inclusion formation (Figure 6-2). Thus, the elimination of endogenous SOD1 signal in mouse TK negative is not sufficient to allow visualization of inclusions formed by mutant human SOD1.

Another possible explanation regarding inclusion visualization may be explained by the amount of detergent-soluble SOD1 protein *vs.* the amount of detergent-insoluble aggregated SOD1 protein. Indeed the amount of detergent-soluble SOD1 protein expressed in HEK293FT cells is very high. In transient 24 hour transfections, the levels of detergent-soluble SOD1 protein in HEK293FT cells expressing mutant SOD1 is about 2 (A4V) to 10 (D101N) times higher than the levels of detergent-insoluble aggregated proteins (Figure 6-3). Thus, it seems reasonable to explain our inability to observe inclusions that might derive from detergent-insoluble SOD1 protein based on the fact that the amount of such aggregated species is too low compared to the overall levels of soluble SOD1 protein that is normally expressed in transfected cell lines.

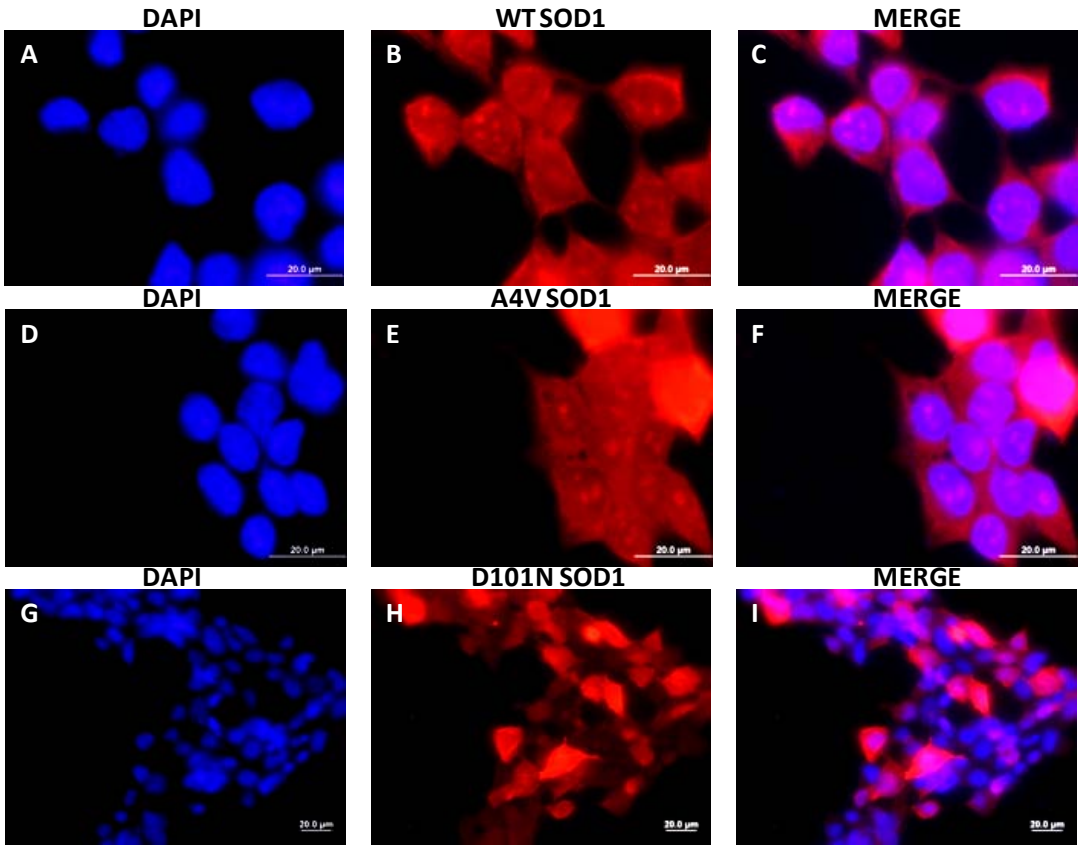

Figure 6-1. HEK293FT cells expressing SOD1 proteins do not form cellular inclusions. A-I) Cells were cultured in glass coverslips previously coated with 0.5 mg/ml poly-L-and transfected with WT (A-C), A4V (D-F), or D101N (G-H) SOD1 for 24 hours. Fixed cells were stained with human SOD1 antibody overnight. A secondary fluorescent (594 nm) antibody was used to visualize SOD1 staining. Co-staining with 4',6-diamidino-2-phenylindole (DAPI) was performed together with secondary antibody incubation. Pictures were taken with either a 100x immersion oil objective, bar 50 µm (A-F); or a 40x objective, bar 20 µm (G-H).

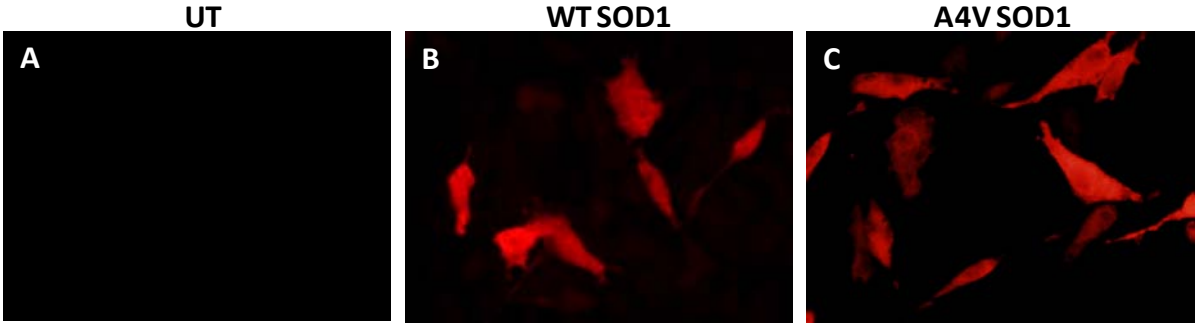

Figure 6-2. TK negative cells transfected with SOD1 constructs for 48 hours and stained for human SOD1 as explained in Figure 6-1. Pictures were taken with a 40x objective.

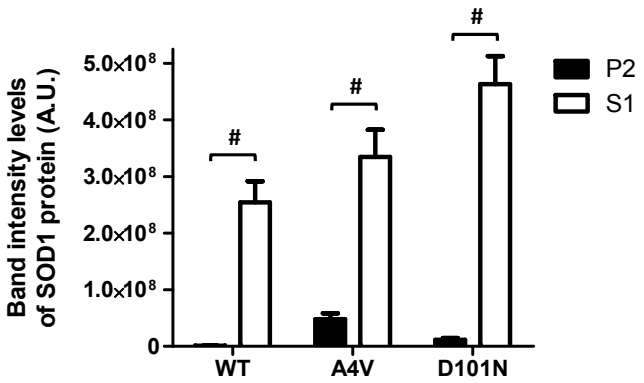

Figure 6-3. HEK293FT transfected cells express higher levels of detergent-soluble SOD1 than detergent-insoluble SOD1 aggregated protein. Band intensities were calculated from western blots of P2 (black bars) and S1 (white bars) fractions, and adjusted for the amount of total protein loaded on the SDS-PAGE gels. The data represented here derives from at least five independent transfection experiments. Significant differences exist between the levels of P2 *vs*. S1 fractions for each SOD1 protein expressed; paired student *t*-test: $^{\#}p \leq 0.005$.

In order to eliminate soluble SOD1 protein, we chose a technique that consists in treating HEK293FT cells with saponin, a mild detergent that open pores on the cellular membranes (Francis et al., 2002). This mild treatment does not kill cells right away and it is intended to allow diffusion of soluble proteins out of the cell. Treatment of cells with such detergent efficiently eliminated part of SOD1 protein that can be visualized through normal immunofluorescence staining techniques, with most of the SOD1 protein concentrated in, and maybe also around, the nuclei. However, we did not observe any obvious immunoreactive inclusion (Figure 6-4). An exception was found in a single cell transfected with A4V SOD1, which presented a few small dot-like inclusions (Figure 6-4E, arrow heads). We also performed the mild detergent treatment in TK negative cells, observing similar pattern of staining to that found in HEK293FT cells treated with saponin (Figure 6-5). However, in this case we observed more obvious punctuate structures. This might be due to the slightly different detergent treatment (digitonin

instead of saponin), but the punctuate structures were not different between cells expressing WT and mutant human SOD1 (Figure 6-5). Thus, we believe that the punctuate staining does not correspond to detergent-insoluble aggregates or inclusions of mutant SOD1 proteins.

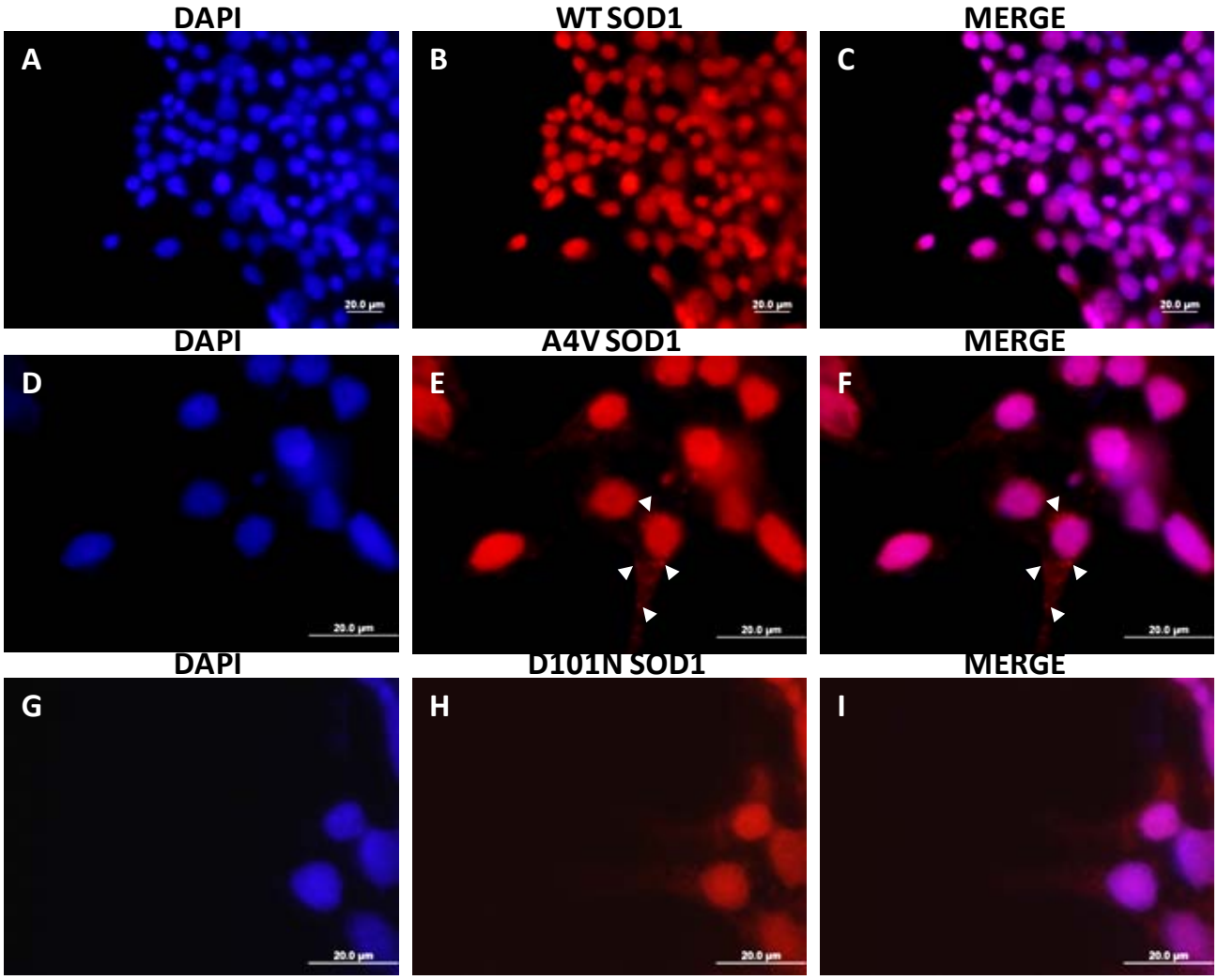

Figure 6-4. Saponin eliminates most of the cytosolic SOD1 protein, but does not uncover the presence of SOD1 positive inclusions. A-I) HEK293FT cells were transfected and stained as explained in Figure 6-1. Saponin treatment was performed prior fixation for 30 minutes at a concentration of 0.01% in 1x PBS. Pictures of WT were taken with a 40x objective (A-C), while A4V (D-F) and D101N (G-I) pictures were taken with an immersion oil 100x objective. All bars represent 20 µm.

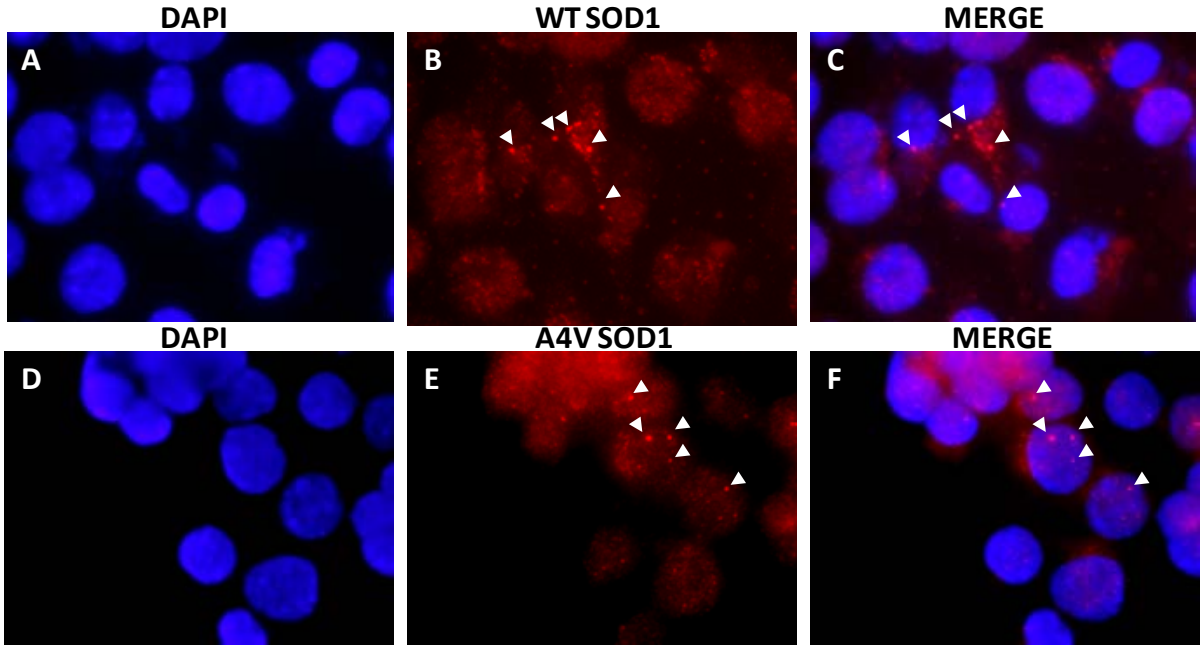

Figure 6-5. Digitonin treatment in TK negative cells show a dot-like pattern of SOD1 that is not exclusive of cells expressing mutant SOD1 proteins. A-F) TK negative cells transfected for 48 hours, treated with 0.01% digitonin in 1x PBS, and stained for human SOD1. Transfection, detergent treatment and staining of TK negative cells was performed as described for HEK293FT cells in Figure 6-4. Pictures corresponding to WT (A-C) and A4V (D-F) were taken using an immersion oil 100x objective.

In conclusion, the use of mild detergent treatments on cells does not allow us to detect aggregates of mutant SOD1. Additionally, this data provides evidence that demonstrate that detergent-insoluble aggregates of mutant SOD1, which we detect through western blot analysis, may be of different nature than big cellular inclusions. Alternatively, it is possible that such aggregated structures may be washed out by the detergent method applied to the cells. Thus, in order to quantify the efficacy of mild detergents (saponin and digitonin) in eliminating detergent-soluble SOD1 from cultured cells (and leaving aggregates inside), we performed a 30 minute incubation of live cells with either saponin or digitonin prior to harvest of the cells; and then we performed analysis of detergent-solubility as previously described (Karch and Borchelt,

2008;Prudencio et al., 2009a;Prudencio et al., 2009b). In both saponin and digitionin treatments, a significant amount of SOD1 protein came out of the cell and into the cell culture media (Figure 6-6). In the case of cells transfected with WT SOD1, it appears that almost the totality of the protein (in S1) was released into the media (Figures 6-6A to 6-6C). However, the overall levels of WT protein expressed are much lower than those of the mutants (Figures 6-6C to 6-6E), indicating that the apparent more effective treatment on cells expressing WT SOD1 is due to the overall lower levels of protein expressed. In each case (WT, A4V, or G93A), the levels of SOD1 released are very similar but not high enough to get rid of all soluble SOD1 protein from the cells. Thus, mild detergent treatments were only partially effective in removing the non-aggregated forms of mutant SOD1 proteins. However, saponin or digitonin treated cells retained the detergent-insoluble aggregated fraction of mutant SOD1. Thus, the SOD1 immunostaining of saponin or digitonin treated cells suggests that detergent-insoluble SOD1 aggregates of mutant SOD1 may be either smaller than visible cellular inclusions, unable to be detected with our current antibodies, or too diffuse to be detected by the described immunocytochemistry techniques.

In view of our observations, we were unable to evaluate the morphology and location of mutant SOD1 aggregates through simple immunofluorescence techniques that do not alter cellular homeostasis or that covalent modify the SOD1 expressed protein. Thus, we decided to study SOD1 inclusions by a protein tagging system. We chose SOD1::YFP (SOD1 fused to YFP) proteins because they are increasingly being used to study aggregation and toxicity in *C. elegans* model (Wang et al., 2009a;Gidalevitz et al., 2009) and in the recently created ALS mouse model expressing

SOD1::YFP (Wang et al., 2009b). The fluorescent tag in these models does not affect SOD1 activity or folding of the YFP tag (Wang et al., 2009a;Gidalevitz et al., 2009).

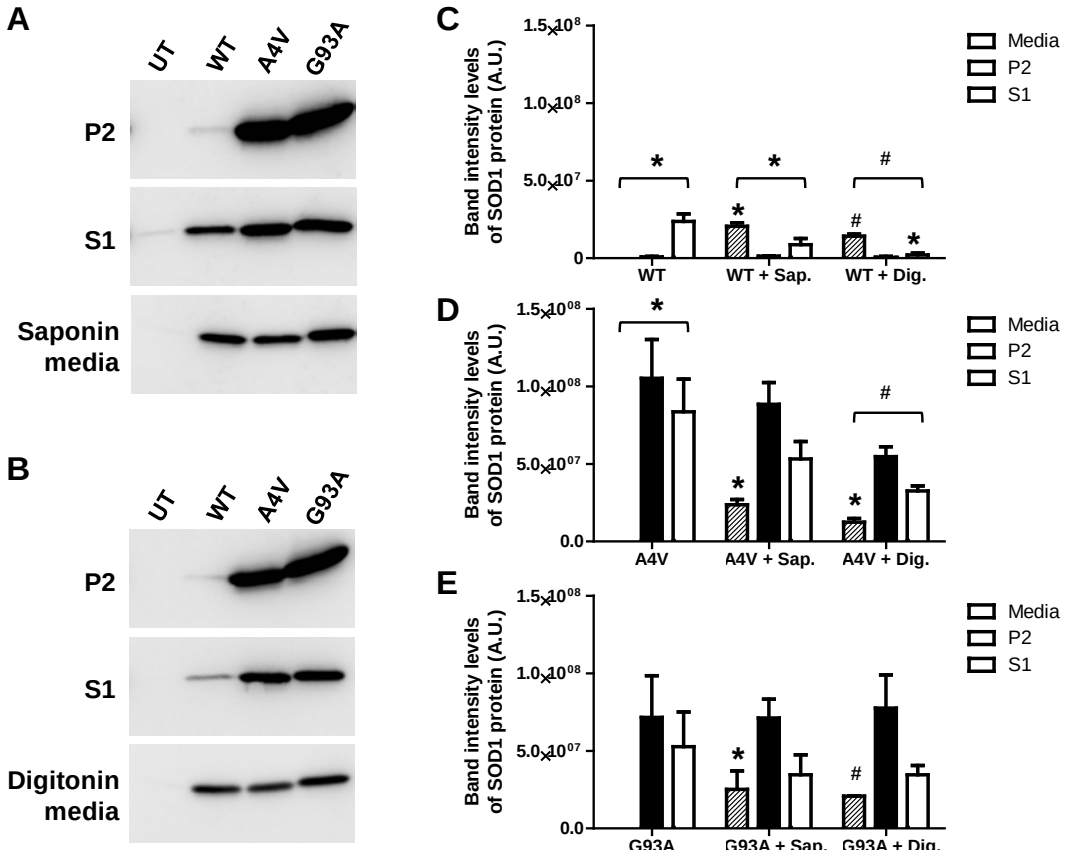

Figure 6-6. Similar effects of saponin and digitonin on eliminating soluble SOD1 protein from HEK293FT cells expressing WT or highly aggregating SOD1 mutant proteins. A, B) Immunoblots of HEK293FT cells transfected with the indicated SOD1 constructs for 48 hours. Prior harvest, cells were incubated 30 minutes in 0.01% detergent, 1x PBS. Then the harvested cell pellets were analyzed by detergent extraction and centrifugation assays. The amount of SOD1 protein released into the cell media was also evaluated. C-E) Quantification of SOD1 protein found in the extracellular space (Media), P2 and S1 fractions of cells untreated or treated with saponin (Sap.) or digitonin (Dig.), and expressing WT (C), A4V (D), or G93A (E). Symbols over bars indicate differences from corresponding non-treated control, or as indicated. Unpaired *t*-tests: $^{*}p \leq 0.05$; $^{\#}p \leq 0.005$.

Transient transfections for 24 hours of WT::YFP (WT SOD1 tagged with YFP) in HEK293FT showed uniform distributions of fluorescence, similar to cells expressing non-tagged WT SOD1 proteins (Figure 6-7B). In this case WT::YFP did not seem to

localize as much protein in the nuclei, being mostly located in the cytosol. We also created a construct to expressed YFP protein by itself. We noted that in this case we can observe a very strong presence of YFP protein in the nuclei (Figure 6-7A), while all our tagged YFP SOD1 proteins (WT and mutants) are mainly located in the cytosol (Figures 6-7B to 6-7L). This outcome can just simply be explained by the bigger size of the fusion protein (about 50 kDa) that impedes SOD1, when tagged, to get easily into the nucleus. In general, cells transfected with high to slow aggregating SOD1::YFP mutants presented from small and many to fewer and larger SOD1 inclusions (Figures 6-7C to 6-7L). Closer observation of inclusion formation in high *vs*. slow aggregating SOD1 mutants suggest possible differences (see Chapters 2 and 3 for more information about selected SOD1 mutants). While YFP or SOD::WT proteins are uniformly spread in the cells, cells expressing the highly aggregating mutants A4V::YFP (Figure 6-7C), G37R::YFP (Figure 6-7D), G85R::YFP (Figure 6-7F), and MDG6FS111Y::YFP (Figure 6-7L) present multiple small inclusions. However, the slowest aggregating mutants H80R::YFP (Figure 6-7E), D101N::YFP (Figure 6-7G), D125H::YFP (Figure 6-7H), E133ΔE::YFP (Figure 6-7I), and S134N::YFP (Figure 6-7J) expressed in cells appeared to be contained in larger discrete areas surrounding nuclei. Interestingly, SODMD protein, which is unable to form detectable levels of detergent-insoluble SOD1 aggregates in cells (see Chapter 2), when tagged with YFP (MD::YFP) produces a fluorescent fusion protein that can be sparsely found concentrating in inclusion structures in different areas of the cell (Figure 6-7K). Note that the SODMD variant that is modified to increase its aggregation propensity, by altering residues at positions 6

and 111 to encode ALS mutations (MDG6FS111Y, see Chapter 2) produces larger and more obvious fluorescent inclusions (Figure 6-7L).

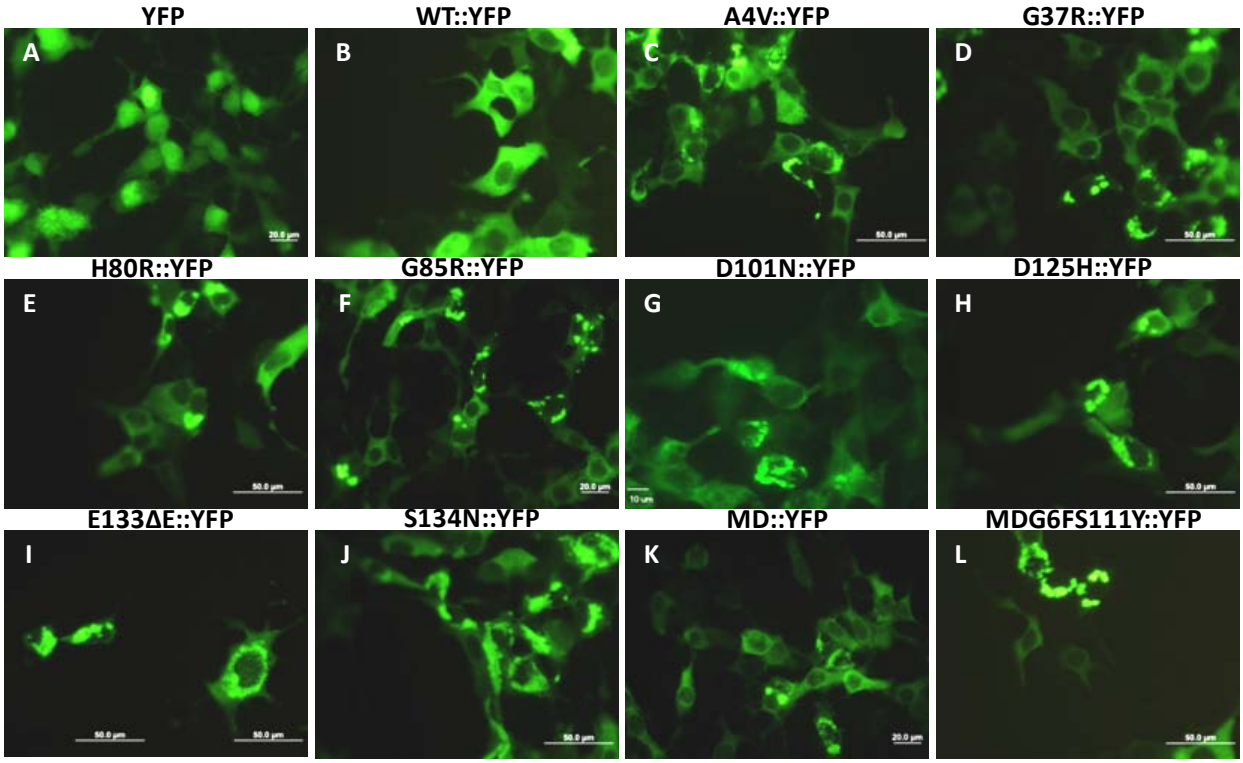

Figure 6-7. Mutant SOD::YFP proteins present variable size and number of inclusions. A-L) HEK293FT cells were transfected in poly-L-lysine coated glass coverslips for 24 hours as described in Figure 6-1. Cells were fixed and observed under a fluorescence microscope. All pictures were taken using a 40x objective, bars10 (G), 20 (A, F, K) or 50 (C-E, H-J, L) µm.

It is possible that the YFP tag may alter the normal location of mutant SOD1 aggregates. However, the impossibility to determine morphology of inclusions of untagged mutant SOD1 in cell culture by simple immunofluorescence techniques makes it a more difficult task. Additionally, the large size of the SOD1::YFP inclusions suggested us that they are unlikely localize in a particular organelle. Thus, we decided to further explore the ability of SOD1::YFP proteins to form inclusions and whether inclusion formation relates to the amount of detergent-insoluble aggregates they can accumulate.

While analyzing SOD1::YFP inclusions we noticed that, in cells expressing WT or the non-aggregating SODMD variant fused to YFP, certain cells appear to accumulate SOD1::YFP protein similar to slow aggregating mutants (see Figure 6-7), while they are known not to be able to form detergent-insoluble aggregated species in cell culture. Thus, we decided to express WT::YFP, D101N::YFP (untagged D101N does not form detergent-insoluble aggregates at 24 hours, but do at 48 hours), and MD::YFP constructs in HEK293FT cells for longer transfection intervals (48 hours) to determine whether inclusions may become more prominent. Effectively, we were able to see increased accumulation of SOD1::YFP proteins in all transfected cells (Figure 6-8). This data confirms our suspicion that YFP tagged SOD1 proteins present a higher tendency to misfold and aggregate that is not common of untagged SOD1 protein.

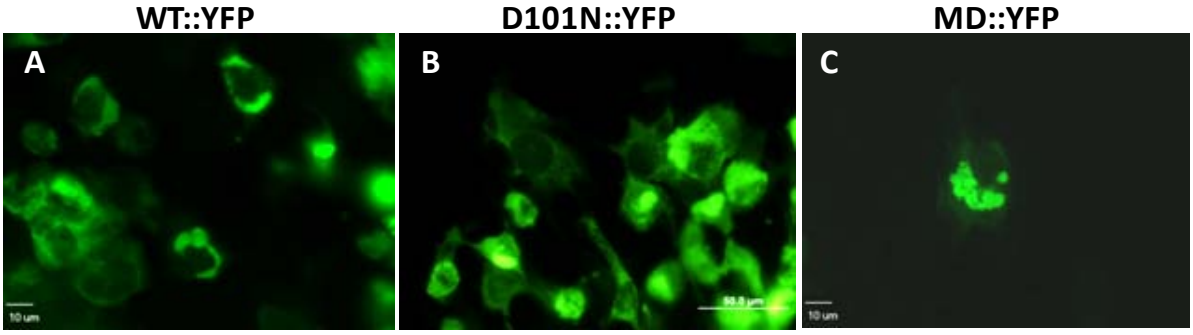

Figure 6-8. Tagged WT::YFP and MD::YFP variants are able to form inclusions, similarly to slow aggregating D101N::YFP proteins when expressed in cells for 48 hours. A-C) HEK293FT cells were transfected for 48 hours with WT::YFP (A), D101N::YFP (B), or MD::YFP (C), and visualized as explained in Figure 6-7. Bars represent either 10 (A, C) or 50 (B) µm, in pictures taken using a 40x objective.

We also explored the ability of WT::YFP to form inclusions in other cell types after a 48 hours transfection. For example, in NIH3T3 cells expressing WT::YFP no obvious inclusion was found (Figure 6-9). Additionally, the number of NIH3T3 cells containing mutant SOD1::YFP inclusions was lower (Figure 6-9), suggesting that the ability of

WT::YFP to form inclusions is time and concentration dependent, as the protein expression levels of our selected plasmids are lower in NIH3T3 than in HEK293FT cells.

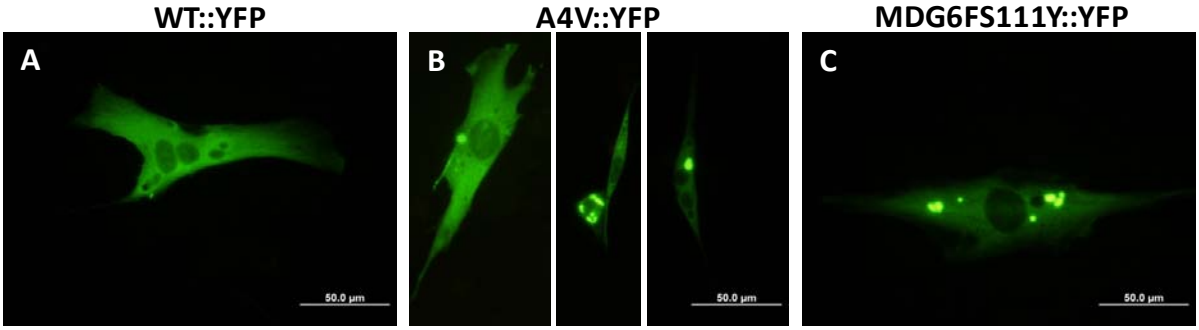

Figure 6-9. NIH3T3 cells express less SOD1::YFP inclusions than HEK293FT after 48 hour transfections. A-C) NIH3T3 cells expressing WT::YFP (A), A4V::YFP (B), or MDG6FS111Y::YFP (C) for 48 hours. Inclusion visualization was performed as described in Figure 6-7. Bars represent 50 µm, in pictures taken using a 40x objective.

Furthermore, we briefly evaluated the ability of other fluorescent tags in inducing mutant SOD1 inclusion formation. We made WT, A4V and D101N SOD1::RFP variants (RFP fused) and tested them in cell culture. At 24 hours the inclusion patterns of A4V::RFP and D101N::RFP (Figures 6-10B and 6-10C) are very similar to A4V::YFP and D101N::YFP, respectively. However, we detected WT::RFP inclusions that resemble those in mutant SOD1::RFP (Figure 6-10A).

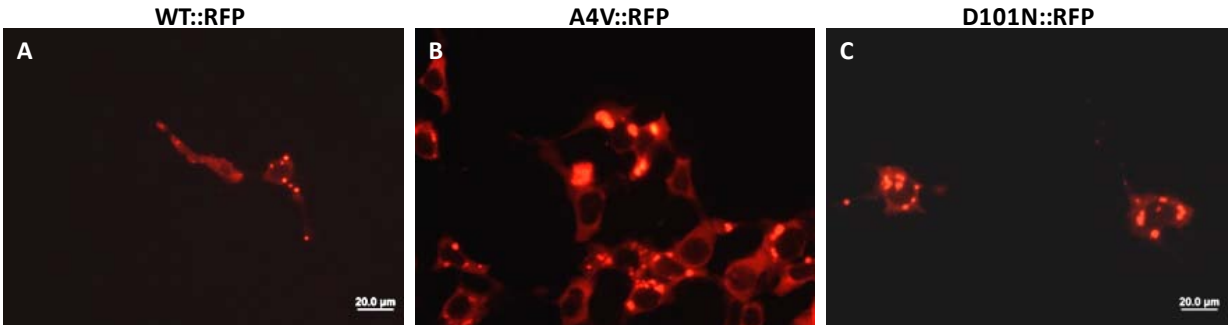

Figure 6-10. WT::RFP proteins form inclusions similar to those formed by mutant SOD1::RFP in HEK293FT cells after 24 hour transfections. A-C) HEK293FT cells expressing WT::RFP (A), A4V::RFP (B), or MDG6FS111Y::RFP (C) for 24 hours. Inclusion visualization was performed as described in Figure 6-7. Bars represent 20 µm, in pictures taken using a 40x objective.

This outcome is similar to a recently published study that reported the ability of WT SOD1 to form inclusions when fused to DsRed2 fluorescent protein (Witan et al., 2009). However, it is unclear why this particular tag can induce WT SOD1 to form inclusions.

In order to determine the relationship between the inclusion structures formed by mutant SOD1::YFP fusion proteins and the detergent-insoluble aggregates formed by untagged mutant SOD1, we examined the detergent solubility of SOD1::YFP fusion proteins. All SOD1::YFP fusion proteins produce some level of detergent insoluble protein, including the WT SOD1::YFP protein (Figure 6-11), which is normally virtually completely soluble without the YFP tag (see Chapters 2 to 5). However, cells transfected with mutant SOD1::YFP fusion proteins accumulated more detergent insoluble SOD1 protein than WT::YFP (Figure 6-11). Additionally, the slow aggregating SOD1 mutants D101N and S134N are known to form detectable levels of detergent-insoluble SOD1 protein at transfection intervals of at least 48 hours (Prudencio et al., 2009b). Here, the D101N::YFP and S134N::YFP protein significantly aggregate, now not different from highly aggregating mutants A4V::YFP or G85R::YFP (Figure 6-11). Similarly, SODMD is able to aggregate when fused to YFP protein (Figure 6-11, see inclusions in Figure 6-8). This data confirms that inclusion formation in HEK293FT cells expressing SOD1::YFP proteins correlates with a higher amount of detergent-insoluble SOD1 protein.

We have previously shown that untagged WT can modulate aggregation of untagged mutant SOD1 proteins (see Chapters 4 and 5). To determine whether the YFP tag in SOD1 interferes with other SOD1 properties, we also examined the effect of WT::YFP and WT SOD1 proteins in modulating aggregation of SOD1 tagged and

untagged A4V and G85R proteins for 24 and 48 hours (Figures 6-12 and 6-13). At 48 hours after transfection, the differences between WT and WT::YFP aggregation propensities are more obvious, while WT SOD1 (untagged) does not significantly aggregate (Figure 6-12). This data suggests that the ability of WT::YFP to form detergent-insoluble SOD1 aggregates may alter its ability to modulate mutant SOD1 aggregation.

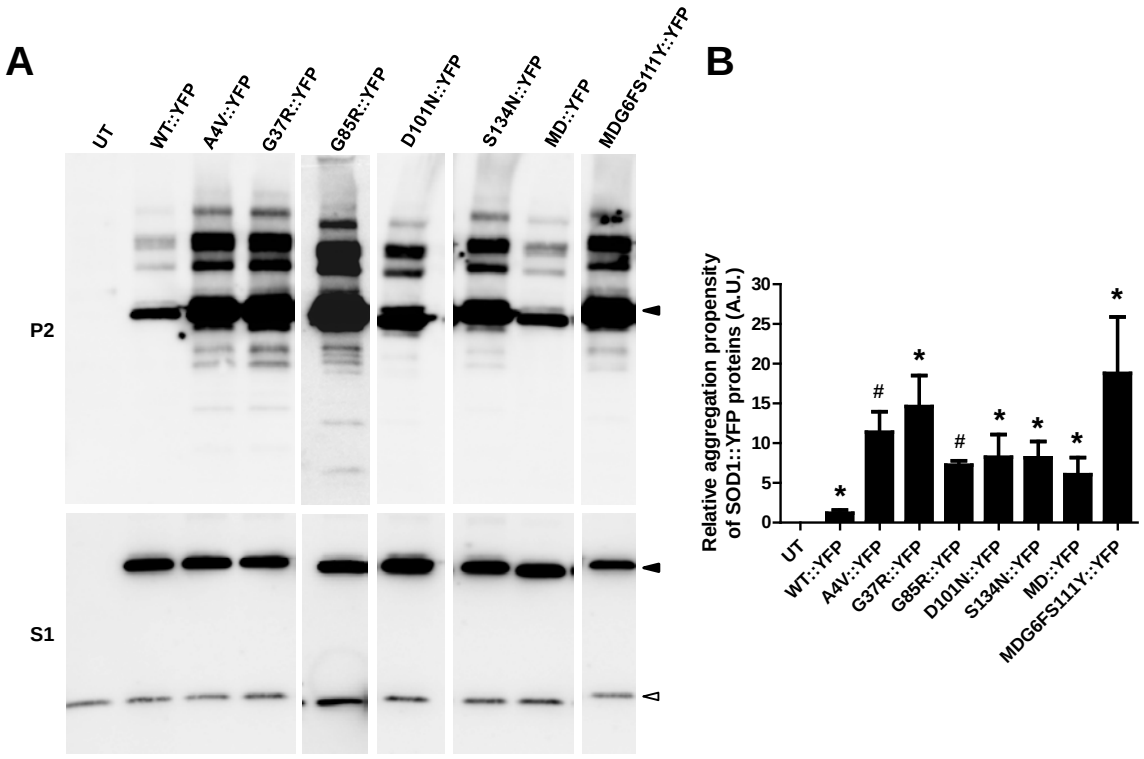

Figure 6-11. All HEK293FT cells expressing a SOD1::YFP variant contain detergent-insoluble aggregates. A) Immunoblot of P2 and S1 protein fractions of cells expressing SOD1::YFP proteins for 24 hours. The SOD1::YFP protein runs at a size corresponding to 50 kDa (filled arrowhead), while endogenous WT SOD1 monomer runs at 16 kDa (open arrowhead), like untagged SOD1. B) Quantification of the aggregation propensity (P2/S1) of cells expressing SOD1::YFP proteins. Paired student *t*-tests were performed to compare the aggregation propensity of WT::YFP or mutant SOD1::YFP with that of untransfected cells: $^{*}p \leq 0.05$; $^{\#}p \leq 0.005$.

Similarly, the aggregation propensity of tagged A4V::YFP is higher than that of untagged A4V, even at 48 hours (Figure 6-12). While in untagged WT and A4V co-

transfections A4V aggregation is reduced to WT levels at 24 hours, WT SOD1 when co-transfected for 24 hours with A4V::YFP does not seem to slow the ability of A4V::YFP to aggregate (Figures 6-12A and 6-12B). A similar outcome is observed at 48 hour co-transfection of A4V::YFP with untagged WT, with the only difference of the incorporation of WT SOD1 into the aggregate (Figures 6-12C and 6-12D). On the other hand, untagged WT is able to slow aggregation of WT::YFP tagged variant at 24 and 48 hours (Figures 6-12A to 6-12D). In the case of modulation of aggregation by tagged variant WT::YFP, the outcome is somewhat different. At 24 hour co-transfections, WT::YFP aggregation is markedly increased in the presence of untagged A4V (Figures 6-12A and 6-12B), while the aggregation propensity of WT::YFP at 48 hours does not differ from WT::YFP when co-expressed with untagged A4V at 48 hours (Figures 6-12C and 6-12D). Additionally, the levels of aggregated A4V in the A4V + WT::YFP 48 hour co-transfection are the same as A4V SOD1 transfected alone for 48 hours (Figures 6-12B and 6-12D).

Similar outcomes are observed when we performed the same experiments using the G85R tagged and untagged variants (Figure 6-13). In this case G85R::YFP and G85R SOD1 aggregation is reduced at 24 hours when they are co-expressed with either untagged or tagged WT SOD1, respectively (Figures 6-13A and 6-13C). At the 48 hour transfection interval, the aggregation propensity of G85R::YFP, when co-expressed with WT SOD1, appear slightly reduced compared to singly transfected G85R::YFP (Figures 6-13B and 6-13D).Moreover, the levels of aggregated WT::YFP and G85R at the 48 hour co-transfection represent the sum of the aggregation capability of each individual mutants (Figure 6-13D).

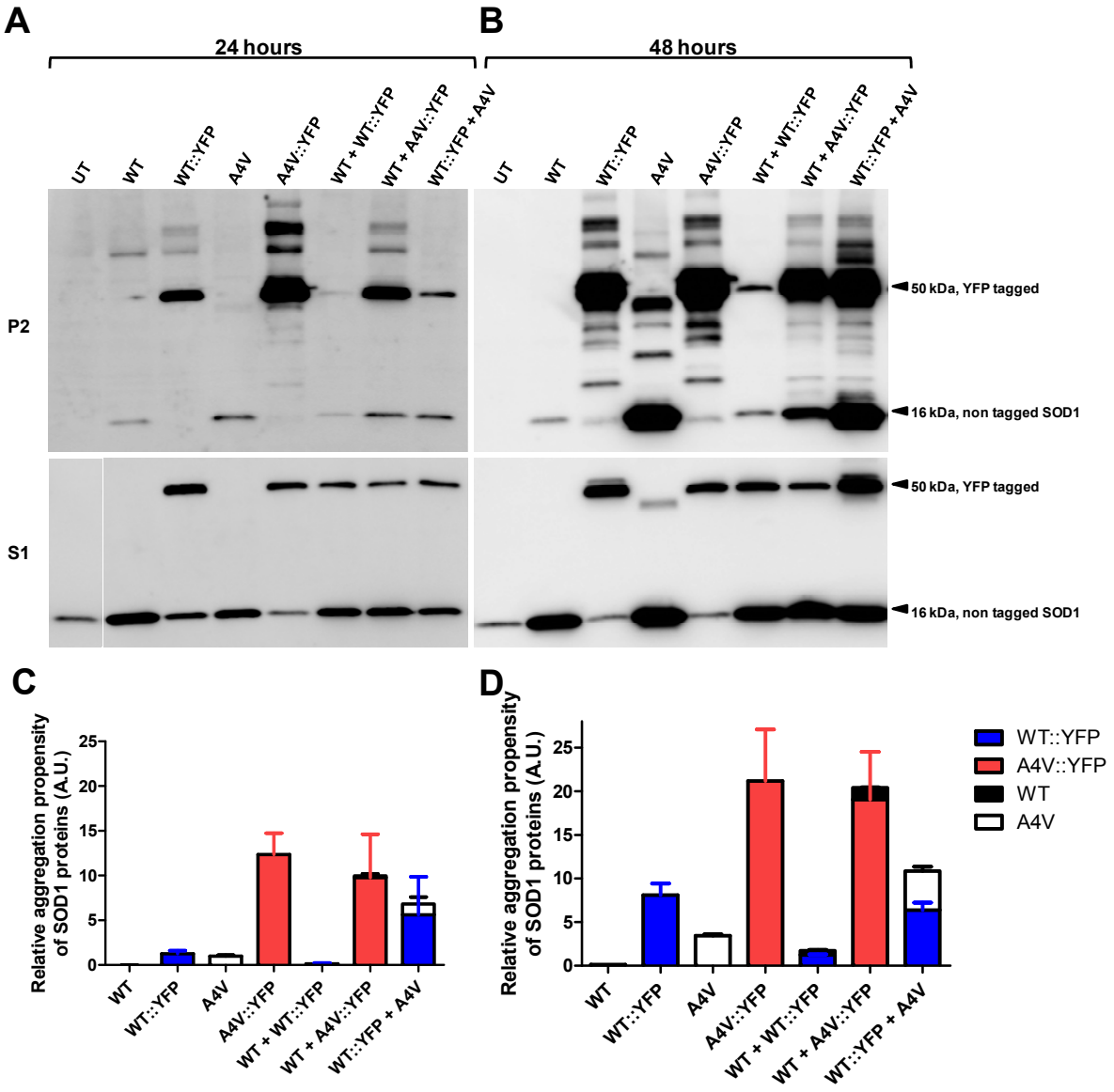

Figure 6-12. Tagged and untagged SOD1 protein co-expressions determine different ability of tagged SOD1 to modulate aggregation of A4V SOD1. A, B) Immunoblots of P2 and S1 fractions of HEK293FT cells co-transfected with the indicated SOD1 constructs for 24 (A) or 48 (B) hours and blotted with an antibody that recognizes mouse and human SOD1. Tagged SOD1::YFP proteins run on SDS-PAGE at a level corresponding to 50 kDa, while untagged SOD1 variants run at about 16 kDa. C, D) Quantification of the aggregation propensities (P2/S1) of tagged and untagged proteins from singly or doubly transfected cells. Note that aggregation propensity values have been normalized to the aggregation propensity of untagged A4V at 24 hours (set to 1). Additionally, the background generated by endogenous WT SOD1 has been subtracted from the value of band intensity for each untagged variant.

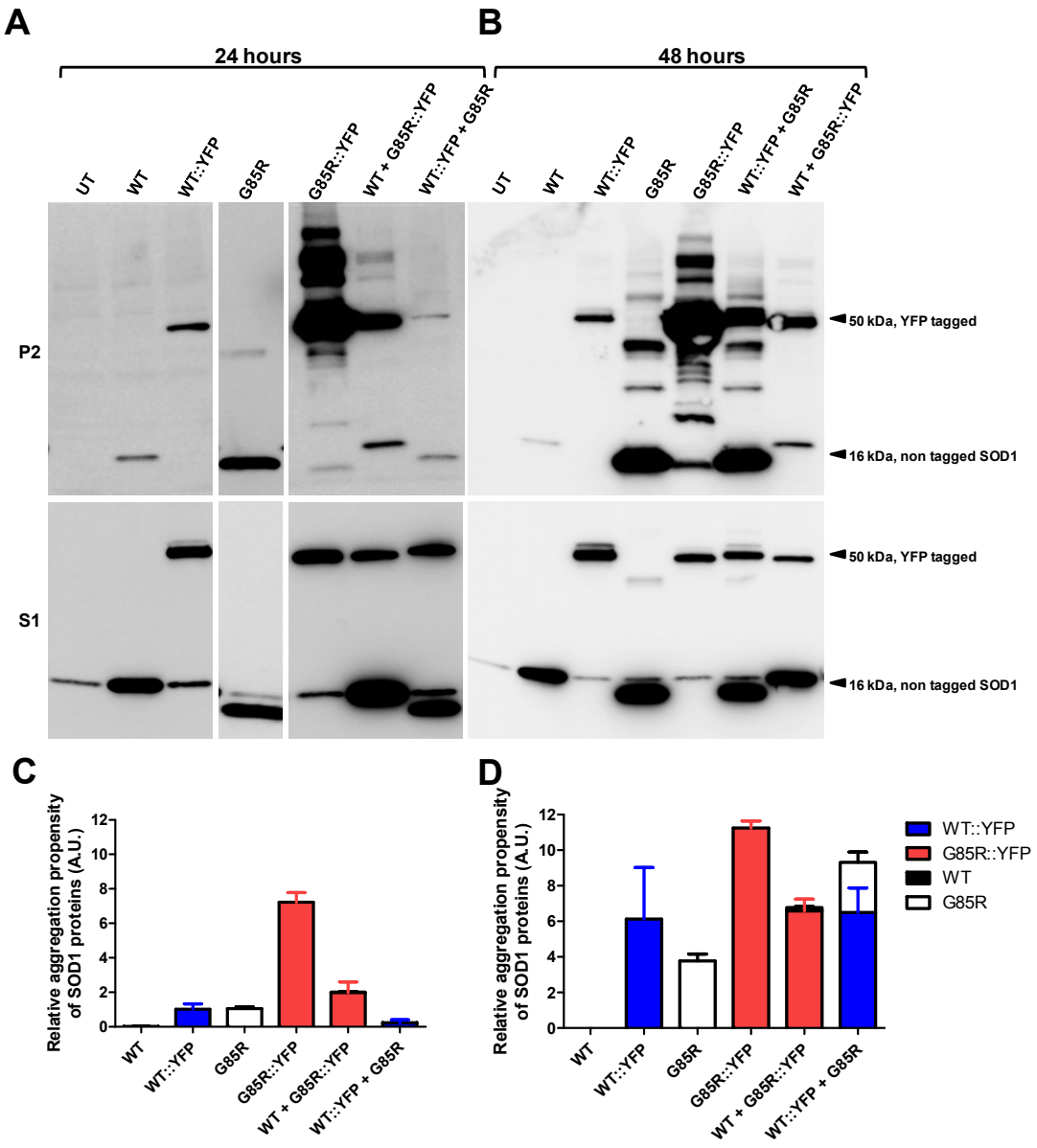

Figure 6-13. Tagged and untagged SOD1 protein co-expressions determine different ability of tagged protein to modulate aggregation of G85R SOD1. A, B) Immunoblots of P2 and S1 fractions of HEK293FT cells co-transfected with the indicated SOD1 constructs for 24 (A) or 48 (B) hours and blotted with an antibody that recognized mouse and human SOD1 protein. Tagged SOD1::YFP proteins run on SDS-PAGE at a level corresponding to 50 kDa, while untagged SOD1 variants run at about 16 kDa. C, D) Quantification of the aggregation propensities (P2/S1) of tagged and untagged proteins from singly or doubly transfected cells. Note that aggregation propensity values have been normalized to the aggregation propensity of untagged A4V at 24 hours (set to 1). Additionally, the background generated by endogenous WT SOD1 has been subtracted from the value of band intensity for each untagged variant

Overall, it appears that the delay in aggregate formation in some of the untagged and tagged SOD1 protein co-transfections is just temporary, as such effect in some cases is not present at 48 hour after co-transfection. Additionally, the length of time that this interaction may occur seems to be dependent on the similarity of the proteins co-expressed. For example, WT + WT::YFP SOD1 co-expression delays aggregate formation of WT::YFP even at the 48 hour interval (Figure 6-12), while little effect is observed with the G85R SOD1 mutant (Figure 6-13) and none with the A4V SOD1 mutant (Figure 6-12) proteins. These results differ from the outcome observed in untagged SOD1 proteins co-transfections, in which the effect of WT SOD1 in slowing A4V SOD1 aggregation was stronger than for the G85R SOD1 mutant (see Chapter 4). Thus, this data indicates that it is possible that the YFP tag may interfere with WT and mutant SOD1 interactions, which could be the explanation for such differences.

Next we sought to investigate how the co-expression of tagged and untagged SOD1 proteins affects the process of inclusion formation. Analysis of cells co-transfected with A4V::YFP or G85R::YFP and untagged WT SOD1 (Figures 6-14B and 6-14E) were still able to form visible inclusions at 24 hours, like in singly transfected cells with A4V::YFP or G85R::YFP (Figures 6-14A and 6-14D). However, the number of inclusions per cell appeared to be lower, and such inclusions were of bigger calibers than in cells expressing the SOD1::YFP mutation alone (data not rigorously quantified). The effect of WT SOD1 on reducing the number of inclusions formed by G85R::YFP protein was more pronounced (Figure 6-14E), which correlates to the effect of WT SOD1 on the formation of detergent-insoluble SOD1 aggregates of mutant SOD1::YFP (see Figure 6-13). Interestingly, untagged mutant proteins (A4V or G85R) did not affect

the ability of WT::YFP protein to form inclusions (Figures 6-14C and 6-14F). Additionally, co-expression of A4V with A4V::YFP does not alter the ability of A4V::YFP to form inclusions (Figure 6-15). Thus, mixtures of untagged and tagged mutant SOD1 proteins can produce fluorescent inclusions, but mixtures of untagged mutant with tagged WT SOD1 do not.

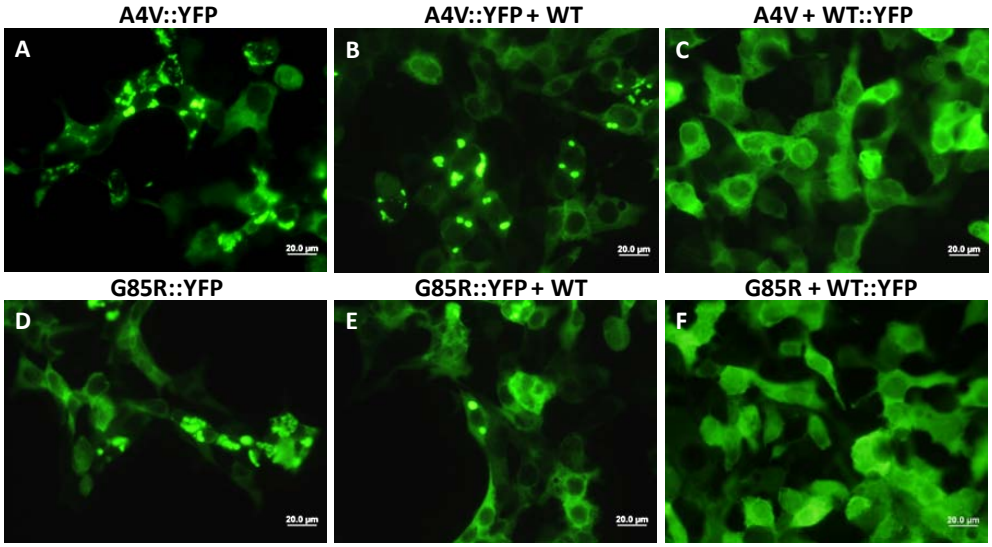

Figure 6-14. WT SOD1 affects inclusion formation in mutant SOD1::YFP proteins, but not mutant SOD1 on WT::YFP proteins. A-F) HEK293FT cells expressing for 24 hours: A4V::YFP (A) or G85R::YFP (D) alone, or with WT SOD1 (B and E); or WT::YFP with either untagged A4V (C) or G85R (F) SOD1. Inclusion visualization was performed as described in Figure 6-7. Bars represent 20 µm, in pictures taken using a 40x objective.

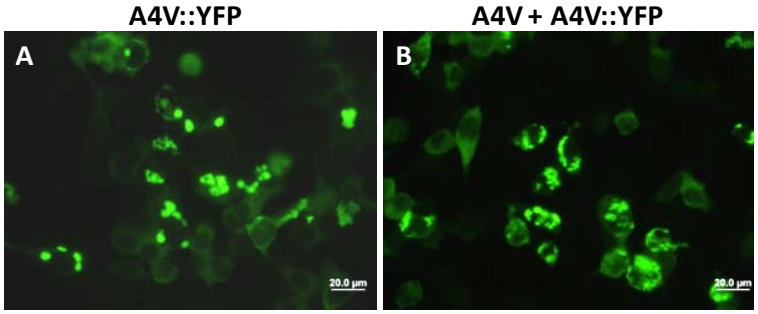

Figure 6-15. Untagged A4V SOD1 does not alter inclusion formation in A4V::YFP expressing cells. A, B) HEK293FT cells expressing A4V::YFP alone (A) or with untagged A4V SOD1 (B). Inclusion visualization was performed as described in Figure 6-7. Bars represent 20 µm, in pictures taken using a 40x objective.

To further understand whether tagged SOD1 proteins can template inclusion formation of WT::YFP, we took advantage of our WT::RFP construct which can form visible inclusions. Co-transfections of WT::YFP and WT::RFP constructs suggest the ability of WT::RFP inclusion formation capability to interact with WT::YFP and induce inclusion formation containing both of the tagged WT variants (Figures 6-16A to 6-15C). Similarly, cells co-transfected with A4V::YFP and A4V::RFP contain inclusions expressing both proteins (Figures 6-16D to 6-16F). This data suggest that the fluorescent tags may not interfere with SOD1 protein-protein interactions.

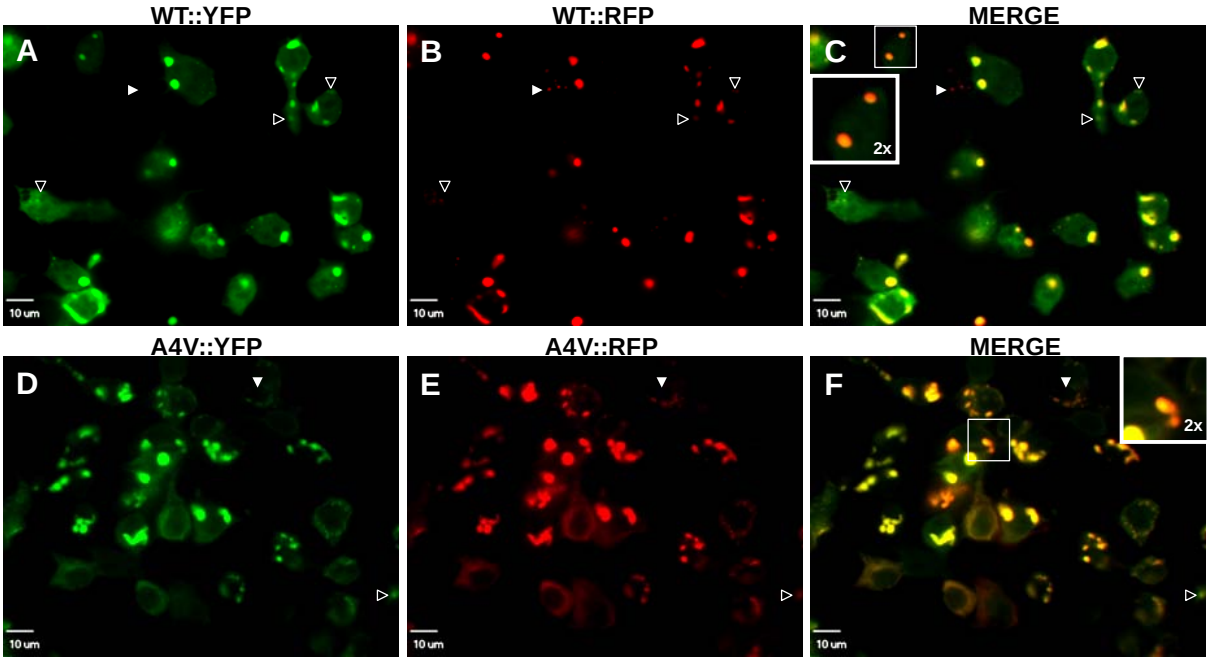

Figure 6-16. WT::RFP can induce inclusion formation of WT::YFP. A-F) HEK293FT cells co-transfected with either WT::YFP + WT::RFP (A-C) or A4V::YFP + A4V::RFP (D-F) for 24 hours. Cells were fixed and visualized under a spinning disc confocal microscope. Pictures were taken using a 60x water immersion objective, bars 10 µm. Squared areas in C and F are double amplification of the area in the smaller square to show inclusions in which the core contains SOD1::YFP and SOD1::RFP, surrounded by SOD1::RFP only. White arrowheads indicate inclusions expressing just SOD1::RFP, while open arrowheads indicate inclusions expressing just SOD1::YFP.

In order to determine whether co-localization of SOD1::YFP and SOD::RFP proteins require the YFP and RFP tags, or whether involve possible SOD1-SOD1 interactions, we performed co-transfections of YFP (no SOD1) and either WT::RFP or A4V::RFP (Figure 6-17). Results from these transfections suggest that YFP does not likely interact with either WT::RFP (Figures 6-17A to 6-17C) or A4V::RFP (Figures 6-17D to 6-17E) to co-localize within inclusions.

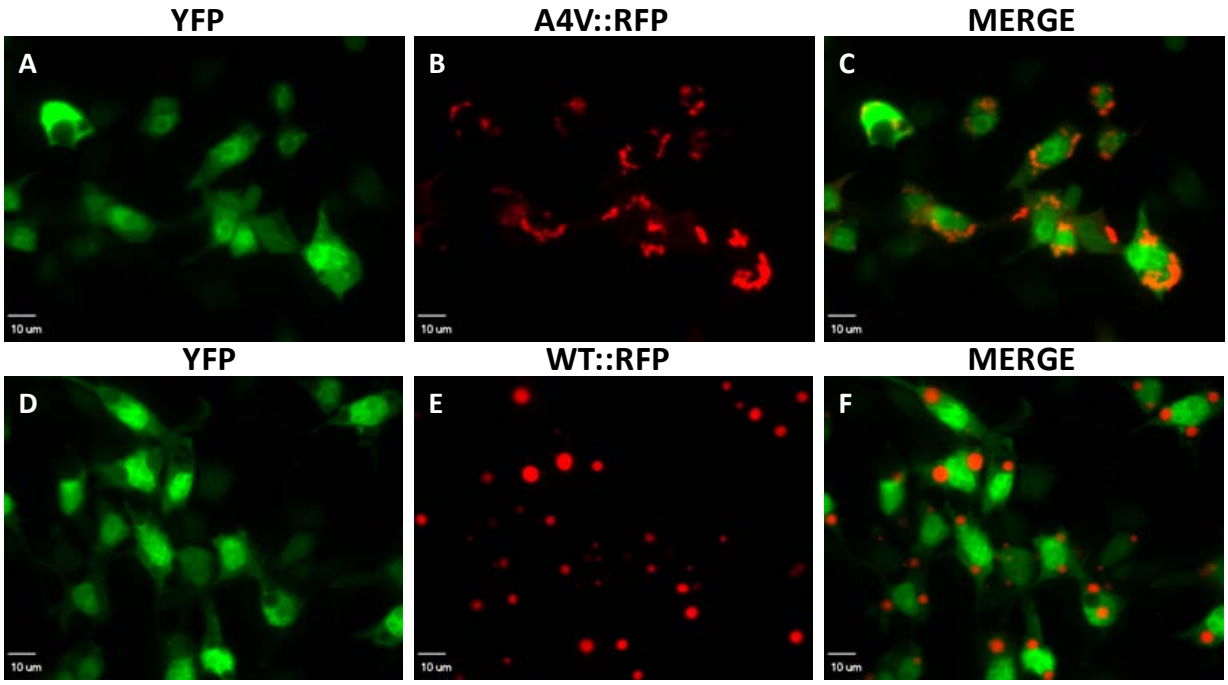

Figure 6-17. YFP does not alter inclusion formation ability of A4V::RFP or WT::RFP. A-F) HEK293FT cells co-transfected with YFP and either A4V::RFP (A-C) or WT::RFP (D-F) for 24 hours. Cells were fixed and visualized under a spinning disc confocal microscope. Pictures were taken using a 60x water immersion objective, bars 10 µm.

Additionally, we performed co-transfections of WT::RFP + A4V::YFP and WT::YFP + A4V::RFP to investigate interactions between WT and mutant SOD1 in the ability to form inclusions containing WT and mutant SOD1 (Figure 6-18). In WT::RFP + A4V::YFP co-transfections, we observed inclusions of both WT and mutant SOD1 that did not co-localize, but that in some cases A4V::YFP surrounded WT::RFP inclusions (Figures 6-

18A to 6-18C). In the other hand, WT::YFP + A4V::RFP showed a very different outcome. While in some cells we observed diffuse fluorescence of WT::YFP and A4V::RFP that overlapped completely (Figures 6-18D to 6-18F), A4V::RFP inclusions appeared to co-localize with more condensed areas of WT::YFP (Figures 6-18G to 6-18I). However, WT::YFP did not seem to form a lot of inclusions at the 24 hour co-transfection interval. This data suggests that SOD1 inclusion formation is favored when the proteins involved are of the same protein sequence, that is, just WT or just a certain type of SOD1 mutation.

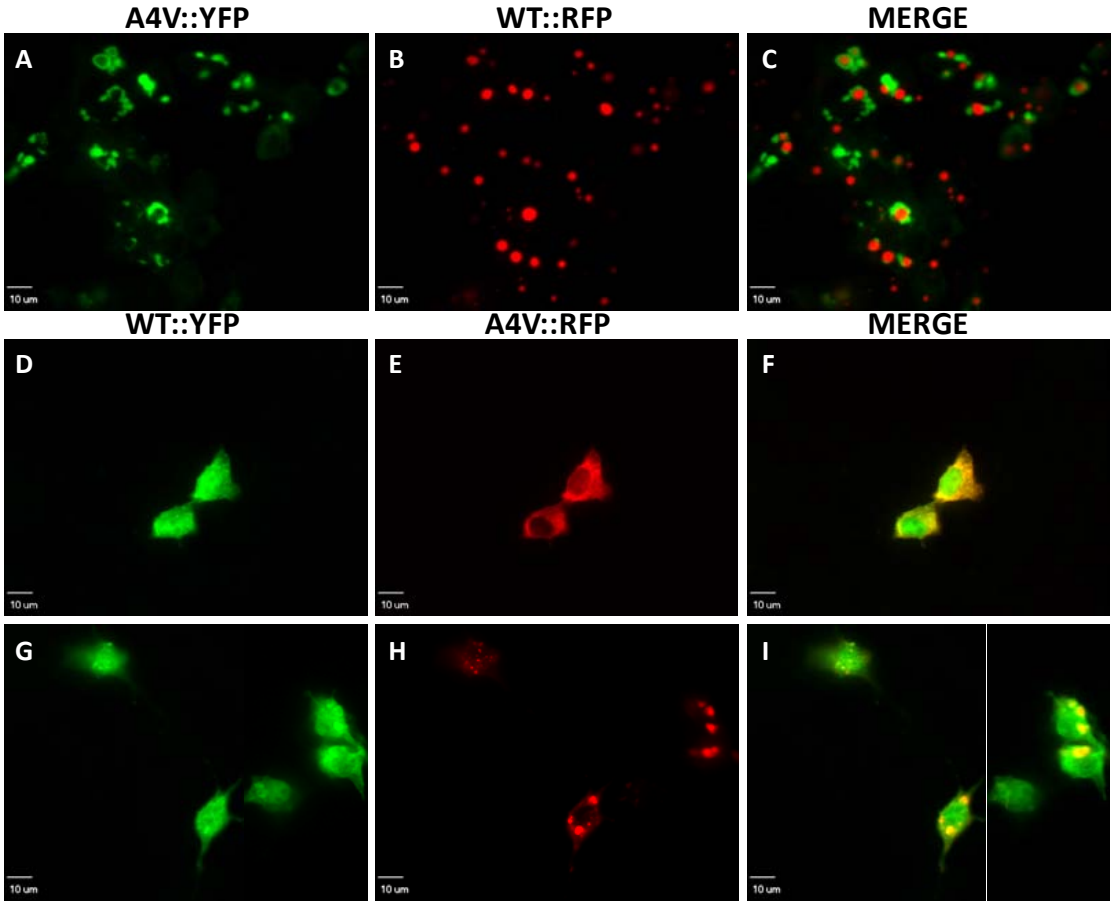

Figure 6-18. WT and mutant SOD1 proteins do not easily form hybrid inclusions but both proteins may interact at the soluble level. A-I) HEK293FT cells co-transfected with A4V::YFP + WT::RFP (A-C) or WT::YFP + A4V::RFP (D-I) for 24 hours. Pictures were taken with a 60x water immersion objective in a spinning disc confocal microscope, bars 10 µm.

Discussion

Mutant SOD1 proteins associated with ALS are characterized by their insolubility in non-ionic detergents. Moreover, the formation of such species is a characteristic pathological feature in mouse models for SOD1-associated ALS. However, little is known about the morphology and location of these detergent-insoluble aggregated species within cells. Here, we have used our HEK293FT cell culture model to determine that such aggregated species are cannot be detected through conventional immunofluorescence techniques. However, cytosolic inclusions can be observed by tagging SOD1 mutant proteins with a fluorescent protein. Cells expressing SOD1::YFP proteins contain inclusions that are easily visualized, thus may be of larger caliber than the detergent-insoluble aggregates of mutant SOD1. Alternatively, SOD1 antibodies may be incapable of detecting inclusions formed of detergent-insoluble aggregated SOD1 proteins. We have established that the amount of detergent-insoluble SOD1 mutant protein in cells expressing mutant SOD1::YFP variants is about 6 fold or higher. This data suggest that a higher concentration of the mutant untagged SOD1 protein might be required to form detectable inclusions, with the detergent-insoluble aggregates being precursors of inclusions. Alternatively, it is also possible that detergent-insoluble aggregated species are a type of SOD1 aggregates that are different from the inclusions seen by tagging SOD1 with fluorescent tags. In terms of the ability of WT in modulating mutant SOD1 aggregation, tagged proteins do not show as big of an impact when WT and mutant are co-expressed, compared to untagged WT and mutant SOD1 co-expression. However, interactions of tagged WT and mutant SOD1 proteins can be observed, with stronger interactions within same WT or mutant proteins and different tags. Additional data suggest that in terms of tagged proteins, it appears that WT and

mutant are more likely to interact at the soluble level, defining soluble in this case as the ability to be expressed but without forming cellular inclusions. However, further analyses are under way to support this hypothesis.

Inclusion Formation in Cells Expressing Untagged SOD1 Proteins

Disease associated variants of SOD1 differ from WT SOD1 in their ability to form detergent-insoluble SOD1 aggregates in cell culture an animal models. To asses aggregation propensity of SOD1 proteins we have previously used a biochemical assay and western blotting (Karch and Borchelt, 2008;Karch et al., 2009;Prudencio et al., 2009a;Prudencio et al., 2009b). However, we have never before assessed their morphology and or location in cells. Using cell culture techniques, we attempted to isolate and visualize such detergent-insoluble SOD1 species. However, the amount of soluble SOD1 proteins expressed in the cells may overshadow the low levels of detergent-insoluble SOD1 aggregates. Additionally, techniques that eliminate part of the detergent-soluble SOD1 proteins indicate that aggregates of mutant SOD1 that are insoluble in non-ionic detergents form structures that cannot be observed through the fluorescence microscopy techniques we employed. These data suggest that the difficulty to identify SOD1 inclusions in pathogenic tissue might be due to the usual small size of such aggregates, or to the inability of the antibodies to detect them.

Subcellular Location of SOD1::YFP Inclusions

We have observed that tagging SOD1 proteins with fluorescent tags increases the amount of detergent-insoluble SOD1 aggregates that forms in 24 or 48 hour transfection intervals. Additionally, the fluorescent tags induce inclusion formation in cell culture, even for WT SOD1 (with RFP tag, or with YFP tag and expressed for long period of times). Similar to the detection of detergent-insoluble aggregates

biochemically, the number of inclusions depends on the amount of protein expressed. Cells that express our SOD1::YFP vectors with lower efficiency than HEK293FT (NIH3T3 or TK negative cells) contained a lower number of cells with inclusions. Additionally, at long transfection intervals, SOD1 proteins that do not normally form detergent-insoluble species in cell culture of HEK293FT cells (WT, and MD) can be seen within protein inclusions (see Figure 6-8).

Furthermore, the large size of SOD1::YFP inclusions suggested us that they may not likely interact with subcellular organelles. Although, we did not extensively explore this avenue, preliminary data was obtained from a few co-localization analyses of SOD1::YFP proteins (see Appendix E). However, the results of these experiments are not conclusive.

Effect on Detergent Solubility in SOD1::YFP Inclusion Formation

We have described the higher inherent propensity of SOD1::YFP proteins to become insoluble in non-ionic detergent, with WT::YFP accumulating significant amounts of insoluble aggregates. However, although the levels of detergent-insoluble aggregates of WT::YFP at 48 hours are not different from those of G85R::YFP at 48 hours (compare G85R::YFP from Figure 6-13C with WT::YFP from Figure 6-13D), the ability of WT::YFP to form inclusions is very low (see Figure 6-8A). Thus, it might be that the amount of detergent-insoluble WT::YFP protein needed to form inclusions is much higher than for mutant SOD1 proteins, due to a very low inherent propensity of WT to aggregate. Alternatively, it is possible that detergent-insoluble SOD1 aggregates and SOD1::YFP inclusions are structures of very different nature, suggesting that other differences between WT and mutant YFP tagged proteins may account for such differences in their ability to form inclusions. Interestingly, we have preliminary data that

suggest a higher ability to aggregate for WT::RFP than for WT::YFP. However we cannot demonstrate whether detergent-insoluble aggregates are precursors of SOD1::YFP inclusions or if they are different species.

WT Modulation of Aggregation and Inclusion Formation

Interactions of WT and mutant SOD1 proteins are an important feature that modulates aggregation and lifespan in mice expressing a human SOD1 mutation (see Chapters 4 and 5). However, the ability of untagged WT to slow mutant SOD1 aggregation in cell culture differs from the ability of untagged WT to modulate mutant SOD1::YFP aggregation, or different from the ability of WT::YFP to modulate aggregate formation of untagged mutant SOD1 proteins. These differences may rely on at least two possibilities: 1) the ability of WT::YFP protein to slow aggregation of mutant proteins may be altered as a consequence of this protein (WT::YFP) to accumulate significant levels of aggregated protein, and 2) the presence of the YFP tag in either WT or mutant SOD1 proteins may introduce subtle modifications in the SOD1 structure, or hide possible exposed amino acid sequences in SOD1, which would translate into weaker ability for WT and mutant SOD1 to interact and modulate aggregate formation.

However, we can still observe a smaller effect on modulating aggregation when one of the SOD1 proteins is tagged with YFP (see Figures 6-12 and 6-13) suggesting that interactions between WT and mutant SOD1 might still occur, but at a much lower level.

The amount of detergent-insoluble SOD1 aggregates produced by untagged mutant SOD1 proteins (A4V or G85R) does not appear to be sufficient to induce inclusion formation of WT::YFP (see Figures 6-14C and 6-14F). In the other hand, the lower ability of untagged mutant proteins to aggregate (compared to WT::YFP, see

Chapter 3 and Figure 6-7) may explain that the addition of these detergent-insoluble aggregates of untagged mutant SOD1 to WT::YFP aggregates when co-transfected, is not sufficient to make WT::YFP to rapidly create cellular inclusions. Clearly the ability of WT::RFP to form inclusions can induce WT::YFP to be included in such species, while YFP does not in the presence of WT::RFP. Similar results are observed with A4V::YFP and A4V::RFP proteins. Thus, interactions occur between the SOD1 proteins that do not involve the fluorescent tags. Additionally, the RFP tag induces a higher ability of SOD1 to readily aggregate (data not shown).

However, interactions of WT and mutant tagged proteins do appear to easily occur. Interestingly, WT::RFP and A4V::YFP co-expression results in the formation of inclusions of each of the expressed proteins, with in some cases A4V::YFP encapsulating the WT::RFP aggregates, but not co-localizing. In the other hand, co-expression of WT::YFP and A4V::RFP resulted in a very different outcome. While some cells lacked of any inclusions and presented WT::YFP and A4V::RFP uniformly distributed within cells (note that A4V::YFP has not been observed before as diffused expression, see Figures 6-10B, 6-16E and 6-17B), cells presenting A4V::RFP inclusions appear to also recruit WT::YFP. In this latter case, WT::YFP did not easily accumulate within inclusions, as a very high fluorescent intensity was also observed all over the cell.

In summary, in terms of WT and mutant interactions within inclusions we can observe that: 1) Tagged WT and mutant SOD1 proteins do not easily interact with each other to form inclusions, different from WT::YFP + WT::RFP or A4V::YFP + A4V::RFP; but 2) Inclusions expressing both WT and mutant tagged proteins can be observed when the WT SOD1 protein expressed is tagged to YFP, the variant less prone to

inclusion formation. Thus, it is possible that interactions between WT and mutant tagged proteins may take place at state prior to inclusion formation. Then, we would explain the inability of WT::RFP and A4V::YFP to interact within inclusions to the fact that WT::RFP has a very high propensity to form inclusions, not allowing enough time to interact with mutant SOD1.

Conclusions

In conclusion, the data presented here is consistent with the idea that the formation of inclusions is accompanied may require an accumulation of a large amount of detergent-insoluble SOD1 protein. WT::YFP seems to show this after 48 hour transfection, where we can observe some inclusions. However, we cannot yet demonstrate whether detergent-insoluble SOD1 aggregates could represent a precursor of inclusions, since we cannot normally detect inclusions in cultured cells expressing untagged mutant SOD1 proteins. It is possible that the structures formed by untagged mutant SOD1 are small and dispersed, but we do not discard the possibility of having a problem of epitope detection with the available antibodies. The presence of a fluorescent tag in SOD1 proteins seems to affect WT and mutant SOD1 interactions, but not WT and WT or mutant and mutant interactions. Thus, inclusions containing tagged WT and mutant SOD1 proteins are less likely to occur, but this process appear to be favored if WT and mutant SOD1 can spend enough time at a state previous to inclusion formation.

CHAPTER 7
CONCLUSIONS

SOD1-associated ALS is a devastating neurodegenerative motor neuron disease, with neither effective developed treatments nor cure. The main reason is likely explained by the uncertainty of what triggers motor neuron death. Several hypothesis exist that try to explain how mutations in SOD1 provide the protein with a toxic property that kills primarily motor neurons. In the work presented here, we have focused on one of these hypotheses, which suggests that some type of aggregated species of mutant SOD1 is responsible for the toxicity in ALS. In particular, we have performed a exhaustive study to understand the role of aggregates of mutant SOD1 that are insoluble in non-ionic detergents and that can be isolated through a previously described biochemical assay (Karch and Borchelt, 2008;Prudencio et al., 2009a). The goals of these studies were to determine whether all mutant SOD1 proteins are able to form detergent-insoluble SOD1 aggregates, and whether aggregation is a common feature in SOD1-associated ALS. Additionally, we intended to evaluate the role of these structures on disease and determine whether aggregation correlates with any disease feature in humans.

ALS is normally dominantly inherited, thus SOD1-associated ALS patients express a SOD1 mutation but also the normal, WT SOD1 protein. Thus, in a second part of this project, we have investigated whether WT SOD1 plays a role in disease and/or in modulating aggregation. And finally, we have further characterized in a cell culture model the detergent-insoluble aggregates of mutant SOD1, and how a fluorescent tag SOD1 system may be useful to study WT and mutant SOD1 co-aggregation.

Detergent-Insoluble Mutant SOD1 Aggregates and ALS.

Over 140 mutations in SOD1 are associated with familial ALS. From all these disease causing mutations about 10% had been analyzed in cell culture and animal models previous to the present study. All these analyzed proteins share the common feature of being able to form detergent-insoluble aggregates in cell culture and animal models, while they differ in several other protein features. The work presented in Chapter 2 demonstrates that not all mutations in the SOD1 protein induce the formation of such detergent-insoluble SOD1 aggregated structures, and that lack of aggregation correlates with lack of disease development. These studies then suggest all SOD1-associated ALS mutations may not have the same inherent propensity to aggregate. Thus, in Chapter 3 we extended the number of studied SOD1-associated ALS mutations to over 30%. We demonstrated the different ability of SOD1 disease causing mutations to aggregate in cell culture. Additionally, the variability in aggregation potential cannot be explained by a single characteristic of the SOD1 protein (stability, metal binding, change in protein charge, etc). However, we determined that higher rates of aggregation predict shorter disease durations in humans, while aggregation did not seem to direct onset. We were not able, however, to find a SOD1 mutation that does not form aggregates but cause ALS in humans or animal models. Thus, it appears that protein aggregation represents at least an important pathological feature of SOD1-associated ALS.

WT SOD1 as a Modulator of Aggregate Formation

In Chapters 2 and 3 we have demonstrated the importance of detergent-insoluble SOD1 aggregates in disease. Additionally, it appears that high aggregation rates are characteristic of shorter disease durations in humans. However, we did not find

statistically significant correlations between aggregation propensity in cell culture and disease duration in humans. Specially, mutants with moderate aggregation propensity presented a large variability in disease durations when expressed in humans. Since no intrinsic protein property of mutant SOD1 by itself could explain the variability in aggregation rates, we considered important to determine whether other proteins could be involve in modulating aggregates of mutant SOD1. Thus, we sought to study whether WT SOD1 protein, which is normally present in affected individuals, could modulate aggregation (Chapters 4 and 5). Effectively, WT SOD1 slows aggregation of several SOD1 mutant proteins (A4V, G37R, G85R, G93A and L126Z) expressed in cell culture for 24 hours. This apparent reduction in aggregation is not permanent, and at longer incubation intervals (48 hours), some cells are able to significantly form detergent-insoluble aggregates. Additionally in several cases we have determined the presence of both, WT and mutant SOD1 proteins, in such aggregates. This data suggest that interactions of WT and mutant SOD1 proteins may occur to modulate aggregate formation. In Chapter 4, we have also demonstrated that human as well as mouse WT SOD1 proteins can slow aggregation of mutant SOD1 proteins, but only human WT SOD1 is capable of co-aggregate with mutant protein. The lack of cysteine 111 in mouse SOD1 did not explain its inability to co-aggregate, as human WT SOD1 without this cysteine can still co-aggregate with human mutant SOD1. Additionally, the effect of WT on slowing aggregation of the truncation mutant L126Z in cell culture suggest that interactions between WT and mutant human SOD1 protein may take place involving human amino acids present in the first 126 residues of the protein. Further studies

looking at the differences between mouse and human WT SOD1 may help us to understand the co-aggregation phenomenon.

Effect of WT SOD1 on Aggregation and ALS in Transgenic Mice

In Chapter 5 we have shown that in transgenic mice, co-aggregation of WT and mutant human SOD1 proteins is a common feature of symptomatic mice overexpressing both human SOD1 proteins. However, in some cases the effect on accelerating disease onset was not as pronounced (compare the effect of WT on PrPG37R and L126Z mice). We have demonstrated that stronger effects on accelerating disease onset are dependent on the dose of WT SOD1 protein expressed. Additionally, such effect varies from mutant to mutant, which could be explained by the existing differences between WT and mutant SOD1 (in terms of sequence or other properties), and that could account for different ability of WT and mutant SOD1 to interact. Due to a more rapid disease development in mutant/WT SOD1 mice, we can detect WT and mutant co-aggregation at earlier time points, coinciding with disease endstage. It is possible that the more rapid disease development correlates with a more rapid rate of aggregation induced by WT SOD1, rather than an earlier development of aggregates (see Figure 5-10). Thus, while WT SOD1 protein initially delays aggregate formation of mutant SOD1, possibly due to WT-mutant SOD1 interactions and protein turnover, once a WT/mutant nucleation complex has been formed the rate of aggregation would be increased. At the same time, other abnormalities in the cell, if not caused by some kind of aggregated species, would be accelerated in parallel and leading to a more rapid onset of paralysis symptoms.

It is known that several abnormalities occur prior to hindlimb weakness in mutant SOD1 mice (gliosis, muscle denervation, etc), but these cannot be evaluated in alive

mice. Thus, future studies should be focused on elucidating easily markers of disease initiation. This data could help us to understand whether WT SOD1 exert a toxic effect in initial stages of the disease or along disease progression. Overall, our studies demonstrate that the presence of WT SOD1 in mutant SOD1 transgenic mice is detrimental, with WT SOD1 altering rates of aggregate formation.

Detergent-Insoluble SOD1 Aggregates are Difficult to Observe in Cells

In order to determine the possible toxic effect of detergent-insoluble SOD1 proteins, we used our cell culture model of HEK293FT to further study these aggregates *in vitro*. However, we were unable to detect aggregates in cell culture using standard fluorescent microscopy techniques. Thus, it is unclear where detergent-insoluble SOD1 aggregates accumulate and/or exert their toxicity. In the studies presented in Chapter 6 we did not determine whether our SOD1 antibodies are capable of detecting protein that forms part of inclusions. However, due to the fact that mutant SOD1::YFP inclusions can be formed in cells expressing very high levels of detergent-insoluble protein, it is possible that the size of detergent-insoluble SOD1 aggregates may be smaller than visible cellular inclusions.

SOD1 Fluorescent-Tagged Inclusions, Detergent-Insoluble Aggregates and WT-Mutant Interactions.

Inclusions of SOD1 proteins can be obtained by using fluorescent tags attached to the C-terminus of SOD1. With such tags, even WT SOD1 can be induced to form inclusions. We have also determined that the addition of the protein tag accelerates the formation of detergent-insoluble SOD1 aggregates. In terms of SOD1::YFP inclusions, these are of such large diameters that we think unlikely their presence within any particular organelle. However, we did not present enough data here to support such

statements (data in Appendix E). Instead, the work presented in Chapter 6 on fluorescent tagged SOD1 demonstrated to be a useful technique to study possibly study protein-protein interactions between WT and mutant human SOD1 proteins. Our co-localization data suggest that WT and mutant SOD1 can interact but with lower efficiency than WT-WT or mutant-mutant SOD1 proteins. We were able to observe, that WT and mutant SOD1 co-localizations, when both proteins are tagged, can take place when they are not already forming SOD1 inclusions (WT::YFP + A4V::RFP); but WT::RFP, which forms inclusions very rapidly, does appear to co-localize with A4V::YFP inclusions. From these studies we suggest WT-mutant protein interactions may take place at the soluble level, before the proteins become part of visible cellular inclusions. In order to establish direct protein-protein interactions between WT and mutant SOD1, further experiments should be performed, such as immunoprecipitation or FRET analyses.

Composition of Detergent-Insoluble SOD1 Aggregates

Previous studies on detergent-insoluble SOD1 aggregates have established that they are composed of full-length unmodified mutant SOD1 (Shaw et al., 2008). Additionally, other studies have demonstrated that a fraction of different SOD1 proteins is in an immature disulfide reduced state *in vivo* (Jonsson et al., 2006a;Zetterstrom et al., 2007). Here we have demonstrated that as little as 10% of soluble WT SOD1 protein can be found as a disulfide immature state in mouse spinal cords. Additionally, soluble SOD1 mutant proteins are found mostly in a disulfide reduced state in cell culture, while all detergent-insoluble SOD1 species are in a disulfide reduced state (Figure 7-1). On the other hand, a larger proportion of WT SOD1 protein is observed as disulfide oxidized protein in cells after 48 hours (Figure 7-1).

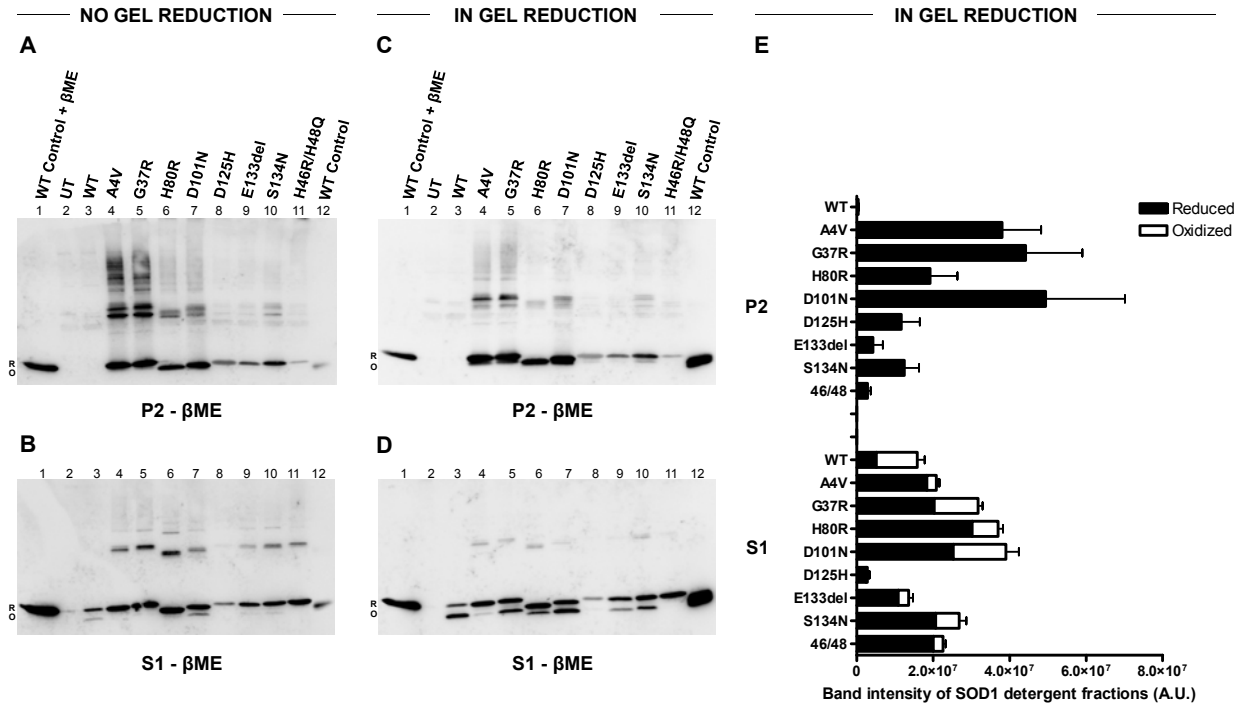

Figure 7-1. SOD1 mutant proteins remain mostly disulfide reduced in cell culture. A-D) Immunoblots of detergent extracted HEK293FT cells that had been transfected for 48 hours with SOD1 constructs and analyzed by western blotting excluding βME (β-mercaptoethanol) from the loading buffer. A technique of in-gel reduction has been performed in C and D that consist in incubating the gels in 2% βME and transfer buffer prior protein transfer. This procedure favors antibody binding to the oxidized form. A protein control for disulfide reduced (R) and disulfide oxidized (O) WT SOD1 protein has been included in each blot as controls. UT denotes untransfected cells. E) Quantification of the relative levels of SOD1 protein that is disulfide reduced (black bars) and oxidized (white bars) forms from immunoblots in C and D. Each experiment was repeated a minimum of 3 times. A very similar figure was included in the published manuscript of Karch *et al*., Prot Natl Acad Sci (2009), 106(19):7774-7779.

Additionally, we have observed a similar outcome with several SOD1 mutant proteins in cell culture and animal models, with maybe the latter presenting a higher proportion of mutant oxidized protein in the detergent-soluble state (Karch et al., 2009). The subtle differences between cells and animal models could be attributed to the lower availability of factors for the maturation of a very large amount SOD1 protein expressed (availability of metals or other co-factors). By analyzing the disulfide status of a smaller

set of mutant SOD1 proteins at 24 and 48 hours, we observed that in cell culture the amount of disulfide reduced and oxidized soluble SOD1 proteins increases over time (Figure 7-2). However, a higher proportion of disulfide reduced protein is more commonly observed in cells expressing mutant SOD1 (Figure 7-2). Interestingly, WT-like proteins, such as D101N present similar proportions of reduced and oxidized proteins at 48 hours to WT SOD1 (Figure 7-2). Thus, our studies suggest that over time much of the SOD1 protein may not completely mature and accumulates in the disulfide reduced state.

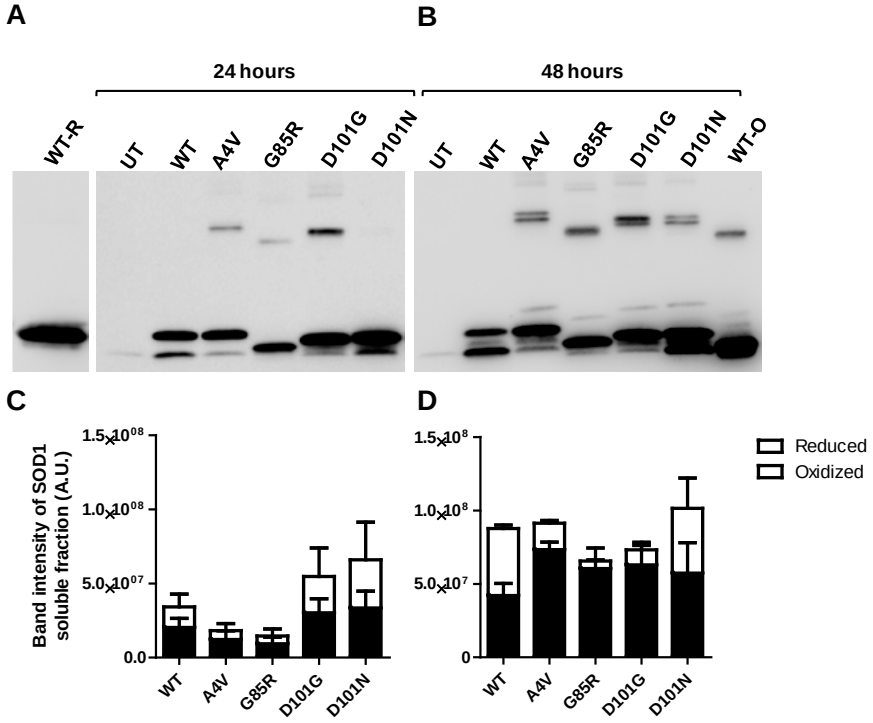

Figure 7-2. Progressive accumulation of disulfide reduced SOD1 proteins in cell culture. A, B) Immunoblots of detergent-soluble SOD1 proteins expressed for 24 (A) or 48 (B) hours in HEK293FT cells and processed as explained in Figures 7-2C and 7-2D. WT-R: WT SOD1 protein control of disulfide reduced protein, WT-O: WT SOD1 protein control of disulfide oxidized protein. C, D) Quantification of the relative levels of SOD1 protein that is disulfide reduced (black bars) and oxidized (white bars) from immunoblots in A and D. Each experiment was repeated a minimum of three times. This figure will be published in a manuscript that studies the kinetics of mutant SOD1 aggregation.

Furthermore, we have also observed that for the formation of detergent-insoluble SOD1 aggregates, the protein does not necessarily need to be able to form a dimer. Studies using a WT SOD1 protein that is unable to dimerize, due to a couple amino acid substitutions in the dimer interface (Bertini et al., 1994), is capable of forming detergent-insoluble SOD1 aggregates (Figure 7-3). These studies suggest that monomeric, and possible disulfide reduced, SOD1 protein may be precursors of detergent-insoluble aggregates. However, more ongoing studies in the lab will further help to corroborate this hypothesis.

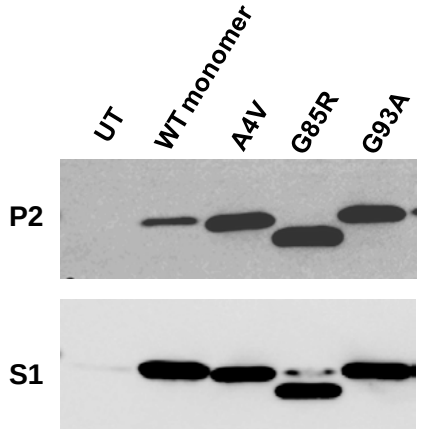

Figure 7-3. The engineered WT SOD1 monomer presents inherent propensity to aggregate, similar to other SOD1 mutant proteins. Immunoblot of detergent-insoluble (P2) and detergent-soluble (S1) fractions of HEK293FT transfected with the indicated SOD1 constructs for 24 hours and analyzed by detergent extraction and centrifugation assay, as described in Methods in Appendix C.

Another important feature of mutant SOD1 aggregates, is that they do not only contain mutant SOD1 proteins, but human WT SOD1 can also form part of the aggregate. This feature is an intriguing finding since the levels of WT SOD1 protein modulate disease. Thus, the presence of WT SOD1 in mutant SOD1 aggregates should be taken into account to determine the specific toxic role of these species.

Summary

The work presented in this dissertation demonstrates that: 1) All ALS causing SOD1 mutations share the ability to form detergent-insoluble structures of SOD1, 2) High aggregation propensity values of mutant SOD1 proteins predict a rapid disease course in humans, 3) The lack of statistical correlation of aggregation propensity in cell culture with disease duration in humans could be explained by the ability of WT SOD1 to modulate aggregation, which has not been considered in those studies, 3) The role of WT SOD1 in modulating mutant SOD1 aggregation is complex, 4) WT and mutant human SOD1 protein can co-aggregate in cell culture and animal models, 5) The dose of WT SOD1 protein in mice determines its ability to accelerate paralysis, the higher the dose, the earlier the onset of paralysis symptoms in mice; 6) Earlier disease onset in WT/mutant mice correlates with the appearance of detergent-insoluble SOD1 aggregates of both, WT and mutant human SOD1 proteins, 7) Detergent-insoluble SOD1 aggregates cannot be easily visualized within cells, 8) Fluorescent tagged SOD1 variants can form visible protein inclusions in cell culture, 9) Fluorescent tagged SOD1 variants form extremely high levels of detergent-insoluble SOD1 protein, 10) The presence of the tag alter protein-protein interaction patterns of SOD1 proteins, and 11) Although with low efficiency, WT and mutant tagged SOD1 proteins can interact to form SOD1 inclusions, but such interactions may likely occur prior inclusion formation, as this is not observed when one of the mutants aggregate very rapidly.

Future Directions

Further studies should be directed to determine the kinetics of aggregate formation and at what time point WT SOD1 intervenes in modulating such process. Additionally, it would be important to continue to study WT and mutant SOD1 interactions through

immunoprecipitation assays in which one of the proteins is tagged and/or through FRET analysis. Additionally, further experiments could be conducted to study what amino acids within the human SOD1 sequence are important for WT-mutant SOD1 interactions. Determination of the location of detergent-insoluble SOD1 structures would provide important information of the role of these structures in disease, thus additional techniques should be developed with this goal. Finally, screening for drugs that might slow aggregate formation, or disrupt WT and mutant SOD1 interactions may provide a benefit in slowing progression in SOD1-associated ALS patients. Alternatively, the ongoing clinical trial of antisense oligonucleotide that targets SOD1 protein to reduce its levels, represents a promising therapy for ALS.

APPENDIX A
LIST OF SOD1-ASSOCIATED ALS MUTATIONS

Table A-1. List of published SOD1-associated ALS mutations.

Mutations	Class	Principal references
Exon 1		
1. A4→S, T, V	B	(Nakanishi et al., 1998;Nakano et al., 1994;Rosen et al., 1994),
2. C6→F, G	B	(Morita et al., 1996;Kohno et al., 1999)
3. V7→E	B	(Hirano et al., 1994)
4. L8→Q, V	B	(Siddique and Deng, 1996;Andersen et al., 2003)
5. G10→ R, V	B	(Kim et al., 2003)
6. G12→R	B	(Penco et al., 1999)
7. V14→G, M	B	(Andersen et al., 1997;Deng et al., 1995)
8. G16→A, S	B	(Andersen et al., 2003;Kawamata et al., 1997)
9. N19→S	B	(Andersen et al., 2003)
10. F20→C	B	(Andersen et al., 2003)
11. E21→G, K	B	(Siddique and Deng, 1996;Jones et al., 1994b)
12. Q22→L	B	(Andersen et al., 2003)
Exon 2		
13. V29→insA	B	(Shi et al., 2004)
14. G37→R	B	(Rosen et al., 1993)
15. L38→R, V	B	(Boukaftane et al., 1998;Rosen et al., 1993)
16. G41→D, S	B	(Rosen et al., 1993)
17. H43→R	B	(Rosen et al., 1993)
18. F45→C	B	(Gellera et al., 2001)
19. H46→R	M	(Aoki et al., 1993)
20. V47→F	B	(Andersen et al., 2003)
21. H48→Q, R	M	(Enayat et al., 1995;Andersen et al., 2003)
22. E49→K	B	(Boukaftane et al., 1998)
23. T54→R	D	(Andersen et al., 2003)
24. C57→R	D	(Andersen, 2006)
Exon 3		
25. S59→I	D	(Andersen et al., 2003)
26. N65→S	M	(Garcia-Redondo et al., 2002)
27. L67→R	M	(Boukaftane et al., 1998)
28. G72→C, S	M	(Stewart et al., 2006;Shaw et al., 1998)
29. D76→V, Y	M	(Segovia-Silvestre et al., 2002;Andersen et al., 1997)
Exon 4		
30. H80→R	M	(Alexander et al., 2002)
31. L84→F, V	M	(Shaw et al., 1998;Aoki et al., 1995)
32. G85→R	M	(Rosen et al., 1993)
33. N86→D, K, S	B	(Andersen, 2006;Beck et al., 2007;Hayward et al., 1998)
34. V87→A	B	(Andersen et al., 2003)
35. T88→ΔTAD	B	(Andersen et al., 2003)
36. A89→T, V	B	(Andersen et al., 2003;Rezania et al., 2003)
37. D90→A, V	B	(Andersen et al., 1995;Chou et al., 2005)
38. G93→A, C, D, R, S, V	B	(Rosen et al., 1993;Esteban et al., 1994;Elshafey et al., 1994;Siddique and Deng, 1996;Hosler et al., 1996)
39. A95→T, V	B	(Gellera et al., 2001;Chio et al., 2008)
40. D96→N	B	(Hand et al., 2001)

Table A-1. Continued.

Mutations	Class	Principal references
41. V97→M	B	(Andersen et al., 2003)
42. E100→G, K	B	(Rosen et al., 1993;Siddique and Deng, 1996)
43. D101→G, H, N,Y	B	(Yulug et al., 1995;Sato et al., 2004;Jones et al., 1994a;Tan et al., 2004)
44. I104→F	B	(Ikeda et al., 1995)
45. S105→L, ΔSL	B	(Andersen et al., 2003)
46. L106→V	B	(Rosen et al., 1993)
47. G108→V	B	(Orrell et al., 1997)
48. D109→Y	B	(Naini et al., 2007)
49. C111→Y	B	(Shibata et al., 2007)
50. I112→M, T	B	(Garcia-Redondo et al., 2002;Esteban et al., 1994)
51. I113→F, T	B	(Andersen et al., 2003;Rosen et al., 1993)
52. G114→A	B	(Andersen et al., 2003)
53. R115→G	B	(Kostrzewa et al., 1994)
54. T116→R	B	(Andersen, 2006)
55. V118→L, L ins (stop 122)	B	(Andersen et al., 2003;Shimizu et al., 2000;Jackson et al., 1997)
Exon 5		
56. D124→G, V	M	(Andersen et al., 2003;Hosler et al., 1996)
57. D125→H	M	(Enayat et al., 1995)
58. L126→S, ΔL (stop 131), stop	B	(Takehisa et al., 2001;Siddique and Deng, 1996;Pramatarova et al., 1994)
59. G127→ins (stop 133)	B	(Andersen et al., 1997)
60. E132→ins (stop 133)	B	(Orrell et al., 1997)
61. E133→ΔE*	B	(Hosler et al., 1996)
62. S134→N	M	(Watanabe et al., 1997)
63. N139→H, K	B	(Nogales-Gadea et al., 2004;Pramatarova et al., 1995)
64. A140→G	B	(Naini et al., 2002)
65. G141→E, stop	B	(Sato et al., 2004;Andersen et al., 2003)
66. L144→F, S	B	(Deng et al., 1993;Sapp et al., 1995)
67. A145→G, T	B	(Andersen et al., 2003;Sapp et al., 1995)
68. C146→R	D	(Siddique and Deng, 1996)
69. G147→R	B	(Andersen et al., 2003)
70. V148→G, I	B	(Deng et al., 1993;Ikeda et al., 1995)
71. I149→T	B	(Pramatarova et al., 1995)
72. I151→S, T	B	(Andersen et al., 2003;Kostrzewa et al., 1996)

B: β-Barrel Mutants; M: Metal binding region mutants; D: Disulfide loop mutants. A similar version of this table has been included in a review paper (Seetharaman et al., 2009).

APPENDIX B
MATERIALS

Table B-1. Cell culture reagents.

Reagent	Description	Manufacturer	Catalog number
10x PBS	Phosphate buffered saline solution	Invitrogen	14200-166
12-well plates	Plates for tissue culture	Fisher/Nunc	353043
60 mm normal tissue culture dishes	Tissue culture dishes	Fisher Scientific	08-772-021
60 mm Poly-L-lysine Biocoat dishes	Poly-lysine coated dishes to grow low adherent cell lines	Fisher Scientific	356517
Cell lifters	Cell scrapers for tissue culture	Fisher Scientific	3008
Coverslips 24 x 50 mm	Coverslips for microscope slides	Fisher Scientific	12-545-88
DMEM	Tissue culture media	Thermo Scientific	SH30022.01
DMSO dimethyl sulfoxide	Storage cell reagent	Fisher Scientific	BP231-1
Fetal bovine serum	Supplement for tissue culture media	Invitrogen	26140-076
Glass round coverslips	Coverslips to grow cells on	Fisher Scientific	12-545-84 18CIR-1D
HEK293FT cells	Human embryonic kidney cell lines	Invitrogen	R700-07
Horse serum	Supplement for tissue culture media	Invitrogen	26050-088
L-glutamine	Amino acid supplement for tissue culture media	Invitrogen	25030-156
Lipofectamine 2000	Transfection reagent	Invitrogen	11668-019
TK negative (L-M) cells	Mouse connective tissue cell line	ATCC	CCL-1.3
MEM	Tissue culture media	Invitrogen	11140-050
Neuro-2a cells	Mouse Neuroblastoma cell line	ATCC	CCL-131
New born calf serum	Supplement for tissue culture media	Invitrogen	16010-159
NIH-3T3 cells	Mouse Embryonic Fibroblast cell line	ATCC	CRL-1658
Opti-MEM I	Tissue culture media for transfections	Invitrogen	31985-070
Poly-L-lysine	Coating reagent for tissue culture plates	Sigma	P2636
Trypsin-EDTA 0.25%	Trysin	Invitrogen	25200-072

Table B-2. Reagents for detergent extraction and centrifugation assay, BCA assay, SDS-PAGE, and Western blotting.

Reagent	Description	Manufacturer	Catalog number
18% Tris-Glicine, 12 well SDS-PAGE gels	Polyacrylamide gels	Invitrogen	EC6505BOX
96-well plates	To measure absorbance	Fisher/Nunc	167008
BCA reagents A and B	To determine absorbance	Thermo Scientific	Reagent A: 23224 Reagent B: 23228
Bench mark pre-stain	Protein ladder marker	Invitrogen	10748-010
Bromophenol blue	Dye for loading dye	Fisher Scientific	BP114-25
BSA reagents	Bovine Serum Albumin	New England Biolabs	B9001S
Deoxycolate	Acid salt	Fisher Scientific	BP349-100
ECL reagent	Membrane protein developer	Fisher/Pierce	PI32106
EDTA	Quelator	Fisher Scientific	BP120-500
Filter paper, 3MM	Filter paper	Whatman	3030662
Glycerol	Reagent	Fisher Scientific	BP229-1
Iodoacetamide	Thiol modifier agent	Sigma	I1149-5G
Magic XP Marker	Protein ladder marker	Invitrogen	LC5602
Methanol	Alcohol	Fisher Scientific	A412-4
Nitrocellulose membrane, 0,45µm	OptiTran BA-S 85 Reinforced	Whatman	10439196
Nonidet-P40 (NP-40)	Non-ionic detergent	US Biological	N3500
PBS	Phosphate buffered saline solution	Amresco	0780-2PK
Powdered non-fat milk	Caranation milk for membrane blocking for western blotting	Publix	Not available
Protease inhibitor cocktail (PI)	Inhibitor of proteases	Sigma	P8340-5ML
Sodium chloride (NaCl)	Salt	Fisher Scientific	BP358-212
Sodium dodecyl sulfate (SDS)	Ionic detergent	Fisher Scientific	BP166-500
TG-SDS	Tris-Glycine, sodium dodecyl sulfate (for running SDS-PAGE)	Mid Scientific	0147-40L
Tris	Buffer	Fisher Scientific	BP152-1
Tween 20	Detergent	Fisher Scientific	BP337-500
Ultracentrifuge tubes	Airfuge tubes 5MM PA	Beckman	342630
β-mercaptoethanol (βME)	Sulfide reduction agent	Fisher Scientific	BP-176-100

Table B-3. Histochemistry and cytochemistry reagents.

Reagent	Description	Manufacturer	Catalog number
2-2-2 Tribromoethanol, 97%	Euthanizing reagent	Sigma	T48402-25G

Table B-3. Continued.

Reagent	Description	Manufacturer	Catalog number
3-methylbutane	Alcohol for tissue freezing	Fisher Scientific	03551-4
ABC kit Vectastain rabbit IgG for DAB	Reagents and antibody for DAB staining	Vector Labs	PK-6101
Ammonium hydroxide	Silver staining reagent	Fisher Scientific	A-669
Cedarwood oil	Paraffin embedding reagent	Electron Microscopy Sciences	12420
Citric acid	Silver staining reagent	Fisher Scientific	A940-500
DAB	3,3 Diamino benzidine tetrahydrochlorida	Sigma	D5905-50TAB
DAPI staining solution	4',6-diamidino-2-phenyl-indole, dehydrochloride	Invitrogen	D1306
Digitonin	Mild detergent	Sigma	D141-100MG
D-Sucrose	Sugar	Fisher Scientific	BP220-1
Eosin Y	Tissue staining reagent	Fisher Scientific	E-511
Ethanol 100%	Alcohol 200 proof	Fisher Scientific	NC9977258
Flash Freeze-it	Reagent for instant OCT freezing	Fisher Scientific	23-022524
Flourescent mounting media	Mounting media for fluorescent sections	Polysciences, Inc.	18606
Formaldehyde 37%	Reagent	Amresco	0493-500ML
Glacial acetic acid	Acid	Fisher Scientific	BP2401-212
Glass round coverslips	To grow cells for cytochemistry	Fisher Scientific	12-545-84 18CIR-1D
Histoclear	Histological clearing agent	National Diagnostics	HS-200
Hydrogen peroxide (H_2O_2)	H_2O_2, 30%	Sigma	H1009-100ML
Methanol	Alchohol 100%	Fisher Scientific	A412-4
Methil Salicylate	Paraffin embedding reagent	Fisher Scientific	O395-500
Modified Meyer's Hematoxylin	Tissue staining reagent	Richard-Allan Scientific	72804
Nitric acid (HNO_3)	Silver staining reagent	Fisher Scientific	A200-500
Normal goat serum	Serum for blocking tissue using secondary antibodies raised in rabbits	Invitrogen	16210-064
OCT	Tissue freezing media	Electron Microscopy Sciences/Fisher	62550-12
PAP pen	Hydrophobic slide marker	Research Products International Corp.	Not available
Paraformaldehyde	Fixing cell reagent	Electron Microscopy Sciences	19202

Table B-3. Continued.

Reagent	Description	Manufacturer	Catalog number
Paraplast X-tra tissue embedding medium	Paraffin	Fisher Scientific	23-021-401
PBS	Phosphate buffered saline solution	Amresco	0780-2PK
Permount	Mounting media for non-fluorescent sections	Fisher Scientific	SP15-100
Phloxine B	Histochemistry dye	Fisher Scientific	P387-25
Saponin	Mild detergent	Fluka	47036
Silver nitrate	Silver staining reagent	EMD	SX0205-5
Sodium thiosulfate pentahydrate ($Na_2S_2O_3$)	Silver staining reagent	Fisher Scientific	S78930-1
Superfrost plus slides	Microscope slides	Fisher Scientific	12-550-15
Tissue Path Cassettes IV white	Cassettes for tissue embedding with paraffin	Fisher Scientific	22-272416
Tissue Path disposable base molds	Molds for paraffin embedding	Fisher Scientific	22-038-217
Triton-X-100	Detergent to permeabilize cells for staining	Fisher Scientific	BP151-500
Ultraclean	Detergent	Spectrum Medical Laboratories	105-544

Table B-4. Reagents for clonning, genotyping, and general DNA work.

Reagent	Description	Manufacturer	Catalog number
Agarose Low EEO	Agarose for DNA gels	Fisher Scientific	BP160-500
Alkaline phosphatase	Enzyme to eliminate phosphate groups	Roche	NC9305850
Amonium acetate	Reagent	Fisher Scientific	A637-500
ATP, 100mM	Adenosine triphosphate		272056
Bacto Agar	Agar for bacterial medium plates	BD Biosciences	214010
Beta agarase I	Agarose digestion enzymes	New England Biolabs	M0392S
Bromophenol blue	Dye for loading dyes	Fisher	BP114-25
Carbenicillin	Antibiotic	Midwest Scientific/Amresco	J358-1G
Cesium chloride	Plasmid prep reagent	Fisher Scientific	BP210-500
Chloroform	Reagent	Fisher Scientific	BP1145-1
Circlegrow capsules	Bacterial medium reagent	BIO101 Systems	3000-131
Deoxiribonucleotides triphosphate (dNTPs)	Nucleotides for PCR reaction, 100 mM set	Invitrogen	10297-018

Table B-4. Continued.

Reagent	Description	Manufacturer	Catalog number
DH5α subclonning efficiency cells	Cells for transformation	Invitrogen	18265017
DNA columns Ultrafree DA	DNA extraction from agarose	Millipore	42600
DNA Hyperladder I	DNA gel marker	Fisher Scientific	NC9841467
DNA ladder 1Kb plus	DNA gel marker	Invitrogen	10787-018
EDTA	Quelator	Fisher Scientific	BP120-500
Ethanol 100%	Alcohol 200 proof	Fisher Scientific	NC9977258
Ethidium bromide	Intercalating DNA agent	Fisher Scientific	BP1302-10
Fast miniprep kit	DNA isolation, low scale for sequencing	Eppendorff	955150619
Glass beads, 4MM	For plating transformed bacteria	Fisher Scientific	11-312B
Glacial acetic acid	Acid	Fisher Scientific	BP2401-212
Glucose, D anhydrous	Sugar	Amresco	0188-1KG
Isopropanol	Alcohol	Fisher Scientific	BP2632-4
LB capsules	LB bacterial medium reagent	MP Biomedicals, LCC	3002-031
Lysozyme, egg white	Enzyme	Amresco	12650-88-3
NcoI	Restriction enzyme	New England Biolabs	R0193S
Phenol	Reagent	Amresco	0945-400ML
Platinum Pfx DNA polymerase	DNA polymerase enzyme	Invitrogen	11708-021
Potassium acetate	Reagent	Fisher Scientific	BP364-500
Proteinase K	Proteinase enzyme	Invitrogen	25530015
PureLink PCR microkit	To purify PCR products	Invitrogen	K310010
RNAse A, pancreatic	Enzyme	Amresco	0675-250MG
SalI	Restriction enzyme	New England Biolabs	R0138S
SeaPlaque GTG Agarose	Low melting point agarose for DNA gels	Lonza	50111
Small Kimwipes	Task wipers	Fisher Scientific	06-666A
S.O.C. medium	Bacterial medium	Invitrogen	15544034
Sodium chloride (NaCl)	Salt	Fisher Scientific	BP358-212
Sodium dodecyl sulfate (SDS)	Ionic detergent	Fisher Scientific	BP166-500
SuperscriptIII RT/Platinum Taq HiFi	Enzyme for RT-PCR reaction	Invitrogen	12574-030
T4 DNA ligase	DNA ligase enzyme	New England Biolabs	M0202S
TAE	Tris, Tris Acetate, EDTA	Amresco	0912-2PK
Taq DNA polymerase	PCR polymerase	New England Biolabs	M0273L
Tris	Buffer	Fisher Scientific	BP152-1
tRNA yeast	Reagent	Invitrogen	15401-029
Ultracentrifuge tubes	Plasmid prep tubes	Beckmann	362185
XhoI	Restriction enzyme	New England Biolabs	R0146S
X-gal	Reagent	Amresco	7240-90-6

Table B-5. Reagents RNA extraction and northern blotting.

Reagent	Description	Manufacturer	Catalog number
Bromophenol blue	Dye for loading dyes	Fisher	BP114-25
BSA for northern	Serum albumin	Amresco	0332-100G
Chloroform	Reagent	Fisher Scientific	BP1145-1
Clear UV 96-well transparent plates	To measure RNA concentration	Costar/Corning	3635
Diethyl Pyrocarbonate (DEPC)	Reagent for Northern	Sigma	D-5758
DNA-Ready to Go-label beads dCTP	To label DNA probes for Northern	GE Healthcare, Amhersan	27-9240-01
Ethidium bromide	Intercalating DNA agent	Fisher Scientific	BP1302-10
Filter paper, 3MM	Filter paper	Whatman	3030662
Formaldehyde 37%	Reagent	Amresco	0493-500ML
Formamide	Reagent	Sigma	47670
GeneScreen Plus Nylon membrane	Nylon membranes for Northern	Perkin-Elmer	NEF 976
Glycerol	Preservative	Fisher Scientific	BP229-1
Ilustra Probe Quant G-50 MicroColumns	Columns to purify radioactive labeled probes	GE Healthcare, Amhersan	27-5335-01
Isopropanol	Alcohol	Fisher Scientific	BP2632-4
MOPS buffer, 10x	Buffer	Amresco	E526-500ML
Nylon membrane	Membrane for Northern	GeneScreen Plus	NEF976001PK
RNAse AWAY	Reagent to eliminate RNA	Molecular Bioproducts	7002
RNAse free agarose low EEO	Free RNA agarose	Fisher Scientific	BP160-500
Sodium chloride	Salt	Fisher Scientific	BP358-212
Sodium citrate	Salt	Fisher Scientific	BP327-1
Sodium phosphate ($NaHPO_4$)	Salt	Fisher Scientific	
TRIzol reagent	RNA extraction reagent	Invitrogen	15596-026

APPENDIX C
METHODS

Chapter 2 Methods

Creation of Genomic SODMD Construct for Expression in Transgenic Mice.

Mutations in the genomic sequence of human SOD1 were introduced using PCR strategies. The selected mutations are indicated in Figure 2-1. The resulting 12 kb genomic mutant DNA fragment was then injected into mouse embryos, as previously described for other SOD1 transgenic mouse lines (Wong et al., 1995). The elaboration of the genomic SODMD DNA was entirely performed by Ms. Hilda Slunt-Brown.

Identification of the Presence of the Human SOD1 Transgene/s in Mice: Genotyping of SODMD Mice and Mice from the SODMD x SJL WT Matings.

Extraction of DNA from mouse tails

- Mouse tails were cut at approximately 0.6 cm in length. The procedures for tail cutting have been reviewed and approved by an Institutional Animal Care and Use Committee (IACUC) at the University of Florida. Collected tails are then digested or stored at -20°C.
- The day before DNA extraction, digest each mouse tail in 600 µl of TNES buffer (50 mM Tris base, pH 7.5; 400 mM NaCl; 100 mM EDTA, pH 8.0; 0.5% SDS) and 18 µl of Proteinase K at 20 mg/ml (dissolve 20 mg of proteinase K in 1 ml of distilled H_2O, vortex and store in aliquots at -20°C, once thawed do not reuse). Incubate overnight in a 55°C water bath.
- Remove tails from the water bath and mix well. Add 167 µl of supersaturated 6 M NaCl to each digested tail and mix well for 15 seconds (do not vortex).
- Centrifuge at 14,000 rpm for 5 minutes. Remove 650 µl of supernatant and place into a new microfuge tube. Try to get below the floating “scum” on the surface when removing the supernatant.
- Centrifuge at 14,000 rpm for 5 minutes. Remove 600 µl of supernatant and place into a new microfuge tube.
- Add 600 µl of cold 100% ethanol to each microfuge tube and mix well for 15 seconds (do not vortex). Centrifuge at 14,000 rpm for 5 minutes.

- Discard the supernatant and add 1 ml of cold 70% ethanol to each microfuge tube. Centrifuge at 14,000 rpm for 2 minutes.

- Discard the supernatant and turn each tube upside-down to air dry for 15-20 minutes.

- Resuspend the DNA by adding 200 µl of TE buffer (10 mM Tris base, pH 7.5; 1 mM EDTA, pH 8.0) to each microfuge tube. Mix and allow the DNA to dissolve at room temperature for at least 1 hour (can be longer, even overnight).

- Proceed to PCR analysis or store DNA at -20°C till needed.

PCR protocol for identification of genomic human SOD1

- Mix the following reagents for each tail DNA sample:
  - Distilled H_2O 20.14 µl
  - 10x PCR Buffer (with $MgCl_2$ from New England Biolabs) 2.50 µl
  - 5 mM dNTP's 0.50 µl
  - 50 µM Hu-S primer 0.38 µl
  - 50 µM H/M-AS primer 0.38 µl
  - Taq DNA Polymerase (from New England Biolabs) 0.10 µl
  - Tail DNA 1.00 µl
  - Total reaction volume 25.00 µl
- Hu-S primer: 5'-TCA AGC GAT TCT CCT GCC T-3'
- H/M-AS primer: 5'-CAC ATT GCC CAR GTC TCC A-3' (R=A/G)
- Set the above samples into a thermocycler and perform the next PCR program:
  - Heat blot pre-start
  - 94°C for 5 minutes
  - 94°C for 30 seconds
  - 60°C for 1 minute
  - 72°C for 5 minutes

  ] x 35 cycles
  - 72°C for 10 minutes
  - Hold at 10°C
- The transgenic band has a size of ~1200 bp
- Note that genotyping of SODMD mice was entirely performed by Ms. Susan E. Fromholt.

For SODMD x WT SJL mice, I performed DNA extraction and PCR genotyping as described above. In order to distinguish human mutant from human WT SOD1, DNA from mouse tails positive for the human SOD1 transgene were re-amplified by the method described above and the resulting DNA product was then purified using the PureLink PCR micro kit from Inivitrogen (Carlsbad, CA), following the manufacturer

protocol. The purified DNA fragments were then sent for automated sequence analysis together with the sequence primer SOD1-I3-AS (5'CTA TCG AAA GAC CTC AAG TAT AC-3'), which allows identification of amino acid sequences in exon 3.

RNA Extraction from Spinal Cords of SOD1 Transgenic Mice

The RNA extraction protocol presented here is a more detailed version of the TRIzol Reagent Protocol from Invitrogen (Carlsbad, CA):

- Weight the spinal cord tissue and calculate the amount of TRIzol needed per sample (do not add till just before homogenizing each sample)
- Homogenize tissue samples in 1 ml of TRIzol per 60-70 mg of tissue using Polytron power homogenizer (minimum speed is 11, start at 11 and increase but do not go over 20). NOTE: use tubes that leave enough space for the homogenizer to go into solution but do not cause overflowing. This step is performed at room temperature.
- Phase separation: incubate homogenized samples for 5 minutes at room temperature, or till the rest of the samples are homogenized. Then add chloroform: 0.2 ml per ml of TRIzol reagent. Then shake tubes vigorously for 15 seconds and incubate at room temperature for 2-3 minutes. Centrifuge samples at 12000 xg for 8 minutes (at room temperature in bench-centrifuge is fine).
- RNA precipitation: Transfer aqueous phase to a fresh tube (top), and save the organic phase if isolation of DNA or protein is desired (interfase for both). Precipitate RNA by mixing through vortexing briefly with isopropyl alcohol (use an aliquot obtained in a clean, just opened falcon tube when a new bottle of isopropanol is opened for the first time) at 0.5 ml per ml of TRIzol used. Incubate samples at room temperature for 10 minutes (or over lunch at 4C), centrifuge at 12000 xg for 10 minutes.
- RNA wash: remove supernatant and wash pellet once with 75% ethanol (1 ml per ml of TRIzol; can do 1ml per sample). Vortex, and centrifuge no more than 7500 xg for 5 minutes.
- Redissolving the RNA: air dry pellet for 10-20 minutes. It is important not to let pellet dry completely. Resuspend RNA in X µl of DEPC treated water (0.1% DEPC in distilled water overnight, autoclave to eliminate DEPC) by incubating for 10 minutes at 50°C (X µl = mg tissue/2).

Determination of Total RNA Concentration

Concentration of resulting RNA can be determined through absorbance in a spectrophotometer microplate reader and using 96-well clear UV transparent plates

Northern Blotting

Run gel, transfer to membrane and crosslink

- On an RNAse free agarose gel run about 5 or 10 µg of RNA with 3x volumes of Northern loading dye (For 730 µl: 360 µl: formamide, 80 µl of 10x MOPS buffer, 130 µl 37% formaldehyde, 50 µl glycerol, and 10 µl of 1% bromophenol blue).
- Heat at 100°C, 2-3 minutes. Cool on ice.
- Add 0.5 µl of 0.5 µg/µl ethidium bromide in DEPC treated water.
- Load on gel (For 125 ml: weight 1.25 g RNAse free agarose and put into 106.26 ml DEPC treated water, boil to melt agarose and cool, add 12.5 ml 10x MOPS buffer and 6.75 ml of 37% formaldehyde). Run loaded gel at 120 volts, until the bromophenol blue of the loading dye is about two-thirds of the way to the bottom (it approximately takes 2-3 hours).
- Soak gel in distilled H_2O for 40-60 minutes with three changes, to remove formaldehyde.
- Take a picture of the gel with a fluorescent ruler.
- Transfer RNA from gel to nitrocellulose or nylon membrane by capillary action overnight using 10x SSC (20x SSC stock: 350.6 g of sodium chloride and 174.4 g of sodium citrate in 2 liters of DEPC treated water). We use GeneScreen Plus, Nylon membrane. See scheme of transfer set up on Figure C-1.

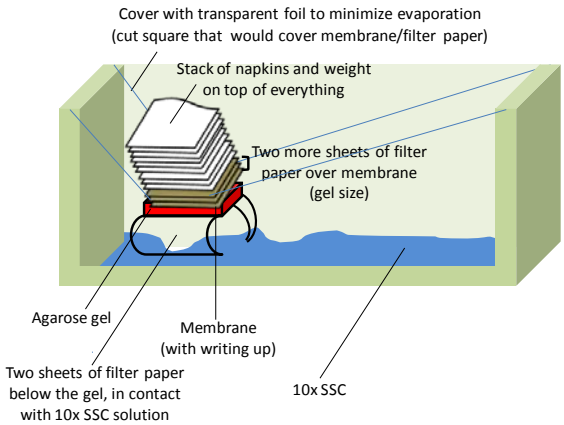

Figure C-1. Scheme of transfer arrangement for northern blotting.

- Crosslink to membrane, using the autocrosslink function of the Stratalinker (put membrane onto filter paper. Letters down. Start, about 45 seconds; then wrap in transparent foil and store at room temperature).

Northern blotting hybridization protocol

- NOTE: the whole protocol is carried out at 65°C

- Pre-hybridize membrane for 5 minutes to 5 hours (1 hour is good). Use 10-20 ml of hybridization buffer (1% BSA, 1 mM EDTA at pH 8.0, 0.5 M NaHPO4 at pH 7.2, 7% SDS, in distilled water) for the 35 x 150 ml hybridization cylinders/bottles (The side of membrane with RNA -face with no writing- facing the inside of the cylinder). Discard buffer.

- Add new hybridization buffer and boiled probe (see next section for labeling the probe). Use 10 ml of hybridization buffer in each hybridization cylinder and $0.5 \cdot 10^6$ to $5 \cdot 10^6$ cpm/ml of boiled probe per cylinder/bottle (add to buffer, not to the membrane). We used 24-25 µl of labeled probe at $1.4 \cdot 10^6$ cpm/ml (total $14 \cdot 10^6$ cpm).

- Hybridize for 8 to 24 hours.

- Washes (warm buffers prior washing): pour off hybridization buffer into radioactive waste (it can be saved and re-used within two weeks if needed). Rinse blot and bottle with wash buffer 1 (0.1% BSA, 1 mM EDTA at pH 8.0, 40 mM $NaHPO_4$ at pH 7.2, 5% SDS, in distilled water). Pour all buffers into radioactive waste. Perform 3 x 30 minute washes with buffer 1. Wash twice, 30 minute each with wash buffer 2 (1 mM EDTA at pH 8.0, 40 mM $NaHPO_4$ at pH 7.2, 1% SDS, in distilled water).

- Wrap wet blot in transparent foil and expose to film in developing cassette for 24 hours at -80°C.

DNA probe labeling with ^{32}P for northern blotting

For labeling the DNA probe we use DNA-Ready to Go-label beads dCTP from GE Healthcare (Amhersan) to prepare the template and label, following the manufacturer protocol. We used DNA insert/fragment as SOD1 probe that has been purified with DNA columns (Ultrafree DA, Millipore). A total of 25-50 ng of DNA probe was used for the labeling reaction. So, for SOD1 at 4 ng/µl we used 8 µl (32 ng) and denatured it at 95°C for 3 minutes and then put on ice as recommended. For PrP loading control, the probe was a fragment of 4 kb at 1 ng/µl purified from a low melting point agarose gel. In this

case the PrP DNA was denatured at 95°C for 7 minutes, then incubated at 37°C for 10 minutes before labeling reaction. Follow labeling reaction as described in manufacturer protocol. Once the probe is labeled, the probe is purified using the Illustra ProbeQuant G-50 Micro Columns from GE Healthcare as described by the manufacturer.

Preparation of Crude Supernatant (Total Protein Fraction) from Mouse Spinal Cords

- Calculate net weight of each spinal cord to analyze and sonicate cords till dissolved (about 2 times for 15 seconds, place on ice in between) in 5 weight volumes of 1x TEN buffer (10 mM Tris, pH 7.5; 1 mM EDTA, pH 8.0; 100 mM NaCl) with protease inhibitor cocktail at 1:100.
- Spin down homogenized tissue at 8000 xg for 10 minutes and discard pellet. Keep supernatant as crude supernatant.

Detergent Extraction and Centrifugation Assay Protocol for Mouse Spinal Cords.

This assay generates two fractions termed S1 (detergent-soluble cellular protein) and P2 (detergent-insoluble cellular protein). The latter containing detergent-insoluble aggregated forms of mutant SOD1. This assay is performed as follows:

A total of 300 µl of spinal cord crude supernatant was extracted by adding an equal volume of buffer 1 (to final concentration of 10 mM Tris, pH 7.5; 1 mM EDTA, pH 8.0; 100 mM NaCl; 0.5% NP-40, 1:100 v/v protease inhibitor cocktail), and sonicated 3 times for 10 seconds each. Then the samples are transferred into airfuge tubes, 200 µl per tube, and centrifuge at maximum speed for 5min (> 100000 xg). The supernatant is saved as the detergent soluble (S1) fraction. The pellet (P1) is further washed with 200 µl/tube of the same extraction buffer (sonicate twice, 15 seconds each) and the supernatant is discarded after another 5 minute high speed spin. The remaining pellet represents the detergent-insoluble (P2) fraction, which is resuspended in 30-40 µl of extraction buffer containing SDS and deoxycolate (10 mM Tris, pH 7.5; 1 mM EDTA, pH

8.0; 100 mM NaCl; 0.5% NP-40, 0.25% SDS, 0.5% deoxycolate, 1:100 v/v protease inhibitor cocktail), and combined into one tube. The total volumes corresponding to S1 and P2 fractions are of 600 and 100 µl, respectively. Protein concentration of S1 and P2 are determined by BCA assay, as described in the corresponding section. For western blot analysis, 5 µg of S1 and 20 µg of P2 total protein are used to load onto 18% SDS-PAGE gels. Western blotting is performed as described in "SDS-PAGE Electrophoresis and Western Blotting".

BCA Assay for Determination of Protein Concentration

- Protein concentrations are obtained using the bicinchoninic acid assay (BCA assay) from Pierce Biotechnology. We use 96-well plates for measuring protein concentration on a plate reader. For detergent-soluble (S1) and insoluble (P2) fractions, the protein was diluted 1:4 (2.5 µl of total protein in 10 µl total volume, diluted in water). For any other lysates a dilution 1:10 is enough. Use 10 µl for each BSA standard (range between 0 and 2.4 µg/µl).
- To wells containing either a standard or a sample, add 200 µl of BCA reagent mixture (50:1, Reagent A: Reagent B).
- Incubate plate at 37C for 20-30 minutes. Alternatively, the reaction can take longer at room temperature (1 hour).
- Read plate at 562 nm. Protein concentrations and the standard curves are calculated through the Kinetical KC4 3.4 software (Bio-Tek Instruments, Inc. Winooski, VT).

SDS-PAGE Electrophoresis and Western Blotting

- For crude supernatants: Prior loading the gel, prepare the 5 µg protein, add 1x TEN up to a 15 µl volume. For detergent extracted samples, prepare 5 µg of S1 fractions and 20 µg of P2 fractions in 1x TEN up to a volume of 15 µl.
- Add 5 µl of 4x Laemmli sample buffer to each sample and boil (or use heat block at 95°C) for 5 minutes. Load samples on 18% SDS-PAGE gel and run at 125 volts for 110 minutes.
- Protein is then transferred from the gel onto nitrocellulose membranes (Optitran BA-S 85 from Whatman Inc). Label the bottom of membrane and pre-wet in distilled water, then wet in transfer buffer. Set into transfer cassette (black electrode, sponge, filter paper, gel, membrane, filter paper, sponge, red electrode). Set transfer at 100

mAmps for overnight transfer in big transfer box. Alternatively you can do 2 hour transfers at 400 mAmps.

- To reduce nonspecific antibody binding, membranes were blocked in 5% nonfat milk, 1x PBS for 15-30min before incubating them with the corresponding antibodies. Incubate membrane in milk with the primary antibody overnight (SOD1 can be done for 1 hour). For antibodies concentrations check the antibody list on Appendix D.

- Wash membrane with 1x PBS-T (0.1% Tween 20 in 1x PBS) for 10 minutes, 3 times.

- Incubate membrane in milk with the corresponding secondary antibody (goat anti rabbit-HRP in this case) for 1 hour at room temperature.

- Wash 3 times with 1x PBS-T for 10 minutes each.

- Secondary chemiluminescence was visualized on a Fujifilm imaging system (FUJIFILM Life Science) using ECL reagent mixture (1:1, total of 800 µl per membrane).

Sciatic Nerve Extraction for Cryosection from SOD1 Transgenic Mice

NOTE: this protocol has been adapted from Dr. Lucia Notterpek's lab protocols.

- Prepare a container with liquid nitrogen.

- Immerse a small beaker with 3-methylbutane (it freezes becoming white). Do not let the liquid nitrogen get into the beaker. The liquid nitrogen is just to freeze the 3-methylbutane.

- Extend legs of sacrified mice and hold with needles. Then, spray animal with water to get hair smoothen down.

- Cut out skin on the legs and the lower back. Try to avoid getting hair left on the animal. Once the muscle is exposed, cut it with 2 straight cuts, then lift muscle layers to see the sciatic nerve. See scheme in Figure C-2 for instructions on how to extract the sciatic nerve from mice.

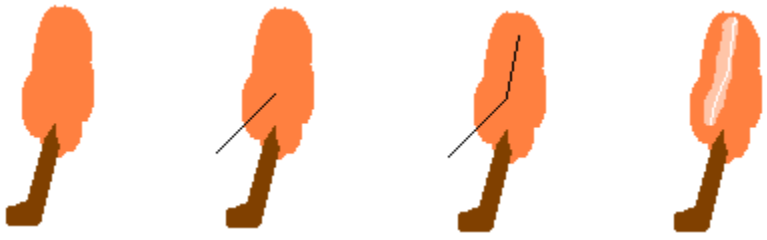

Figure C-2. Schematic representation of how to make cuts in mouse limbs to extract the sciatic nerve.

- Hold the nerve with forceps like in the middle (try to handle it on just one place), and cut underneath the nerve to release it from other tissues. Then cut at the lower end and follow till the upper end and cut. Keep in mind that when it gets close to the spinal cord there is a lateral connection that needs to be cut too.

- Remove extra skin if present and extend the nerve on a piece of filter paper. Get the other nerve and do the same.

- Get the beaker that contains 3-methylbutane out of the liquid nitrogen and once it thaws, immerse the filter paper with the nerve into the 3-methylbutane solution. Leave a few seconds and then immerse in liquid nitrogen. Introduce into crystorage tubes and leave into liquid nitrogen till all animals are done. Store in crystorage, in contact with liquid nitrogen.

Sciatic Nerve Cryosection and Immunostaining

NOTE: This protocol has been adapted from Dr. Lucia Notterpek's lab protocol.

- Cut frozen tissue sections at 5 µm thickness, with chamber at -25ºC: For longitudinal sections, OCT is applied on the base, then a small piece of sciatic nerve is laid on top of OCT (do not embed). Apply Flash Freezing spray from Fisher (note that if the OCT is very liquid, the spray will splash OCT away). Carefully put the longitudinally placed sciatic nerve parallel to the blade, so the tissue will not be in an angle with respect to the blade. For transverse sections the tissue needs to be embedded in OCT. A trick to maintain the sciatic nerve perpendicular to the base is to add a little OCT to the base first, then immerse half of a small piece of sciatic nerve in OCT in vertical orientation. Then, fast freeze the sample. This will maintain the sciatic nerve rigid and can be then completely covered by OCT.

- Cut sections are placed on superfrost plus microscope slides at room temperature (touch straightened out tissue with the slide quickly, which allows the tissue to quickly adhere to the slide. Slides can be stored at -80ºC till staining steps.

- For staining procedures, let the tissue dry (or come to room temperature if stored at -80°C) for about 1 hour at room temperature before beginning staining procedure.

- Circle entire sample area with a PAP pen (if not available, use rubber cement)

- Fixation/permeabilization: for MBP in sciatic nerve or mouse tissue the next method works really well

    - Incubate in 4% paraformaldehyde 10 minutes at room temperature.

    - Permeabilize 5-10 minutes with 100% COLD (-20ºC) methanol.

- Rinse 3 times with 1x PBS for 10 minutes each.

- Blocking: incubate 1 hour at room temperature with 20% goat serum in 1x PBS (can do longer than 2 hours at 4ºC).

- Primary antibody: MBP from Chemicon in 20% goat serum in PBS o/n at 4ºC (for antibody dilutions check antibody list on Appendix D).

- Rinse 3 times with 1x PBS for 10 minutes each.

- Secondary antibody: Alexa fluor goat anti-rabbit 594 nm in 20% goat serum in PBS for 1 hour. Also include DAPI (4´,6-diamidino-2-phenylindole, dihydrochloride, stock 14.3 mM from Invitrogen) at 1:2000 (if forget to add, it can be done later in 1x PBS for a minimum of 5 minutes, 5-10 minutes is good).

- Rinse 3 times with 1x PBS for 10 minutes each.

- Mount cells with Aqua/Poly mount from Polysciences Inc. Mount coverslips over tissue sections. Store slides at 4ºC in the dark.

Paraffin Embedding

- Put perfused spinal cord tissues into small tissue path cassettes from Fisher, and wash in distilled water for 30 minutes. Then follow the next incubation series in the indicated reagents at room temperature with shaking unless otherwise indicated:

- 70% Ethanol for 15 minutes x 2
- 80% Ethanol for 15 minutes x 2
- 95% Ethanol for 15 minutes x 2
- 100% Ethanol: 4 quick rinses
- 100% Cedarwood oil for 15 minutes x 3
- Pre-warmed Cedarwood oil at 37°C oven for 2 hours
- Cedarwood/Methyl Salicylate for 40 minutes x 2
- Leave in Cedarwood/Methyl Salicylate overnight
- Methyl Salicylate for 30 minutes x 3
- Paraffin at 60°C oven for 30 minutes x 5
- Use new paraffin in the last time for 1 hour (tissues cannot be left in hot paraffin for too long, such as overnight.)

- Embed in 65°C paraffin. Blocks can then be stored or sectioned. For sectioning we performed 10 µm thick sections and when the tissues appeared to be dry, we rehydrated them by applying a small piece of paper wet in a solution of 0.01% Triton X-100.

Deparaffinization and Dehydration of Paraffin Sections.

- Prior staining of paraffin sections we need to deparaffinize them. After the chosen staining method is performed, sections are dehydrated and permount solution is used to cover the slides.

- Deparaffinize slides: incubate slides in a 60°C oven till paraffin appears clear. Then pass the slides to a series of solutions in the following order for about 2 minutes in each: histoclear, 100% ethanol, 95% ethanol. 70% ethanol, distilled water.

- Dehydrate by immersing slides for 2 minutes in each of the following solutions in the same order: 70%, 95% and 100% ethanol, and histoclear solution. Mount coverslips with Permount solution.

Heammatoxylin and Eosin Staining of Paraffin Sections.

- Deparaffinize slides.

- Immerse slides into filtered Modified Mayer's Hematoxylin solution for 5 minutes.

- Soak in distilled H_2O till it turns blue (or in warm tap water; it takes around 2 minutes). Check under the miscroscope, if good then go to next step.

- Immerse in eosin solution (0.1% eosin, 0.01% phloxine, 74% alcohol, 0,4% glacial acetic acid in water) for 2 minutes, then water for 1 minute. If too dark longer washes can be done in water till the desired color is obtained.

- Dehydrate and coverslip.

Silver Staining of Paraffin Sections

- The day prior staining we need to wash the glassware we will use: slide jars, 200 ml beakers; 250 ml flasks. Wash them in tap water carefully with detergent, rinse carefully. Follow by immersing them in tap water with 20% bleach for at least 2 hours. Then, wash thoroughly in tap water. Place them in Ultraclean overnight (20 ml ultraclean per liter of distilled water).

- The next day we rinse glassware in running distilled water carefully and perform silver staining as described here.

- Deparaffinize the slides as previously described.

- For about 32 sections, prepare 100 ml of ~20% $AgNO_3$ solution (20 g $AgNO_3$ in 100 ml H_2O).

- Place slides in 50 ml of 20% $AgNO_3$ in the dark for 20 minutes for impregnation

- Titrate the other 50 ml of 20% $AgNO_3$ solution by ammonium hydroxide: add drop by drop until it becomes black and continue till the solution becomes clear again.

- Wash the slides by distilled water thoroughly, drain the slides carefully

- Place slides into titrated $AgNO_3$ for 20 minutes in the dark.

- Pour the titrated $AgNO_3$ into a beaker and add 2 drops of developer (30 ml distilled water, 5 ml of 37% formaldehyde, 1.5 g citric acid, and 1 drop of concentrated HNO_3. Mix and return to slide jar.

- Place the slides into developing solution, normally it takes from 8 to 20 minutes. Be careful to check under a microscope, do not go too dark.

- Wash by ammonium hydroxide in water (10 drop of ammonium hydroxide in ~300 ml of distilled water).

- Wash by distilled water

- Place slides in 5% $Na_2S_2O_3$ in water for 30 seconds

- Wash by distilled water again

- Dehydrate and coverslip using permount

GFAP-DAB Staining of Paraffin Sections

- Deparaffinize sections. The rest of the protocol is performed at room temperature.

- DAB-pretreatment for 5 min in 0.3% hydrogen peroxide, 10% methanol in 1x PBS

- Wash with 1x PBS for 10 minutes, 3 times. Block in 20% NGS, 0.1% Triton X-100 in 1x PBS for 45 minutes.

- Primary antibody (rabbit GFAP) incubation in 20% NGS, 0.1% Triton X-100 in 1x PBS overnight.

- Wash with 1x PBS for 10 minutes x 3

- Incubate slides in biotinylated secondary anti-rabbit antibody (1:200) in 20% NGS, 0.1% Triton X-100 in 1x PBS for 1 hour.

- Wash with 1x PBS for 10 minutes once.

- Make ABC reagent (NOTE MAKE 30minutes BEFORE USE): 2 drops of reagent A into 10 ml of 1x PBS solution, mix and add 2 drops of reagent B, mix well and allow to stand 30 minutes before use

- Incubation in ABC reagent for 30 minutes

- Wash with 1x PBS for 10 minutes, x 3

- Make DAB: 10 mg (one tablet) in 100 ml PBS. Filter and add 10 µl hydrogen peroxide (or 5 µl into 50 ml DAB).

- Put sections in DAB for about 5-20 minutes (watch for color change, remove immediately upon browning)
- Wash with 1x PBS for 10 minutes, once
- Counter-stain with haematoxylin (5 minutes) and dehydrate. Use permount to coverslip.

Creation of SODMD and SODMD cDNA Variants

The SODMD cDNA was obtained from the genomic version of this mutant protein by RT-PCR. This step was performed by Ms. Hilda Slunt-Brown. Then, by PCR techniques I added XhoI sites at 3' and 5' ends of the cDNA, which allowed for subcloning into a version of pEF-BOS vector with a SalI site in the cloning site (XhoI and SalI sites are compatible, but ligation is not reversible).

For SODMD cDNA variants, the SODMD cDNA was used as a template and new mutations were performed by PCR techniques, in which the primers contain the desire mutation. Additionally, we added to this new versions new restriction sites for cloning into our most updated version of the pEF-BOS vector: NcoI at 5' end and SalI at 3' end. These different restriction sites in inserts and the pEF-BOS vector allows easier cloning as it allows directional orientation of inserts.

Transfection into HEK293FT Cells for Biochemical Analysis of Detergent-Insoluble Aggregates.

HEK293FT cells express the SV40 large T-antigen, which allows for episomal replication of the pEF-BOS plasmid as well as strong enhancement of transcription, and were purchased from Invitrogen (Carlsbad, CA, USA). HEK293FT cells were cultured in 60 mm lysine-coated dishes and transiently transfected, at 90-95% confluency, with either one SOD1 construct (4 µg), or equimolar amounts of two SOD1 constructs (~2 µg

each). Transfections were performed using Lipofectamine 2000, following the manufacturer's protocol. Prepare the next samples separately:

- 4 µg DNA + 250 µl OptiMEM
- 10 µl Lipofectamine 2000 + 250 µl OptiMEM

Then combine both mixes into the same tube and incubate for 20 minutes at room temperature.

In the mean time wash cells to transfect with 1x PBS, aspirate and add 2 ml (for untransfected control) or 1.5 ml (for transfected cells) of OptiMEM. Add complex to the cells following the 20 minute incubation.

In some cases, for 24 hour transfections, 3 to 4 hour following addition of DNA complex to the cells, complete DMEM media (with L-glutamine and horse serum) was added (2 ml, total of ~5 ml total media volume). In some other cases, cells were left in OptiMEM media for a total of 24 hours, to enhance transfection efficiency. For 48 hour transfections, cells were left in OptiMEM + DNA complex for 24 hours, at which point it was exchanged by complete cell media (complete DMEM media). Note than when an experiment was performed with a set of conditions, the repetitions were carried out following exactly the same conditions.

Collect Transfected HEK293FT Cells

Cells were harvested 24 or 48 hours after transfection by scraping in 1x PBS. Cell pellets are then washed twice in 1.5ml tubes with 1x PBS. When needed, cell pellets are stored at -20°C.

Detergent Extraction and Centrifugation Assay of HEK293FT Collected Cells

The method used for HEK293FT cells is the same as decribed for mouse spinal cord (see "Detergent Extraction and Centrifugation Assay for Mouse Spinal Cords"). For

cell culture studies, the whole cell pellet is used and lysed by sonication in 200 µl of non-ionic detergent (10mM Tris, pH 7.5; 1mM EDTA, pH 8.0; 100mM NaCl; 0.5% NP-40, 1:100 v/v protease inhibitor), 3 times 10 seconds each. This step is equivalent as using 1x TEN and adding equal volumes of detergent extraction buffer 1. The rest of the protocol is followed as described for spinal cord samples, including BCA assay (see "BCA Assay for Determination of Protein Concentration"), SDS-PAGE and western blotting (see "SDS-PAGE Electrophoresis and Western Blotting").

Chapter 3 Methods

Creation of SOD1 cDNA Expression Plasmids

All of the WT and mutant human SOD1 cDNAs are expressed from plasmids based on the mammalian pEF-BOS expression vector, and cloned through PCR strategies, through either a unique SalI site or a directional 5' NcoI and 3' SalI restriction sites. A few of the SOD1 mutants cDNAs used here were previously created into the pEF-BOS system (single SalI site) by Ms. Hilda Slunt-Brown (WT, A4V, G37R, G41D, H46R/H48Q, G85R, G93A, G93C, L126X or L126Z, and L126delTT SOD1) (Wang et al., 2005a;Borchelt et al., 1994;Wang et al., 2003); however, many other mutants were kindly provided, in the YEp351 yeast vector, by the Hart lab (Dr. Stephen Holloway, University of Texas Health Sciences Center San Antonio, TX), which I subcloned into our pEF-BOS mammalian vector through NcoI and SalI restriction sites (A4T, V14G, V14M, E21G, E21K, G41S, H43R, H80R, G93D, G93R, G93S, G93V, L84V, D90A, E100G, E100K, D101G, D101N, D124V, D125H, E133ΔE, S134N, N139K, L144F, L144S, V148G and V148I SOD1).

The sequences of all mutants in the vectors were verified by automated sequence analysis.

HEK293FT Transfections and Analysis by Detergent Extraction

The rest of the methods used in Chapter 3 has been described in Chapter 2 Methods: see “HEK293FT Transfection for Detergent Extraction and Centrifugation Assay”, “Collect Transfected HEK293FT Cells”, “Detergent Extraction and Centrifugation Assay of HEK293FT Collected Cell Pellets”, “BCA Assay for Determination of Protein Concentration”, and “SDS-PAGE Electrophoresis and Western Blotting”

N2a Cell Transfection and Analysis of Detergent-Insoluble and Soluble Fractions

The work of N2a cells was performed following the same procedures as described for HEK293FT cells.

Chapter 4 Methods

SOD1 cDNA and GFP Expression Plasmids

All SOD1 cDNA constructs used here have been described in “Creation of SOD1 cDNA Expression Plasmids” from Chapter 3 Methods. Similar techniques were performed to create the mouse WT SOD1 and C111S cDNAs (Karch and Borchelt, 2008).

The GFP cDNA was purchased from Clontech (Mountain View, CA, USA) and inserted into pcDNA3.1(A)-STOP-Myc through a XhoI site prior the vector Myc tag (Invitrogen, Carlsbad, CA, USA) by Ms. Hilda Slunt-Brown.

HEK293FT Transfections and Analysis by Detergent Extraction

Additional methods used in Chapter 4 has been described in Chapter 2 Methods: see “HEK293FT Transfection for Detergent Extraction and Centrifugation Assay” (note that when co-transfections of SOD1 and GFP were performed, equimolar amounts of one SOD1 construct and the GFP construct were used, total 4 µg), “Collect Transfected

HEK293FT Cells", "Detergent Extraction and Centrifugation Assay of HEK293FT Collected Cell Pellets" (note that for detergent extractions in the presence of high levels of β-mercaptoethanol, βME, all buffers were adjusted to contain 30% βME), "BCA Assay for Determination of Protein Concentration", and "SDS-PAGE Electrophoresis and Western Blotting"

Analysis of S1 and P2 Fractions by Hybrid Linear Ion-trap Fourier-transform Ion Cyclotron Resonance Mass Spectrometry (FTMS)

For mass spectrometry analysis, six 60 mm culture dishes were co-transfected with WT and G93A human SOD1 constructs, then combined and extracted in detergent. Ultimately, the S1 and P2 fractions were combined into final volumes of 600 µl and 100 µl respectively. Portions of these fractions were chromatographed by HPLC as previously described (Shaw et al., 2008). SOD1 containing fractions from HPLC chromatography were quickly thawed and 7 µl was loaded into nano-electrospray emitters (Proxeon) for immediate analysis using a nano-electrospray source equipped mass spectrometer (LTQ-FT Ultra, Thermo, San Jose). Samples were analyzed in positive ion mode with 1.8 kV typically required for stable nanospray performance. Full mass spectra were recorded over a mass range 600-2000 (m/z, Da) with resolution set at 100,000 at m/z = 400. Typically, 50 transients were averaged prior to recording a single MS spectrum. FTMS analyses were repeated twice. The FTMS analyses were performed by Dr. Armando Durazo from the laboratory of Dr. Julian Whitelegge at UCLA.

Chapter 5 Methods

SOD1 cDNA Expression Plasmids

All SOD1 cDNA constructs used here have been described in “Creation of SOD1 cDNA Expression Plasmids” from Chapter 3 Methods.

HEK293FT Transfections and Analysis by Detergent Extraction

The rest of the cell culture methods used in Chapter 5 has been described in Chapter 2 Methods: see “HEK293FT Transfection for Detergent Extraction and Centrifugation Assay” (note that when co-transfections of SOD1 and GFP were performed, equimolar amounts of one SOD1 construct and the GFP construct were used, total 4 µg), “Collect Transfected HEK293FT Cells”, “Detergent Extraction and Centrifugation Assay of HEK293FT Collected Cell Pellets”, “BCA Assay for Determination of Protein Concentration”, and “SDS-PAGE Electrophoresis and Western Blotting”.

Mouse Lines

All mouse lines used in this study has been previously described: PrPG37R (Wang et al., 2005b), L126Z (Wang et al., 2005a), SJL WT and Cg WT lines (Gurney et al., 1994), and L76 WT Wong line (Wong et al., 1995).

Identification of Double Mutant/WT Transgenic Mice: Genotyping

Genotyping and maintenance of individual PrPG37R, L126Z, and L76 WT mouse lines was performed entirely by Ms. Susan E. Fromholt.

Extraction of DNA from mouse tails was performed as described in Chapter 2 Methods, but different PCR protocols were used for identification of mutant and WT transgenes in matings resulting from PrPG37R or L126Z crossed to SJL WT, Cg WT, or L76 WT.

PCR protocol for identification of PrPG37R cDNA

- Mix the following reagents for each tail DNA sample:
  - Distilled H_2O 20.6 µl
  - 10x PCR Buffer (with $MgCl_2$ from New England Biolabs) 2.5 µl
  - 5 mM dNTP's 0.5 µl
  - 50 µM PrP-S 0.2 µl
  - 50 µM PrP-AS 0.1 µl
  - Taq DNA Polymerase (from New England Biolabls) 0.1 µl
  - Tail DNA 1.0 µl
  - Total reaction volume 25.0 µl
- PrP-S primer: 5'-GGG ACT ATG TGG ACT GAT GTC GG-3'
- PrP-AS primer: 5'-CCA AGC CTA GAC CAC GAG AAT GC-3'
- Set above samples into a thermocycler and perform the next PCR program:
  - Heat blot pre-start
  - 94°C for 5 minutes
  - 94°C for 30 seconds
  - 60°C for 1 minute
  - 72°C for 5 minutes

  ] x 35 cycles
  - 72°C for 10 minutes
  - Hold at 10°C
- The PrPG37R transgenic band has a size of ~500 bp.

For identifying human WT SOD1 from the different PrPG37R x WT matings, I performed the "PCR Protocol for Identification of Genomic Human SOD1" as described in Chapter 2 Methods.

PCR protocol for identification of L126Z and/or WT SOD1

For identifying either L126Z or WT human SOD1 from the different L126Z x WT matings, I performed the "PCR Protocol for Identification of Genomic Human SOD1" as described in Chapter 2 Methods, in which the L126Z transgene gives a band of ~500 bp and the WT transgene gives a band of ~1200 bp.

RNA Extraction and Northern Blotting

For RNA analysis and northern blotting of WT lines, we followed the same protocols that we described in Chapter 2 Methods: see "RNA Extraction from Spinal

Cords of SOD1 Transgenic Mice", "Determination of Total RNA Concentration", and "Northern Blotting".

Protein Analysis and Western Blotting of Mouse Spinal Cords

For protein analysis and western blotting of spinal cord samples, we followed protocols that are described in Chapter 2 Methods: see "Preparation of Crude Supernantant (Total Protein Fraction) from Mouse Spinal Cords" (note that together with SOD1 primary antibody incubations we use a primary antibody that recognizes β-TubulinIII, which represents a protein loading control), "Detergent Extraction and Centrifugation Assay Protocol for Mouse Spinal Cords", "BCA assay for Determination of Protein Concentration", and "SDS-PAGE Electrophoresis and Western Blotting".

Analysis of S1 and P2 Fractions by Hybrid Linear Ion-Trap Furier-transform Ion Cyclotron Resonance Mass Specctrometry (FTMS)

FTMS analysis of S1 and P2 of spinal cords was performed as described for cell culture samples in Chapter 2 Methods. Here, the spinal cord fractions were prepared by combining three spinal cords into one sample and extracted in detergent to obtain 1.2 ml of S1 and 600 µl of P2 fractions. These analyses were preformed twice by Dr. Armando Durazo from the laboratory of Dr. Julian Whitelegge at UCLA.

Visualization of Reduced and Oxidized SOD1 Proteins

To observe the redox state of WT and mutant SOD1 proteins, iodoacetamide was included in the extraction buffer (at concentration of 100 mM), which serves as a modifier agent of free SH-groups in order to prevent the random formation of disulfide bonds by air oxidation.

Extracted samples were run onto SDS-PAGE gels as described in "SDS-PAGE Electrophoresis and Western Blotting" from Chapter 2 Methods, with the following modifications:

- Samples are boiled in a Laemmli sample buffer lacking β-mercaptoethanol.
- To allow visualization of the oxidized state, gels were incubated in transfer buffer containing 2% of β-mercaptoethanol for 10 minutes prior transfer onto membranes (in gel reduction). Alternatively, a "in membrane reduction" can be done (incubation of membrane instead of the gel). This step allows for a better binding of the antibody to oxidized forms of the protein (Jonsson et al., 2006a;Zetterstrom et al., 2007).

RT-PCR of Mouse WT Lines

- RNA extracted from WT lines was used in RT-PCR reactions as follows:
  - 500 ng of RNA
  - 2x Reaction buffer 25 µl
  - HuSOD-S genomic primer 10 µM 1 µl
  - HuSOD-AS genomic primer 10 µM 1 µl
  - Enzyme mix (SuperscriptIII RT/Platinum Taq HiFi, from Invitrogen) 1 µl
  - Distilled DEPC treated H_2O up to 50 µl
- HuSOD-S genomic primer: 5'-CTA GCG AGT TAT GGC GAC GAA G-3'
- HuSOD-AS genomic primer: 5'-GAA TGT TTA TTG GGC GAT CCC-3'
- Set above samples into a thermocycler and perform the next PCR program:
  - Heat blot pre-start
  - 55 ^{o}C for 30 minutes
  - 94^{o}C for 2 minutes
  - 94^{o}C for 15 seconds
  - 50^{o}C for 30 seconds } x 25 cycles
  - 68^{o}C for 45 seconds
  - 68^{o}C foor 5 minutes
  - Hold at 4^{o}C

Chapter 6 Methods

Creation of SOD1 cDNA Expression Plasmids

SOD1 of non-tagged cDNA constructs were described in "Creation of SOD1 cDNA Expression Plasmids" from Chapter 3 Methods.

SOD1 tagged cDNA variants were created from a worm expression SOD1::eYFP-pPD30 construct provided from Dr. Rick Morimoto's lab. This SOD1::eYFP construct contains a small linker between SOD1 and YFP that was modified by Ms. Hilda Slunt-

Brown to introduce a SalI restriction site. This SOD1::YFP DNA was then cloned in to our mammalian pEF-BOS vector. Different SOD1 mutants were introduced in this construct to generate different SOD1::YFP expression plasmids (WT::YFP, A4V::YFP, G37R::YFP, H80R::YFP, G85R::YFP, D101N::YFP, D125H::YFP, E133ΔE::YFP, S134N::YFP, MD::YFP, and MD-G6F-S111Y::YFP). Similarly in some cases, the YFP cDNA was replaced by a Turbo RFP cDNA (in pTRIPZ empty vector from Open Biosystems, Huntsville, AL) to create WT::RFP, A4V::RFP and D101N::RFP.

Transfection into HEK293FT, TK-Negative or NIH3T3 Cells for Immunocytochemistry Analysis.

Transfection was performed on coverslips previously coated with 0.5 mg/ml poly-L-lysine, 1x PBS in 12-well plates. We followed the same protocol as described in "Transfection into HEK293FT Cells for Biochemical Analysis of Detergent-Insoluble Aggregates" from Chapter 2 Methods, with the variation that only 2 µg of SOD1 cDNA was transfected per sample.

Immunocytochemistry of Transfected Cells

NOTE: for fluorescent tagged SOD1 transfections that did not need additional staining, only fixation or fixation and DAPI staining was performed.

- Rinse transfected cells once with 1x PBS. Go directly to step 4 if saponin treatment is not needed.
- Incubate cells for 30 minutes in 0.01% freshly made saponin (or alternatively 0.01% freshly made digitonin) in 1x PBS at room temperature.
- Wash with 1x PBS, 10 minutes once
- Fix cells in 4% paraformaldehyde in 1x PBS at room temperature for 15 minutes.
- Wash cells 3 times with 1x PBS, 10 minutes each.
- Permeabilize cells with cold (-20°C) 100% methanol for 5 minutes and replace by 1x PBS (do not let cells dry).

- Block a minimum of 30 minutes in 20% goat serum, 1x PBS (or serum type in which secondary antibody was raised) at room temperature.
- Incubate cells with primary antibody (see antibody table in Appendix D for working dilutions) in 10% goat serum, 1x PBS at 4°C overnight.
- Wash cells 3 times with 1x PBS, 10 minutes each.
- Incubate cells with secondary antibody (see antibody table in Appendix D for working dilutions) in 10% goat serum, 1x PBS at room temperature for 1-2 hours. Also add DAPI solution at 1:2000 with secondary antibody incubation (DAPI: 4´,6-diamidino-2-phenylindole, dihydrochloride, stock 14.3 mM from Invitrogen). NOTE: if adding DAPI is forgotten, it can be added in one of the washes; 5 minutes of DAPI at 1:2000 is enough for good nuclei staining.
- Wash cells 3 times with 1x PBS, 10 minutes each.
- Mount cells with Aqua/Poly mount from Polysciences Inc.

Statistical Analysis

Estimation of Aggregation Propensity

The aggregation propensity of SOD1 mutants was assessed by comparing the ratio of immunolabeled SOD1 protein in the P2 *vs*. S1 fractions. Notably, the amount of protein analyzed by immunoblots from these two fractions was not equivalent; in all cases 20 µg of protein was analyzed from the P2 fraction and 5 µg from the S1 fraction. The intensities of the SOD1 immunoreactive bands in the S1 and P2 fractions establish a ratio value for a particular mutant in a particular immunoblot. To normalize the data from different experiments, each immunoblot that was quantified included a positive control (A4V, with exception of G85R for Figure 4-3), which were used to normalize the data (A4V and G85R show equivalent aggregation propensities and the ratio values for these positive controls was set to 1).

Statistical Tests

Statistical analyses included paired and unpaired student *t*-tests, and correlations studies that were performed as indicated in the corresponding figure or chapter. All these analyses were performed using the GraphPad Prism 5.0 Software (San Diego, CA, USA). In order to perform significant statistical test, each experiment was repeated a minimum of three times.

Cloning Methods

A compilation of some of the cloning methods used in this research project is described below.

Ligation

Ligations are performed using 0.01 pmol of vector and 0.05 pmol of insert, and the following reaction components:

- 10mM ATP (no more than 1 month old) 2 µl
- 10x ligase T4 buffer (from Roche) 2 µl
- Ligase T4 (Roche) 1 µl
- Distilled H_2O up to 20 µl
- Incubate ligation reaction 2 hours at room temperature, or alternatively overnight at 15°C.

Transformation

- Thaw DH5α cells on hand and place quickly on ice.
- Add to 50 µl of cells: 4 µl of ligation, 2 µl of pUC19 control plasmid, or 2-2.5 µg of plasmid DNA.
- Incubate on ice for 30 minutes.
- Heat shock at 37ºC for 20-30 seconds.
- Add 940 µl SOC media.
- Incubate 1 hour at 37ºC with shaking.

- While incubating, plate 100 µl of 2% X-gal on carbenicillin plates and incubate at 37ºC till the 1 hour incubation is over (STEP FOR pBlueScript ONLY).

- Briefly spin down samples (EXCEPT CONTROL). Eliminate ~850µl and resuspend pellet in remaining ~150µl media and plate all (PLATE 100µl CONTROL).

- Incubate plates overnight.

Minipreps

- Pick a (white) colony from transfermed plates into 2.5 ml media with carbenicillin and grow overnight in a 37°C shaking incubator.

- Transfer ~1.5 ml of overnight growth to a 1.5 ml microfuge tube and spin 30 seconds at full speed. (Use a little less media if using Circle-Grow, use a little more if using LB.) Discard supernatant.

- Resuspend cell pellet in 100 µl of cold Solution I (50 mM Tris, pH 8; 5 mM EDTA, pH 8; 1% glucose) by vortexing gently. Incubate 2-5 minutes at room temperature.

- Add 200 µl of Solution II (0.2 M NaOH, 1 % SDS, make fresh before each use). Mix gently by inverting tube three times. Incubate on ice 2-5 minutes.

- Add 150 µl Solution III (3M K/5M Ac: for 100 ml mix 29.44 grams of potassium acetate, 11.5 ml of glacial acetic acid in distilled water). Mix thoroughly by inverting tube on vortexer. Incubate on ice 2-5 minutes.

- Pellet cell debris for 2 minutes at full speed in microfuge. Transfer supernatant to a new tube and discard the pellet.

- Optional: Phenol-Chloroform extract. (This is important only when DNA is to be sequenced.).

- Precipitate DNA by adding 1 ml 100% ethanol. Vortex and incubate at least 2 or more minutes at -20°C (About 30 minutes is good. This is a good place to stop, if necessary. Store samples at -20°C.).

- Pellet DNA for 5 minutes at full speed in microfuge. Aspirate supernatant.

- Rinse pellet with 150 µl of 70% ethanol. Vortex briefly and spin for 2 minutes at full speed in microfuge. Aspirate supernatant.

- Allow pellet to dry for 15- 20 minutes at room temperature.

- Resuspend pellet in 50 µl distilled H_2O.

NOTE: an alternative plasmid DNA isolation protocol can be use following the Fast Plasmid Miniprep kit, especially when this DNA is to be sequenced.

Digestion of Plasmid DNA

The following reaction works well to digest about 2 µl of miniprep DNA, or 1 µg of total DNA (in the latter case use double of restriction enzymes):

- 10x NEBuffer 2.5 µl
- RNAase A 1.0 µl
- NEB Restriction enzyme 0.5 µl of each (1 µl for 1 µg DNA or 10 µl miniprep)
- Distilled H_2O up to 20.0 µl
- Incubate digestion reaction 1 hour at the corresponding temperature, usually it is at 37°C.

Plasmid Preps

- Innoculate 50 ml of autoclaved Circle-Grow with carbenicillin (100 ng/ml) and with miniprep culture. Grow overnight at 37°C in shaking incubator. (For large plasmids, such as PrP, use 100 ml LB).

- Spin cells down for 5 minutes at 5200 rpm in HS-4 rotor in Superspeed centrifuge at 4°C.

- Pour off supernatant and resuspend cells in 7.5 ml ice cold Solution I (25 mM Tris, pH 8; 50 mM EDTA, pH 8; 1% glucose; sterile filter) with a pinch of lysozyme added just prior used to ~1 mg/ml. Incubate on ice 5-10 minutes.

- Add 15.75 ml Solution II (0.2 M NaOH; 1% SDS, make fresh from stock solutions before each use). Invert three times to mix gently. Incubate on ice 5-10 minutes.

- Add 11.6 ml Solution III (3M K/5M Ac: for 100 ml mix 29.44 grams of potassium acetate, 11.5 ml of glacial acetic acid in distilled water). Shake vigorously and incubate on ice for 10-15 minutes.

- Spin tubes for 10 minutes at 6000 rpm in HS-4 in Superspeed centrifuge at 4°C.

- Filter supernatant through a Kimwipe funnel (alternatively cheese cloth can be used).

- Add 2 volumes 100% ethanol. Shake to mix and incubate 5-10 minutes at room temperature.

- Spin down DNA for 10 minutes at 6000 rpm in HS-4 in Superspeed centrifuge at 4°C.

- Pour off supernatant. Allow pellet to dry at room temperature for 15-20 minutes.
- Resuspend pellet in 4 ml distilled H_2O, (or TE). Be sure the DNA is completely in solution.
- Add 4.25 grams of cesium chloride solution (CsCl solution: 42.5 grams CsCl and 40 ml distilled H_2O). Mix well to dissolve completely.
- Pour into ultracentrifuge tube. Top with CsCl solution.
- Remove 100 µl solution from tube and replace with 100 µl ethidium bromide (10 mg/ml). Cap and seal tube, balance tubes and place into TV865 rotor immediately.
- Spin in ultracentrifuge at 20°C, at 45,000 rpm overnight.
- Tap lower band with a needle and syringe.
- Add 3 volumes of salt-saturated isopropanol (200 ml isopropanol, 200 ml 5 M NaCl, shake to mix, and allow phases to separate; Add NaCl crystals until it no longer dissolves; Use the top layer only) in the syringe. Shake thoroughly and allow phases to separate. Bend needle and push off the top layer, which is pink. Repeat two more times (till layers are clear).
- Transfer aqueous phase to a new tube. Add two volumes distilled H_2O. Mix.
- Add two times the resulting volume 100% ethanol. Mix.
- Incubate at -20°C, for 30 min to overnight.
- Spin for 20 minutes at 7000 rpm in HS-4 rotor in Superspeed centrifuge at 4°C.
- Pour off supernatant. Add 2-5 ml of 70% ethanol.
- Spin for 10 minutes at 7000 rpm in HS-4 rotor in Superspeed centrifuge at 4°C.
- Pour off supernatant. Allow pellet to dry.
- Resuspend pellet in 300 µl TE or distilled H_2O.
- Check concentration by measuring OD 260 nm of a 1:100 dilution made in 50 mM Tris, pH 8.

Optional:

- If you don't need Cesium quality DNA, stop before adding CsCl to DNA and add 4 ml of TNES (50 mM Tris, pH 7.5, 100 mM EDTA, 400 mM NaCl, 0.5% SDS).

- Add RNase A to 25 µg/ml (20 µl of a 10 mg/ml stock), and incubate 30 minutes at 37°C.
- Add Proteinase K to 100 µg/ml (40 µl of a 20 mg/ml stock), and incubate 30 minutes at 37°C.
- Phenol-Chloroform extraction
- Precipitate aqueous phase with two volumes 100% ethanol.
- Resuspend DNA in 300 µl TE or distilled H_2O. OD at 1:100 dilution.

Phenol-Choloform Extraction

- Bring the volume of DNA to purify (to eliminate enzymes, etc) to 100 µl (with 1x TEN) and transfer your sample to a 1.5 ml eppendorff tube. (60 µl of 1x TEN to 40 µl of PCR product).
- Add 100 µl of Phenol-Chloroform solution (1:1; mix well 5 ml phenol with 5 ml of chloroform, and centrifuge at 5000 rpm for 5 minutes. Do NOT use upper layer, keep at 4ºC and discard when the solution gets too pink). Vortex.
- Centrifuge 3 minutes at maximum speed. Take upper layer to a new eppendorff and add 1 µl of tRNA (yeast 10mg/ml).
- Add 100 µl of 5M ammonium acetate (NH_4OAc: 19.27grams in 50 ml of distilled water; molecular weight 77.08). Vortex well.
- Add 2.5 volumes of 100% ethanol (500µl). Vortex.
- Leave on ice (good stop point) at least 10 minutes (usually leave at -20ºC).
- Spin down 5 minutes at maximum speed. Discard supernatant.
- Rinse pellet with 100 µl of 70% ethanol and spin down again. Discard supernatant and air dry pellet for 15-20 minutes.
- Resuspend pelleted DNA in 16 µl of distilled H_2O (variable).

β-Agarase Digestion

- Weight empty eppendorff. Cut out band from low melting point agarose gel and put into eppendorff.
- Weight band in tube and calculate net weight of band [weight(band+tube)-weight(tube)]. Assume 1 mg = 1 µl

- Add 1 µl of 10x agarase buffer to 10 µl band (example: to a 0.12 gram band add 12 µl buffer).
- Melt band and buffer at 65ºC, 10 minutes (or till dissolved).
- Equilibrate band at 42ºC, for 10 minutes.
- Add 1 µl agarase enzyme per 125 mg band
- Incubate at 42ºC, for 1 hour.
- Inactivate enzyme at 95ºC, for 2 minutes.

Other Useful Protocols

Freezing Cells

- Wash cells from an almost confluent 75 cm^2 flask with 5 ml 1x dPBS.
- Trypsinize with 1 ml of Trypsin.
- Add media up to 9.5 ml. Take out 9 ml to a 15 ml falcon tube and spin down at 500 rpm for 5 minutes. To the rest 1.5 ml cells + media, add 8.5 ml or 18.5 ml of media to propagate (1:10 or 1:20 dilutions respectively).
- Resuspend pellet in 5 ml media with 5% DMSO (4.75 ml media + 250 µl DMSO).
- Store at -80ºC for at least a day and then put cells in liquid nitrogen. Thaw cells after a while to check they grow fine.

Thawing Cells

- Thaw cells in water bath at 37ºC, then transfer cells to a 15 ml falcon tube and add media up to 10 ml.
- Spin down cells to get rid of the DMSO (5000 rpm, 5 minutes).
- Resuspend cell pellet in 5 ml of media and put in 25 cm^2 flask.
- Transfer to a 75 cm^2 flask when they get confluent in the 25 cm^2 flask.

APPENDIX D
ANTIBODY LIST

Table D-1. List of primary antibodies.

Species	Antigen	Source	Dilution WB	Dilution ICC/IHC
Rabbit	hSOD1	(Borchelt et al., 1994)	1:2500	1:500
Rabbit	h/m SOD1	(Pardo et al., 1995)	1:2500	1:500
Rabbit	LGP120	Gift from Dr. William Dunn Jr.	1:2000	1:250
Rabbit	GFAP	Dako, Cat# Z 0334		1:500
Rabbit	MBP	Gift from Dr. Notterpek (Chemicon)		1:500
Mouse	Dynactin p50	BD Biosciences, Cat# 611003		1:500
Rabbit	hUbiquitin	Dako, Cat# Z0458		1:500
Rabbit	αβ-Tubulin III	Covance, Cat# PRB-435P		1:500
Rabbit	VDAC	Abcam, Cat# ab7783		1:500

WB: Western blot; ICC: Immunocytochemistry; IHC: immunohistochemistry; LGP-120: lysosome glycoprotein 120; VDAC: Voltage-Dependent Anion Channel (commonly known as porin); MBP: Myelin basic protein; GFAP: glial fibrillary acidic protein.

Table D-2. List of secondary antibodies.

Antibody	Source	Dilution WB	Dilution ICC/IHC
Alexa Fluor goat anti-rabbit 594 nm	Invitrogen, Cat# A11012		1:2000
Goat anti-rabbit IgG	KPL, Cat# 074-1516	1:5000	

WB: Western blot; ICC: Immunocytochemistry; IHC: immunohistochemistry.

APPENDIX E
CO-LOCALIZATION STUDIES OF SOD1::YFP INCLUSIONS

Previous studies have determined association of mutant SOD1 with the cytosolic face of mitochondria (Liu et al., 2004). Thus, we sought to determine whether any of these SOD1::YFP fusion proteins appear to accumulate in areas with abundant mitochondrial organelles. Expression of SOD1::YFP mutant proteins for 24 hours and staining of such cells with an antibody that recognizes the voltage-dependent anion channel (VDAC) of mitochondria, does not appear to indicate strong co-localizations of WT or mutant SOD1 inclusions with mitochondria, nor mitochondrial reorganization derived from mutant SOD1::YFP expression (Figure E-1). Interestingly, apparent accumulations of mitochondria were found in different cells, but in areas devoid of SOD1::YFP inclusions (Figure E-1, open arrowheads). Mitochondrial immunoreactivity appeared to colocalize some with WT::YFP or D101N::YFP proteins (Figures E-1A to 1-1L). Only in one case we found a cell with an abnormal high number of mitochondrial immunoreactivity, however this cell did not express SOD1::YFP (Figures E-1G and E-1H, filled arrowhead). Thus, our data suggest that SOD1::YFP inclusions do not co-localize with mitochondria, however more extensive analysis at higher magnifications may be needed.

Ubiquitin-positive inclusions are a common feature in ALS patients. However, ubiquitin and SOD1 co-staining does not appear to take place (Shibata et al., 1996a). Studies in ALS mouse models expressing mutant SOD1 indicate that insoluble SOD1 is partly oligoubiquitinated at disease endstage (Basso et al., 2006). Additionally, other studies in animal models indicate a reduction in proteasome activity in symptomatic mice (Cheroni et al., 2005). In cell culture, studies have previously shown association of

mutant SOD1, but not WT, with components of the ubiquitin proteasome system (Urushitani et al., 2002), indicating that they might be targeted for proteasomal degradation. In order to study whether our cell model expressing mutant SOD1::YFP also contain ubiquitin positive inclusions, we stained cells expressing fusion SOD1 proteins with an antibody that recognizes ubiquitin. We did not observe ubiquitin inclusions of similar size to SOD1::YFP inclusions (Figure E-2). Additionally, cells expressing a SOD1::YFP protein appeared to be less immunoreactive to ubiquitin (Figures E-2C, E-2D, E-2G, and E-2H), while when bigger ubiquitin positive areas were found, they did not seem to co-localize with SOD1::YFP (Figures E-2K and E-2L).

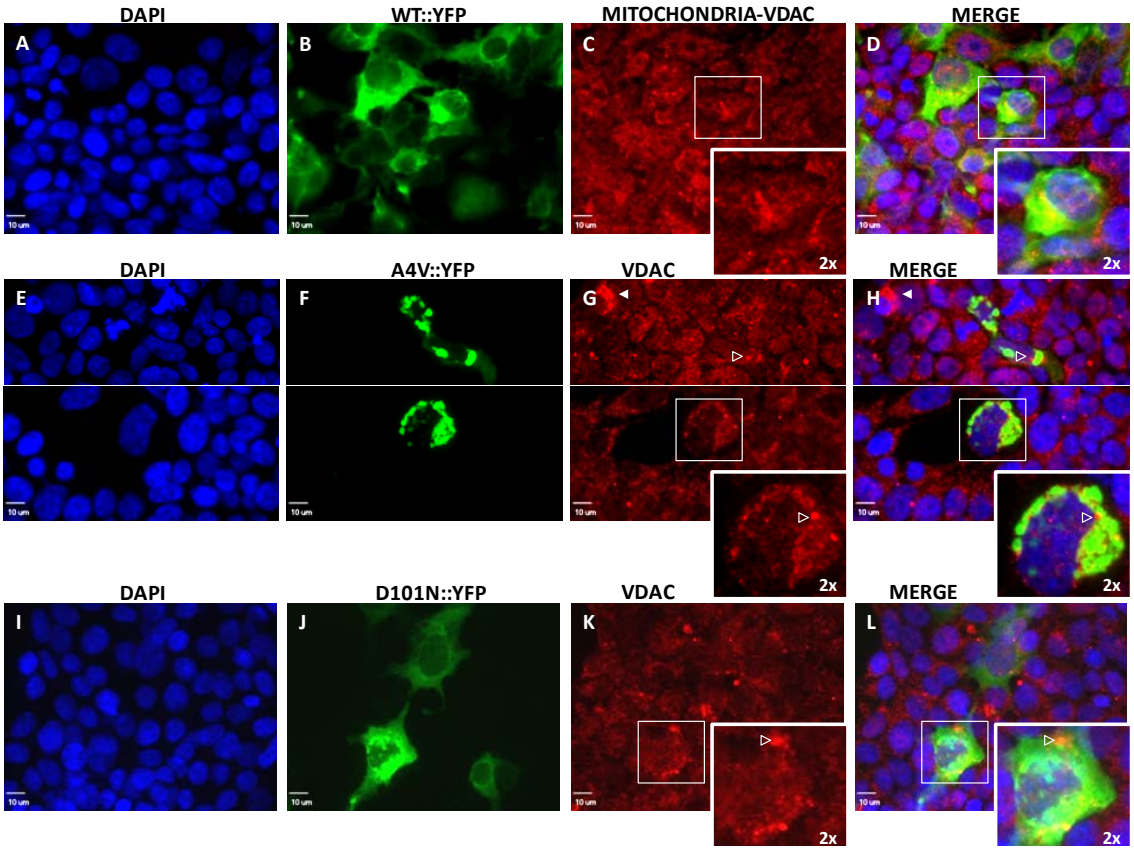

Figure E-1. SOD1::YFP inclusions do not co-localize with mitochondria. A-L) HEK293FT transfected for 24 hours with SOD1::YFP fusion constructs and stained for mitochondrial membrane protein VDAC following a staining procedure as described for Figure 6-1. Pictures were taken using a spinning disk confocal microscope, with a 60x water immersion objective, bars 10 µm.

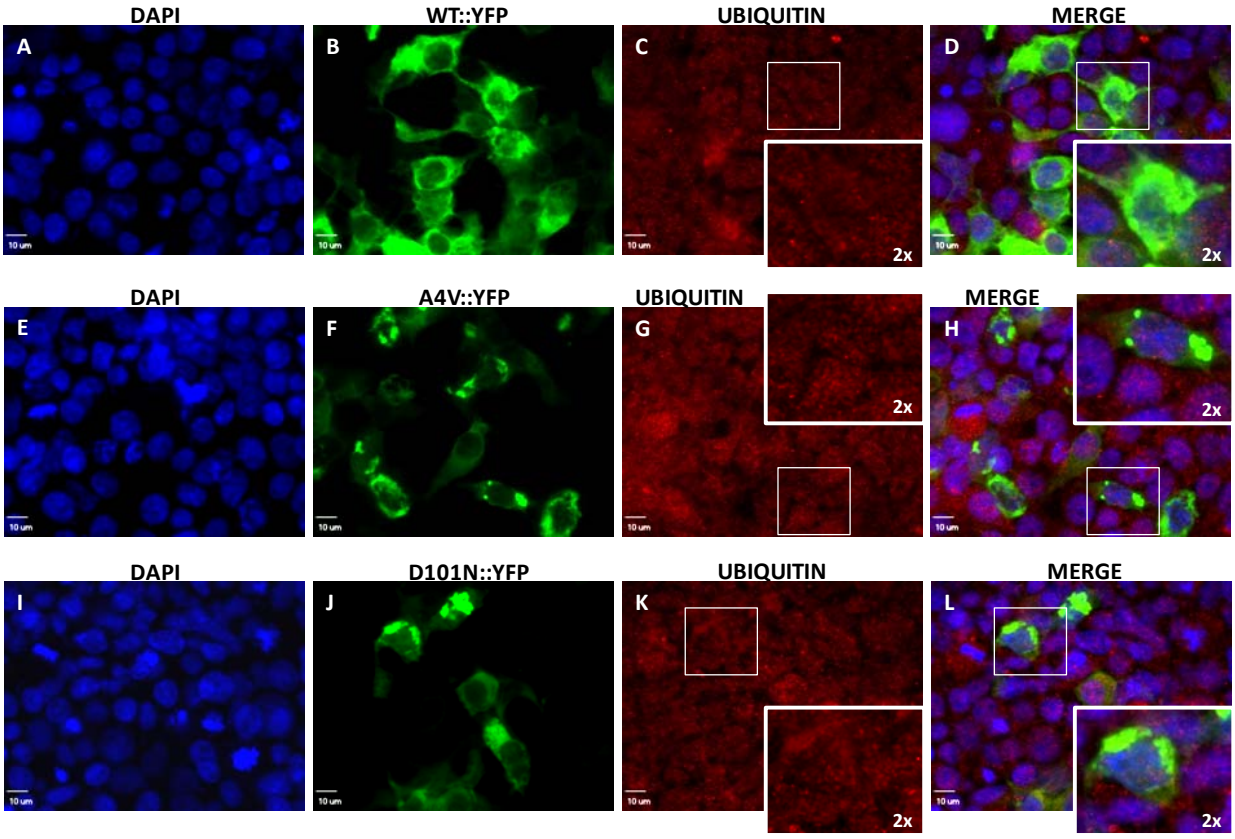

Figure E-2. Ubiquitin does not concentrate to SOD1::YFP inclusions. A-L) HEK293FT cells transfected for 24 hours with SOD1::YFP fusion constructs and stained like explained on Figure E-1 but stained here with an antibody recognizing ubiquitin. Pictures were taken using a spinning disk confocal microscope, with a 60x water immersion objective, bars 10 µm.

Thus, it is unclear the role that ubiquitination may play on SOD1::YFP inclusions and further studies should be conducted. In our hands, we did not observe interactions of ubiquitin with either WT or mutant SOD1 when tagged with YFP.

An alternative mode of degradation of mutant SOD1::YFP proteins could involve lysosomes. Thus, to determine whether SOD1::YFP inclusions may concentrate into lysosomal compartments, we performed similar immunostaining techniques using an antibody that recognizes LGP120, a lysosomal transmembrane glycoprotein. Similar to mitochondrial staining, WT::YFP proteins were the only ones that we observed to clearly co-localize with lysosomes, while mutant SOD1::YFP inclusions did not (Figure E-3).

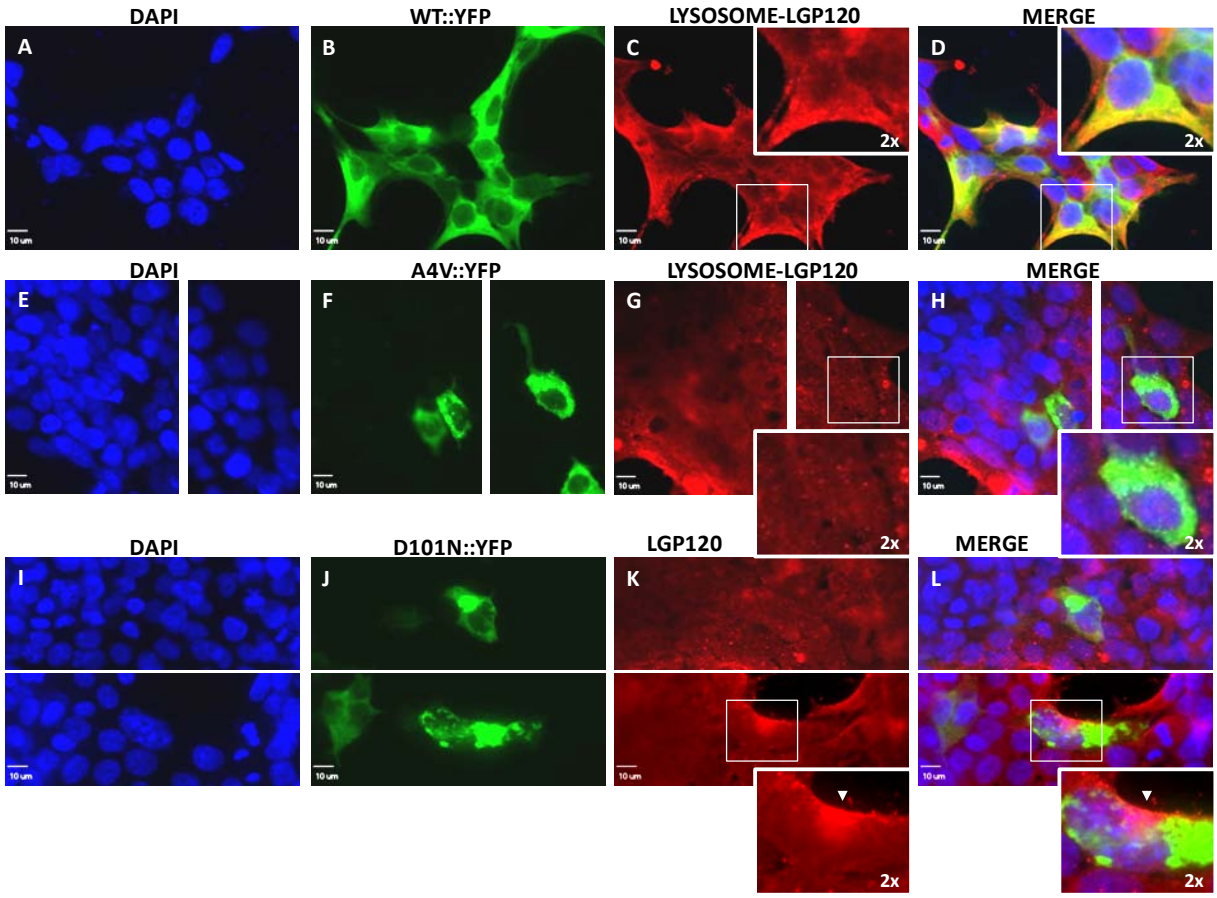

Figure E-3. Mutant SOD1::YFP inclusions do not localize within lysosomes. A-L) HEK293FT cells transfected for 24 hours with SOD1::YFP constructs and stained as described in Figure E-1, using the lysosome marker LGP120. Pictures were taken using a spinning disk confocal microscope, with a 60x water immersion objective, bars 10 µm. White arrowhead in K and L indicate strong immunoreactivity to LGP120, in an area free of SOD1::YFP protein.

Additional studies suggest that interactions of SOD1 with components of the axonal transport are required for inclusion formation (Strom et al., 2008). In particular, overexpression of dynactin protein p50 abolishes dynein-SOD1::GFP protein interactions. In our case, we wanted to see whether interactions of p50 dynactin complex with SOD1::YFP inclusions are obvious in our cell culture system. However, we did not observe clear co-localization, and it appeared that a lower immunoreactivity of p50 was present in cells containing SOD1::YFP inclusions (Figure E-4). Thus, our

data does not provide indication of interactions of SOD1::YFP inclusions with the p50 protein. However, we are aware that the data presented here is too limited to draw conclusions, and additional experiments should be performed to further study this possibility.

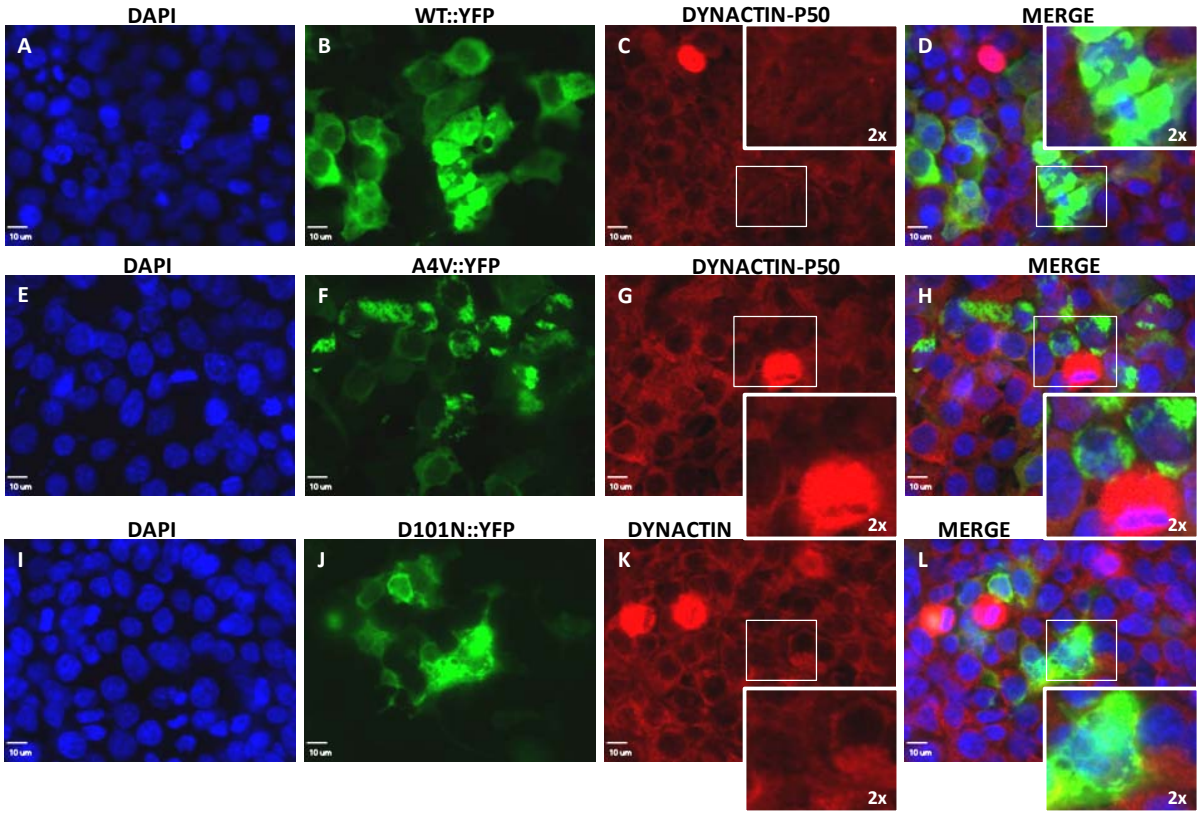

Figure E-4. Lower expression of dynactin protein p50 in SOD1::YFP containing cells. A-L) HEK293FT cells transfected for 24 hours with SOD1::YFP constructs and stained as described in Figure E-1 using the dynactin marker p50. Pictures were taken using a spinning disk confocal microscope, with a 60x water immersion objective, bars 10 µm.

In all the described immunofluorescence studies we did not observe co-localization with SOD1::YFP inclusions. Additionally, we did not see an obvious redistribution of any of the markers that we employed. This can be confirmed when comparing the staining of all these markers in SOD1::YFP expressing cells with untransfected cells (Figure E-5).

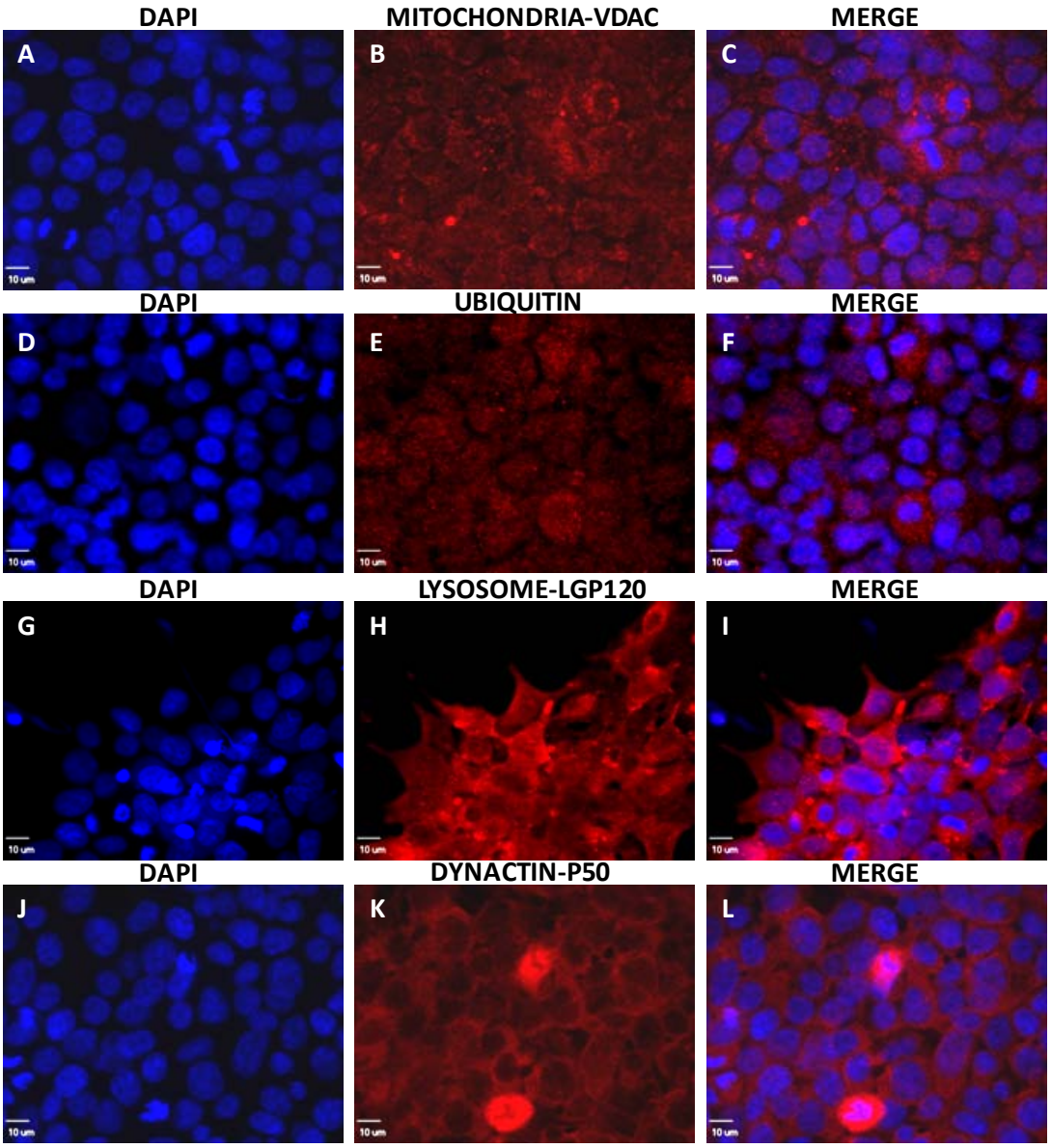

Figure E-5. HEK293FT untransfected cells present similar staining pattern of cellular markers as SOD1::YFP transfected cells. A-L) HEK293FT cells untransfected and stained as described in Figure E-1 after 24 hour of culture using markers for mitochondria (A-C), ubiquitin (D-F), lysosome (G-I), and dynactin (J-L). Pictures were taken using a spinning disk confocal microscope, with a 60x water immersion objective, bars 10 µm.

Although not extensive studies are presented here, we suspect the lack of strong co-localizations due to the size of the inclusions of SOD1::YFP fusion proteins. Only in certain cases we observed co-localization of WT::YFP with either mitochondria (see Figure E-1) or lysosomes (see Figure E-2). However, we do not have enough data to

demonstrate whether such interactions with non-inclusion forming WT::YFP occur on the surface of the organelle, or whether the fusion protein can be internalized. It appears, however, that even WT::YFP has a hard time to get into the nucleus, while YFP is highly expressed there. This suggests that SOD1::YFP proteins are likely not easily being transported inside organelles. Then, interactions may occur at the levels of more “soluble” states of the protein (not forming inclusions). Thus, in the case of SOD1::YFP inclusions, the lack of association with organelles could be explained by their rapid ability to form such structures, which would not allow for interactions to occur at the non-inclusion level.

LIST OF REFERENCES

Aisen, M.L., D.Sevilla, L.Edelstein, and J.Blass. 1996. A double-blind placebo-controlled study of 3,4-diaminopyridine in amytrophic lateral sclerosis patients on a rehabilitation unit. *J. Neurol. Sci.* 138:93-96.

Aisen, M.L., D.Sevilla, G.Gibson, H.Kutt, A.Blau, L.Edelstein, J.Hatch, and J.Blass. 1995. 3,4-diaminopyridine as a treatment for amyotrophic lateral sclerosis. *J. Neurol. Sci.* 129:21-24.

Al-Chalabi, A., P.M.Andersen, B.Chioza, C.Shaw, P.C.Sham, W.Robberecht, G.Matthijs, W.Camu, S.L.Marklund, L.Forsgren, G.Rouleau, N.G.Laing, P.V.Hurse, T.Siddique, P.N.Leigh, and J.F.Powell. 1998. Recessive amyotrophic lateral sclerosis families with the D90A SOD1 mutation share a common founder: evidence for a linked protective factor. *Hum. Mol. Genet.* 7:2045-2050.

Al-Chalabi, A., M.D.Scheffler, B.N.Smith, M.J.Parton, M.E.Cudkowicz, P.M.Andersen, D.L.Hayden, V.K.Hansen, M.R.Turner, C.E.Shaw, P.N.Leigh, and R.H.Brown, Jr. 2003. Ciliary neurotrophic factor genotype does not influence clinical phenotype in amyotrophic lateral sclerosis. *Ann. Neurol.* 54:130-134.

Albo, F., M.Pieri, and C.Zona. 2004. Modulation of AMPA receptors in spinal motor neurons by the neuroprotective agent riluzole. *J. Neurosci. Res.* 78:200-207.

Alexander, M.D., B.J.Traynor, N.Miller, B.Corr, E.Frost, S.McQuaid, F.M.Brett, A.Green, and O.Hardiman. 2002. "True" sporadic ALS associated with a novel SOD-1 mutation. *Ann. Neurol.* 52:680-683.

Andersen, P.M. 2006. Amyotrophic lateral sclerosis associated with mutations in the CuZn superoxide dismutase gene. *Curr. Neurol. Neurosci. Rep.* 6:37-46.

Andersen, P.M., P.Nilsson, M.L.Keranen, L.Forsgren, J.Hagglund, M.Karlsborg, L.O.Ronnevi, O.Gredal, and S.L.Marklund. 1997. Phenotypic heterogeneity in motor neuron disease patients with CuZn-superoxide dismutase mutations in Scandinavia. *Brain* 120 (Pt 10):1723-1737.

Andersen, P.M., P.Nilsson, V.la-Hurula, M.L.Keranen, I.Tarvainen, T.Haltia, L.Nilsson, M.Binzer, L.Forsgren, and S.L.Marklund. 1995. Amyotrophic lateral sclerosis associated with homozygosity for an Asp90Ala mutation in CuZn-superoxide dismutase. *Nat. Genet.* 10:61-66.

Andersen, P.M., K.B.Sims, W.W.Xin, R.Kiely, G.O'Neill, J.Ravits, E.Pioro, Y.Harati, R.D.Brower, J.S.Levine, H.U.Heinicke, W.Seltzer, M.Boss, and R.H.Brown, Jr. 2003. Sixteen novel mutations in the Cu/Zn superoxide dismutase gene in amyotrophic lateral sclerosis: a decade of discoveries, defects and disputes. *Amyotroph. Lateral. Scler. Other Motor Neuron Disord.* 4:62-73.

Antonyuk, S., J.S.Elam, M.A.Hough, R.W.Strange, P.A.Doucette, J.A.Rodriguez, L.J.Hayward, J.S.Valentine, P.J.Hart, and S.S.Hasnain. 2005. Structural consequences of the familial amyotrophic lateral sclerosis SOD1 mutant His46Arg. *Protein Sci.* 14:1201-1213.

Aoki, M., K.Abe, K.Houi, M.Ogasawara, Y.Matsubara, T.Kobayashi, S.Mochio, K.Narisawa, and Y.Itoyama. 1995. Variance of age at onset in a Japanese family with amyotrophic lateral sclerosis associated with a novel Cu/Zn superoxide dismutase mutation. *Ann. Neurol.* 37:676-679.

Aoki, M., M.Ogasawara, Y.Matsubara, K.Narisawa, S.Nakamura, Y.Itoyama, and K.Abe. 1993. Mild ALS in Japan associated with novel SOD mutation. *Nat. Genet.* 5:323-324.

Arisato, T., R.Okubo, H.Arata, K.Abe, K.Fukada, S.Sakoda, A.Shimizu, X.H.Qin, S.Izumo, M.Osame, and M.Nakagawa. 2003. Clinical and pathological studies of familial amyotrophic lateral sclerosis (FALS) with SOD1 H46R mutation in large Japanese families. *Acta Neuropathol. (Berl)* 106:561-568.

Arrasate, M., S.Mitra, E.S.Schweitzer, M.R.Segal, and S.Finkbeiner. 2004. Inclusion body formation reduces levels of mutant huntingtin and the risk of neuronal death. *Nature* 431:805-810.

Basso, M., T.Massignan, G.Samengo, C.Cheroni, B.S.De, M.Salmona, C.Bendotti, and V.Bonetto. 2006. Insoluble mutant SOD1 is partly oligoubiquitinated in amyotrophic lateral sclerosis mice. *J. Biol. Chem.* 281:33325-33335.

Beal, M.F., R.J.Ferrante, S.E.Browne, R.T.Matthews, N.W.Kowall, and R.H.Brown, Jr. 1997. Increased 3-nitrotyrosine in both sporadic and familial amyotrophic lateral sclerosis. *Ann. Neurol.* 42:644-654.

Beck, M., P.Flachenecker, T.Magnus, R.Giess, K.Reiners, K.V.Toyka, and M.Naumann. 2005. Autonomic dysfunction in ALS: a preliminary study on the effects of intrathecal BDNF. *Amyotroph. Lateral. Scler. Other Motor Neuron Disord.* 6:100-103.

Beck, M., M.Sendtner, and K.V.Toyka. 2007. Novel SOD1 N86K mutation is associated with a severe phenotype in familial ALS. *Muscle Nerve* 36:111-114.

Beckman, G. and A.Pakarinen. 1973. Superoxide dismutase. A population study. *Hum. Hered.* 23:346-351.

Beckman, J.S., M.Carson, C.D.Smith, and W.H.Koppenol. 1993. ALS, SOD and peroxynitrite. *Nature* 364:584.

Beghi, E., A.Chio, M.Inghilleri, L.Mazzini, A.Micheli, G.Mora, M.Poloni, R.Riva, L.Serlenga, D.Testa, and P.Tonali. 2000. A randomized controlled trial of

recombinant interferon beta-1a in ALS. Italian Amyotrophic Lateral Sclerosis Study Group. *Neurology* 54:469-474.

Bence, N.F., R.M.Sampat, and R.R.Kopito. 2001. Impairment of the ubiquitin-proteasome system by protein aggregation. *Science* 292:1552-1555.

Bendotti, C. and M.T.Carri. 2004. Lessons from models of SOD1-linked familial ALS. *Trends Mol. Med.* 10:393-400.

Bertini, I., M.Piccioli, M.S.Viezzoli, C.Y.Chiu, and G.T.Mullenbach. 1994. A spectroscopic characterization of a monomeric analog of copper, zinc superoxide dismutase. *Eur. Biophys. J.* 23:167-176.

Bertram, L. and R.E.Tanzi. 2008. Thirty years of Alzheimer's disease genetics: the implications of systematic meta-analyses. *Nat. Rev. Neurosci.* 9:768-778.

Bird, T.D. 2008. Genetic aspects of Alzheimer disease. *Genet. Med.* 10:231-239.

Boillee, S., V.C.Vande, and D.W.Cleveland. 2006a. ALS: a disease of motor neurons and their nonneuronal neighbors. *Neuron* 52:39-59.

Boillee, S., K.Yamanaka, C.S.Lobsiger, N.G.Copeland, N.A.Jenkins, G.Kassiotis, G.Kollias, and D.W.Cleveland. 2006b. Onset and progression in inherited ALS determined by motor neurons and microglia. *Science* 312:1389-1392.

Borchelt, D.R. 1998. Metabolism of presenilin 1: influence of presenilin 1 on amyloid precursor protein processing. *Neurobiol. Aging* 19:S15-S18.

Borchelt, D.R., M.Guarnieri, P.C.Wong, M.K.Lee, H.S.Slunt, Z.S.Xu, S.S.Sisodia, D.L.Price, and D.W.Cleveland. 1995. Superoxide dismutase 1 subunits with mutations linked to familial amyotrophic lateral sclerosis do not affect wild-type subunit function. *J. Biol. Chem.* 270:3234-3238.

Borchelt, D.R., M.K.Lee, H.S.Slunt, M.Guarnieri, Z.S.Xu, P.C.Wong, R.H.Brown, Jr., D.L.Price, S.S.Sisodia, and D.W.Cleveland. 1994. Superoxide dismutase 1 with mutations linked to familial amyotrophic lateral sclerosis possesses significant activity. *Proc. Natl. Acad. Sci. U. S. A* 91:8292-8296.

Borchelt, D.R., P.C.Wong, M.W.Becher, C.A.Pardo, M.K.Lee, Z.S.Xu, G.Thinakaran, N.A.Jenkins, N.G.Copeland, S.S.Sisodia, D.W.Cleveland, D.L.Price, and P.N.Hoffman. 1998. Axonal transport of mutant superoxide dismutase 1 and focal axonal abnormalities in the proximal axons of transgenic mice. *Neurobiol. Dis.* 5:27-35.

Boukaftane, Y., J.Khoris, B.Moulard, F.Salachas, V.Meininger, A.Malafosse, W.Camu, and G.A.Rouleau. 1998. Identification of six novel SOD1 gene mutations in familial amyotrophic lateral sclerosis. *Can. J. Neurol. Sci.* 25:192-196.

Brooks, B.R. 1994. El Escorial World Federation of Neurology criteria for the diagnosis of amyotrophic lateral sclerosis. Subcommittee on Motor Neuron Diseases/Amyotrophic Lateral Sclerosis of the World Federation of Neurology Research Group on Neuromuscular Diseases and the El Escorial "Clinical limits of amyotrophic lateral sclerosis" workshop contributors. *J Neurol Sci*. 124 Suppl:96-107.

Brown, R.H., Jr., S.L.Hauser, H.Harrington, and H.L.Weiner. 1986. Failure of immunosuppression with a ten- to 14-day course of high-dose intravenous cyclophosphamide to alter the progression of amyotrophic lateral sclerosis. *Arch. Neurol.* 43:383-384.

Bruijn, L.I., M.W.Becher, M.K.Lee, K.L.Anderson, N.A.Jenkins, N.G.Copeland, S.S.Sisodia, J.D.Rothstein, D.R.Borchelt, D.L.Price, and D.W.Cleveland. 1997. ALS-linked SOD1 mutant G85R mediates damage to astrocytes and promotes rapidly progressive disease with SOD1-containing inclusions. *Neuron* 18:327-338.

Bruijn, L.I., M.K.Houseweart, S.Kato, K.L.Anderson, S.D.Anderson, E.Ohama, A.G.Reaume, R.W.Scott, and D.W.Cleveland. 1998. Aggregation and motor neuron toxicity of an ALS-linked SOD1 mutant independent from wild-type SOD1. *Science* 281:1851-1854.

Bruijn, L.I., T.M.Miller, and D.W.Cleveland. 2004. Unraveling the mechanisms involved in motor neuron degeneration in ALS. *Annu. Rev. Neurosci.* 27:723-749.

Bush, A.I. 2002. Is ALS caused by an altered oxidative activity of mutant superoxide dismutase? *Nat. Neurosci.* 5:919-920.

Calamai, M., N.Taddei, M.Stefani, G.Ramponi, and F.Chiti. 2003. Relative influence of hydrophobicity and net charge in the aggregation of two homologous proteins. *Biochemistry* 42:15078-15083.

Chang-Hong, R., M.Wada, S.Koyama, H.Kimura, S.Arawaka, T.Kawanami, K.Kurita, T.Kadoya, M.Aoki, Y.Itoyama, and T.Kato. 2005. Neuroprotective effect of oxidized galectin-1 in a transgenic mouse model of amyotrophic lateral sclerosis. *Exp. Neurol.* 194:203-211.

Charcot JM and A J. 1869. Deux cas d'atrophie musculaire progressive avec lésions de la substance grise et des faiseaux antérolatéraux de la moelle épinière. *Arch Physiol Neurol Path.* 744-754.

Chattopadhyay, M., A.Durazo, S.H.Sohn, C.D.Strong, E.B.Gralla, J.P.Whitelegge, and J.S.Valentine. 2008. Initiation and elongation in fibrillation of ALS-linked superoxide dismutase. *Proc. Natl. Acad. Sci. U. S. A* 105:18663-18668.

Chen, Y.Z., C.L.Bennett, H.M.Huynh, I.P.Blair, I.Puls, J.Irobi, I.Dierick, A.Abel, M.L.Kennerson, B.A.Rabin, G.A.Nicholson, M.uer-Grumbach, K.Wagner, J.P.De,

J.W.Griffin, K.H.Fischbeck, V.Timmerman, D.R.Cornblath, and P.F.Chance. 2004. DNA/RNA helicase gene mutations in a form of juvenile amyotrophic lateral sclerosis (ALS4). *Am. J. Hum. Genet.* 74:1128-1135.

Cheroni, C., M.Peviani, P.Cascio, S.Debiasi, C.Monti, and C.Bendotti. 2005. Accumulation of human SOD1 and ubiquitinated deposits in the spinal cord of SOD1G93A mice during motor neuron disease progression correlates with a decrease of proteasome. *Neurobiol. Dis.* 18:509-522.

Chio, A., A.Cucatto, A.A.Terreni, and D.Schiffer. 1998. Reduced glutathione in amyotrophic lateral sclerosis: an open, crossover, randomized trial. *Ital. J. Neurol. Sci.* 19:363-366.

Chio, A., B.J.Traynor, F.Lombardo, M.Fimognari, A.Calvo, P.Ghiglione, R.Mutani, and G.Restagno. 2008. Prevalence of SOD1 mutations in the Italian ALS population. *Neurology* 70:533-537.

Chiti, F., M.Calamai, N.Taddei, M.Stefani, G.Ramponi, and C.M.Dobson. 2002. Studies of the aggregation of mutant proteins in vitro provide insights into the genetics of amyloid diseases. *Proc. Natl. Acad. Sci. U. S. A* 99 Suppl 4:16419-16426.

Chou, C.M., C.J.Huang, C.M.Shih, Y.P.Chen, T.P.Liu, and C.T.Chen. 2005. Identification of three mutations in the Cu,Zn-superoxide dismutase (Cu,Zn-SOD) gene with familial amyotrophic lateral sclerosis: transduction of human Cu,Zn-SOD into PC12 cells by HIV-1 TAT protein basic domain. *Ann. N. Y. Acad. Sci.* 1042:303-313.

Clinical Trials. 2009. U. S. National Institute of Health Clinical Trials, 08/2009. www.clinicaltrials.gov.

Cozzolino, M., I.Amori, M.G.Pesaresi, A.Ferri, M.Nencini, and M.T.Carri. 2008a. Cysteine 111 Affects Aggregation and Cytotoxicity of Mutant Cu,Zn-superoxide Dismutase Associated with Familial Amyotrophic Lateral Sclerosis. *J. Biol. Chem.* 283:866-874.

Cozzolino, M., A.Ferri, and M.T.Carri. 2008b. Amyotrophic lateral sclerosis: from current developments in the laboratory to clinical implications. *Antioxid. Redox. Signal.* 10:405-443.

Crapo, J.D., T.Oury, C.Rabouille, J.W.Slot, and L.Y.Chang. 1992. Copper,zinc superoxide dismutase is primarily a cytosolic protein in human cells. *Proc. Natl. Acad. Sci. U. S. A* 89:10405-10409.

Crow, J.P., J.B.Sampson, Y.Zhuang, J.A.Thompson, and J.S.Beckman. 1997. Decreased zinc affinity of amyotrophic lateral sclerosis-associated superoxide dismutase mutants leads to enhanced catalysis of tyrosine nitration by peroxynitrite. *J. Neurochem.* 69:1936-1944.

Cudkowicz, M.E., D.kenna-Yasek, P.E.Sapp, W.Chin, B.Geller, D.L.Hayden, D.A.Schoenfeld, B.A.Hosler, H.R.Horvitz, and R.H.Brown. 1997. Epidemiology of mutations in superoxide dismutase in amyotrophic lateral sclerosis. *Ann. Neurol.* 41:210-221.

Cudkowicz, M.E., J.M.Shefner, D.A.Schoenfeld, R.H.Brown, Jr., H.Johnson, M.Qureshi, M.Jacobs, J.D.Rothstein, S.H.Appel, R.M.Pascuzzi, T.D.Heiman-Patterson, P.D.Donofrio, W.S.David, J.A.Russell, R.Tandan, E.P.Pioro, K.J.Felice, J.Rosenfeld, R.N.Mandler, G.M.Sachs, W.G.Bradley, E.M.Raynor, G.D.Baquis, J.M.Belsh, S.Novella, J.Goldstein, and J.Hulihan. 2003. A randomized, placebo-controlled trial of topiramate in amyotrophic lateral sclerosis. *Neurology* 61:456-464.

Cudkowicz, M.E., J.M.Shefner, D.A.Schoenfeld, H.Zhang, K.I.Andreasson, J.D.Rothstein, and D.B.Drachman. 2006. Trial of celecoxib in amyotrophic lateral sclerosis. *Ann. Neurol.* 60:22-31.

Dal Canto, M.C. and M.E.Gurney. 1994. Development of central nervous system pathology in a murine transgenic model of human amyotrophic lateral sclerosis. *Am. J. Pathol.* 145:1271-1279.

Dal Canto, M.C. and M.E.Gurney. 1997. A low expressor line of transgenic mice carrying a mutant human Cu,Zn superoxide dismutase (SOD1) gene develops pathological changes that most closely resemble those in human amyotrophic lateral sclerosis. *Acta Neuropathol. (Berl)* 93:537-550.

Danciger, E., N.Dafni, Y.Bernstein, Z.Laver-Rudich, A.Neer, and Y.Groner. 1986. Human Cu/Zn superoxide dismutase gene family: molecular structure and characterization of four Cu/Zn superoxide dismutase-related pseudogenes. *Proc. Natl. Acad. Sci. U. S. A* 83:3619-3623.

Deng, H.X., A.Hentati, J.A.Tainer, Z.Iqbal, A.Cayabyab, W.Y.Hung, E.D.Getzoff, P.Hu, B.Herzfeldt, R.P.Roos, and . 1993. Amyotrophic lateral sclerosis and structural defects in Cu,Zn superoxide dismutase. *Science* 261:1047-1051.

Deng, H.X., H.Jiang, R.Fu, H.Zhai, Y.Shi, E.Liu, M.Hirano, M.C.Dal Canto, and T.Siddique. 2008. Molecular dissection of ALS-associated toxicity of SOD1 in transgenic mice using an exon-fusion approach. *Hum. Mol. Genet.* 17:2310-2319.

Deng, H.X., Y.Shi, Y.Furukawa, H.Zhai, R.Fu, E.Liu, G.H.Gorrie, M.S.Khan, W.Y.Hung, E.H.Bigio, T.Lukas, M.C.Dal Canto, T.V.O'Halloran, and T.Siddique. 2006. Conversion to the amyotrophic lateral sclerosis phenotype is associated with intermolecular linked insoluble aggregates of SOD1 in mitochondria. *Proc. Natl. Acad. Sci. U. S. A* 103:7142-7147.

Deng, H.X., J.A.Tainer, H.Mitsumoto, A.Ohnishi, X.He, W.Y.Hung, Y.Zhao, T.Juneja, A.Hentati, and T.Siddique. 1995. Two novel SOD1 mutations in patients with familial amyotrophic lateral sclerosis. *Hum. Mol. Genet.* 4:1113-1116.

Drachman, D.B., V.Chaudhry, D.Cornblath, R.W.Kuncl, A.Pestronk, L.Clawson, E.D.Mellits, S.Quaskey, T.Quinn, A.Calkins, and . 1994. Trial of immunosuppression in amyotrophic lateral sclerosis using total lymphoid irradiation. *Ann. Neurol.* 35:142-150.

Duff, K., C.Eckman, C.Zehr, X.Yu, C.M.Prada, J.Perez-tur, M.Hutton, L.Buee, Y.Harigaya, D.Yager, D.Morgan, M.N.Gordon, L.Holcomb, L.Refolo, B.Zenk, J.Hardy, and S.Younkin. 1996. Increased amyloid-beta42(43) in brains of mice expressing mutant presenilin 1. *Nature* 383:710-713.

Elam, J.S., A.B.Taylor, R.Strange, S.Antonyuk, P.A.Doucette, J.A.Rodriguez, S.S.Hasnain, L.J.Hayward, J.S.Valentine, T.O.Yeates, and P.J.Hart. 2003. Amyloid-like filaments and water-filled nanotubes formed by SOD1 mutant proteins linked to familial ALS. *Nat. Struct. Biol.* 10:461-467.

Elia, A.J., T.L.Parkes, K.Kirby, P.St George-Hyslop, G.L.Boulianne, J.P.Phillips, and A.J.Hilliker. 1999. Expression of human FALS SOD in motorneurons of Drosophila. *Free Radic. Biol. Med.* 26:1332-1338.

Elshafey, A., W.G.Lanyon, and J.M.Connor. 1994. Identification of a new missense point mutation in exon 4 of the Cu/Zn superoxide dismutase (SOD-1) gene in a family with amyotrophic lateral sclerosis. *Hum. Mol. Genet.* 3:363-364.

Enayat, Z.E., R.W.Orrell, A.Claus, A.Ludolph, R.Bachus, J.Brockmuller, K.Ray-Chaudhuri, A.Radunovic, C.Shaw, J.Wilkinson, and . 1995. Two novel mutations in the gene for copper zinc superoxide dismutase in UK families with amyotrophic lateral sclerosis. *Hum. Mol. Genet.* 4:1239-1240.

Esteban, J., D.R.Rosen, A.C.Bowling, P.Sapp, D.kenna-Yasek, J.P.O'Regan, M.F.Beal, H.R.Horvitz, and R.H.Brown, Jr. 1994. Identification of two novel mutations and a new polymorphism in the gene for Cu/Zn superoxide dismutase in patients with amyotrophic lateral sclerosis. *Hum. Mol. Genet.* 3:997-998.

Estevez, A.G., J.P.Crow, J.B.Sampson, C.Reiter, Y.Zhuang, G.J.Richardson, M.M.Tarpey, L.Barbeito, and J.S.Beckman. 1999. Induction of nitric oxide-dependent apoptosis in motor neurons by zinc-deficient superoxide dismutase. *Science* 286:2498-2500.

Estevez, A.G., N.Spear, S.M.Manuel, L.Barbeito, R.Radi, and J.S.Beckman. 1998. Role of endogenous nitric oxide and peroxynitrite formation in the survival and death of motor neurons in culture. *Prog. Brain Res.* 118:269-280.

Feeney, S.J., P.A.McKelvie, L.Austin, M.J.Jean-Francois, R.Kapsa, S.M.Tombs, and E.Byrne. 2001. Presymptomatic motor neuron loss and reactive astrocytosis in

the SOD1 mouse model of amyotrophic lateral sclerosis. *Muscle Nerve* 24:1510-1519.

Ferrante, R.J., S.E.Browne, L.A.Shinobu, A.C.Bowling, M.J.Baik, U.MacGarvey, N.W.Kowall, R.H.Brown, Jr., and M.F.Beal. 1997. Evidence of increased oxidative damage in both sporadic and familial amyotrophic lateral sclerosis. *J. Neurochem.* 69:2064-2074.

Fischer, L.R., D.G.Culver, P.Tennant, A.A.Davis, M.Wang, A.Castellano-Sanchez, J.Khan, M.A.Polak, and J.D.Glass. 2004. Amyotrophic lateral sclerosis is a distal axonopathy: evidence in mice and man. *Exp. Neurol.* 185:232-240.

Forman, H.J. and I.Fridovich. 1973. On the stability of bovine superoxide dismutase. The effects of metals. *J. Biol. Chem.* 248:2645-2649.

Francis, G., Z.Kerem, H.P.S.Makkar, and K.Becker. 2002. The biological action of saponins in animal systems: a review. *British Journal of Nutrition* 88:587-605.

Friedlander, R.M., R.H.Brown, V.Gagliardini, J.Wang, and J.Yuan. 1997. Inhibition of ICE slows ALS in mice. *Nature* 388:31.

Fumagalli, E., M.Funicello, T.Rauen, M.Gobbi, and T.Mennini. 2008. Riluzole enhances the activity of glutamate transporters GLAST, GLT1 and EAAC1. *Eur. J. Pharmacol.* 578:171-176.

Furukawa, Y., R.Fu, H.X.Deng, T.Siddique, and T.V.O'Halloran. 2006. Disulfide cross-linked protein represents a significant fraction of ALS-associated Cu, Zn-superoxide dismutase aggregates in spinal cords of model mice. *Proc. Natl. Acad. Sci. U. S. A* 103:7148-7153.

Garcia-Redondo, A., F.Bustos, Y.S.Juan, H.P.Del, S.Jimenez, Y.Campos, M.A.Martin, J.C.Rubio, F.Canadillas, J.Arenas, and J.Esteban. 2002. Molecular analysis of the superoxide dismutase 1 gene in Spanish patients with sporadic or familial amyotrophic lateral sclerosis. *Muscle Nerve* 26:274-278.

Gellera, C., B.Castellotti, M.C.Riggio, V.Silani, L.Morandi, D.Testa, C.Casali, F.Taroni, D.S.Di, M.Zeviani, and C.Mariotti. 2001. Superoxide dismutase gene mutations in Italian patients with familial and sporadic amyotrophic lateral sclerosis: identification of three novel missense mutations. *Neuromuscul. Disord.* 11:404-410.

Gidalevitz, T., T.Krupinski, S.Garcia, and R.I.Morimoto. 2009. Destabilizing protein polymorphisms in the genetic background direct phenotypic expression of mutant SOD1 toxicity. *PLoS. Genet.* 5:e1000399.

Gitcho, M.A., R.H.Baloh, S.Chakraverty, K.Mayo, J.B.Norton, D.Levitch, K.J.Hatanpaa, C.L.White, III, E.H.Bigio, R.Caselli, M.Baker, M.T.Al-Lozi, J.C.Morris, A.Pestronk,

R.Rademakers, A.M.Goate, and N.J.Cairns. 2008. TDP-43 A315T mutation in familial motor neuron disease. *Ann. Neurol.* 63:535-538.

Gong, B., M.C.Lim, J.Wanderer, A.Wyttenbach, and A.J.Morton. 2008. Time-lapse analysis of aggregate formation in an inducible PC12 cell model of Huntington's disease reveals time-dependent aggregate formation that transiently delays cell death. *Brain Res. Bull.* 75:146-157.

Gong, Y.H., A.S.Parsadanian, A.Andreeva, W.D.Snider, and J.L.Elliott. 2000. Restricted expression of G86R Cu/Zn superoxide dismutase in astrocytes results in astrocytosis but does not cause motoneuron degeneration. *J. Neurosci.* 20:660-665.

Gordon, P.H., D.H.Moore, R.G.Miller, J.M.Florence, J.L.Verheijde, C.Doorish, J.F.Hilton, G.M.Spitalny, R.B.Macarthur, H.Mitsumoto, H.E.Neville, K.Boylan, T.Mozaffar, J.M.Belsh, J.Ravits, R.S.Bedlack, M.C.Graves, L.F.McCluskey, R.J.Barohn, and R.Tandan. 2007. Efficacy of minocycline in patients with amyotrophic lateral sclerosis: a phase III randomised trial. *Lancet Neurol.* 6:1045-1053.

Gourie-Devi, M., A.Nalini, and D.K.Subbakrishna. 1997. Temporary amelioration of symptoms with intravenous cyclophosphamide in amyotrophic lateral sclerosis. *J. Neurol. Sci.* 150:167-172.

Graf, M., D.Ecker, R.Horowski, B.Kramer, P.Riederer, M.Gerlach, C.Hager, A.C.Ludolph, G.Becker, J.Osterhage, W.H.Jost, B.Schrank, C.Stein, P.Kostopulos, S.Lubik, K.Wekwerth, R.Dengler, M.Troeger, A.Wuerz, A.Hoge, C.Schrader, N.Schimke, K.Krampfl, S.Petri, S.Zierz, K.Eger, S.Neudecker, K.Traufeller, M.Sievert, B.Neundorfer, and M.Hecht. 2005. High dose vitamin E therapy in amyotrophic lateral sclerosis as add-on therapy to riluzole: results of a placebo-controlled double-blind study. *J. Neural Transm.* 112:649-660.

Gredal, O., L.Werdelin, S.Bak, P.B.Christensen, G.Boysen, M.O.Kristensen, J.H.Jespersen, L.Regeur, H.H.Hinge, and T.S.Jensen. 1997. A clinical trial of dextromethorphan in amyotrophic lateral sclerosis. *Acta Neurol. Scand.* 96:8-13.

Groeneveld, G.J., J.H.Veldink, d.T.van, I, S.Kalmijn, C.Beijer, V.M.de, J.H.Wokke, H.Franssen, and L.H.van den Berg. 2003. A randomized sequential trial of creatine in amyotrophic lateral sclerosis. *Ann. Neurol.* 53:437-445.

Gurney, M.E. 1994. Transgenic-mouse model of amyotrophic lateral sclerosis. *N. Engl. J. Med.* 331:1721-1722.

Gurney, M.E., H.Pu, A.Y.Chiu, M.C.Dal Canto, C.Y.Polchow, D.D.Alexander, J.Caliendo, A.Hentati, Y.W.Kwon, H.X.Deng, and . 1994. Motor neuron degeneration in mice that express a human Cu,Zn superoxide dismutase mutation. *Science* 264:1772-1775.

Gusella, J.F. and M.E.MacDonald. 2006. Huntington's disease: seeing the pathogenic process through a genetic lens. *Trends Biochem. Sci.* 31:533-540.

Hadano, S., C.K.Hand, H.Osuga, Y.Yanagisawa, A.Otomo, R.S.Devon, N.Miyamoto, J.Showguchi-Miyata, Y.Okada, R.Singaraja, D.A.Figlewicz, T.Kwiatkowski, B.A.Hosler, T.Sagie, J.Skaug, J.Nasir, R.H.Brown, Jr., S.W.Scherer, G.A.Rouleau, M.R.Hayden, and J.E.Ikeda. 2001. A gene encoding a putative GTPase regulator is mutated in familial amyotrophic lateral sclerosis 2. *Nat. Genet.* 29:166-173.

Hand, C.K., J.Khoris, F.Salachas, F.Gros-Louis, A.A.Lopes, V.Mayeux-Portas, C.G.Brewer, R.H.Brown, Jr., V.Meininger, W.Camu, and G.A.Rouleau. 2002. A novel locus for familial amyotrophic lateral sclerosis, on chromosome 18q. *Am. J. Hum. Genet.* 70:251-256.

Hand, C.K., V.Mayeux-Portas, J.Khoris, V.Briolotti, P.Clavelou, W.Camu, and G.A.Rouleau. 2001. Compound heterozygous D90A and D96N SOD1 mutations in a recessive amyotrophic lateral sclerosis family. *Ann. Neurol.* 49:267-271.

Harrington, H., M.Hallett, and H.R.Tyler. 1984. Ganglioside therapy for amyotrophic lateral sclerosis: a double-blind controlled trial. *Neurology* 34:1083-1085.

Hayward, C., D.J.Brock, R.A.Minns, and R.J.Swingler. 1998. Homozygosity for Asn86Ser mutation in the CuZn-superoxide dismutase gene produces a severe clinical phenotype in a juvenile onset case of familial amyotrophic lateral sclerosis. *J. Med. Genet.* 35:174.

Hayward, L.J., J.A.Rodriguez, J.W.Kim, A.Tiwari, J.J.Goto, D.E.Cabelli, J.S.Valentine, and R.H.Brown, Jr. 2002. Decreased metallation and activity in subsets of mutant superoxide dismutases associated with familial amyotrophic lateral sclerosis. *J. Biol. Chem.* 277:15923-15931.

Hegedus, J., C.T.Putman, and T.Gordon. 2007. Time course of preferential motor unit loss in the SOD1 G93A mouse model of amyotrophic lateral sclerosis. *Neurobiol. Dis.* 28:154-164.

Hentati,A., K.Ouahchi, M.A.Pericak-Vance, D.Nijhawan, A.Ahmad, Y.Yang, J.Rimmler, W.Hung, B.Schlotter, A.Ahmed, M.Ben-Hamida, F.Hentati, and T.Siddique. 1998. Linkage of a commoner form of recessive amyotrophic lateral sclerosis to chromosome 15q15-q22 markers. *Neurogenetics* 55-60.

Higgins, C.M., C.Jung, and Z.Xu. 2003. ALS-associated mutant SOD1G93A causes mitochondrial vacuolation by expansion of the intermembrane space and by involvement of SOD1 aggregation and peroxisomes. *BMC. Neurosci.* 4:16.

Hirano, M., J.Fujii, Y.Nagai, M.Sonobe, K.Okamoto, H.Araki, N.Taniguchi, and S.Ueno. 1994. A new variant Cu/Zn superoxide dismutase (Val7-->Glu) deduced from

lymphocyte mRNA sequences from Japanese patients with familial amyotrophic lateral sclerosis. *Biochem. Biophys. Res. Commun.* 204:572-577.

Hosler, B.A., G.A.Nicholson, P.C.Sapp, W.Chin, R.W.Orrell, J.S.de Belleroche, J.Esteban, L.J.Hayward, D.kenna-Yasek, L.Yeung, A.K.Cherryson, J.E.Dench, S.D.Wilton, N.G.Laing, R.H.Horvitz, and R.H.Brown, Jr. 1996. Three novel mutations and two variants in the gene for Cu/Zn superoxide dismutase in familial amyotrophic lateral sclerosis. *Neuromuscul. Disord.* 6:361-366.

Hosler, B.A., T.Siddique, P.C.Sapp, W.Sailor, M.C.Huang, A.Hossain, J.R.Daube, M.Nance, C.Fan, J.Kaplan, W.Y.Hung, D.kenna-Yasek, J.L.Haines, M.A.Pericak-Vance, H.R.Horvitz, and R.H.Brown, Jr. 2000. Linkage of familial amyotrophic lateral sclerosis with frontotemporal dementia to chromosome 9q21-q22. *JAMA* 284:1664-1669.

Howland, D.S., J.Liu, Y.She, B.Goad, N.J.Maragakis, B.Kim, J.Erickson, J.Kulik, L.DeVito, G.Psaltis, L.J.DeGennaro, D.W.Cleveland, and J.D.Rothstein. 2002. Focal loss of the glutamate transporter EAAT2 in a transgenic rat model of SOD1 mutant-mediated amyotrophic lateral sclerosis (ALS). *Proc. Natl. Acad. Sci. U. S. A* 99:1604-1609.

Hsiao, K.K., D.Groth, M.Scott, S.L.Yang, H.Serban, D.Rapp, D.Foster, M.Torchia, S.J.DeArmond, and S.B.Prusiner. 1994. Serial transmission in rodents of neurodegeneration from transgenic mice expressing mutant prion protein. *Proc. Natl. Acad. Sci. U. S. A* 91:9126-9130.

Huang, C.S., J.H.Song, K.Nagata, D.Twombly, J.Z.Yeh, and T.Narahashi. 1997a. G-proteins are involved in riluzole inhibition of high voltage-activated calcium channels in rat dorsal root ganglion neurons. *Brain Res.* 762:235-239.

Huang, C.S., J.H.Song, K.Nagata, J.Z.Yeh, and T.Narahashi. 1997b. Effects of the neuroprotective agent riluzole on the high voltage-activated calcium channels of rat dorsal root ganglion neurons. *J. Pharmacol. Exp. Ther.* 282:1280-1290.

Hutton, M., C.L.Lendon, P.Rizzu, M.Baker, S.Froelich, H.Houlden, S.Pickering-Brown, S.Chakraverty, A.Isaacs, A.Grover, J.Hackett, J.Adamson, S.Lincoln, D.Dickson, P.Davies, R.C.Petersen, M.Stevens, G.E.de, E.Wauters, B.J.van, M.Hillebrand, M.Joosse, J.M.Kwon, P.Nowotny, L.K.Che, J.Norton, J.C.Morris, L.A.Reed, J.Trojanowski, H.Basun, L.Lannfelt, M.Neystat, S.Fahn, F.Dark, T.Tannenberg, P.R.Dodd, N.Hayward, J.B.Kwok, P.R.Schofield, A.Andreadis, J.Snowden, D.Craufurd, D.Neary, F.Owen, B.A.Oostra, J.Hardy, A.Goate, S.J.van, D.Mann, T.Lynch, and P.Heutink. 1998. Association of missense and 5'-splice-site mutations in tau with the inherited dementia FTDP-17. *Nature* 393:702-705.

Ikeda, M., K.Abe, M.Aoki, M.Sahara, M.Watanabe, M.Shoji, P.H.St George-Hyslop, S.Hirai, and Y.Itoyama. 1995. Variable clinical symptoms in familial amyotrophic lateral sclerosis with a novel point mutation in the Cu/Zn superoxide dismutase gene. *Neurology* 45:2038-2042.

Islinger, M., K.W.Li, J.Seitz, A.Volkl, and G.H.Luers. 2009. Hitchhiking of Cu/Zn Superoxide Dismutase to Peroxisomes-Evidence for a Natural Piggyback Import Mechanism in Mammals. *Traffic.*

Jaarsma, D., E.D.Haasdijk, J.A.Grashorn, R.Hawkins, D.W.van, H.W.Verspaget, J.London, and J.C.Holstege. 2000. Human Cu/Zn superoxide dismutase (SOD1) overexpression in mice causes mitochondrial vacuolization, axonal degeneration, and premature motoneuron death and accelerates motoneuron disease in mice expressing a familial amyotrophic lateral sclerosis mutant SOD1. *Neurobiol. Dis.* 7:623-643.

Jaarsma, D., F.Rognoni, D.W.van, H.W.Verspaget, E.D.Haasdijk, and J.C.Holstege. 2001. CuZn superoxide dismutase (SOD1) accumulates in vacuolated mitochondria in transgenic mice expressing amyotrophic lateral sclerosis-linked SOD1 mutations. *Acta Neuropathol. (Berl)* 102:293-305.

Jaarsma, D., E.Teuling, E.D.Haasdijk, C.I.De Zeeuw, and C.C.Hoogenraad. 2008. Neuron-specific expression of mutant superoxide dismutase is sufficient to induce amyotrophic lateral sclerosis in transgenic mice. *J. Neurosci.* 28:2075-2088.

Jackson, M., A.Al-Chalabi, Z.E.Enayat, B.Chioza, P.N.Leigh, and K.E.Morrison. 1997. Copper/zinc superoxide dismutase 1 and sporadic amyotrophic lateral sclerosis: analysis of 155 cases and identification of a novel insertion mutation. *Ann. Neurol.* 42:803-807.

Jarrett, J.T. and P.T.Lansbury, Jr. 1992. Amyloid fibril formation requires a chemically discriminating nucleation event: studies of an amyloidogenic sequence from the bacterial protein OsmB. *Biochemistry* 31:12345-12352.

Johnston, J.A., M.J.Dalton, M.E.Gurney, and R.R.Kopito. 2000. Formation of high molecular weight complexes of mutant Cu, Zn-superoxide dismutase in a mouse model for familial amyotrophic lateral sclerosis. *Proc. Natl. Acad. Sci. U. S. A* 97:12571-12576.

Jones, C.T., P.J.Shaw, G.Chari, and D.J.Brock. 1994a. Identification of a novel exon 4 SOD1 mutation in a sporadic amyotrophic lateral sclerosis patient. *Mol. Cell Probes* 8:329-330.

Jones, C.T., R.J.Swingler, and D.J.Brock. 1994b. Identification of a novel SOD1 mutation in an apparently sporadic amyotrophic lateral sclerosis patient and the detection of Ile113Thr in three others. *Hum. Mol. Genet.* 3:649-650.

Jonsson, P.A., K.Ernhill, P.M.Andersen, D.Bergemalm, T.Brannstrom, O.Gredal, P.Nilsson, and S.L.Marklund. 2004. Minute quantities of misfolded mutant superoxide dismutase-1 cause amyotrophic lateral sclerosis. *Brain* 127:73-88.

Jonsson, P.A., K.S.Graffmo, P.M.Andersen, T.Brannstrom, M.Lindberg, M.Oliveberg, and S.L.Marklund. 2006a. Disulphide-reduced superoxide dismutase-1 in CNS of transgenic amyotrophic lateral sclerosis models. *Brain* 129:451-464.

Jonsson, P.A., K.S.Graffmo, T.Brannstrom, P.Nilsson, P.M.Andersen, and S.L.Marklund. 2006b. Motor neuron disease in mice expressing the wild type-like D90A mutant superoxide dismutase-1. *J. Neuropathol. Exp. Neurol.* 65:1126-1136.

Julien, J.P. and J.Kriz. 2006. Transgenic mouse models of amyotrophic lateral sclerosis. *Biochim. Biophys. Acta* 1762:1013-1024.

Kabashi, E., J.N.Agar, D.M.Taylor, S.Minotti, and H.D.Durham. 2004. Focal dysfunction of the proteasome: a pathogenic factor in a mouse model of amyotrophic lateral sclerosis. *J. Neurochem.* 89:1325-1335.

Kabashi, E., P.N.Valdmanis, P.Dion, D.Spiegelman, B.J.McConkey, V.C.Vande, J.P.Bouchard, L.Lacomblez, K.Pochigaeva, F.Salachas, P.F.Pradat, W.Camu, V.Meininger, N.Dupre, and G.A.Rouleau. 2008. TARDBP mutations in individuals with sporadic and familial amyotrophic lateral sclerosis. *Nat. Genet.* 40:572-574.

Kalra, S., A.Genge, and D.L.Arnold. 2003. A prospective, randomized, placebo-controlled evaluation of corticoneuronal response to intrathecal BDNF therapy in ALS using magnetic resonance spectroscopy: feasibility and results. *Amyotroph. Lateral. Scler. Other Motor Neuron Disord.* 4:22-26.

Karch, C.M. and D.R.Borchelt. 2008. A Limited Role for Disulfide Cross-linking in the Aggregation of Mutant SOD1 Linked to Familial Amyotrophic Lateral Sclerosis. *J. Biol. Chem.* 283:13528-13537.

Karch, C.M., M.Prudencio, D.D.Winkler, P.J.Hart, and D.R.Borchelt. 2009. Role of mutant SOD1 disulfide oxidation and aggregation in the pathogenesis of familial ALS. *Proc. Natl. Acad. Sci. U. S. A*.

Kato, M., M.Aoki, M.Ohta, M.Nagai, F.Ishizaki, S.Nakamura, and Y.Itoyama. 2001a. Marked reduction of the Cu/Zn superoxide dismutase polypeptide in a case of familial amyotrophic lateral sclerosis with the homozygous mutation. *Neurosci. Lett.* 312:165-168.

Kato, S., S.Horiuchi, J.Liu, D.W.Cleveland, N.Shibata, K.Nakashima, R.Nagai, A.Hirano, M.Takikawa, M.Kato, I.Nakano, and E.Ohama. 2000a. Advanced glycation endproduct-modified superoxide dismutase-1 (SOD1)-positive inclusions are common to familial amyotrophic lateral sclerosis patients with SOD1 gene mutations and transgenic mice expressing human SOD1 with a G85R mutation. *Acta Neuropathol. (Berl)* 100:490-505.

Kato, S., S.Horiuchi, K.Nakashima, A.Hirano, N.Shibata, I.Nakano, M.Saito, M.Kato, K.Asayama, and E.Ohama. 1999a. Astrocytic hyaline inclusions contain

advanced glycation endproducts in familial amyotrophic lateral sclerosis with superoxide dismutase 1 gene mutation: immunohistochemical and immunoelectron microscopical analyses. *Acta Neuropathol. (Berl)* 97:260-266.

Kato, S., M.Saito, A.Hirano, and E.Ohama. 1999b. Recent advances in research on neuropathological aspects of familial amyotrophic lateral sclerosis with superoxide dismutase 1 gene mutations: neuronal Lewy body-like hyaline inclusions and astrocytic hyaline inclusions. *Histol. Histopathol.* 14:973-989.

Kato, S., M.Shimoda, Y.Watanabe, K.Nakashima, K.Takahashi, and E.Ohama. 1996. Familial amyotrophic lateral sclerosis with a two base pair deletion in superoxide dismutase 1: gene multisystem degeneration with intracytoplasmic hyaline inclusions in astrocytes. *J. Neuropathol. Exp. Neurol.* 55:1089-1101.

Kato, S., H.Sumi-Akamaru, H.Fujimura, S.Sakoda, M.Kato, A.Hirano, M.Takikawa, and E.Ohama. 2001b. Copper chaperone for superoxide dismutase co-aggregates with superoxide dismutase 1 (SOD1) in neuronal Lewy body-like hyaline inclusions: an immunohistochemical study on familial amyotrophic lateral sclerosis with SOD1 gene mutation. *Acta Neuropathol.* 102:233-238.

Kato, S., M.Takikawa, K.Nakashima, A.Hirano, D.W.Cleveland, H.Kusaka, N.Shibata, M.Kato, I.Nakano, and E.Ohama. 2000b. New consensus research on neuropathological aspects of familial amyotrophic lateral sclerosis with superoxide dismutase 1 (SOD1) gene mutations: inclusions containing SOD1 in neurons and astrocytes. *Amyotroph. Lateral. Scler. Other Motor Neuron Disord.* 1:163-184.

Kawamata, H. and G.Manfredi. 2008. Different regulation of wild-type and mutant Cu,Zn superoxide dismutase localization in mammalian mitochondria. *Hum. Mol. Genet.* 17:3303-3317.

Kawamata, J., S.Shimohama, S.Takano, K.Harada, K.Ueda, and J.Kimura. 1997. Novel G16S (GGC-AGC) mutation in the SOD-1 gene in a patient with apparently sporadic young-onset amyotrophic lateral sclerosis. *Hum. Mutat.* 9:356-358.

Kelenyi, G. 1967. Thioflavin S fluorescent and Congo red anisotropic stainings in the histologic demonstration of amyloid. *Acta Neuropathol. (Berl)* 7:336-348.

Keller, G.A., T.G.Warner, K.S.Steimer, and R.A.Hallewell. 1991. Cu,Zn superoxide dismutase is a peroxisomal enzyme in human fibroblasts and hepatoma cells. *Proc. Natl. Acad. Sci. U. S. A* 88:7381-7385.

Kennel, P.F., F.Finiels, F.Revah, and J.Mallet. 1996. Neuromuscular function impairment is not caused by motor neurone loss in FALS mice: an electromyographic study. *Neuroreport* 7:1427-1431.

Kim, N.H., H.J.Kim, M.Kim, and K.W.Lee. 2003. A novel SOD1 gene mutation in a Korean family with amyotrophic lateral sclerosis. *J. Neurol. Sci.* 206:65-69.

Kohno, S., Y.Takahashi, H.Miyajima, M.Serizawa, and K.Mizoguchi. 1999. A novel mutation (Cys6Gly) in the Cu/Zn superoxide dismutase gene associated with rapidly progressive familial amyotrophic lateral sclerosis. *Neurosci. Lett.* 276:135-137.

Kokubo, Y., S.Kuzuhara, Y.Narita, K.Kikugawa, R.Nakano, T.Inuzuka, S.Tsuji, M.Watanabe, T.Miyazaki, S.Murayama, and Y.Ihara. 1999. Accumulation of neurofilaments and SOD1-immunoreactive products in a patient with familial amyotrophic lateral sclerosis with I113T SOD1 mutation. *Arch. Neurol.* 56:1506-1508.

Kostrzewa, M., U.Burck-Lehmann, and U.Muller. 1994. Autosomal dominant amyotrophic lateral sclerosis: a novel mutation in the Cu/Zn superoxide dismutase-1 gene. *Hum. Mol. Genet.* 3:2261-2262.

Kostrzewa, M., M.S.Damian, and U.Muller. 1996. Superoxide dismutase 1: identification of a novel mutation in a case of familial amyotrophic lateral sclerosis. *Hum. Genet.* 98:48-50.

Krishnan, J., R.Lemmens, W.Robberecht, and B.L.Van Den. 2006. Role of heat shock response and Hsp27 in mutant SOD1-dependent cell death. *Exp. Neurol.* 200:301-310.

Kunst, C.B. 2004. Complex genetics of amyotrophic lateral sclerosis. *Am. J. Hum. Genet.* 75:933-947.

Kwiatkowski, T.J., Jr., D.A.Bosco, A.L.Leclerc, E.Tamrazian, C.R.Vanderburg, C.Russ, A.Davis, J.Gilchrist, E.J.Kasarskis, T.Munsat, P.Valdmanis, G.A.Rouleau, B.A.Hosler, P.Cortelli, P.J.de Jong, Y.Yoshinaga, J.L.Haines, M.A.Pericak-Vance, J.Yan, N.Ticozzi, T.Siddique, D.kenna-Yasek, P.C.Sapp, H.R.Horvitz, J.E.Landers, and R.H.Brown, Jr. 2009. Mutations in the FUS/TLS gene on chromosome 16 cause familial amyotrophic lateral sclerosis. *Science* 323:1205-1208.

Lacomblez, L., G.Bensimon, P.N.Leigh, C.Debove, R.Bejuit, P.Truffinet, and V.Meininger. 2002. Long-term safety of riluzole in amyotrophic lateral sclerosis. *Amyotroph. Lateral. Scler. Other Motor Neuron Disord.* 3:23-29.

Lacomblez, L., G.Bensimon, P.N.Leigh, P.Guillet, L.Powe, S.Durrleman, J.C.Delumeau, and V.Meininger. 1996. A confirmatory dose-ranging study of riluzole in ALS. ALS/Riluzole Study Group-II. *Neurology* 47:S242-S250.

Lange, D.J., P.L.Murphy, B.Diamond, V.Appel, E.C.Lai, D.S.Younger, and S.H.Appel. 1998. Selegiline is ineffective in a collaborative double-blind, placebo-controlled trial for treatment of amyotrophic lateral sclerosis. *Arch. Neurol.* 55:93-96.

Leitch, J.M., P.J.Yick, and V.L.Culotta. 2009. The right to choose: Multiple pathways for activating Cu/Zn superoxide dismutase. *J. Biol. Chem.*

Levin, B.J., G.Thompson, L.H.Mitsumoto, and P.Kaufmann. 2006. Pentoxifylline in ALS: a double-blind, randomized, multicenter, placebo-controlled trial. *Neurology* 66:1786-1787.

Lindberg, M.J., L.Tibell, and M.Oliveberg. 2002. Common denominator of Cu/Zn superoxide dismutase mutants associated with amyotrophic lateral sclerosis: decreased stability of the apo state. *Proc. Natl. Acad. Sci. U. S. A* 99:16607-16612.

Lino, M.M., C.Schneider, and P.Caroni. 2002. Accumulation of SOD1 mutants in postnatal motoneurons does not cause motoneuron pathology or motoneuron disease. *J. Neurosci.* 22:4825-4832.

Liu, J., C.Lillo, P.A.Jonsson, V.C.Vande, C.M.Ward, T.M.Miller, J.R.Subramaniam, J.D.Rothstein, S.Marklund, P.M.Andersen, T.Brannstrom, O.Gredal, P.C.Wong, D.S.Williams, and D.W.Cleveland. 2004. Toxicity of familial ALS-linked SOD1 mutants from selective recruitment to spinal mitochondria. *Neuron* 43:5-17.

Lobsiger, C.S., S.Boillee, M.onis-Downes, A.M.Khan, M.L.Feltri, K.Yamanaka, and D.W.Cleveland. 2009. Schwann cells expressing dismutase active mutant SOD1 unexpectedly slow disease progression in ALS mice. *Proc. Natl. Acad. Sci. U. S. A* 106:4465-4470.

Lynch, T., M.Sano, K.S.Marder, K.L.Bell, N.L.Foster, R.F.Defendini, A.A.Sima, C.Keohane, T.G.Nygaard, S.Fahn, and . 1994. Clinical characteristics of a family with chromosome 17-linked disinhibition-dementia-parkinsonism-amyotrophy complex. *Neurology* 44:1878-1884.

MARKOWITZ, H., G.E.CARTWRIGHT, and M.M.WINTROBE. 1959. Studies on copper metabolism. XXVII. The isolation and properties of an erythrocyte cuproprotein (erythrocuprein). *J. Biol. Chem.* 234:40-45.

Matsumoto, G., A.Stojanovic, C.I.Holmberg, S.Kim, and R.I.Morimoto. 2005. Structural properties and neuronal toxicity of amyotrophic lateral sclerosis-associated Cu/Zn superoxide dismutase 1 aggregates. *J. Cell Biol.* 171:75-85.

Matsumoto, S., S.Goto, H.Kusaka, T.Imai, N.Murakami, Y.Hashizume, H.Okazaki, and A.Hirano. 1993. Ubiquitin-positive inclusion in anterior horn cells in subgroups of motor neuron diseases: a comparative study of adult-onset amyotrophic lateral sclerosis, juvenile amyotrophic lateral sclerosis and Werdnig-Hoffmann disease. *J. Neurol. Sci.* 115:208-213.

Matsumoto, S., H.Kusaka, H.Ito, N.Shibata, T.Asayama, and T.Imai. 1996. Sporadic amyotrophic lateral sclerosis with dementia and Cu/Zn superoxide dismutase-positive Lewy body-like inclusions. *Clin. Neuropathol.* 15:41-46.

Mazzini, L., D.Testa, C.Balzarini, and G.Mora. 1994. An open-randomized clinical trial of selegiline in amyotrophic lateral sclerosis. *J. Neurol.* 241:223-227.

McCord, J.M. and I.Fridovich. 1969. Superoxide dismutase. An enzymic function for erythrocuprein (hemocuprein). *J. Biol. Chem.* 244:6049-6055.

Meininger, V., B.Asselain, P.Guillet, P.N.Leigh, A.Ludolph, L.Lacomblez, and W.Robberecht. 2006. Pentoxifylline in ALS: a double-blind, randomized, multicenter, placebo-controlled trial. *Neurology* 66:88-92.

Meininger, V., G.Bensimon, W.R.Bradley, B.Brooks, P.Douillet, A.A.Eisen, L.Lacomblez, P.N.Leigh, and W.Robberecht. 2004. Efficacy and safety of xaliproden in amyotrophic lateral sclerosis: results of two phase III trials. *Amyotroph. Lateral. Scler. Other Motor Neuron Disord.* 5:107-117.

Miller, R., W.Bradley, M.Cudkowicz, J.Hubble, V.Meininger, H.Mitsumoto, D.Moore, H.Pohlmann, D.Sauer, V.Silani, M.Strong, M.Swash, and E.Vernotica. 2007a. Phase II/III randomized trial of TCH346 in patients with ALS. *Neurology* 69:776-784.

Miller, R.G., J.D.Mitchell, M.Lyon, and D.H.Moore. 2007b. Riluzole for amyotrophic lateral sclerosis (ALS)/motor neuron disease (MND). *Cochrane. Database. Syst. Rev.*CD001447.

Miller, R.G., D.H.Moore, D.F.Gelinas, V.Dronsky, M.Mendoza, R.J.Barohn, W.Bryan, J.Ravits, E.Yuen, H.Neville, S.Ringel, M.Bromberg, J.Petajan, A.A.Amato, C.Jackson, W.Johnson, R.Mandler, P.Bosch, B.Smith, M.Graves, M.Ross, E.J.Sorenson, P.Kelkar, G.Parry, and R.Olney. 2001. Phase III randomized trial of gabapentin in patients with amyotrophic lateral sclerosis. *Neurology* 56:843-848.

Miller, R.G., R.Shepherd, H.Dao, A.Khramstov, M.Mendoza, J.Graves, and S.Smith. 1996a. Controlled trial of nimodipine in amyotrophic lateral sclerosis. *Neuromuscul. Disord.* 6:101-104.

Miller, R.G., S.A.Smith, J.R.Murphy, J.R.Brinkmann, J.Graves, M.Mendoza, M.L.Sands, and S.P.Ringel. 1996b. A clinical trial of verapamil in amyotrophic lateral sclerosis. *Muscle Nerve* 19:511-515.

Miller, T.M., S.H.Kim, K.Yamanaka, M.Hester, P.Umapathi, H.Arnson, L.Rizo, J.R.Mendell, F.H.Gage, D.W.Cleveland, and B.K.Kaspar. 2006. Gene transfer demonstrates that muscle is not a primary target for non-cell-autonomous toxicity in familial amyotrophic lateral sclerosis. *Proc. Natl. Acad. Sci. U. S. A* 103:19546-19551.

Mockett, R.J., A.C.Bayne, L.K.Kwong, W.C.Orr, and R.S.Sohal. 2003. Ectopic expression of catalase in Drosophila mitochondria increases stress resistance but not longevity. *Free Radic. Biol. Med.* 34:207-217.

Morita, M., M.Aoki, K.Abe, T.Hasegawa, R.Sakuma, Y.Onodera, N.Ichikawa, M.Nishizawa, and Y.Itoyama. 1996. A novel two-base mutation in the Cu/Zn

superoxide dismutase gene associated with familial amyotrophic lateral sclerosis in Japan. *Neurosci. Lett.* 205:79-82.

Munsat, T.L., J.Taft, I.M.Jackson, P.L.Andres, D.Hollander, L.Skerry, M.Ordman, D.Kasdon, and L.Finison. 1992. Intrathecal thyrotropin-releasing hormone does not alter the progressive course of ALS: experience with an intrathecal drug delivery system. *Neurology* 42:1049-1053.

Nagai, M., M.Aoki, I.Miyoshi, M.Kato, P.Pasinelli, N.Kasai, R.H.Brown, Jr., and Y.Itoyama. 2001. Rats expressing human cytosolic copper-zinc superoxide dismutase transgenes with amyotrophic lateral sclerosis: associated mutations develop motor neuron disease. *J. Neurosci.* 21:9246-9254.

Naini, A., M.Mehrazin, J.Lu, P.Gordon, and H.Mitsumoto. 2007. Identification of a novel D109Y mutation in Cu/Zn superoxide dismutase (sod1) gene associated with amyotrophic lateral sclerosis. *J. Neurol. Sci.* 254:17-21.

Naini, A., O.Musumeci, L.Hayes, F.Pallotti, B.M.Del, and H.Mitsumoto. 2002. Identification of a novel mutation in Cu/Zn superoxide dismutase gene associated with familial amyotrophic lateral sclerosis. *J. Neurol. Sci.* 198:17-19.

Nakanishi, T., M.Kishikawa, A.Miyazaki, A.Shimizu, Y.Ogawa, S.Sakoda, T.Ohi, and H.Shoji. 1998. Simple and defined method to detect the SOD-1 mutants from patients with familial amyotrophic lateral sclerosis by mass spectrometry. *J. Neurosci. Methods* 81:41-44.

Nakano, R., T.Inuzuka, K.Kikugawa, H.Takahashi, K.Sakimura, J.Fujii, N.Taniguchi, and S.Tsuji. 1996. Instability of mutant Cu/Zn superoxide dismutase (Ala4Thr) associated with familial amyotrophic lateral sclerosis. *Neurosci. Lett.* 211:129-131.

Nakano, R., S.Sato, T.Inuzuka, K.Sakimura, M.Mishina, H.Takahashi, F.Ikuta, Y.Honma, J.Fujii, N.Taniguchi, and . 1994. A novel mutation in Cu/Zn superoxide dismutase gene in Japanese familial amyotrophic lateral sclerosis. *Biochem. Biophys. Res. Commun.* 200:695-703.

Nishimura, A.L., M.Mitne-Neto, H.C.Silva, A.Richieri-Costa, S.Middleton, D.Cascio, F.Kok, J.R.Oliveira, T.Gillingwater, J.Webb, P.Skehel, and M.Zatz. 2004. A mutation in the vesicle-trafficking protein VAPB causes late-onset spinal muscular atrophy and amyotrophic lateral sclerosis. *Am. J. Hum. Genet.* 75:822-831.

Nogales-Gadea, G., E.Garcia-Arumi, A.L.Andreu, C.Cervera, and J.Gamez. 2004. A novel exon 5 mutation (N139H) in the SOD1 gene in a Spanish family associated with incomplete penetrance. *J. Neurol. Sci.* 219:1-6.

Norris, F.H., Y.Tan, R.J.Fallat, and L.Elias. 1993. Trial of oral physostigmine in amyotrophic lateral sclerosis. *Clin. Pharmacol. Ther.* 54:680-682.

Ohi, T., K.Saita, S.Takechi, K.Nabesima, H.Tashiro, K.Shiomi, S.Sugimoto, T.Akematsu, T.Nakayama, T.Iwaki, and S.Matsukura. 2002. Clinical features and neuropathological findings of familial amyotrophic lateral sclerosis with a His46Arg mutation in Cu/Zn superoxide dismutase. *J. Neurol. Sci.* 197:73-78.

Okado-Matsumoto, A. and I.Fridovich. 2002. Amyotrophic lateral sclerosis: a proposed mechanism. *Proc. Natl. Acad. Sci. U. S. A* 99:9010-9014.

Okamoto, K., S.Hirai, M.Amari, M.Watanabe, and A.Sakurai. 1993. Bunina bodies in amyotrophic lateral sclerosis immunostained with rabbit anti-cystatin C serum. *Neurosci. Lett.* 162:125-128.

Orrell, R.W., J.J.Habgood, I.Gardiner, A.W.King, F.A.Bowe, R.A.Hallewell, S.L.Marklund, J.Greenwood, R.J.Lane, and J.deBelleroche. 1997. Clinical and functional investigation of 10 missense mutations and a novel frameshift insertion mutation of the gene for copper-zinc superoxide dismutase in UK families with amyotrophic lateral sclerosis. *Neurology* 48:746-751.

Oztug Durer, Z.A., J.A.Cohlberg, P.Dinh, S.Padua, K.Ehrenclou, S.Downes, J.K.Tan, Y.Nakano, C.J.Bowman, J.L.Hoskins, C.Kwon, A.Z.Mason, J.A.Rodriguez, P.A.Doucette, B.F.Shaw, and V.J.Selverstone. 2009. Loss of metal ions, disulfide reduction and mutations related to familial ALS promote formation of amyloid-like aggregates from superoxide dismutase. *PLoS. ONE.* 4:e5004.

Pardo, C.A., Z.Xu, D.R.Borchelt, D.L.Price, S.S.Sisodia, and D.W.Cleveland. 1995. Superoxide dismutase is an abundant component in cell bodies, dendrites, and axons of motor neurons and in a subset of other neurons. *Proc. Natl. Acad. Sci. U. S. A* 92:954-958.

Parkes, T.L., A.J.Elia, D.Dickinson, A.J.Hilliker, J.P.Phillips, and G.L.Boulianne. 1998. Extension of Drosophila lifespan by overexpression of human SOD1 in motorneurons. *Nat. Genet.* 19:171-174.

Pasinelli, P., M.E.Belford, N.Lennon, B.J.Bacskai, B.T.Hyman, D.Trotti, and R.H.Brown, Jr. 2004. Amyotrophic lateral sclerosis-associated SOD1 mutant proteins bind and aggregate with Bcl-2 in spinal cord mitochondria. *Neuron* 43:19-30.

Pasinelli, P., D.R.Borchelt, M.K.Houseweart, D.W.Cleveland, and R.H.Brown, Jr. 1998. Caspase-1 is activated in neural cells and tissue with amyotrophic lateral sclerosis-associated mutations in copper-zinc superoxide dismutase. *Proc. Natl. Acad. Sci. U. S. A* 95:15763-15768.

Penco, S., A.Schenone, D.Bordo, M.Bolognesi, M.Abbruzzese, O.Bugiani, F.Ajmar, and C.Garre. 1999. A SOD1 gene mutation in a patient with slowly progressing familial ALS. *Neurology* 53:404-406.

Persichetti, F., J.Srinidhi, L.Kanaley, P.Ge, R.H.Myers, K.D'Arrigo, G.T.Barnes, M.E.MacDonald, J.P.Vonsattel, J.F.Gusella, and . 1994. Huntington's disease

CAG trinucleotide repeats in pathologically confirmed post-mortem brains. *Neurobiol. Dis.* 1:159-166.

Petty, S.A., T.Adalsteinsson, and S.M.Decatur. 2005. Correlations among morphology, beta-sheet stability, and molecular structure in prion peptide aggregates. *Biochemistry* 44:4720-4726.

Petty, S.A. and S.M.Decatur. 2005. Intersheet rearrangement of polypeptides during nucleation of {beta}-sheet aggregates. *Proc. Natl. Acad. Sci. U. S. A* 102:14272-14277.

Potter, S.Z., H.Zhu, B.F.Shaw, J.A.Rodriguez, P.A.Doucette, S.H.Sohn, A.Durazo, K.F.Faull, E.B.Gralla, A.M.Nersissian, and J.S.Valentine. 2007. Binding of a single zinc ion to one subunit of copper-zinc superoxide dismutase apoprotein substantially influences the structure and stability of the entire homodimeric protein. *J. Am. Chem. Soc.* 129:4575-4583.

Pramatarova, A., D.A.Figlewicz, A.Krizus, F.Y.Han, I.Ceballos-Picot, A.Nicole, M.Dib, V.Meininger, R.H.Brown, and G.A.Rouleau. 1995. Identification of new mutations in the Cu/Zn superoxide dismutase gene of patients with familial amyotrophic lateral sclerosis. *Am. J. Hum. Genet.* 56:592-596.

Pramatarova, A., J.Goto, E.Nanba, K.Nakashima, K.Takahashi, A.Takagi, I.Kanazawa, D.A.Figlewicz, and G.A.Rouleau. 1994. A two basepair deletion in the SOD 1 gene causes familial amyotrophic lateral sclerosis. *Hum. Mol. Genet.* 3:2061-2062.

Pramatarova, A., J.Laganiere, J.Roussel, K.Brisebois, and G.A.Rouleau. 2001. Neuron-specific expression of mutant superoxide dismutase 1 in transgenic mice does not lead to motor impairment. *J. Neurosci.* 21:3369-3374.

Proescher, J.B., M.Son, J.L.Elliott, and V.C.Culotta. 2008. Biological effects of CCS in the absence of SOD1 enzyme activation: implications for disease in a mouse model for ALS. *Hum. Mol. Genet.* 17:1728-1737.

Prudencio, M., A.Durazo, J.P.Whitelegge, and D.R.Borchelt. 2009a. Modulation of mutant superoxide dismutase 1 aggregation by co-expression of wild-type enzyme. *J. Neurochem.* 108:1009-1018.

Prudencio, M., P.J.Hart, D.R.Borchelt, and P.M.Andersen. 2009b. Variation in aggregation propensities among ALS-associated variants of SOD1: Correlation to human disease. *Human Molecular Genetics*ddp260.

Puls, I., C.Jonnakuty, B.H.LaMonte, E.L.Holzbaur, M.Tokito, E.Mann, M.K.Floeter, K.Bidus, D.Drayna, S.J.Oh, R.H.Brown, Jr., C.L.Ludlow, and K.H.Fischbeck. 2003. Mutant dynactin in motor neuron disease. *Nat. Genet.* 33:455-456.

Ralph, G.S., P.A.Radcliffe, D.M.Day, J.M.Carthy, M.A.Leroux, D.C.Lee, L.F.Wong, L.G.Bilsland, L.Greensmith, S.M.Kingsman, K.A.Mitrophanous, N.D.Mazarakis, and M.Azzouz. 2005. Silencing mutant SOD1 using RNAi protects against neurodegeneration and extends survival in an ALS model. *Nat. Med.* 11:429-433.

Raoul, C., A.G.Estevez, H.Nishimune, D.W.Cleveland, O.deLapeyriere, C.E.Henderson, G.Haase, and B.Pettmann. 2002. Motoneuron death triggered by a specific pathway downstream of Fas. potentiation by ALS-linked SOD1 mutations. *Neuron* 35:1067-1083.

Ratovitski, T., L.B.Corson, J.Strain, P.Wong, D.W.Cleveland, V.C.Culotta, and D.R.Borchelt. 1999. Variation in the biochemical/biophysical properties of mutant superoxide dismutase 1 enzymes and the rate of disease progression in familial amyotrophic lateral sclerosis kindreds. *Hum. Mol. Genet.* 8:1451-1460.

Reaume, A.G., J.L.Elliott, E.K.Hoffman, N.W.Kowall, R.J.Ferrante, D.F.Siwek, H.M.Wilcox, D.G.Flood, M.F.Beal, R.H.Brown, Jr., R.W.Scott, and W.D.Snider. 1996. Motor neurons in Cu/Zn superoxide dismutase-deficient mice develop normally but exhibit enhanced cell death after axonal injury. *Nat. Genet.* 13:43-47.

Rezania, K., J.Yan, L.Dellefave, H.X.Deng, N.Siddique, R.T.Pascuzzi, T.Siddique, and R.P.Roos. 2003. A rare Cu/Zn superoxide dismutase mutation causing familial amyotrophic lateral sclerosis with variable age of onset, incomplete penetrance and a sensory neuropathy. *Amyotroph. Lateral. Scler. Other Motor Neuron Disord.* 4:162-166.

Rodriguez, J.A., B.F.Shaw, A.Durazo, S.H.Sohn, P.A.Doucette, A.M.Nersissian, K.F.Faull, D.K.Eggers, A.Tiwari, L.J.Hayward, and J.S.Valentine. 2005. Destabilization of apoprotein is insufficient to explain Cu,Zn-superoxide dismutase-linked ALS pathogenesis. *Proc. Natl. Acad. Sci. U. S. A* 102:10516-10521.

Rodriguez, J.A., J.S.Valentine, D.K.Eggers, J.A.Roe, A.Tiwari, R.H.Brown, Jr., and L.J.Hayward. 2002. Familial amyotrophic lateral sclerosis-associated mutations decrease the thermal stability of distinctly metallated species of human copper/zinc superoxide dismutase. *J. Biol. Chem.* 277:15932-15937.

Rosen, D.R., A.C.Bowling, D.Patterson, T.B.Usdin, P.Sapp, E.Mezey, D.kenna-Yasek, J.O'Regan, Z.Rahmani, R.J.Ferrante, and . 1994. A frequent ala 4 to val superoxide dismutase-1 mutation is associated with a rapidly progressive familial amyotrophic lateral sclerosis. *Hum. Mol. Genet.* 3:981-987.

Rosen, D.R., T.Siddique, D.Patterson, D.A.Figlewicz, P.Sapp, A.Hentati, D.Donaldson, J.Goto, J.P.O'Regan, H.X.Deng, and . 1993. Mutations in Cu/Zn superoxide dismutase gene are associated with familial amyotrophic lateral sclerosis. *Nature* 362:59-62.

Rothstein, J.D., L.J.Martin, and R.W.Kuncl. 1992. Decreased glutamate transport by the brain and spinal cord in amyotrophic lateral sclerosis. *N. Engl. J. Med.* 326:1464-1468.

Rothstein, J.D., K.M.Van, A.I.Levey, L.J.Martin, and R.W.Kuncl. 1995. Selective loss of glial glutamate transporter GLT-1 in amyotrophic lateral sclerosis. *Ann. Neurol.* 38:73-84.

Ryberg, H., H.Askmark, and L.I.Persson. 2003. A double-blind randomized clinical trial in amyotrophic lateral sclerosis using lamotrigine: effects on CSF glutamate, aspartate, branched-chain amino acid levels and clinical parameters. *Acta Neurol. Scand.* 108:1-8.

Sandelin, E., A.Nordlund, P.M.Andersen, S.S.Marklund, and M.Oliveberg. 2007. Amyotrophic lateral sclerosis-associated copper/zinc superoxide dismutase mutations preferentially reduce the repulsive charge of the proteins. *J. Biol. Chem.* 282:21230-21236.

Sapp, P.C., B.A.Hosler, D.kenna-Yasek, W.Chin, A.Gann, H.Genise, J.Gorenstein, M.Huang, W.Sailer, M.Scheffler, M.Valesky, J.L.Haines, M.Pericak-Vance, T.Siddique, H.R.Horvitz, and R.H.Brown, Jr. 2003. Identification of two novel loci for dominantly inherited familial amyotrophic lateral sclerosis. *Am. J. Hum. Genet.* 73:397-403.

Sapp, P.C., D.R.Rosen, B.A.Hosler, J.Esteban, D.kenna-Yasek, J.P.O'Regan, H.R.Horvitz, and R.H.Brown, Jr. 1995. Identification of three novel mutations in the gene for Cu/Zn superoxide dismutase in patients with familial amyotrophic lateral sclerosis. *Neuromuscul. Disord.* 5:353-357.

Sasaki, S., M.Nagai, M.Aoki, T.Komori, Y.Itoyama, and M.Iwata. 2007. Motor neuron disease in transgenic mice with an H46R mutant SOD1 gene. *J. Neuropathol. Exp. Neurol.* 66:517-524.

Sasaki, S., Y.Ohsawa, K.Yamane, H.Sakuma, N.Shibata, R.Nakano, K.Kikugawa, T.Mizutani, S.Tsuji, and M.Iwata. 1998. Familial amyotrophic lateral sclerosis with widespread vacuolation and hyaline inclusions. *Neurology* 51:871-873.

Sasaki, S., H.Warita, T.Murakami, N.Shibata, T.Komori, K.Abe, M.Kobayashi, and M.Iwata. 2005. Ultrastructural study of aggregates in the spinal cord of transgenic mice with a G93A mutant SOD1 gene. *Acta Neuropathol. (Berl)* 109:247-255.

Sato, T., Y.Yamamoto, T.Nakanishi, K.Fukada, F.Sugai, Z.Zhou, T.Okuno, S.Nagano, S.Hirata, A.Shimizu, and S.Sakoda. 2004. Identification of two novel mutations in the Cu/Zn superoxide dismutase gene with familial amyotrophic lateral sclerosis: mass spectrometric and genomic analyses. *J. Neurol. Sci.* 218:79-83.

Scherzinger, E., A.Sittler, K.Schweiger, V.Heiser, R.Lurz, R.Hasenbank, G.P.Bates, H.Lehrach, and E.E.Wanker. 1999. Self-assembly of polyglutamine-containing

huntingtin fragments into amyloid-like fibrils: implications for Huntington's disease pathology. *Proc. Natl. Acad. Sci. U. S. A* 96:4604-4609.

Schiffer, D., L.utilio-Gambetti, A.Chio, P.Gambetti, M.T.Giordana, F.Gullotta, A.Migheli, and M.C.Vigliani. 1991. Ubiquitin in motor neuron disease: study at the light and electron microscope. *J. Neuropathol. Exp. Neurol.* 50:463-473.

Seetharaman, S.V., M.Prudencio, C.Karch, S.P.Holloway, D.R.Borchelt, and P.J.Hart. 2009. Immature Copper-zinc Superoxide Dismutase and Familial Amyotrophic Lateral Sclerosis. *Exp. Biol. Med. (Maywood.)*.

Segovia-Silvestre, T., A.L.Andreu, C.Vives-Bauza, E.Garcia-Arumi, C.Cervera, and J.Gamez. 2002. A novel exon 3 mutation (D76V) in the SOD1 gene associated with slowly progressive ALS. *Amyotroph. Lateral. Scler. Other Motor Neuron Disord.* 3:69-74.

Seilhean, D., J.Takahashi, K.H.El Hachimi, H.Fujigasaki, A.S.Lebre, V.Biancalana, A.Durr, F.Salachas, J.Hogenhuis, T.H.de, J.J.Hauw, V.Meininger, A.Brice, and C.Duyckaerts. 2004. Amyotrophic lateral sclerosis with neuronal intranuclear protein inclusions. *Acta Neuropathol. (Berl)* 108:81-87.

Shaw, B.F., H.L.Lelie, A.Durazo, A.M.Nersissian, G.Xu, P.K.Chan, E.B.Gralla, A.Tiwari, L.J.Hayward, D.R.Borchelt, J.S.Valentine, and J.P.Whitelegge. 2008. Detergent-insoluble aggregates associated with amyotrophic lateral sclerosis in transgenic mice contain primarily full-length, unmodified superoxide dismutase-1. *J. Biol. Chem.* 283:8340-8350.

Shaw, B.F. and J.S.Valentine. 2007. How do ALS-associated mutations in superoxide dismutase 1 promote aggregation of the protein? *Trends Biochem. Sci.* 32:78-85.

Shaw, C.E., Z.E.Enayat, B.A.Chioza, A.Al-Chalabi, A.Radunovic, J.F.Powell, and P.N.Leigh. 1998. Mutations in all five exons of SOD-1 may cause ALS. *Ann. Neurol.* 43:390-394.

Shi, S.G., L.S.Li, K.N.Chen, and X.Liu. 2004. [Identification of the mutation of SOD1 gene in a familial amyotrophic lateral sclerosis]. *Zhonghua Yi. Xue. Yi. Chuan Xue. Za Zhi.* 21:149-152.

Shibata, N., K.Asayama, A.Hirano, and M.Kobayashi. 1996a. Immunohistochemical study on superoxide dismutases in spinal cords from autopsied patients with amyotrophic lateral sclerosis. *Dev. Neurosci.* 18:492-498.

Shibata, N., A.Hirano, M.Kobayashi, T.Siddique, H.X.Deng, W.Y.Hung, T.Kato, and K.Asayama. 1996b. Intense superoxide dismutase-1 immunoreactivity in intracytoplasmic hyaline inclusions of familial amyotrophic lateral sclerosis with posterior column involvement. *J. Neuropathol. Exp. Neurol.* 55:481-490.

Shibata, N., M.Kawaguchi, K.Uchida, A.Kakita, H.Takahashi, R.Nakano, H.Fujimura, S.Sakoda, Y.Ihara, K.Nobukuni, Y.Takehisa, S.Kuroda, Y.Kokubo, S.Kuzuhara, T.Honma, Y.Mochizuki, T.Mizutani, S.Yamada, S.Toi, S.Sasaki, M.Iwata, A.Hirano, T.Yamamoto, Y.Kato, T.Sawada, and M.Kobayashi. 2007. Protein-bound crotonaldehyde accumulates in the spinal cord of superoxide dismutase-1 mutation-associated familial amyotrophic lateral sclerosis and its transgenic mouse model. *Neuropathology.* 27:49-61.

Shimizu, T., A.Kawata, S.Kato, M.Hayashi, K.Takamoto, H.Hayashi, S.Hirai, S.Yamaguchi, T.Komori, and M.Oda. 2000. Autonomic failure in ALS with a novel SOD1 gene mutation. *Neurology* 54:1534-1537.

Shorter, J. and S.Lindquist. 2005. Prions as adaptive conduits of memory and inheritance. *Nat. Rev. Genet.* 6:435-450.

Siddique, T. and H.X.Deng. 1996. Genetics of amyotrophic lateral sclerosis. *Hum. Mol. Genet.* 5 Spec No:1465-1470.

Smith, S.A., R.G.Miller, J.R.Murphy, and S.P.Ringel. 1994. Treatment of ALS with high dose pulse cyclophosphamide. *J. Neurol. Sci.* 124 Suppl:84-87.

Son, M., Q.Fu, K.Puttaparthi, C.M.Matthews, and J.L.Elliott. 2009. Redox susceptibility of SOD1 mutants is associated with the differential response to CCS over-expression in vivo. *Neurobiol. Dis.* 34:155-162.

Son, M., K.Puttaparthi, H.Kawamata, B.Rajendran, P.J.Boyer, G.Manfredi, and J.L.Elliott. 2007. Overexpression of CCS in G93A-SOD1 mice leads to accelerated neurological deficits with severe mitochondrial pathology. *Proc. Natl. Acad. Sci. U. S. A* 104:6072-6077.

Sorenson, E.J., A.J.Windbank, J.N.Mandrekar, W.R.Bamlet, S.H.Appel, C.Armon, P.E.Barkhaus, P.Bosch, K.Boylan, W.S.David, E.Feldman, J.Glass, L.Gutmann, J.Katz, W.King, C.A.Luciano, L.F.McCluskey, S.Nash, D.S.Newman, R.M.Pascuzzi, E.Pioro, L.J.Sams, S.Scelsa, E.P.Simpson, S.H.Subramony, E.Tiryaki, and C.A.Thornton. 2008. Subcutaneous IGF-1 is not beneficial in 2-year ALS trial. *Neurology* 71:1770-1775.

Sreedharan, J., I.P.Blair, V.B.Tripathi, X.Hu, C.Vance, B.Rogelj, S.Ackerley, J.C.Durnall, K.L.Williams, E.Buratti, F.Baralle, B.J.de, J.D.Mitchell, P.N.Leigh, A.Al-Chalabi, C.C.Miller, G.Nicholson, and C.E.Shaw. 2008. TDP-43 mutations in familial and sporadic amyotrophic lateral sclerosis. *Science* 319:1668-1672.

Stevenson, A., D.M.Yates, C.Manser, K.J.De Vos, A.Vagnoni, P.N.Leigh, D.M.McLoughlin, and C.C.Miller. 2009. Riluzole protects against glutamate-induced slowing of neurofilament axonal transport. *Neurosci. Lett.* 454:161-164.

Stewart, H.G., I.R.Mackenzie, A.Eisen, T.Brannstrom, S.L.Marklund, and P.M.Andersen. 2006. Clinicopathological phenotype of ALS with a novel G72C SOD1 gene mutation mimicking a myopathy. *Muscle Nerve* 33:701-706.

Stieber, A., Y.Chen, S.Wei, Z.Mourelatos, J.Gonatas, K.Okamoto, and N.K.Gonatas. 1998. The fragmented neuronal Golgi apparatus in amyotrophic lateral sclerosis includes the trans-Golgi-network: functional implications. *Acta Neuropathol. (Berl)* 95:245-253.

Stieber, A., J.O.Gonatas, J.Collard, J.Meier, J.Julien, P.Schweitzer, and N.K.Gonatas. 2000a. The neuronal Golgi apparatus is fragmented in transgenic mice expressing a mutant human SOD1, but not in mice expressing the human NF-H gene. *J. Neurol. Sci.* 173:63-72.

Stieber, A., J.O.Gonatas, and N.K.Gonatas. 2000b. Aggregates of mutant protein appear progressively in dendrites, in periaxonal processes of oligodendrocytes, and in neuronal and astrocytic perikarya of mice expressing the SOD1(G93A) mutation of familial amyotrophic lateral sclerosis. *J. Neurol. Sci.* 177:114-123.

Stieber, A., J.O.Gonatas, and N.K.Gonatas. 2000c. Aggregation of ubiquitin and a mutant ALS-linked SOD1 protein correlate with disease progression and fragmentation of the Golgi apparatus. *J. Neurol. Sci.* 173:53-62.

Strom, A.L., P.Shi, F.Zhang, J.Gal, R.Kilty, L.J.Hayward, and H.Zhu. 2008. Interaction of amyotrophic lateral sclerosis (ALS)-related mutant copper-zinc superoxide dismutase with the dynein-dynactin complex contributes to inclusion formation. *J. Biol. Chem.* 283:22795-22805.

Sturtz, L.A., K.Diekert, L.T.Jensen, R.Lill, and V.C.Culotta. 2001. A fraction of yeast Cu,Zn-superoxide dismutase and its metallochaperone, CCS, localize to the intermembrane space of mitochondria. A physiological role for SOD1 in guarding against mitochondrial oxidative damage. *J. Biol. Chem.* 276:38084-38089.

Subramaniam, J.R., W.E.Lyons, J.Liu, T.B.Bartnikas, J.Rothstein, D.L.Price, D.W.Cleveland, J.D.Gitlin, and P.C.Wong. 2002. Mutant SOD1 causes motor neuron disease independent of copper chaperone-mediated copper loading. *Nat. Neurosci.* 5:301-307.

Takehisa, Y., H.Ujike, H.Ishizu, S.Terada, T.Haraguchi, Y.Tanaka, T.Nishinaka, K.Nobukuni, Y.Ihara, R.Namba, T.Yasuda, M.Nishibori, T.Hayabara, and S.Kuroda. 2001. Familial amyotrophic lateral sclerosis with a novel Leu126Ser mutation in the copper/zinc superoxide dismutase gene showing mild clinical features and lewy body-like hyaline inclusions. *Arch. Neurol.* 58:736-740.

Tan, C.F., Y.S.Piao, S.Hayashi, H.Obata, Y.Umeda, M.Sato, T.Fukushima, R.Nakano, S.Tsuji, and H.Takahashi. 2004. Familial amyotrophic lateral sclerosis with bulbar onset and a novel Asp101Tyr Cu/Zn superoxide dismutase gene mutation. *Acta Neuropathol.* 108:332-336.

Tandan, R., M.B.Bromberg, D.Forshew, T.J.Fries, G.J.Badger, J.Carpenter, P.B.Krusinski, E.F.Betts, K.Arciero, and K.Nau. 1996. A controlled trial of amino acid therapy in amyotrophic lateral sclerosis: I. Clinical, functional, and maximum isometric torque data. *Neurology* 47:1220-1226.

Testa, D., T.Caraceni, and V.Fetoni. 1989. Branched-chain amino acids in the treatment of amyotrophic lateral sclerosis. *J. Neurol.* 236:445-447.

Tiwari, A. and L.J.Hayward. 2005. Mutant SOD1 instability: implications for toxicity in amyotrophic lateral sclerosis. *Neurodegener. Dis.* 2:115-127.

Tobisawa, S., Y.Hozumi, S.Arawaka, S.Koyama, M.Wada, M.Nagai, M.Aoki, Y.Itoyama, K.Goto, and T.Kato. 2003. Mutant SOD1 linked to familial amyotrophic lateral sclerosis, but not wild-type SOD1, induces ER stress in COS7 cells and transgenic mice. *Biochem. Biophys. Res. Commun.* 303:496-503.

Tohgi, H., T.Abe, K.Yamazaki, T.Murata, E.Ishizaki, and C.Isobe. 1999. Remarkable increase in cerebrospinal fluid 3-nitrotyrosine in patients with sporadic amyotrophic lateral sclerosis. *Ann. Neurol.* 46:129-131.

Tu, P.H., P.Raju, K.A.Robinson, M.E.Gurney, J.Q.Trojanowski, and V.M.Lee. 1996. Transgenic mice carrying a human mutant superoxide dismutase transgene develop neuronal cytoskeletal pathology resembling human amyotrophic lateral sclerosis lesions. *Proc. Natl. Acad. Sci. U. S. A* 93:3155-3160.

Urbani, A. and O.Belluzzi. 2000. Riluzole inhibits the persistent sodium current in mammalian CNS neurons. *Eur. J. Neurosci.* 12:3567-3574.

Urushitani, M., J.Kurisu, K.Tsukita, and R.Takahashi. 2002. Proteasomal inhibition by misfolded mutant superoxide dismutase 1 induces selective motor neuron death in familial amyotrophic lateral sclerosis. *J. Neurochem.* 83:1030-1042.

Valentine,J.S., P.A.Doucette, and S.Z.Potter. Copper-Zinc Superoxide Dismutase and Amyotrophic Lateral Sclerosis. 2005.
Ref Type: Generic

Valentine, J.S. and P.J.Hart. 2003. Misfolded CuZnSOD and amyotrophic lateral sclerosis. *Proc. Natl. Acad. Sci. U. S. A* 100:3617-3622.

Vance, C., B.Rogelj, T.Hortobagyi, K.J.De Vos, A.L.Nishimura, J.Sreedharan, X.Hu, B.Smith, D.Ruddy, P.Wright, J.Ganesalingam, K.L.Williams, V.Tripathi, S.Al-Saraj, A.Al-Chalabi, P.N.Leigh, I.P.Blair, G.Nicholson, B.J.de, J.M.Gallo, C.C.Miller, and C.E.Shaw. 2009. Mutations in FUS, an RNA processing protein, cause familial amyotrophic lateral sclerosis type 6. *Science* 323:1208-1211.

VASSAR, P.S. and C.F.CULLING. 1959. Fluorescent stains, with special reference to amyloid and connective tissues. *Arch. Pathol.* 68:487-498.

Vijayvergiya, C., M.F.Beal, J.Buck, and G.Manfredi. 2005. Mutant Superoxide Dismutase 1 Forms Aggregates in the Brain Mitochondrial Matrix of Amyotrophic Lateral Sclerosis Mice. *Journal of Neuroscience* 25:2463-2470.

Vyth, A., J.G.Timmer, P.M.Bossuyt, E.S.Louwerse, and J.M.de Jong. 1996. Survival in patients with amyotrophic lateral sclerosis, treated with an array of antioxidants. *J. Neurol. Sci.* 139 Suppl:99-103.

Wang, J., A.Caruano-Yzermans, A.Rodriguez, J.P.Scheurmann, H.H.Slunt, X.Cao, J.Gitlin, P.J.Hart, and D.R.Borchelt. 2007. Disease-associated mutations at copper ligand histidine residues of superoxide dismutase 1 diminish the binding of copper and compromise dimer stability. *J. Biol. Chem.* 282:345-352.

Wang, J., G.W.Farr, D.H.Hall, F.Li, K.Furtak, L.Dreier, and A.L.Horwich. 2009a. An ALS-linked mutant SOD1 produces a locomotor defect associated with aggregation and synaptic dysfunction when expressed in neurons of Caenorhabditis elegans. *PLoS. Genet.* 5:e1000350.

Wang, J., G.W.Farr, C.J.Zeiss, D.J.Rodriguez-Gil, J.H.Wilson, K.Furtak, D.T.Rutkowski, R.J.Kaufman, C.I.Ruse, J.R.Yates, III, S.Perrin, M.B.Feany, and A.L.Horwich. 2009b. Progressive aggregation despite chaperone associations of a mutant SOD1-YFP in transgenic mice that develop ALS. *Proc. Natl. Acad. Sci. U. S. A* 106:1392-1397.

Wang, J., H.Slunt, V.Gonzales, D.Fromholt, M.Coonfield, N.G.Copeland, N.A.Jenkins, and D.R.Borchelt. 2003. Copper-binding-site-null SOD1 causes ALS in transgenic mice: aggregates of non-native SOD1 delineate a common feature. *Hum. Mol. Genet.* 12:2753-2764.

Wang, J., G.Xu, and D.R.Borchelt. 2002a. High molecular weight complexes of mutant superoxide dismutase 1: age-dependent and tissue-specific accumulation. *Neurobiol. Dis.* 9:139-148.

Wang, J., G.Xu, and D.R.Borchelt. 2006. Mapping superoxide dismutase 1 domains of non-native interaction: roles of intra- and intermolecular disulfide bonding in aggregation. *J. Neurochem.* 96:1277-1288.

Wang, J., G.Xu, V.Gonzales, M.Coonfield, D.Fromholt, N.G.Copeland, N.A.Jenkins, and D.R.Borchelt. 2002b. Fibrillar inclusions and motor neuron degeneration in transgenic mice expressing superoxide dismutase 1 with a disrupted copper-binding site. *Neurobiol. Dis.* 10:128-138.

Wang, J., G.Xu, H.Li, V.Gonzales, D.Fromholt, C.Karch, N.G.Copeland, N.A.Jenkins, and D.R.Borchelt. 2005a. Somatodendritic accumulation of misfolded SOD1-L126Z in motor neurons mediates degeneration: alphaB-crystallin modulates aggregation. *Hum. Mol. Genet.* 14:2335-2347.

Wang, J., G.Xu, H.H.Slunt, V.Gonzales, M.Coonfield, D.Fromholt, N.G.Copeland, N.A.Jenkins, and D.R.Borchelt. 2005b. Coincident thresholds of mutant protein for paralytic disease and protein aggregation caused by restrictively expressed superoxide dismutase cDNA. *Neurobiol. Dis.* 20:943-952.

Wang, L., H.X.Deng, G.Grisotti, H.Zhai, T.Siddique, and R.P.Roos. 2009c. Wild-type SOD1 overexpression accelerates disease onset of a G85R SOD1 mouse. *Hum. Mol. Genet.* 18:1642-1651.

Wang, Q., J.L.Johnson, N.Y.Agar, and J.N.Agar. 2008. Protein aggregation and protein instability govern familial amyotrophic lateral sclerosis patient survival. *PLoS. Biol.* 6:e170.

Watanabe, M., M.Aoki, K.Abe, M.Shoji, T.Iizuka, Y.Ikeda, S.Hirai, K.Kurokawa, T.Kato, H.Sasaki, and Y.Itoyama. 1997. A novel missense point mutation (S134N) of the Cu/Zn superoxide dismutase gene in a patient with familial motor neuron disease. *Hum. Mutat.* 9:69-71.

Watanabe, M., M.Dykes-Hoberg, V.C.Culotta, D.L.Price, P.C.Wong, and J.D.Rothstein. 2001. Histological evidence of protein aggregation in mutant SOD1 transgenic mice and in amyotrophic lateral sclerosis neural tissues. *Neurobiol. Dis.* 8:933-941.

Watanabe, S., S.Nagano, J.Duce, M.Kiaei, Q.X.Li, S.M.Tucker, A.Tiwari, R.H.Brown, Jr., M.F.Beal, L.J.Hayward, V.C.Culotta, S.Yoshihara, S.Sakoda, and A.I.Bush. 2007. Increased affinity for copper mediated by cysteine 111 in forms of mutant superoxide dismutase 1 linked to amyotrophic lateral sclerosis. *Free Radic. Biol. Med.* 42:1534-1542.

Watanabe, Y., K.Yasui, T.Nakano, K.Doi, Y.Fukada, M.Kitayama, M.Ishimoto, S.Kurihara, M.Kawashima, H.Fukuda, Y.Adachi, T.Inoue, and K.Nakashima. 2005. Mouse motor neuron disease caused by truncated SOD1 with or without C-terminal modification. *Brain Res. Mol. Brain Res.* 135:12-20.

Wiedau-Pazos, M., J.J.Goto, S.Rabizadeh, E.B.Gralla, J.A.Roe, M.K.Lee, J.S.Valentine, and D.E.Bredesen. 1996. Altered reactivity of superoxide dismutase in familial amyotrophic lateral sclerosis. *Science* 271:515-518.

Williamson, T.L. and D.W.Cleveland. 1999. Slowing of axonal transport is a very early event in the toxicity of ALS-linked SOD1 mutants to motor neurons. *Nat. Neurosci.* 2:50-56.

Witan, H., P.Gorlovoy, A.M.Kaya, I.Koziollek-Drechsler, H.Neumann, C.Behl, and A.M.Clement. 2009. Wild-type Cu/Zn superoxide dismutase (SOD1) does not facilitate, but impedes the formation of protein aggregates of amyotrophic lateral sclerosis causing mutant SOD1. *Neurobiol. Dis.*

Witan, H., A.Kern, I.Koziollek-Drechsler, R.Wade, C.Behl, and A.M.Clement. 2008. Heterodimer formation of wild-type and amyotrophic lateral sclerosis-causing mutant Cu/Zn-superoxide dismutase induces toxicity independent of protein aggregation. *Hum. Mol. Genet.* 17:1373-1385.

Wong, P.C., C.A.Pardo, D.R.Borchelt, M.K.Lee, N.G.Copeland, N.A.Jenkins, S.S.Sisodia, D.W.Cleveland, and D.L.Price. 1995. An adverse property of a familial ALS-linked SOD1 mutation causes motor neuron disease characterized by vacuolar degeneration of mitochondria. *Neuron* 14:1105-1116.

Wroe, R. 2009. The ALS association online database (alsod), 8/2009, http://alsod.iop.kcl.ac.uk/Als/index.aspx.

Yamagishi, S., Y.Koyama, T.Katayama, M.Taniguchi, J.Hitomi, M.Kato, M.Aoki, Y.Itoyama, S.Kato, and M.Tohyama. 2007. An in vitro model for Lewy body-like hyaline inclusion/astrocytic hyaline inclusion: induction by ER stress with an ALS-linked SOD1 mutation. *PLoS. ONE.* 2:e1030.

Yamanaka, K., S.Boillee, E.A.Roberts, M.L.Garcia, M.onis-Downes, O.R.Mikse, D.W.Cleveland, and L.S.Goldstein. 2008. Mutant SOD1 in cell types other than motor neurons and oligodendrocytes accelerates onset of disease in ALS mice. *Proc. Natl. Acad. Sci. U. S. A* 105:7594-7599.

Yang, Y., A.Hentati, H.X.Deng, O.Dabbagh, T.Sasaki, M.Hirano, W.Y.Hung, K.Ouahchi, J.Yan, A.C.Azim, N.Cole, G.Gascon, A.Yagmour, M.Ben-Hamida, M.Pericak-Vance, F.Hentati, and T.Siddique. 2001. The gene encoding alsin, a protein with three guanine-nucleotide exchange factor domains, is mutated in a form of recessive amyotrophic lateral sclerosis. *Nat. Genet.* 29:160-165.

Yim, H.S., J.H.Kang, P.B.Chock, E.R.Stadtman, and M.B.Yim. 1997. A familial amyotrophic lateral sclerosis-associated A4V Cu, Zn-superoxide dismutase mutant has a lower Km for hydrogen peroxide. Correlation between clinical severity and the Km value. *J. Biol. Chem.* 272:8861-8863.

Yim, M.B., P.B.Chock, and E.R.Stadtman. 1990. Copper, zinc superoxide dismutase catalyzes hydroxyl radical production from hydrogen peroxide. *Proc. Natl. Acad. Sci. U. S. A* 87:5006-5010.

Yim, M.B., J.H.Kang, H.S.Yim, H.S.Kwak, P.B.Chock, and E.R.Stadtman. 1996. A gain-of-function of an amyotrophic lateral sclerosis-associated Cu,Zn-superoxide dismutase mutant: An enhancement of free radical formation due to a decrease in Km for hydrogen peroxide. *Proc. Natl. Acad. Sci. U. S. A* 93:5709-5714.

Yulug, I.G., N.Katsanis, B.J.de, J.Collinge, and E.M.Fisher. 1995. An improved protocol for the analysis of SOD1 gene mutations, and a new mutation in exon 4. *Hum. Mol. Genet.* 4:1101-1104.

Zetterstrom, P., H.G.Stewart, D.Bergemalm, P.A.Jonsson, K.S.Graffmo, P.M.Andersen, T.Brannstrom, M.Oliveberg, and S.L.Marklund. 2007. Soluble misfolded subfractions of mutant superoxide dismutase-1s are enriched in spinal cords throughout life in murine ALS models. *Proc. Natl. Acad. Sci. U. S. A* 104:14157-14162.

Zhang, B., P.h.Tu, F.Abtahian, J.Q.Trojanowski, and V.M.Y.Lee. 1997. Neurofilaments and Orthograde Transport Are Reduced in Ventral Root Axons of Transgenic Mice that Express Human SOD1 with a G93A Mutation. *The Journal of Cell Biology* 139:1307-1315.

Zona, C., A.Siniscalchi, N.B.Mercuri, and G.Bernardi. 1998. Riluzole interacts with voltage-activated sodium and potassium currents in cultured rat cortical neurons. *Neuroscience* 85:931-938.

BIOGRAPHICAL SKETCH

Mercedes Prudencio Álvarez was born in Badajoz (Spain) in 1982 to Máximo and Joaquina. She graduated with Honors from I.E.S. Maestro Domingo Cáceres in 2000, and obtained an English degree at the Escuela Oficial de Idiomas that same year. In 2000, she attended Universidad de Extremadura for her undergraduate studies, where she graduated with a 5-year Bachelor of Science in biology in 2005. Mercedes began her graduate studies in biomedical sciences (neuroscience) at the University of Florida in 2005, where she joined the laboratory of Dr. David R. Borchelt in 2006.